Université de Montréal

Études fonctionnelles de deux nouvelles protéines centrosomales, NPHP5 et Cep76, et leurs implications dans les maladies humaines

par
Marine Barbelanne

Département de Pathologie et Biologie Cellulaire
Faculté de Médecine

Thèse présentée à la Faculté de Médecine
en vue de l'obtention du grade de philosophiae doctor (Ph.D.)
en Pathologie et Biologie Cellulaire
option Biologie Cellulaire

août 2015

Université de Montréal
Faculté de médecine

Cette thèse intitulée :

Études fonctionnelles de deux nouvelles protéines centrosomales, NPHP5 et Cep76, et leurs implications dans les maladies humaines

Présentée par :
Marine Barbelanne

a été évaluée par un jury composé des personnes suivantes :

Dr Gilles Hickson, président-rapporteur

Dr William Tsang, directeur de recherche

Dr Benjamin Kwok, membre du jury

Dr Michel Leroux, examinateur externe

Dr Jean-François Côté, représentant de la doyenne

Résumé

Les centrosomes sont de petits organites qui régulent divers processus cellulaires comme la polarité ou la mitose dans les cellules de mammifères. Ils sont composés de deux centrioles entourés par une matrice péricentriolaire. Ces centrosomes sont les principaux centres organisateurs de microtubules. De plus, ils favorisent la formation de cils, des protubérances sur la surface des cellules quiescentes qui sont critiques pour la transduction du signal. Une grande variété de maladies humaines telles que les cancers ou les ciliopathies sont liées à un mauvais fonctionnement des centrosomes et des cils. C'est pourquoi le but de mes projets de recherche est de comprendre les mécanismes nécessaires à la biogénèse et au fonctionnement des centrosomes et des cils.

Tout d'abord, j'ai caractérisé une nouvelle protéine centrosomale nommée nephrocystine - 5 (NPHP5). Cette protéine est localisée dans les cellules en interphase au niveau de la région distale des centrioles. Sa déplétion inhibe la migration des centrosomes à la surface cellulaire lors de l'étape précoce de la formation des cils. NPHP5 interagit avec la protéine CEP290 via sa région C-terminale qui est essentielle pour la ciliogenèse. Elle interagit également avec la calmoduline ce qui empêche son auto-agrégation. J'ai démontré que les domaines de liaison de NHPH5 à CEP290 et à la calmoduline, ainsi que son domaine de localisation centrosomale sont séparables. De plus, j'ai démontré que les protéines NPHP5 présentant des mutations pathogènes ne peuvent plus interagir avec CEP290 et ne sont plus localisées aux centrosomes, rendant ainsi ces protéines non fonctionnelles. Enfin, en utilisant une approche pharmacologique pour moduler les événements en aval dans la voie ciliogénique, j'ai montré que la formation des cils peut être restaurée même en absence de NPHP5.

D'autre part, j'ai étudié le rôle de NPHP5 dans l'assemblage et le trafic du complexe BBSome dans le cil. Le BBSome est composé de huit sous-unités différentes qui s'assemblent en un complexe fonctionnel dont on sait peu de chose sur la régulation spatiotemporelle de son processus d'assemblage. J'ai précédemment montré que NPHP5 favorisait la formation des cils et que son dysfonctionnement contribuait au développement de néphronophtise (NPHP).

Bien que la NPHP et le syndrome de Bardet-Biedl (BBS) soient des ciliopathies qui partagent des caractéristiques cliniques communes, la base moléculaire de ces ressemblances phénotypiques n'est pas comprise. J'ai constaté que NPHP5, localisé à la base du cil, contient deux sites de liaison distincts pour le BBSome. De plus, j'ai démontré que NPHP5 et son partenaire CEP290 interagissent de façon dynamique avec le BBSome pendant la transition de la prolifération à la quiescence. La déplétion de NPHP5 ou CEP290 conduit à la dissociation d'au moins deux sous-unités du BBSome formant alors un sous-complexe dont la capacité de migration dans le cil n'est pas compromise. J'ai montré que le transport des cargos vers le compartiment ciliaire par ce sous-complexe n'est que partiellement altéré.

Enfin, j'ai également concentré mes recherches sur une autre protéine centrosomale peu caractérisée. La protéine centrosomale de 76 kDa (Cep76) a été précédemment impliquée dans le maintien d'une duplication unique des centrioles par cycle cellulaire, et dans une interaction avec la kinase cycline-dépendante 2 (CDK2). Cep76 est préférentiellement phosphorylée par le complexe cycline A/CDK2 sur le site unique S83. Cet événement est essentiel pour supprimer l'amplification des centrioles en phase S. J'ai démontré que Cep76 inhibe cette amplification en bloquant la phosphorylation de Plk1 au niveau des centrosomes. D'autre part, Cep76 peut être acétylée au site K279 en phase G2, ce qui régule négativement son activité et sa phosphorylation sur le site S83.

Ces études permettent d'améliorer notre compréhension de la biologie des centrosomes et des cils et pourraient conduire au développement de nouvelles applications diagnostiques et thérapeutiques.

Mots-clés : Centrosome, cil, NPHP5, Cep76, cycle cellulaire, Cep290, BBSome, CDK2, cycline A, phosphorylation, acétylation, cancer

Abstract

Centrosomes are small organelles that regulate diverse cellular processes such as polarity or mitosis in mammalian cells. They are composed of two centrioles surrounded by a pericentriolar matrix. These centrosomes are the major microtubule organizing centers. Moreover, they promote the formation of cilia, protrusions on the surface of quiescent cells that are critical for signal transduction. A wide variety of human diseases such as cancers or ciliopathies are linked to a malfunction of centrosomes and cilia. Therefore the aim of my research is to understand the mechanisms necessary for the biogenesis and function of centrosomes and cilia.

First, I have characterized a novel centrosomal protein called nephrocystin - 5 (NPHP5). This protein is localized, in interphase cells, in the distal region of centrioles. Its depletion inhibits the migration of centrosomes to the cell surface during the early stage of cilia formation. NPHP5 interacts with CEP290 via its C-terminal region that is essential for ciliogenesis. It also interacts with calmodulin, which prevents its self-aggregation. I have demonstrated that the Cep290- and CaM-binding domains as well as the centrosomal localization domain of NPHP5 are separable. Moreover, I have shown that NPHP5 proteins with pathogenic mutations can no longer interact with CEP290 and are not localized to centrosomes, rendering these proteins non-functional. Finally, using a pharmacological approach to modulate the downstream events in the ciliogenic pathway, I showed that cilia formation can be restored even without NPHP5.

On the other hand, I studied the role of NPHP5 in the assembly and trafficking of the BBSome into the cilium. The BBSome consists of eight different subunits that assemble into a functional complex of which little is known about the spatiotemporal regulation of its assembly process. I have previously shown that NPHP5 favored the formation of cilia and its dysfunction contributes to the development of nephronophthisis (NPHP). Although the NPHP and BBS syndrome (BBS) are ciliopathies that share common clinical features, molecular basis of these phenotypic similarities is not understood. I found that NPHP5, located at the base of the cilium, contains two separate binding sites for BBSome.

Furthermore, I demonstrated that NPHP5 and his partner CEP290 interact dynamically with the BBSome during the transition from quiescence to proliferation. Depletion NPHP5 or CEP290 leads to the dissociation of at least two subunits of BBSome forming a sub-complex that can still traffic into the cilium. I have shown that the transport of cargo to the ciliary compartment through this sub-complex is only partially altered.

Finally, I have also focused my research on another centrosomal protein poorly characterized. The centrosomal protein of 76 kDa (Cep76) was previously involved in the maintenance of a single duplication of centrioles per cell cycle, and interacts with the cyclin-dependent kinase 2 (CDK2). Cep76 is preferentially phosphorylated by cyclin A/CDK2 on the single site S83. This event is essential to suppress centrioles amplification in S phase. I have demonstrated that Cep76 inhibits amplification by blocking the phosphorylation of Plk1 at the centrosome. Moreover, Cep76 can be acetylated at the K279 site in G2 phase, which negatively regulates its activity and phosphorylation on the site S83.

These studies will improve our understanding of the biology of centrosomes and cilia and could lead to development of new diagnostic and therapeutic applications.

Keywords : Centrosome, cilia, NPHP5, Cep76, cell cycle, cancer, Cep290, BBSome, CDK2, cyclin A, phosphorylation, acetylation

Table des matières

Liste des figures

Liste des abréviations

ADN : acide désoxyribonucléique

APC/C : anaphase promoting complex / cyclosome

ARN : acide ribonucléique

BBS : Bardet-Biedl syndrome

CC : coiled-coil

CDC : cell division cycle

CDK : cyclin-dependent kinase

CEP135 : centrosomal protein 135 kDa

CEP290 : centrosomal protein 290 kDa

Cep76 : centrosomal protein 76 kDa

Cep97 : centrosomal protein 97 kDa

CP110 : centriolar protein 110 kDa

CPAP : centrosome P4.1 associated protein

G1 : gap phase 1

G2 : gap phase 2

HU : hydroxyurée

IF : immunofluorescence

IP : immunoprécipitation

IQ : calmodulin binding domain

JBTS : Joubert syndrome

kDa : kilo dalton

LCA : Leber congenital amaurosis

M : mitose

MPC : matrice péricentriolaire

MPF : maturation promoting factor

MPT : modifications post-traductionelles

MT : microtubule

MTOC : microtubule organizing center

NEK2A : NIMA (Never In Mitosis Gene A)-Related Kinase 2

NPHP : néphronophthise

NPHP5 : néphrocystine-5

PLA : proximity ligation assay

PLK1 : polo-like kinase 1

PLK4 : polo-like kinase 4

RPE : retinal pigment epithelium

RPGR : Retinitis Pigmentosa GTPase Regulator

S : synthèse

SAS6 : Spindle Assembly 6

SCF : SKP1-Cullin-F-box

SDM : spectrométrie de masse

SHH : sonic hedgehog

siRNA : small interference RNA

SLSN : Senior-Loken syndrome

Smo : smoothened

STIL : SCL/TAL1 Interrupting Locus

TGL : transglutaminase

TIF : transport intraflagellaire

U2OS : U2-Osteosarcoma

WB : western blot

"If we knew what it was we were doing, it would not be called research, would it?"

— *Albert Einstein*

Remerciements

Ce manuscrit conclut de longues années de travail, je tiens en quelques lignes à exprimer ma reconnaissance et ma gratitude envers toute personne qui a participé de près ou de loin à l'accomplissement de cette thèse.

Je voudrais d'abord remercier mon directeur, le Dr William Tsang pour son aide et ses conseils au cours des cinq dernières années.

Je tiens à remercier les membres du laboratoire, anciens et actuels, spécialement Émilie, Yalda, Alice, Andréa, Matt et Jin. Je vous remercie pour votre temps, votre aide, et tous les moments agréables passés ensemble.

J'aimerais remercier la grande famille de l'Institut de recherches cliniques de Montréal. Vous m'avez apporté un soutien technique, mais encore plus important, un environnement agréable, stimulant et chaleureux. Particulièrement, j'aimerais remercier Nicole Rousseau et Dominic Filion.

Je désire également remercier les membres de mon comité de thèse qui m'ont accompagnée, soutenue et encouragée durant ma formation doctorale.

Je veux remercier le département de pathologie et biologie cellulaire, la fédération des études supérieures et postdoctorales de l'université de Montréal et l'institut de recherches cliniques de Montréal pour leur support financier.

Mille mercis à vous tous d'avoir accepté de lire et corriger ma thèse dans un temps record malgré vos emplois du temps personnels chargés et plus spécialement Dr Reza Sharif Naeini.

Enfin, je tiens à remercier mes proches pour leur support inconditionnel bien qu'à des milliers de kilomètres (surtout toi Hélène). Un énorme merci à mes parents, en particulier ma mère, pour leur présence, leur écoute et leurs encouragements dans les meilleurs et les pires moments. Deux personnes qui, par leurs sacrifices, m'ont permis d'être où je suis aujourd'hui. Merci d'avoir toujours eu confiance en moi malgré certaines étapes difficiles.

Enfin, une pensée spéciale pour vous qui nous avez quitté trop tôt. J'espère que vous savez à quel point vous me manquez et que vous êtes fiers de cet accomplissement final.

Introduction

Le cycle cellulaire

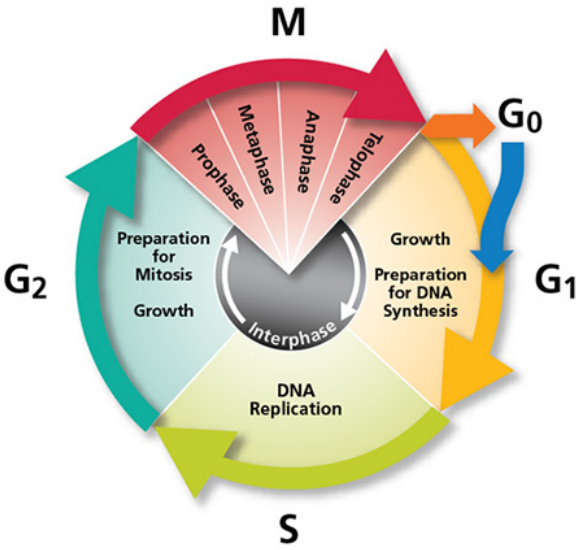

Adaptation du site : http://www.bdbiosciences.com/anz/research/apoptosis/analysis/index.jsp

Figure 1 : Les différentes phases du cycle cellulaire.

Le cycle cellulaire est séparé en deux grandes étapes : l'interphase et la phase mitotique (phase M). L'interphase comporte trois phases successives et distinctes : G1, S et G2.

Le cycle cellulaire est défini par une séquence d'événements qui permet de créer deux cellules filles identiques à partir d'une cellule mère. Le cycle est composé de deux phases : l'interphase et la mitose. L'interphase comprend les phases G0/G1, S et G2 successivement avant d'entrer en mitose (phase M) (Figure 1). L'étape principale de l'interphase est la réplication de l'ADN en phase S avant la complétion de la division en phase M. Les phases G1 et G2 servent quant à elles de transition entre ces étapes, d'où leur nom de ''gap phase'' (1). Chaque étape est caractérisée par des processus cellulaires spécifiques tels que la synthèse de l'ADN, le contrôle de la croissance ou la vérification de l'intégrité génomique. Enfin, la progression du cycle cellulaire se fait grâce à l'expression et l'activation séquentielle des complexes CYCLINES-CDK.

Les différentes phases du cycle cellulaire

La phase G1 est la phase intermédiaire qui couvre le temps entre la formation de la nouvelle cellule fille et la synthèse subséquente de l'ADN en phase S. C'est la phase dont la durée est la plus variable selon le type cellulaire, allant de quelques heures (cellules épithéliales de muqueuse) à plusieurs mois (hépatocytes) (2). Pendant cette période, la cellule grandit en préparation de la réplication de l'ADN et certains composants intracellulaires, comme le centrosome, subissent aussi une duplication. Avant de s'engager en phase S, la cellule doit s'assurer que les conditions sont optimum au niveau cellulaire en contrôlant son environnement mais aussi sa taille. C'est également à ce moment qu'elle peut choisir de rentrer en quiescence, ou phase G0, si les conditions ne sont pas propices. Les cellules quiescentes décident alors si elles vont se différencier ou entrer en sénescence (3-5). La décision de poursuivre en phase S ou d'aller vers la phase G0 est influencée par la composition et la nature du milieu extracellulaire de la cellule (facteurs de croissance, hormones, chemokines, cytokines, ions, etc.) (6). Cette décision se prend au niveau du point de restriction en fin de phase G1 (7).

La phase S, pour synthèse, est la phase du cycle cellulaire où l'ADN, sous forme chromosomes, est répliqué. Cette étape est cruciale car elle permet que chaque cellule fille créée contienne exactement le même matériel génétique à la fin de la division cellulaire. Au cours de cette phase S, la cellule va également continuer à grandir et synthétiser en grand nombre plusieurs protéines et enzymes impliquées dans la réplication de l'ADN (8, 9).

La phase G2, ou phase prémitotique, survient entre la fin de la réplication de l'ADN en phase S et le début de la division cellulaire en phase M. Au cours de cette étape, la cellule va augmenter sa taille due à une synthèse protéique renforcée mais aussi vérifier l'intégrité de son génome répliqué ainsi que les autres composants intracellulaires. C'est pourquoi cette étape est considérée comme une étape de contrôle (10).

Enfin, la mitose se compose elle-même de plusieurs phases successives : prophase, prométaphase, métaphase, anaphase, télophase et cytokinèse. Ces étapes aboutissent à la scission du corps cellulaire et du matériel génétique de la cellule mère pour donner naissance à deux cellules filles identiques. Au cours des phases précédentes, l'ADN de la cellule se trouve sous forme relaxée dans le noyau et c'est durant la mitose que les changements morphologiques importants se produisent. En prophase, l'ADN se condense pour former les chromosomes avec leurs centromères, les nucléoles disparaissent et les centrosomes dupliqués commencent leur migration vers les pôles mitotiques opposés pour former les fuseaux mitotiques. Le cytosquelette commence également à se réorganiser et les microtubules astraux s'allongent. L'événement majeur marquant l'entrée des cellules en prométaphase est la désintégration de l'enveloppe nucléaire en petites vésicules. La rupture de cette enveloppe permet ainsi aux fuseaux mitotiques d'avoir accès aux kinétochores au niveau des centromères grâce aux microtubules. Les centrosomes exercent alors des forces opposées mais égales sur les chromosomes pour les aligner sur la plaque équatoriale au centre de la cellule. Il s'agit de la métaphase. À ce moment précis, les chromatides sœurs de chaque chromosome sont alignées sur la plaque équatoriale et attachées de part et d'autre par les microtubules. Les chromatides sont dites bi-orientées et cet évènement va ensuite déclencher l'anaphase. C'est au cours de cette étape que les chromatides sœurs se séparent grâce à la rétraction vers chaque pôle des microtubules attachés aux kinétochores. Au cours de la dernière étape, la télophase, les chromatides sœurs ont atteint les pôles opposés. Les petites vésicules nucléaires vont également reformer l'enveloppe nucléaire à chaque pôle de la cellule où la chromatine se décondense, créant ainsi une cellule binuclée. Un sillon de clivage va aussi apparaître à l'endroit où s'était formée la plaque équatoriale. Ce sillon va progressivement se resserrer avant de se refermer totalement créant les deux cellules filles qui vont retourner en phase G1. Il s'agit de la cytokinèse. (11-16)

Régulation du cycle cellulaire

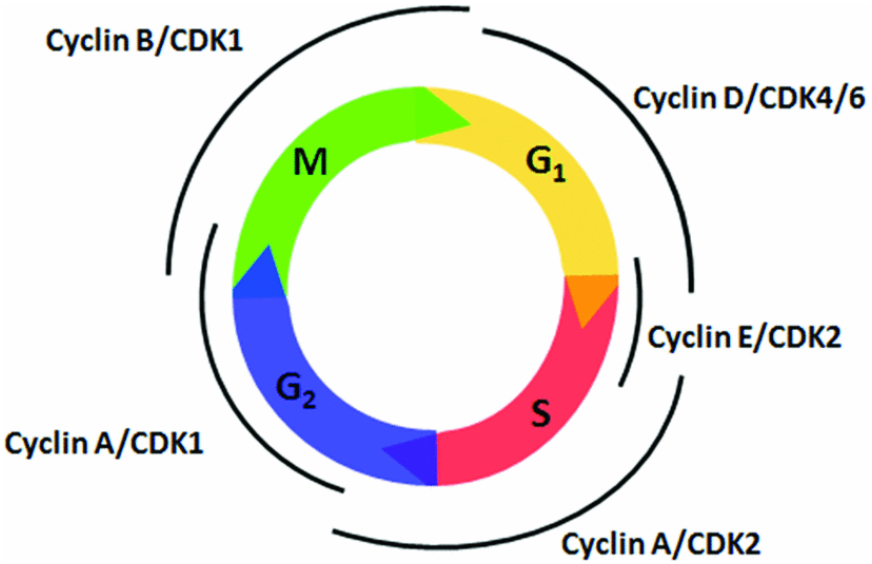

Extrait de Biosci Rep. 2010 Mar 17;30(4):243-55.

Figure 2 : La régulation du cycle cellulaire par les complexes CYCLINE-CDK.
Dans les cellules de mammifères, différents complexes CYCLINE/CDK régulent la progression des cellules à travers les différentes phases du cycle cellulaire.

La progression du cycle cellulaire est finement régulée de manière séquentielle par les complexes CYCLINE-CDK (Kinase dépendante des cyclines). Au cours des cinquante dernières années, plusieurs acteurs moléculaires responsables de cette régulation ont été découverts, comme le facteur MPF (Maturation Promoting Factor) ou plusieurs gènes impliqués dans la division cellulaire (17-19). Cependant, ce fut la découverte des cyclines dans les années 1980 par le professeur Tim Hunt et son équipe qui a permis d'établir le modèle actuel de la régulation du cycle cellulaire (20).

Les complexes CYCLINE-CDK sont des hétérodimères constitués d'une cycline sans activité catalytique et d'une kinase. Les différentes cyclines et CDKs impliquées dans la régulation du cycle cellulaire sont les CYCLINES A, B, D ou E et CDK 1, 2, 4 ou 6.

En s'associant avec une CDK, la cycline va permettre à cette dernière d'être active et de phosphoryler ses substrats. On appelle les cyclines les sous unités régulatrices de ce complexe. L'association transitoire des cyclines avec les CDKs se fait de manière contrôlée et spécifique en fonction des différentes phases du cycle cellulaire (21, 22). (Figure 2)

La phase G1 est contrôlée par les complexes CYCLINE D-CDK4/6 (23) tandis que la transition G1/S et la phase S sont respectivement contrôlées par les complexes CYCLINE E-CDK2 et CYCLINE A -CDK2 (24-30). En début de phase G2, c'est le complexe CYCLINE A-CDK1 qui sera actif puis le complexe CYCLINE B-CDK1 en fin de phase G2 et pour la phase M (31-36). L'expression séquentielle des cyclines dicte l'activité des complexes CYCLINES-CDK propres à chaque phase du cycle cellulaire. Sachant que les CDKs sont des protéines très stables et que leur niveau d'expression ne varie quasiment pas au cours du cycle cellulaire ; la régulation des complexes est due à l'expression puis dégradation séquentielle des cyclines à chaque phase. La dégradation des cyclines est souvent rapide et principalement régulée par deux complexes E3 ubiquitine ligase : le cyclosome APC/C et le complexe SKP1-CULLIN-F-box (SCF). Ces complexes vont poly-ubiquitinyler les cyclines pour les pousser à la dégradation par le protéasome. Le complexe SCF poly-ubiquitinyle les CYCLINES A, D et E en interphase tandis que le complexe APC/C poly-ubiquitinyle les CYCLINES A et B en mitose (37-41).

Points de contrôle du cycle cellulaire

En cas d'erreur lors de la réplication, de lésions génotoxiques ou de problèmes dans la structure de la chromatine, les cellules possèdent des mécanismes qui leur permettent de stopper la progression du cycle cellulaire pour réparer les erreurs ou mourir. Ces mécanismes, ou points de contrôle du cycle cellulaire, arrêtent le cycle à différentes étapes : la transition G1/S, au cours de la phase S, à la transition G2/M et durant la mitose entre la métaphase et l'anaphase. (Figure 3)

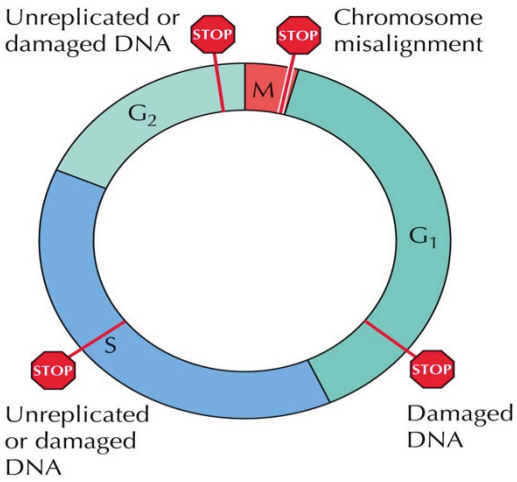

Extrait de The Cell, fourth edition, figure 16.8

Figure 3 : Les points de contrôle du cycle cellulaire.

À certains moments au cours du cycle cellulaire, la cellule s'arrête afin de vérifier que tout est en ordre avant de poursuivre son cycle. Il s'agit des points de contrôle du cycle cellulaire.

Le point de contrôle à la transition G_1/S stoppe l'activation des complexes CYCLINE E-CDK2 nécessaire au passage des cellules en phase S. Cette inactivation se fait via l'inhibition de la phosphatase CDC25A et l'activation de la protéine p21, un inhibiteur du cycle cellulaire (42-45). Le point de contrôle au cours de la phase S va également inactiver les complexes CYCLINE A-CDK2 en inhibant la phosphatase CDC25A. En même temps, la progression des fourches de réplications actives va ralentir et la formation de nouvelles origines de réplication va être bloquée (46-48). Le point de contrôle à la transition G2/M inactive les complexes CYCLINE B-CDK1 par séquestration ou dégradation des trois phosphatases CDC25A, B et C. L'arrêt du cycle cellulaire à cette étape permet de vérifier l'intégrité du génome ainsi que la fidélité de réplication de l'ADN (42, 49, 50). Enfin, le point de contrôle en phase M est activé si les chromatides sœurs des chromosomes dupliqués ne sont pas distribuées de manière équitable en fin de métaphase. L'arrêt du cycle à cette étape se fait par l'inhibition de l'ubiquitine ligase APC/C et la stabilisation des complexes CYCLINE B-CDK1 (51-54).

Les centrosomes

Les centrosomes sont des organelles importantes pour le maintien de la stabilité génomique des cellules. Ils sont les centres organisateurs des microtubules et jouent un rôle essentiel dans l'organisation du fuseau mitotique bipolaire et la séparation des chromosomes pendant la mitose. Ils sont également impliqués dans la formation et la motilité des cils et flagelles dans les cellules différenciées.

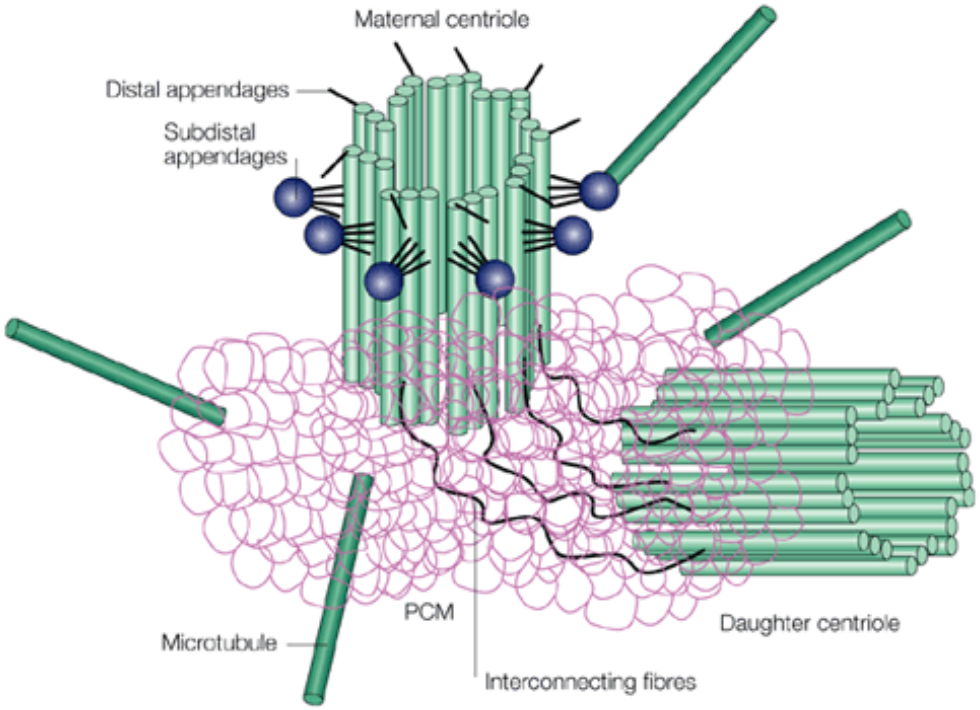

Extrait de Nature Reviews Molecular Cell Biology 2, 688-698

Figure 4 : Structure du centrosome.

Chaque centrosome est composé d'une paire de centrioles, formé de neuf triplets de microtubules chacun, et entouré par une matrice préicentriolaire. Le centriole mère est le seul à disposer des appendices distaux et subdistaux pour la nucléation et l'attachement des microtubules.

Structure

Les centrosomes sont de petits organites périnucléaires constitués de deux centrioles perpendiculaires l'un à l'autre, appelés mère et fille, et entourés d'une matrice protéique appelée matériel péricentriolaire (MPC) (55, 56). Cette matrice contient de nombreuses protéines nécessaires à la nucléation et l'ancrage des microtubules pour la formation des fuseaux mitotiques (57, 58). Les centrioles sont composés d'un arrangement radial et symétrique de neuf triplets de microtubules (MT) et sont reliés l'un à l'autre par un pont protéique flexible composé principalement par les protéines ROOTLETIN et C-NAP1 (Figure 4) (59-62). Le centriole mère est plus long et possède des appendices distaux et sub-distaux nécessaires à l'ancrage des centrosomes à la membrane plasmique, le trafic endosomal ou encore l'attachement des MT (57, 63). Le centriole fille quant à lui est plus court et ne possède pas d'appendice. Il est important de noter que les parties distales et proximales des centrioles ont des fonctions différentes. La partie distale du centriole mère est impliquée dans la ciliogénèse, l'ancrage et la nucléation des MT tandis que la partie proximale des deux centrioles est nécessaire au recrutement des protéines de la MPC et à la formation des procentrioles en phase S lors de leur duplication (59, 63, 64).

Le cycle des centrosomes

La duplication des centrosomes est liée de façon spatio-temporelle au cycle cellulaire, notamment à la réplication de l'ADN, et est strictement régulée à une fois par cycle. Ce processus permet la transmission d'un centrosome mature à chaque cellule fille au moment de la mitose (65-67). Le cycle des centrosomes est constitué de quatre phases distinctes : le désengagement, la duplication, la maturation et enfin la séparation. (Figure 5)

En fin de mitose ou début de phase G1, chaque paire de centrioles ; appelés centrioles mère et fille ou parentaux, va se séparer et perdre son orientation perpendiculaire pour préparer le site d'initiation de la duplication. Il s'agit du désengagement. Cette étape est contrôlée principalement par l'action de la kinase PLK1 et la protéase SÉPARASE. PLK1 va promouvoir l'enlèvement de la COHÉSINE au niveau des centrosomes en prophase mais aussi stimuler son clivage par la SÉPARASE à la sortie de la mitose (68-70). À noter que les centrioles sont toujours liés par le pont protéique flexible (58, 60, 67, 71).

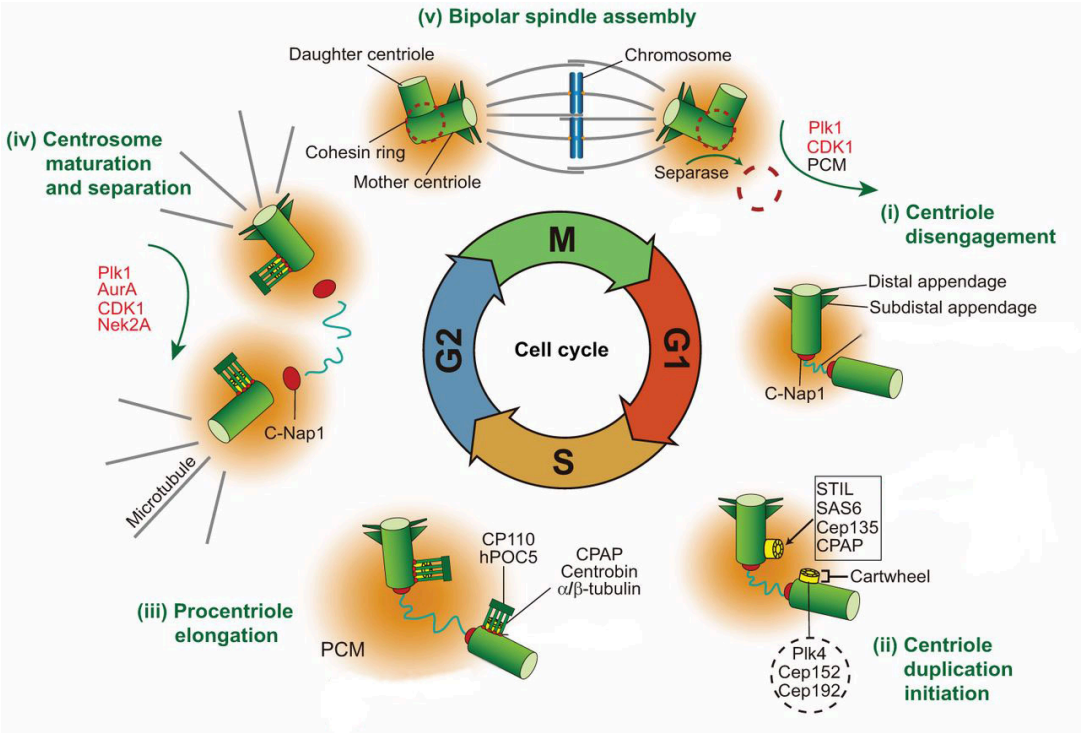

Adaptation de J Cell Sci 127, 4111-4122.

Figure 5 : Cycle des centrosomes.

Le cycle centrosome est composé de plusieurs étapes qui sont liées au cycle cellulaire : (i) le désengagement des centrioles, (ii) la duplication des centrioles, (iii) l'allongement des procentrioles, (iv) la maturation et la séparation des centrioles et enfin (v) l'assemblage du fuseau mitotique bipolaire.

Durant la transition de la phase G1 à la phase S, de nouveaux centrioles ; appelés pro-centrioles, sont dupliqués de manière semi conservative au niveau proximal de chaque centriole parental. La kinase PLK4 va stabiliser les protéines SAS6, STIL et CEP135 sur la paroi du centriole et ainsi leur permettre de former l'arrangement radial et symétrique des nouveaux centrioles (72-76). Cette duplication est concomitante avec la réplication des chromosomes et est aussi régie par les complexes CDK2-CYCLINE A/E (68, 77-82). Au cours des phases S et G2, les pro-centrioles s'allongent jusqu'à maturité et le centriole fille va acquérir les appendices distaux et sub-distaux, composés de nombreuses protéines, pour devenir à son tour centriole mère. L'élongation des microtubules est contrôlée positivement par la protéine CPAP mais la protéine CP110 empêche une élongation excessive en servant de ''cap'' aux centrioles (83-87). Les centrioles vont également recruter massivement et rapidement les protéines de la MPC pour former deux centrosomes parfaitement fonctionnels en fin de phase G2 (55, 71, 82, 88). En début de mitose, le pont protéique entre les centrosomes est détruit activant ainsi leur séparation et migration à chaque pole de la cellule, pour créer le fuseau mitotique bipolaire et permettre la bonne ségrégation des chromosomes. Pour cela, les kinases PLK1 et NEK2A vont phosphoryler les différentes protéines composant le lien fibreux pour soit défaire la structure soit les dégrader (89-91). A la fin de la mitose, chaque cellule fille recevra donc un centrosome mature et un jeu de chromosome identiques (88, 92, 93).

Les centrosomes et les complexes Cycline-CDK

Récemment, les complexes CYCLINE-CDK ont été impliqués dans la duplication des centrosomes en raison de leurs nombreux substrats centrosomaux (93). Il a notamment été montré que la kinase CDK2, impliquée dans la réplication de l'ADN, serait également importante pour la duplication des centrosomes. Cela suggère que le cycle cellulaire et celui des centrosomes seraient liés par l'activation de cette kinase (81, 94). En effet, l'initiation des deux cycles se fait au niveau de la phase G1 par l'activation des complexes CYCLINE E-CDK2 (55). De récentes expériences ont aussi mis en évidence le rôle crucial de CDK2 dans la duplication des centrosomes dans les œufs de xénope (68).

Enfin, de nombreuses protéines centrosomales sont les cibles directes des complexes CYCLINE-CDK2, comme CP110. À noter que la phosphorylation de CP110 par CDK2 est connue pour empêcher la duplication excessive des centrosomes en phase S en bloquant la séparation prématurée des centrosomes (95, 96). Le cycle des centrosomes est donc lié de manière spatio-temporelle au cycle cellulaire et leur régulation précise est primordiale au bon fonctionnement des cellules.

Centrosomes et maladies

Un nombre anormal de centrosomes est une caractéristique commune de beaucoup de cancers humains et corrèle souvent avec l'agressivité tumorale (55, 97-99). La présence d'un nombre anormal de centrosomes peut engendrer des mitoses multipolaires et enrayer la ségrégation équitable des chromosomes créant de l'aneuploïdie (82, 100, 101). Toutefois, la plupart des cellules cancéreuses sont capables de regrouper leurs centrosomes surnuméraires en deux pôles pour éviter la catastrophe mitotique. À ce jour, ces mécanismes d'adaptations sont peu connus mais représentent des cibles prometteuses en thérapie antitumorales (102-105). Ces anomalies centrosomales seraient dues à une dérégulation du cycle des centrosomes, voire du cycle cellulaire. Il est aussi important de noter que de nombreuses mutations ont été détectées dans des gènes codant pour des protéines centrosomales (106-108). Des aberrations dans la duplication ou la maturation des centrosomes peuvent également entrainer des maladies neurodégénératives comme les microcéphalies primaires ou la maladie de Huntington (109-112). Étant donné que de nombreuses maladies humaines sont liées d'une manière ou d'une autre aux centrosomes, il est crucial d'étudier plus en profondeur cette organelle afin de mieux comprendre son organisation et ses fonctions dans le but de trouver de nouvelles cibles thérapeutiques.

Les cils

Les centrosomes jouent également un rôle crucial dans la formation des cils soit la ciliogénèse. Les cils sont présents sur la plupart des cellules post-mitotiques et ressemblent à des antennes qui se projettent dans l'espace extracellulaire. Ils servent à l'échange d'informations avec l'environnement. Plusieurs voies de signalisation du développement ou de la différentiation dont Sonic Hedgehog et Wnt ont d'ailleurs plusieurs protéines localisées au niveau des cils (109, 113-116).

Structure

Deux types de cils se distinguent par leur structure et par leur fonction; le cil primaire ou non-mobile, et le cil mobile. Le cil primaire est composé d'un axonème, formé de neufs doublets de microtubules circulaires (conformation 9+0), qui émane du centrosome mère, alors appelé corps basal. En comparaison, le cil mobile possède en plus une paire de microtubules centraux (conformation 9+2) qui lui permet de se mouvoir (67, 117, 118). Dans les deux cas, l'axonème est recouvert par une membrane plasmique ciliaire dont la composition et la fonction seraient différentes de celles de la membrane plasmique cellulaire (119, 120). Cette différence serait due à un enrichissement en protéines spécifiques ayant des signaux de localisation ciliaire. En effet, la base du cil est constituée d'une zone de transition délimitée par un réseau de fibres en Y et, avec l'aide des corps basaux, cette zone de transition aiderait activement à la sélection des éléments qui entrent et sortent du cil. Puisqu'il n'y a pas de synthèse protéique au niveau du cil, tous ces éléments nécessaires à sa formation et à son maintien doivent être transportés. Le mécanisme moléculaire par lequel les protéines ciliaires sont véhiculées le long de l'axonème est nommé transport intraflagellaire (TIF) (121). Les complexes TIF-A et TIF-B, grâce aux moteurs protéiques dynéine et kinésine, transportent la tubuline, les récepteurs ou encore les molécules de signalisation de façon antérograde et rétrograde dans les cils pour permettre leur formation mais aussi leur maintien et leur fonction (122-126). (Figure 6)

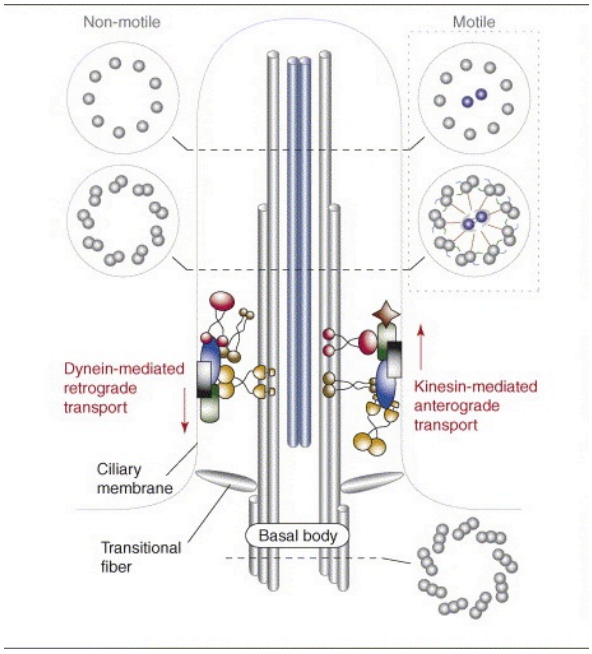

Adapté de Trends Genet. 2006 Sep;22(9):491-500

Figure 6 : Structure du cil.

Les cils, composés de doublets de microtubules (singlets à l'extrémité distale), sont nucléés à partir du centriole mère alors appelé corps basal. Les cils non-mobiles manquent la paire centrale de microtubules. Les coupes transversales montrent l'architecture des microtubules à différentes régions des cils.

Formation du cil ou ciliogénèse

La ciliogénèse est un processus en plusieurs étapes. Premièrement, une vésicule ciliaire transportant diverses protéines est recrutée et fusionnée au niveau distal du centrosome mère grâce aux appendices distaux, créant ainsi le corps basal. Des vésicules ciliaires secondaires fusionnent à leur tour et permettent l'émergence de la zone de transition à partir du corps basal (126-129). Ensuite, cette structure va commencer sa migration vers la membrane plasmique avant de s'y accrocher grâce aux appendices distaux. Au cours de la migration, la zone de transition devient mature et s'allonge toujours par la fusion de vésicules ciliaires secondaires (126).

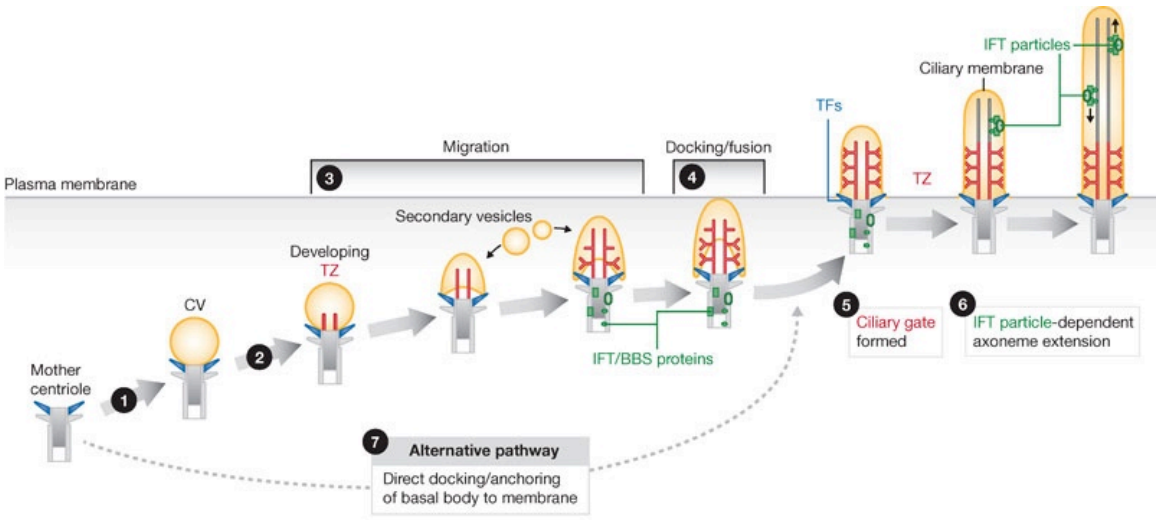

Adapté de EMBO Rep. 2012 Jul; 13(7): 608–618

Figure 7 : Ciliogénèse.

La première étape de la ciliogénèse implique la fusion de vésicules à l'extrémité distale du centriole mère (1). Une zone de transition à émerger et continue à se développer grâce à la fusion des vésicules secondaires (2-3). Le corps basal peut alors migrer vers la membrane plasmatique (3) pour fusionner avec (4), moment auquel la zone de transition forme la porte ciliaire (5). La formation complète de l'axonème est un processus dépendant du trafic intraflagellaire (6). Une autre voie (7) propose que le corps basal migre et fusionne directement avec la membrane plasmique avant la formation de la zone de transition. CV, vésicule ciliaire; IFT, transport intraflagellaire; BBS, syndrome de Bardet-Biedl; TZ, zone de transition.

Au moment de s'attacher à la membrane plasmique, la zone de transition mature forme la porte ciliaire qui va alors permettre la sélection des éléments qui entrent et sortent du cil. Finalement, l'axonème est nucléé vers l'espace extracellulaire par l'action du transport intraflagellaire et devient mature et fonctionnel (129, 130). Cette succession d'étapes est principalement utilisée par les cellules formant des cils primaires, c'est à dire un cil par cellule. En ce qui concerne les cellules multiciliées, soit avec des cils mobiles, la séquence est légèrement différente.

En effet, pour ces cellules, le corps basal va d'abord migrer et s'accrocher à la membrane plasmique avant de former la zone de transition et de nucléer l'axonème mature. Bien que la séquence soit différente, l'élongation de l'axonème se fait toujours par le transport intraflagellaire (126, 131). Il est important de noter que les cils vont être démantelés lorsque la cellule va rentrer de nouveau dans le cycle cellulaire. Cette résorption est nécessaire pour que le corps basal redevienne un centriole mère et donc un centre organisateur de microtubules. (Figure 7)

Cils et maladies

Des défauts dans la structure ou la fonction des cils primaires et mobiles créent des pathologies humaines appelées ciliopathies dont entre autres le syndrome de Joubert, le syndrome de Bardet-Biedl, la néphronophtise ou la maladie polycystique du rein. Ces maladies sont majoritairement dues à des mutations dans un ou plusieurs gènes codant des protéines localisées au niveau du cil et impliquées dans leur formation et/ou leur fonction. Les ciliopathies sont des maladies multi-symptomatiques incluant la dégénérescence de la rétine, des kystes rénaux ou des troubles neurologiques (66, 109, 122, 132-134). Malheureusement, aucun traitement n'est disponible à ce jour pour soigner ces maladies notamment en raison du manque de connaissances au niveau moléculaire. Il est important de signaler qu'au cours des dernières années, certains cancers ont également été liés à des défauts dans les cils, notamment au niveau des voies de signalisation comme Sonic Hedgehog, mais les mécanismes moléculaire sont peu compris (116, 135-137).

La protéine néphrocystine 5 (NPHP5)

Structure

NPHP5 est une protéine centrosomale conservée chez la souris, le rat, le poulet et le poisson zèbre. Cette protéine est formée par quinze exons et contient deux domaines de liaison à la CALMODULINE (IQ) et un domaine coiled-coil putatif (CC) qui servirait à la liaison avec d'autres protéines (138, 139). NPHP5 a deux isoformes : la plus abondante et la plus longue de 598 acides aminés et une plus courte de seulement 465 acides aminés (139). Grâce à une analyse récente par spectrométrie de masse, il a été montré que NPHP5 possède également plusieurs sites de phosphorylation. Enfin, plus de quinze mutations causant des maladies ont été identifiées à ce jour. Il s'agit principalement de mutations hétérozygotes, homozygotes non-sens ou de mutations induisant un décalage du cadre de lecture lors de la traduction de l'ARN messager. Ces mutations provoquent deux types de ciliopathies : le syndrome de Senior Loken, avec des symptômes au niveau de la rétine et du rein, ou l'amaurose congénitale de Leber avec des symptômes rénaux seulement (138, 140-142). (Figure 8)

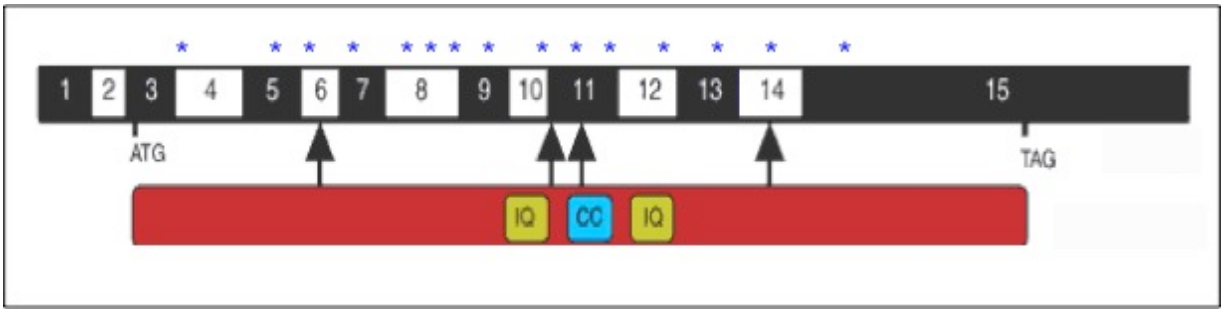

Adapté de Nat Genet. 2005 Mar;37(3):282-8

Figure 8 : Schéma représentatif de la structure de NPHP5.
Cette protéine est formée par quinze exons et contient deux domaines de liaison à la CALMODULINE (IQ) et un domaine coiled-coil putatif (CC).

Fonction

NPHP5 a été détectée, au niveau des centrosomes, comme partenaire de CEP290, une autre protéine centrosomale impliquée dans la ciliogénèse (143, 144). Elle peut aussi s'associer avec RPGR, une protéine mutée chez les patients atteints de rétinite pigmentaire, une autre ciliopathie (138, 145). NPHP5 se localise au niveau des cils dans les cellules rénales, des cils connecteurs dans les cellules photo-réceptrices de l'œil et des centrosomes dans les cellules du rein chez la souris. Il a été démontré également que NPHP5 est nécessaire à la ciliogénèse dans les cellules rénales. De façon intéressante, son ARN messager peut être surexprimé lors de cancer gastro-intestinal mais inhibé en cas de dommage à l'ADN (138, 139, 146). La déplétion de NPHP5 chez le poisson zèbre à l'aide de morpholinos anti-sens provoque la formation de kystes rénaux et des anomalies cérébrales. Ces symptômes sont semblables à ceux observés chez les patients humains (144). Toutefois, la localisation précise de NPHP5 ainsi que sa fonction au niveau du centrosome ou lors de la ciliogénèse restent inconnues à ce jour. À la vue de ces données, il est facile d'imaginer un rôle clé pour NPHP5 dans la formation, le maintien et/ou la fonction du cil. C'est pourquoi il est important de connaître les partenaires impliqués et d'élucider les mécanismes moléculaires auxquels NPHP5 pourrait participer pour potentiellement développer des atouts thérapeutiques contre les ciliopathies.

La protéine centrosomale de 290 kDa (CEP290)

Structure

CEP290, aussi appelée néphrocystine 6 (NPHP6), est une grosse protéine composée de 2479 acides aminés étendus sur 54 exons et ayant un poids moléculaire de 290 kDa.

Cette protéine a premièrement été identifiée lors du séquençage d'une bibliothèque d'ADN du cerveau avant d'être identifiée lors d'un crible protéomique de centrosomes issus de lymphoblastes humains (147, 148). CEP290 contient de nombreux domaines conservés au cours de l'évolution dont des motifs putatifs coiled-coil (CC), des motifs inductibles par protéine kinase ou encore un motif de localisation nucléaire. Ces nombreux domaines semblent impliquer CEP290 dans diverses fonctions au travers différents compartiments de la cellule. Toutefois, le rôle précis de ces nombreux domaines reste largement non élucidé (149). Jusqu'à maintenant, 112 mutations ont été identifiées comprenant des changements de cadre de lecture, des mutations non-sens ou encore des délétions. Ces mutations induisent une perte de fonction de la protéine et provoquent au moins cinq types de ciliopathies humaines avec une variabilité clinique importante : l'amaurose congénitale de Leber (LCA), la néphronophtise (NPHP), le syndrome de Joubert (JBTS), le syndrome de Bardet-Biedl (BBS) et le syndrome de Meckel-Gruber (MKS) (150, 151). En raison de son large spectre phénotypique, CEP290 a été proposé comme étant un ''master regulator'' de la ciliogénèse.

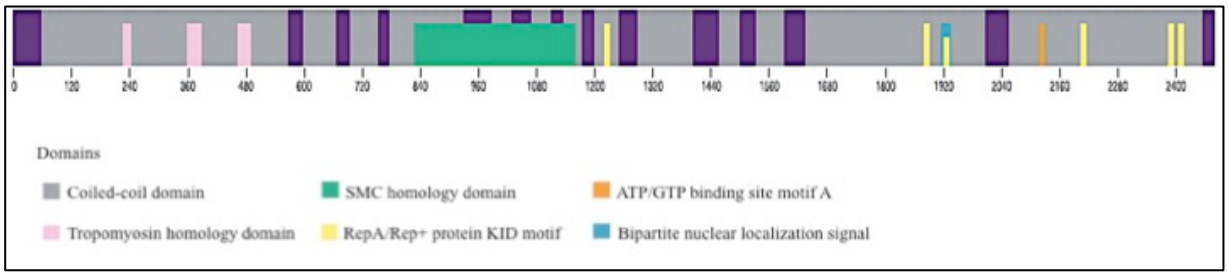

Adaptation de Human Mutation, Volume 31, Issue 10, pages 1097–1108, October 2010

Figure 9 : Schéma représentatif de la structure de Cep290.

Cette protéine est formée de 54 exons et contient de nombreux domaines distincts.

Fonction

La présence des nombreux domaines dans la protéine révèlerait des rôles multiples et variés de CEP290 dans les cellules. CEP290 est localisée principalement dans la partie distale des centrioles et au niveau de la matrice péricentriolaire (satellites) où elle participe à la ciliogénèse et à l'organisation du réseau de microtubules cytoplasmiques, respectivement (143, 147, 149, 152, 153). Au cours des dix dernières années, CEP290 a également été localisée au niveau du noyau où elle activerait des facteurs de transcription comme ATF4 (impliqué dans la formation de kystes rénaux) (143, 149, 152, 154-156).

L'inhibition de CEP290 par ARN interférence induit une baisse drastique du nombre de cellules formant des cils. D'autres protéines normalement situées dans les cils sont également délocalisées dans ces cellules. Les mêmes phénotypes ont été observés dans la rétine du modèle murin rd16 (retinal degeneration 16). Cette souris est caractérisée par une délétion de 298 acides aminés sans changement du cadre de lecture. Il a été observé une relocalisation de certaines protéines ciliaires du segment externe vers le segment interne des photorécepteurs de cette souris. Ces résultats soulignent un rôle important de CEP290 non seulement dans la ciliogénèse mais aussi dans le trafic ciliaire. Toutefois, il est à noter qu'aucun phénotype majeur extra-rétinal n'a été reporté chez cette souris, contrairement aux patients humains qui développent des anomalies dans divers organes dont le rein, le foie ou encore le cerveau en plus de la rétine (143, 157, 158).

Des expériences d'immuno-précipitations sur des extraits de rétines murines ont montrées que CEP290 forme des complexes avec diverses partenaires (centrine, Kif3A, sous unité p150 de la dynactine,…) impliqués dans le transport protéique sur les microtubules (152, 154). CEP290 interagit aussi avec les protéines centrosomales PCM-1 et CP110. Des études de déplétion de CEP290 dans des cellules humaines et chez le poisson zèbre ont montré une redistribution cellulaire de la protéine PCM-1, perturbant ainsi la stabilité du réseau cytoplasmique de microtubules. CEP290 est également importante pour la localisation ciliaire de Rab8; une petite GTPase régulée par le BBSome lors de la ciliogénèse (144, 149, 159-162).

Des études chez le chat Abyssin rdAc (substitution de nucléotide qui entraine un changement du cadre de lecture), dont une portion du C-terminal de CEP290 est manquante, ont montré une dégénération de la rétine avec accumulation de vésicules contenant la rhodopsine au niveau du segment interne du photorécepteur (163).

De plus, des expériences de déplétion par morpholinos chez le poisson zèbre *Dario rerio* entrainent des kystes rénaux, des défauts de la rétine et une hydrocéphalie entre autres. Toutefois, la longueur des cils n'est pas affectée. Le rôle de CEP290 dans ce phénotype pourrait donc être tissu dépendant (144, 149, 164).

Enfin, une perte de fonction de CEP290 chez l'algue *Chlamydomonas reinhardtii* entraine une perturbation de la longueur des cils mais aussi du contenu protéique (165).

CEP290 est importante pour la fonction des centrosomes et des cils. Cependant, les connaissances sur la corrélation entre les mutations de CEP290, sa fonction et les divers phénotypes des maladies sont limitées. Devant un tel éventail de manifestations cliniques, il est important d'étudier plus CEP290 et d'essayer de comprendre les mécanismes moléculaires sous-jacents à ses fonctions.

Le complexe du syndrome de Bardet-Biedl : le BBSome

Structure

Le syndrome de Bardet-Biedl est une ciliopathie autosomique récessive caractérisée par de l'obésité, de la dégénérescence rétinienne, des kystes rénaux, de la polydactylie, du retard mental ou encore de l'hypogénitalisme (166-170). À ce jour, dix neuf locus BBS ont été identifiés et chacun peut causer la maladie indépendamment des autres (171-173).

Huit de ces protéines (BBS1/2/4/5/7/8/9/18) forment le BBSome, un complexe protéique d'environ 438 kDa qui transporte les récepteurs de signalisation vers et depuis les cils (172, 174, 175). Les protéines BBS2/7/9 forment le cœur du complexe auquel sont ajoutées successivement les protéines BBS1/5/8 et enfin BBS4. De plus, les protéines BBS6/10/12 forment, avec la chaperonine ATP-dépendante TRiC/CCT, un complexe de chaperonnes nécessaire à l'assemblage correct du BBSome (175, 176). Les protéines du BBSome contiennent pour ça des domaines connus pour faciliter l'interaction protéique comme des hélices β ou des domaines coiled-coil.

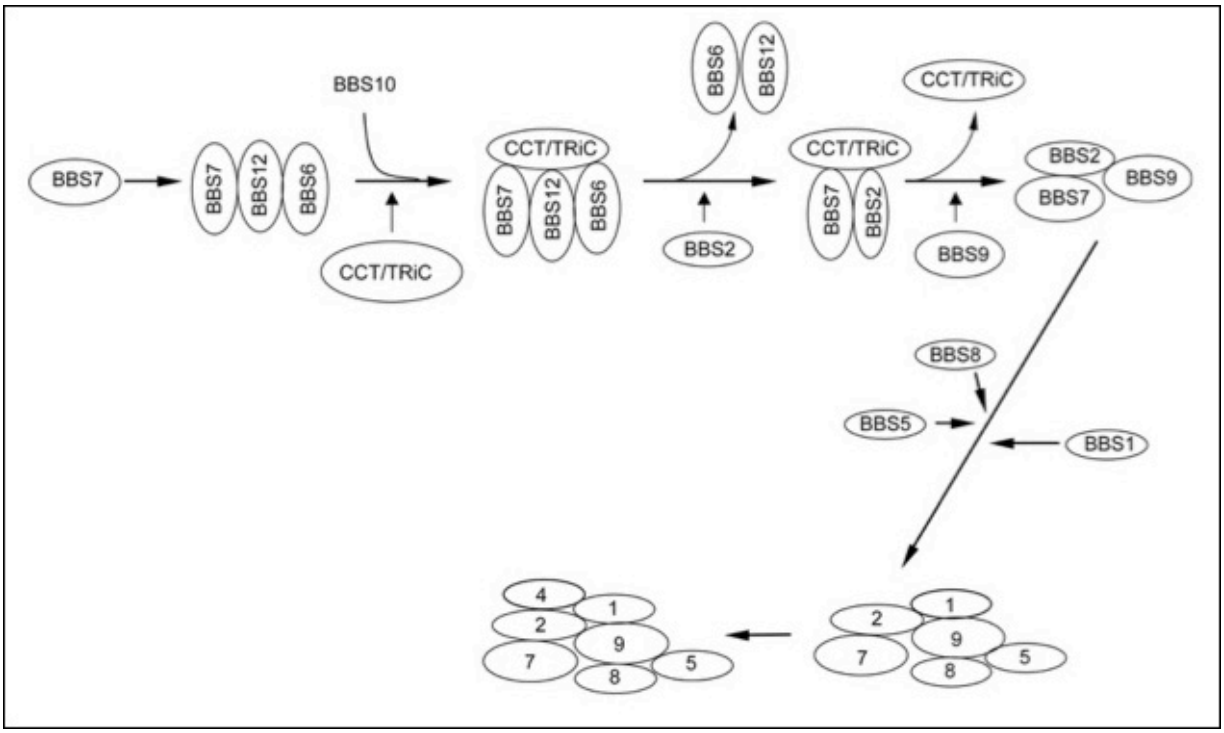

Adaptation de Qihong Zhang et al. J. Biol. Chem. 2012;287:20625-20635

Figure 10. Schéma représentatif de la formation séquentielle du BBSome.

Les protéines BBS2/7/9 forment le cœur du complexe auquel sont ajoutés successivement les protéines BBS1/5/8 et enfin BBS4 à l'aide des chaperonnes BBS6/10/12 et TRiC/CCT.

Fonction

Le BBSome est localisé au niveau des satellites péricentriolaires ainsi qu'au niveau des cils. Il est recruté au niveau du corps basal par la petite GTPase Rab8 et son partenaire Rabin8. Ce recrutement va également activer Rab8 et permettre la fusion des vésicules ciliaires proche de la membrane des cils. Pour être actif comme transporteur de protéines membranaires, le BBSome est alors recruté à la membrane ciliaire par la petite GTPase BBS3 qui va aider à son entrée dans l'organelle. Ces évènements sont essentiels à la ciliogénèse ainsi qu'au mouvement du BBSome dans le cil (174, 175, 177, 178). Le BBSome circule entre la base et l'extrémité du cil grâce aux complexes IFT et module également l'exportation de certaines protéines en dehors des cils. Parmi les protéines transportées par le BBSome, on retrouve plusieurs récepteurs impliqués dans diverses voies de signalisation comme les récepteurs couplés aux protéines G ou Smoothened, un récepteur de la voie Sonic hedgehod (178, 179).

Des études chez la souris et le poisson zèbre soutiennent un rôle du BBSome dans la ciliogénèse et le transport intraflagellaire. Une inhibition des gènes BBS par morpholinos chez le poisson zèbre entraine une perte progressive des cils ainsi qu'une perte de fonction des vésicules de Kupffer (transport rétrograde) (180). Chez les souris knock-out, une accumulation de diverses protéines de signalisation a été observée au niveau des cils, ce qui coïncide avec les expériences chez *C. elegans* et met en évidence des défauts dans les complexes IFT et le transport rétrograde dans les cils. Ces résultats ont également été observés dans les cellules en culture dont les protéines BBS ont été inhibées par ARN interférence (173, 181-189).

Des expériences chez *C. reinhardtii* montrent que plusieurs protéines de signalisation associées à la membrane sont accumulées dans les cils en cas de perturbation du BBSome. Toutefois, cette accumulation serait due à des défauts d'exportation via le BBSome et non à la perturbation des complexes IFT (190, 191).

En raison de la pléiotropie de la maladie, de nombreuses caractéristiques cliniques du syndrome de Bardet-Biedl sont communes à d'autres maladies, ce qui amène souvent à un diagnostic incertain. Il est donc important d'étudier les protéines impliquées dans ce syndrome ainsi que leurs partenaires afin de mieux comprendre les mécanismes moléculaires propres à cette maladie et éventuellement développer des thérapies ciblées.

La protéine centrosomale de 76 kDa (CEP76)

Structure

CEP76 a été identifiée pour la première fois comme protéine centrosomale lors d'une analyse des centrosomes par spectrométrie de masse (147). CEP76 semble être conservée des mammifères au poisson zèbre et au xénope mais aucun homologue n'a été clairement identifié à ce jour chez la drosophile ou la levure (93).

Cette protéine contient un motif WD-40 partiel ; motif connu pour être impliqué dans les interactions entre protéines, ainsi qu'un domaine de liaison au calcium et aux lipides (domaine CaLB)(93). De plus, la structure primaire de CEP76 contient plusieurs sites putatifs de liaison aux cyclines (RXL) et de phosphorylation par les CDKs (SP/TP) suggérant de possibles modifications post-traductionnelles. Récemment, un domaine similaire au transglutaminase (TGL) inactif a été découvert pour CEP76. Ce motif pourrait être essentiel à la liaison de peptides ainsi qu'au contrôle des interactions protéiques durant la ciliogénèse (192). Toutefois, aucune recherche supplémentaire n'a été faite à ce jour pour comprendre la signification de ces différents domaines.

Fonction

CEP76 a été détectée comme partenaire de CP110, un substrat de CDK2 qui régule positivement la duplication des centrosomes, et CEP97, un stabilisateur de CP110 (93, 96). Les niveaux protéiques de CEP76 varient selon les phases du cycle cellulaire : l'expression est faible en quiescence, augmente légèrement en phase G1 et atteint son maximum dans les phases S et G2, soit juste après le début de la duplication des centrioles. Au moment d'entrer en mitose, l'expression de CEP76 diminue de nouveau (93). Cette fluctuation est similaire à celle de l'activité des complexes CDK2-CYCLINEA et CDK2-CYCLINE, comme décrit précédemment.

Lors de travaux précédents, il a été démontré que la déplétion de CEP76 par ARN interférence provoque l'accumulation de structures centriolaires dans certaines lignées cellulaires cancéreuses. Cette accumulation serait due à plusieurs cycles de duplication des centrioles et est dépendante de la présence de CP110 et CEP97 aux centrosomes.(93) De manière intéressante, ces structures intermédiaires sont composées de protéines centriolaires uniquement car la matrice péricentriolaire n'est pas affectée par la déplétion de CEP76. De plus, l'amplification des centrioles causée par un traitement avec hydroxyurée (HU) peut être inhibée si CEP76 est surexprimée dans les cellules. À noter que ce traitement n'affecte pas les niveaux protéiques de CEP76 et que cette surexpression n'empêche pas la duplication normale des centrioles (93).

Ces résultats suggèrent que CEP76 serait impliquée dans la régulation de la duplication des centrioles. CEP76 limiterait ce processus à une fois par cycle cellulaire en veillant à ce que de multiples rondes de duplication ne soient pas possibles. Toutefois, la fonction précise de CEP76 reste toujours inconnue, c'est pourquoi il est important de connaître les partenaires impliqués et d'élucider ces mécanismes moléculaires qui limitent la duplication des centrioles à une fois par cycle cellulaire.

Mise en contexte

Les centrosomes et les cils sont des organelles complexes essentielles pour un large éventail de processus comme l'embryogénèse et le développement, la polarité, la mobilité, la division cellulaire ou encore la sensation de signaux. Au cours des dernières années, des efforts ont été réalisés pour approfondir les recherches sur les centrosomes et les cils. De nombreuses nouvelles protéines ont donc été découvertes, mais peu sont à ce jour étudiées en détail.

De nombreuses maladies humaines telles que les cancers ou les ciliopathies comme le syndrome de Bardet Biedl sont dues à un mauvais fonctionnement des centrosomes et des cils. Précédemment, il a été montré qu'une protéine déficiente dans diverses ciliopathies humaines, Cep290, est une protéine centrosomale exigée pour la formation de cils (160). La caractérisation de protéines associées à Cep290 est donc importante pour comprendre son rôle dans la ciliogénèse et le développement de maladies. Plusieurs preuves suggèrent qu'une nouvelle protéine, NPHP5, ait des liens fonctionnels avec Cep290, bien que l'on ne connaisse pas la fonction précise de NPHP5 (143, 144). Notre hypothèse est que NPHP5 promeut la formation de cils avec Cep290 et que son dysfonctionnement contribue au développement de ciliopathies

La duplication des centrosomes est finement régulée et des dérégulations sont souvent impliquées dans l'instabilité génomique et l'aneuploïdie, deux marques du cancer. Les mécanismes qui régulent la duplication des centrosomes sont peu connus. Récemment, une nouvelle protéine centrosomale, Cep76, a été liée à ce processus. La déplétion de Cep76 entraine une sur-duplication des centrioles tandis que sa surexpression supprime ce phénomène après arrêt en phase S par traitement à l'hydroxyurée. Cependant, le mécanisme par lequel Cep76 agit reste peu connu (93).

L'objectif général de cette thèse était de mieux caractériser ces protéines centrosomales, leurs rôles dans la régulation de processus cellulaires majeurs et leurs implications dans les maladies humaines. Les objectifs particuliers étaient :

1- Caractériser la protéine centrosomale NPHP5 et son rôle dans la ciliogénèse : quels sont sa localisation, sa fonction et ses partenaires potentiels ? (article 1).

2- Étudier la fonction spécifique de NPHP5 et son partenaire Cep290 dans la régulation du BBSome : sont-elles impliquées dans l'assemblage et le maintien du complexe et dans le trafic ciliaire ? (article 2).

3- Caractériser le rôle spécifique de la protéine Cep76 dans la régulation du cycle des centrosomes : par quel(s) mécanisme(s) Cep76 contrôle la duplication des centrioles en phase S à raison d'une fois par cycle cellulaire? (article 3).

Article 1 : Pathogenic NPHP5 mutations impair protein interaction with Cep290, a prerequisite for ciliogenesis

Marine Barbelanne[1,2], Jenny Song[1], Mustafa Ahmadzai[1] and William Y. Tsang[1,2,3,*]

[1] Institut de recherches cliniques de Montréal, 110 avenue des Pins Ouest, Montréal, Québec H2W 1R7, Canada

[2] Faculté de Médecine, Université de Montréal, Montréal, Québec H3C 3J7, Canada

[3] Division of Experimental Medicine, McGill University, Montréal, Québec H3A 1A3, Canada

Article publié dans Human Molecular Genetics, 2013 June 15; 22(12): 2482–2494

Contributions de M.B. : Toutes les expériences sauf clonage et WB des figures 2B, 3B (en partie) et 6B. Créations de toutes les figures/tables et participation dans l'interprétation des résultats et l'écriture du manuscript.

Abstract

Mutations in the human *NPHP5* gene cause retinal and renal disease but the precise mechanisms by which NPHP5 functions are not understood. We report that NPHP5 is a centriolar protein whose depletion inhibits an early step of ciliogenesis, a phenotype reminiscent of Cep290 loss and contrary to IFT88 loss. Functional dissection of NPHP5 interactions with Cep290 and CaM reveals a requirement of the former for ciliogenesis, while the latter prevents NPHP5 self-aggregation. Disease-causing mutations lead to truncated products unable to bind Cep290 and localize to centrosomes, thereby compromising cilia formation. In contrast, a modifier mutation cripples CaM-binding but has no overt effect on ciliogenesis. Drugs that antagonize negative regulators of the ciliogenic pathway can rescue ciliogenesis in cells depleted of NPHP5, with response profiles similar to those of Cep290- but not IFT88-depleted cells. Our results uncover the underlying molecular basis of disease and provide novel insights into mitigating NPHP5 deficiency.

Introduction

Located in close proximity to the nucleus as a non-membrane bound organelle, the centrosome is the principal microtubule-organizing center critical for cell division in most eukaryotic cells (1, 2). A single centrosome, consisting of a pair of centrioles (termed the mother and daughter centrioles) surrounded by a pericentriolar matrix duplicates in S phase. The duplicated centrosomes migrate to opposite poles of a cell and establish the mitotic spindle at the onset of mitosis, ensuring faithful segregation of chromosomes into daughter cells. Upon cell cycle exit, centrosomes in many cell types template the formation of primary cilia, cellular antennae that sense a wide variety of signals important for growth, development and differentiation (3). Cilia biogenesis or ciliogenesis can be arbitrarily divided into discrete steps (4, 5). First, membrane vesicles carrying protein and lipid cargos are formed at, and recruited to, the distal end of the mother centriole. The centrosome then migrates to the cell cortex, wherein the mother centriole, now transformed into a basal body, attaches itself to the cell membrane and nucleates the formation of an axoneme, the skeleton of a cilium. Docking and fusion of membrane vesicles with the cell membrane also occur simultaneously. The final step of ciliogenesis, intraflagellar transport (IFT) mediates bi-directional transport of cargos and is necessary for cilia biogenesis, function and maintenance. Defects in ciliogenesis can give rise to a bewildering array of human ciliary diseases collectively known as ciliopathies (6, 7). Ciliopathies are pleiotropic and exhibit variable clinical manifestations such as kidney cyst formation, hepatic dysfunction, retinal degeneration and neurological disorders.

Although mutations in a number of genes encoding centrosomal and ciliary components are responsible for nearly all ciliopathy cases, the etiology and molecular basis of these diseases remain incompletely understood.

We and others have previously characterized one centrosomal protein, Cep290, whose deficiency is implicated in ciliopathies including Leber congenital amaurosis (LCA; an inherited eye disease characterized by severe loss of vision), Senior-Løken syndrome (SLS; an inherited disorder associated with retinal (severe loss of vision) and renal failure (kidney cyst formation and end-stage renal disease)), nephronophthisis, Joubert syndrome, Bardet-Biedl syndrome and Meckel-Gruber syndrome (8-10). Cep290 participates in primary cilia formation and functions at an early step of the ciliogenic pathway, affecting centrosomal migration and/or anchoring to the cell cortex (11-13). Interestingly, it biochemically interacts with a multitude of proteins, including CP110, a centrosomal protein known to suppress ciliogenesis (12, 14). Identification and characterization of key proteins that associate with Cep290 would greatly enhance our understanding of its roles in ciliogenesis and disease development.

Converging evidence suggests that Cep290 has functional connections with a partially characterized centrosomal/ciliary protein called nephrocystin-5 (NPHP5). First, patients with *NPHP5* mutations exhibit clinical phenotypes that overlap with patients bearing *Cep290* mutations. *NPHP5* mutations constitute a frequent cause of SLS (15, 16). Certain mutations of *NPHP5*, in addition to several SLS-causing mutations, are also detected in patients with LCA, although these patients are believed to be at high risk of developing late-onset renal failure (17, 18).

Second, Cep290 is shown to interact with NPHP5 under certain circumstances and therefore the significance of this interaction remains controversial (19-21). Third, ablation of NPHP5 with anti-sense morpholinos in zebrafish leads to the formation of pronephric cysts and phenocopies Cep290 depletion (19). NPHP5 is highly conserved in higher eukaryotes and possesses a putative coiled-coil and IQ calmodulin (CaM)-binding motifs of unknown function (15, 22). Here, we show that NPHP5 localizes to the distal region of centrioles during interphase and is specifically required for early cilia assembly, a function similar to Cep290 but different from IFT88, a protein participating in IFT at a later step of ciliogenesis. Endogenous NPHP5 interacts with Cep290 and CaM, and detailed domain-mapping studies on NPHP5 reveal three separable and functionally distinct domains, namely, the Cep290-binding domain, the CaM-binding domain and the centrosomal localization domain which encompasses the coiled-coil motif. NPHP5 interaction with Cep290 is strictly required for ciliogenesis, while the association between NPHP5 and CaM is needed to prevent NPHP5 self-aggregation. Pathogenic *NPHP5* mutations known to cause SLS and LCA result in the production of truncated products that are incompetent to bind Cep290 and are mis-localized, thus compromising cilia formation. On the contrary, a *NPHP5* modifier mutation associated with patients with severe retinitis pigmentosa caused by X-linked retinitis pigmentosa GTP regulator (RPGR) deficiency specifically impairs CaM-binding and has no adverse effect on cilia biogenesis. Loss of cilia in the absence of NPHP5 can be rescued by pharmacologically inhibiting negative regulators of ciliogenesis downstream of NPHP5. Interestingly, the response profiles of NPHP5-depleted cells towards different drugs are comparable to those of Cep290- but not IFT88-depleted cells, further suggesting that NPHP5 and Cep290 participate in a common step of the ciliogenic pathway.

Cilia formation in cells expressing disease-causing mutants of NPHP5 and treated with drugs can likewise be rescued. Thus, we have uncovered the functional significance of NPHP5 and its interactions with Cep290 and CaM, delineated the molecular mechanisms underlying the pathogenesis of NPHP5-assoicated ciliopathies, and revealed novel pharmacological approaches for treating NPHP5 deficiency.

Results

NPHP5 localizes to the distal region of centrioles and is present in interphase cells

Although NPHP5 is shown to localize to centrosomes and cilia (15, 21, 23), its localization during the cell cycle has not been fully investigated. We used immunofluorescence microscopy to detect NPHP5 localization in diploid human retinal pigment epithelial (RPE-1) cells. This cell line possesses normal centrosome morphology and number and is a well-established model for primary cilia formation. Antibodies against NPHP5 stained two and four prominent spots in G1 and S phase, respectively (Figure 1A). These spots became more diffused in G2 phase and subsequently disappeared in mitosis (Figure 1A). Identical staining patterns were obtained by the use of three antibodies raised against different regions of NPHP5 and also in U2OS cells (data not shown). NPHP5 staining overlapped substantially with that of centrin (Figures 1A and 1B), which is a canonical centriolar protein found at the distal lumen of centrioles.

Centrosomal localization of NPHP5 was not affected by treatment with nocodazole (Figure S1A), a microtubule de-polymerizing agent, suggesting that NPHP5 is an intrinsic component of centrosomes. In G0 phase, NPHP5 is present at both the mother centriole/basal body and the daughter centriole, but was never observed along the ciliary axoneme (Figure 1C). Notably, NPHP5 staining at the mother centriole/basal body marginally co-localizes with acetylated and polyglutamylated tubulins in the proximal region, but rather is localized to the distal end near the base of the cilium (Figure 1C).

To further confirm the localization of NPHP5 on centrioles, cells were co-stained with antibodies against NPHP5 and a panel of proximal (C-Nap1, Sas-6 and Flag-Plk4) and distal (CP110, Cep290, Cep164) centriolar markers. NPHP5 showed significant overlap with CP110, Cep290 and Cep164 foci but marginal overlap with dots of Flag-Plk4, C-Nap1 and Sas-6 (Figures 1B and 1D). Thus, our data strongly indicate that NPHP5 is a distal centriolar protein and that it could function during interphase.

NPHP5 depletion inhibits an early step of cilia formation

We examined the consequences of depleting NPHP5 using RNA interference (RNAi)-mediated gene silencing. We transfected either pools of four small interfering RNAs (siRNAs) or five individual siRNAs, and microscopically confirmed the near complete removal of NPHP5 (~90%) from centrosomes in RPE-1 cells (Figures 2A and S1B). Similar observations regarding the loss of NPHP5 signal were made in several non-ciliated (U2OS) and ciliated (ARPE-19 and HEK293) cell lines (Figure S1C), and with the use of three different antibodies against NPHP5 (Figure S1D).

To further confirm specificity, Western blot analysis revealed that NPHP5 antibodies recognized one specific band corresponding to a size of ~69kDa, and more importantly, protein levels were elevated in cells over-expressing Flag-NPHP5 and reduced by ~80% in NPHP5 siRNA-treated cells (Figure 2B). Of note, although endogenous NPHP5 was readily detected in HEK293 extracts, it was undetectable in lysates of RPE-1 and U2OS cells (Figure 2B), suggesting that this protein is of low abundance in the latter two cell lines. Next, we determined whether NPHP5 is needed for different aspects of centrosome function. Depletion of NPHP5 did not induce abnormal number of centrin or γ-tubulin foci (Figures S2A-B), abnormal separation of centrin foci (Figure S2C), aberrant mitotic figures (data not shown) or mitotic arrest (Figure S2D), and therefore had no significant impact on centriole/centrosome duplication, centriole/centrosome separation or mitotic division. Further flow cytometric analysis indicated that suppression of NPHP5 did not alter cell cycle progression (Figure S2E).

Given its connection with human ciliopathies, we tested a role for NPHP5 in the assembly of primary cilia. RPE-1 cells were transfected with control or NPHP5 siRNAs, uninduced or induced to quiescence, and stained for ciliary markers including glutamylated tubulin, acetylated tubulin, IFT88 and Gli2. The percentages of ciliated cells are different between proliferative and quiescent states, and hence it is critical to evaluate if NPHP5 perturbs cilia formation under both conditions. Interestingly, ablation of NPHP5 led to a dramatic two-fold reduction in the ability of cells to assemble cilia in cycling and quiescent cells (20% to 10% for cycling and 80% to 40% for quiescent cells; Figure 2C). Similar results were obtained with another retinal pigment epithelial cell line, ARPE-19 (data not shown), and these findings were consistent with a systematic analysis designed to unravel the roles of ciliary disease proteins in cells and tissues (21).

The failure to undergo ciliogenesis in NPHP5-depleted cells was not due to cell cycle defects (Figures S2D-E) or an inability of the cell to enter a quiescent state, as revealed by Ki67 staining (Figure 2D). Subsequently, we pinpointed the step(s) at which cilia formation is blocked. Loss of NPHP5 did not impinge on centrosomal accumulation of Rab11a-positive vesicles, suggesting that early vesicular trafficking events, including the formation of pericentrosomal preciliary compartment (24), are not affected (Figures S2F). In light of the *in vivo* interaction between NPHP5 and Cep290 (Figure 3A) and the role of Cep290 in the migration and/or anchoring of centrosomes to the cell cortex during early ciliogenesis, we examined the distance between centrosomes and nuclei in NPHP5-depleted RPE-1 cells. As a control, we performed identical experiments in cells depleted of IFT88, a protein dispensable for centrosome migration but required for a late step of ciliogenesis (25). Strikingly, ~60% of the centrosomes in quiescent control and IFT88-depleted cells were well separated from the nucleus and were localized close to the cell surface, in contrast to ~30% in NPHP5- and Cep290-depleted cells (Figure 2E). Taken together, depletion of NPHP5, like Cep290, disrupts the migration and/or anchoring of centrioles to the cell cortex and inhibits ciliogenesis.

NPHP5 interaction with Cep290 is critical for ciliogenesis

Despite circumstantial evidence that NPHP5 interacts with Cep290 (19-21), an endogenous interaction between the two proteins has not been demonstrated and its physiological relevance remains unclear. To determine whether endogenous proteins associate *in vivo*, we performed immunoprecipitations with NPHP5 and Cep290 antibodies.

NPHP5 and Cep290 were co-immunoprecipitated by NPHP5 antibodies, and reciprocal immunoprecipitations with Cep290 antibodies confirmed a robust physiological interaction (Figure 3A). Next, we generated a series of Flag-tagged Cep290 truncation mutants, performed anti-Flag immunoprecipitations and examined their ability to interact with NPHP5 in cell extracts. We found that the NPHP5-binding domain of Cep290 was mapped between residues 790-816 (Figures S3A-B), consistent with two previous studies showing a requirement of the N-terminal region for binding to NPHP5 (19, 21). In addition, domain-mapping experiments were performed to identify the region of NPHP5 responsible for its interaction with Cep290. A C-terminal region of NPHP5 interacted with Cep290, and further efforts to delete or mutate conserved residues within this region revealed that residues 509-529 and 549 were both critical for binding (Figures 3B-D). Notably, the Cep290- and calmodulin-binding domains of NPHP5 are separable, as mutants with impaired binding to Cep290 could still associate with CaM (Δ509-529 and A549K; Figures 3B and 3D), and vice versa (ΔIQ123; Figures 5A-B). Both domains are also distinct from the centrosomal localization domain which encompasses the coiled-coil motif (residues 340-371) and residue 547 (Δ340-371, Δ543-555 and A547K; Figures 3C-D, 4C and S4). Thus, we have successfully generated small deletions and single amino acid substitutions that specifically cripple Cep290-binding, CaM-binding or protein localization to the centrosome. Finally, Far-Western blot experiments revealed a direct association of NPHP5 with Cep290 (Figure S3C).

To delineate the biological significance of the NPHP5-Cep290 interaction, we performed reciprocal depletion of NPHP5 and Cep290 using RNAi. Ablation of NPHP5 has no effect on the levels or localization of Cep290. However, loss of Cep290 significantly disrupts NPHP5 centrosomal localization without affecting its protein levels (Figures 4A-B).

Although these observations led to the speculation that Cep290 recruits NPHP5 to the centrosome (21), we do not believe this is the case. We demonstrated from our large collection of NPHP5 mutants that four mutants proficient in Cep290-binding (Δ340-371, A547K, fragments 419-598 and 287-530) could not be targeted to the centrosome, and conversely, two mutants deficient in Cep290-binding (Δ509-529 and A549K) were properly targeted (Figures 3C-D, 4C and S4). These data argue against a role for Cep290 in recruiting NPHP5 to the centrosome and further reinforce the notion that the Cep290-binding and centrosomal localization domains of NPHP5 are separable.

We then carried out rescue experiments in which wild type or mutant NPHP5 was expressed in quiescent cells depleted of endogenous NPHP5. We note that, whereas wild type was able to rescue ciliogenesis, mis-localized mutants (Δ340-371, Δ543-555 and A547K) failed to do so irrespective of their Cep290-binding status (Figures 3D and 4D). Most remarkably, mutants that are localized to centrosomes but do not bind Cep290 (Δ509-529 and A549K) also failed to restore cilia formation (Figures 3D and 4D). These results establish a clear and important mechanistic link between NPHP5-binding to Cep290 and ciliogenesis.

NPHP5 interaction with CaM prevents self-aggregation

The foregoing results suggest that the distinct binding domains for Cep290 and CaM in NPHP5 could serve different biological functions. To begin characterizing the interaction between NPHP5 and CaM, we showed that the two proteins associated with each other in the presence or absence of calcium from extracts supplemented with calcium ($+Ca^{2+}$) or EGTA ($-Ca^{2+}$) (Figure S5A).

Further, both wild type and mutant CaM refractory to Ca^{2+}-binding (CaM1234) interacted equally well with NPHP5 (Figure S5B), and these results together confirmed a previous report that NPHP5 and CaM interact in a Ca^{2+}-dependent and Ca^{2+}-independent manner (22). Bacterially expressed NPHP5 robustly bound to purified CaM *in vitro*, strongly suggestive of a direct interaction (Figure S5C). The Calmodulin Target Database predicts the existence of three putative IQ motifs in NPHP5 (residues 300-328, 391-410 and 420-437 and denoted IQ1, IQ2 and IQ3, respectively; Figure 3C). Using a series of Flag-tagged NPHP5 truncation and deletion mutants wherein the IQ motifs were removed singly or in combination, we demonstrated that the first and second motifs, IQ1 and IQ2, were most critical for binding to CaM (Figures 3B-C, 5A-B). Complete loss of binding, however, was achieved only when all three IQ motifs were deleted (ΔIQ123; Figures 5A-B). Loss of CaM-binding does not compromise Cep290-binding (Figures 5A-B), strengthening an earlier point that the CaM- and Cep290-binding domains of NPHP5 are separable. In addition, we showed that recombinant GFP-NPHP5 and endogenous CaM co-immunoprecipitated with recombinant Flag-Cep290 (Figures S3A-B), and likewise, endogenous Cep290 and GFP-NPHP5 were detected in Flag-CaM immunoprecipitates (Figure S5B). Moreover, antibodies against NPHP5 and Cep290 co-precipitated endogenous CaM (Figure 3A). Taken together, these data indicate that IQ motifs of NPHP5 mediate CaM-binding and that NPHP5 forms a complex with Cep290 and CaM.

Next, we investigated the functional consequences of the NPHP5-CaM interaction. Unlike mutations that specifically cripple the centrosomal localization or the Cep290-binding domain, the CaM-binding mutant, ΔIQ123 still showed centrosomal targeting and was fully able to rescue cilia formation in NPHP5-depleted cells (Figures 5B-C and S5D).

Noticeably, we observed the formation of punctate foci or aggregates in the cytoplasm of mutant cells (Figure 5D and S5D). These cytoplasmic aggregates were devoid of centrosomal markers such as centrin, CP110, γ-tubulin and Cep290 (Figure S5D), suggesting that they do not recruit any centrosomal proteins to extra-centrosomal sites and therefore arise from self-assembly. In addition, aggregate formation is unlikely to be triggered by elevated levels of expression, since the levels of wild type and mutant proteins were comparable (Figure 5A). To further strengthen the correlation between impaired CaM-binding and aggregate formation, we found that removal of the first two IQ motifs (ΔIQ12) or a point mutation in the second IQ motif (I393N) of NPHP5 severely weakened mutant protein interaction with CaM and induced aggregate formation (to a lesser extent compared to ΔIQ123) without affecting protein localization to centrosomes, binding to Cep290, or ciliogenesis (Figures 5A-D and S5D; also see below). In summary, NPHP5 mutants deficient in CaM-binding are aggregation-prone and CaM may serve as a chaperone to protect the mis-folding and aggregation of NPHP5 through direct interaction.

Molecular and functional consequences of *NPHP5* disease mutations

The differential roles of NPHP5 interactions with Cep290 and CaM prompted us to investigate their relevance in human disease. The vast majority of the >15 pathogenic *NPHP5* mutations identified in SLS and LCA patients are compound heterozygous or homozygous non-sense and frameshift mutations. No apparent correlation exists between genotype and phenotype, and the same mutation can often cause LCA and SLS (15-18, 26-28). These mutations are located in the internal regions of the gene and predicted to encode truncated products lacking the C-terminal tail (Figure 6A; (15-18, 26-28)).

Since the C-terminal tail contains the centrosomal localization and Cep290-binding domains, loss of Cep290-binding and protein mis-localization could underlie the disease mechanism in patients carrying *NPHP5* mutations. We examined five *NPHP5* mutations (F142fsX146, R332X, R461X, R502X and H506fsX518) commonly found in disease patients, including two at the extreme 5' and 3' ends, and tested whether they affect protein expression, localization to centrosomes and interaction with Cep290 and CaM, and cilia formation in rescue experiments. R332X and R502X mutations are detected in patients with SLS and LCA, respectively, while F142fsX146, R461X and H506fsX518 mutations are associated with SLS and LCA (Figure 6A). These mutations resulted in shorter and faster-migrating proteins as expected, and their expression levels were relatively similar to full-length protein (Figure 6B). Interestingly, while two mutants, F142fsX146 and R332X failed to interact with CaM, all were incompetent in binding to Cep290 (Figures 6A and 6B), mis-localized (Figures 6C and S6A) and unable to rescue ciliogenesis (Figures 6D and S6B). Thus, disease-causing mutations of *NPHP5* render the resulting proteins non-functional.

In addition to its pathogenic role in SLS and LCA, *NPHP5* is reported to be a modifier gene for a different retinal disorder, namely, retinitis pigmentosa. In this case, a natural polymorphic variation in *NPHP5*, I393N, strongly associates with disease severity in patients with RPGR deficiency (29), suggesting that it may contribute to the development of disease symptoms. Remarkably, we found that I393N mutation induced only subtle molecular and cellular defects, including diminished protein binding to CaM and increased aggregate formation, but had no effect on protein localization to the centrosome and cilia formation (Figures 5A-D and S5D). These results contrast sharply with those of disease-causing mutations (Figure 6).

Pharmacological rescue of cilia formation in the absence of NPHP5

One prediction stemming from our studies is that since NPHP5 is a positive regulator at an early step of ciliogenesis, modulation of downstream events in the ciliogenic pathway could mitigate or correct the effects of NPHP5 deficiency and restore cilia formation. Several cellular processes, such as removal of a "cap" at the distal end of the mother centriole, focal adhesion disassembly, actin de-polymerization and membrane trafficking are known to be important for ciliogenesis (14, 24, 30, 31). These highly dynamic processes are controlled by a number of negative regulators, including CP110, focal adhesion kinase (FAK), actin-related protein 3 (ARP3) and secreted phospholipase A2 Group 3 (PLA2G3) (Figure 7A). In addition, X-lined inhibitor of apoptosis (XIAP) also inhibits cilia biogenesis, although its role in centrosome and cilium biology is virtually unknown (Figure 7A; (24)). Given that loss of these proteins facilitate ciliogenesis in cycling cells (14, 24, 30, 31), we tested whether their depletion or inhibition could rescue cilia formation in cells depleted of NPHP5. We first examined the consequences of knocking down NPHP5, CP110, or both by RNAi. Depletion of CP110 led to aberrant formation of cilia (Figure 7B), consistent with our previous observations (12, 14). However, ablation of both NPHP5 and CP110 suppressed the phenotype associated with CP110 depletion and mimicked NPHP5 ablation (Figure 7B), suggesting that CP110 inhibition cannot compensate for the loss of NPHP5. Next, we determined that treatment of control cells with drugs targeting FAK, actin, ARP3, PLA2G3 and XIAP resulted in a two-fold enhancement of cilia formation following dose optimization (Figures 7A and data not shown). Remarkably, certain drugs dramatically rescued the loss of cilia phenotype caused by depletion of NPHP5 (Figures 7C and S7A).

PF573228, Cytochalasin D and latruculin B, in particular, restored ciliogenesis to levels comparable to control, whereas FAK inhibitor 14, CK548 and embelin were the least potent (Figure 7C). Of note, drug response profiles of NPHP5-depleted cells were remarkably similar, if not identical, to those of Cep290-depleted cells (Figures 7C and S7A), further suggesting that NPHP5 and Cep290 depletion inhibit a common pathway in cilia assembly. The same set of drugs, however, elicited different responses in cells depleted of IFT88, with FAK Inhibitor 14, cytochalasin D, CK548 and embelin being the most potent in rescuing cilia formation (Figure 7C). PF573228 and latruculin B, in striking contrast, were practically ineffective in IFT88-depleted cells (Figure 7C). Finally, we performed experiments in which we depleted endogenous NPHP5, expressed disease-causing mutants of NPHP5 and subsequently treated cells with cytochalasin D, and found that cilia formation was drastically restored (Figure S7B). Considered together, our findings indicate that ciliary defects associated with deficiencies in NPHP5/Cep290 and IFT88 can be differentially rescued by pharmacological means.

Discussion

Ciliogenesis is a poorly understood dynamic process requiring precise coordination of multiple cellular events and proteins. Elucidating the molecular mechanisms through which these proteins function is crucial to understanding their roles in human ciliopathies. We and others have previously described Cep290, a human ciliary disease protein required for ciliogenesis (11-13).

Here, we characterize another ciliopathy protein, NPHP5, and show that the two proteins share a number of common characteristics. First, NPHP5 and Cep290 strictly function at an early step of ciliogenesis and participate in the migration and/or anchoring of centrosomes to the cell cortex. Second, NPHP5 interacts with Cep290 in a physiologically relevant setting and their direct association is necessary for ciliogenesis. Third, drugs that rescue the loss of cilia phenotype associated with NPHP5 depletion are also effective in rescuing the Cep290 depletion phenotype. Despite these similarities, it is also clear that the two proteins differ in several important aspects. Whereas NPHP5 is targeted to centrioles, Cep290 is known to localize to both centrioles and centriolar satellites (11, 20, 32, 33). Furthermore, loss of Cep290 disrupts the localization of a well-known satellite protein percentriolar material-1 (PCM-1) to satellites, a phenotype we did not observe upon NPHP5 depletion (data not shown). Several satellite proteins, including PCM-1, are essential for cilia biogenesis, underscoring the importance of these peculiar structures in cilium biology (34). In addition, the clinical spectrum of *Cep290* mutations is more diverse compared to that of *NPHP5* mutations, implying that Cep290 could possess additional biological roles and/or function in multiple cell and tissue types. Further studies will be needed to dissect the relative contribution of NPHP5 and Cep290 to ciliogenesis and ciliopathies.

Although we have identified critical functional domains in NPHP5, including the centrosomal localization domain, the molecular mechanisms through which NPHP5 is recruited to the centrosome remain unknown. In light of our findings with NPHP5 mutants and reciprocal depletion of NPHP5 and Cep290, we speculate that targeting of NPHP5 could entail an unidentified factor X.

This factor recognizes and binds to the centrosomal localization domain of NPHP5 and transports it to the centrosome. Once there, factor X transiently interacts with a docking platform containing Cep290 wherein it presents NPHP5 to Cep290. Experiments are currently underway to reveal the identity of factor X and to test the validity of our proposed recruitment mechanism.

It is clear from our studies that the differential roles of NPHP5 interactions with Cep290 and CaM have important clinical implications. Disease-causing mutations of *NPHP5* induce two crucial and universal defects, namely protein mis-localization and incompetence in binding Cep290, both of which interfere with cilia assembly. On the other hand, a *NPHP5* modifier mutation identified in patients with RPGR deficiency specifically cripples CaM-binding and causes NPHP5 self-aggregation. Although these aggregates do not appear to affect ciliogenesis, their presence might be detrimental in the long run or under certain pathophysiological conditions. Since it is known that protein aggregation can lead to an accumulation of amyloid fibrils (35), a hallmark of neurodegenerative disorders, it is plausible that NPHP5 aggregates could induce amyloidosis and contribute to the severity of retinitis pigmentosa, a degenerative eye disease. Future experiments aimed at unraveling how this modifier mutation might compromise protein function and/or induce cellular toxicity will greatly enhance our knowledge of disease pathogenesis.

The series of molecular and cellular events leading to cilia formation have not been elucidated. Our work strongly suggests that removal of CP110 “cap” from the distal end of the mother centriole precedes NPHP5-mediated migration and/or anchoring of centrosomes to the cell surface, and a similar relationship between CP110 and Cep290 has previously been documented (12).

On the other hand, PF573228 and latrunculin B dramatically rescue cilia formation in NPHP5- and Cep290- but not IFT88-depleted cells, and therefore, actin de-polymerization and focal adhesion disassembly might lie "downstream" of NPHP5 and Cep290 function. Both drugs are highly specific to their targets: latrunculin B is a membrane-permeable compound known to bind monomeric G-actin in the nanomolar range (IC_{50}=10 nM), while PF573228 (IC_{50}=4 nM) is one of the many potent inhibitors of FAK currently being evaluated for potential utility in cancer therapeutics (36, 37). Thus, one intriguing possibility is that NPHP5 and Cep290 directly or indirectly sequester G-actin and/or inactivate FAK, thereby promoting centrosome migration and/or anchoring to the cell cortex. It will be interesting to determine whether NPHP5 and Cep290 bind to monomeric actin and/or focal adhesion complex, as understanding these mechanisms will provide novel insights into the development of therapeutic strategies for ciliopathies.

Materials and Methods

Cell Culture and Plasmids

Human ARPE-19, U2OS, hTERT RPE-1 and HEK293 cells were grown in DMEM supplemented with 10% FBS at 37°C in a humidified 5% CO2 atmosphere. To generate Flag-tagged NPHP5 fusion proteins, human NPHP5 cDNA fragments encoding residues 1–598 (full-length or FL), 1-157, 168-414, 419-598, 96-279, 287-493, 287-506, 287-530, 287-554, 287-579, 287-598, 336-598 and 380-598 were amplified by PCR using Phusion High-Fidelity DNA Polymerase (New England Biolabs) and sub-cloned into mammalian expression vector

pCBF-Flag (gift from B. Dynlacht). The following NPHP5 deletions and point mutations (Δ340-371, Δ509-529, Δ543-555, A547K, K548A, A549K, K550A, Q551A, Δ300-328 (ΔIQ1), Δ391-410 (ΔIQ2), Δ420-437 (ΔIQ3), Δ300-328Δ391-410 (ΔIQ12), Δ300-328Δ420-437 (ΔIQ13), Δ391-410Δ420-437 (ΔIQ23), Δ300-328Δ391-410Δ420-437 (ΔIQ123), I393N, F142fsX146, R332X, R461X, R502X, H506fsX518) were introduced into full-length cDNA by employing a two-step PCR mutagenesis strategy and sub-cloned into pCBF-Flag. Human NPHP5 was also sub-cloned into mammalian vector pEGFP-C1 and bacterial expression vector pET23a (gift from J.F. Cote) to generate GFP-NPHP5 and NPHP5-His, respectively. To generate Flag-CaM and Flag-CaM1234, rat CaM and CaM1234 (gift from J. Adelman) were amplified by PCR and sub-cloned into mammalian vector pFlag-CMV5. To generate Flag-Cep290, Cep290 fragments encoding residues 696-790, 696-822, 696-896, 720-896, 746-896, 762-896, and 780-896 were amplified by PCR and subcloned into pCBF-Flag. All constructs were verified by DNA sequencing. Other Flag-Cep290 constructs were previously described (12). A plasmid DNA expressing Flag-Plk4 was obtained from K. Lee.

Antibodies

Antibodies used in this study included anti-CP110, anti-CEP290 (Bethyl Laboratories), anti-centrin (Millipore), anti-C-Nap-1, anti-Sas-6, anti-NPHP5, anti-Gli2, anti-Rab11a (all from Santa Cruz), anti-PCM-1 (gift from A. Merdes), anti-α-tubulin, anti-acetylated tubulin, anti-Flag, and anti-γ-tubulin (all from Sigma-Aldrich), anti-glutamylated tubulin GT335, anti-Cep170, anti-Ki67 (all from Invitrogen), anti-IFT88, anti-NPHP5 (ProteinTech), anti-Cep164 (gift from E. Nigg), anti-CaM and anti-NPHP5 (Abcam). To generate rabbit anti-NPHP5 antibodies, a glutathione-S-transferase (GST) fusion protein containing residues 1-131

(IRCM2) and 469-598 (IRCM1) of NPHP5 was expressed in *E. coli* and purified to homogeneity. Antibodies against NPHP5 were purified by affinity chromatography.

Immunoprecipitation, Immunoblotting, and Immunofluorescence Microscopy

Cells were lysed with buffer (50 mM HEPES/pH 7, 250 mM NaCl, 5 mM EDTA/pH 8, 0.1% NP-40, 1 mM DTT, 0.5 mM PMSF, 2 μg/ml leupeptin, 2 μg aprotinin, 10 mM NaF, 50 mM β-glycerophosphate and 10% glycerol) at 4°C for 30 min and extracted proteins were recovered in the supernatant after centrifugation at 16,000g. In experiments involving calcium, 2.5 mM CaCl2 (+Ca2+) or 5 mM EGTA (-Ca2+) was also added to the lysis buffer. After centrifugation, 2 mg of the resulting supernatant was incubated with an appropriate antibody at 4oC for 2 hours and collected using protein A Sepharose. The resin was washed with lysis buffer, and bound proteins were analyzed by SDS-PAGE and immunoblotting using appropriate primary antibodies and horseradish peroxidase (HRP)-conjugated secondary antibodies (VWR). Typically, 50–150 μg of lysate was loaded into the input (IN) lane. For mapping studies, Flag-tagged constructs alone or in combination with GFP-tagged constructs were transfected into HEK293 cells. Cells were harvested 48–72 hr after transfection. Anti-Flag M2 beads (Sigma-Aldrich) were used for immunoprecipitations. For indirect immunofluorescence, cells were grown on glass coverslips, fixed with cold methanol or 4% paraformaldehyde and permeabilized with 1% Triton X-100/PBS. Slides were blocked with 3% BSA in 0.1% Triton X-100/PBS prior to incubation with primary antibodies. Secondary antibodies used were Cy3-, Cy5- or Alexa488- conjugated donkey anti-mouse, anti-rat or anti-rabbit IgG (Jackson Immunolabs and Molecular Probes). Cells were then stained with DAPI, and slides were mounted, observed, and photographed using a Leitz DMRB (Leica)

microscope (100×, NA 1.3) equipped with a Retiga EXi cooled camera. For analysis of the distance between the centrosome and the nucleus, z-sections spaced by 0.2μm were taken using a DM6000 B (Leica) microscope (100×, NA 1.4) equipped with a Hamamatsu Orca-ER camera (model C-4742). The xyz coordinates of the centrosome and the center of the nucleus were determined using Volocity6 (PerkinElmer) and distance was calculated using the formula $d = \sqrt{(x_2-x_1)^2+(y_2-y_1)^2+(z_2-z_1)^2}$. When the distance between the centrosome and the nucleus was >7μm, the centrosome was considered to be migrated to the cell surface. A distance of <7μm signified no migration.

Pharmacological Studies

Cells were treated with varying concentrations of cytochalasin D, CK636, CK548 (Sigma), TPEN, CAY10590, OPC, latrunculin B (Cayman Chemical), embelin, PF573228 or FAK Inhibitor 14 (Tocris Bioscience) and incubated for 8h before fixation. For each drug, the concentration required to induce maximal ciliated cell numbers with minimal toxicity was determined and used in subsequent experiments. As a vehicle control, an equivalent amount of DMSO or ethanol was added, and neither has an effect on cilia formation.

RNA Interference

Synthetic siRNA oligonucleotides were purchased from Dharmacon. Transfection of siRNAs was performed using siImporter (Millipore) per manufacturer's instructions. The 21-nucleotide siRNA sequence for the nonspecific control (NS) and IFT88 were 5-AATTCTCCGAACGTGTCACGT-3' and 5'-CCGAAGCACTTAACACTTATT-3', respectively. The 21-nucleotide siRNA sequences for NPHP5 were: 5'-GAGCAGAATGTCCCTGTTA-3' (oligo 1), 5'-ACCCAAGGATCTTATCTAT-3' (oligo 2),

5’ GAGGCCATGTTGAACTTAT-3’ (oligo 3), 5’-CCAAATAGGATCTGCAGTC-5’ (oligo 4) and 5’-CCCTAAGAATTGACACAAA-3’ (oligo 5). siRNA oligo 2 was used to deplete endogenous NPHP5 unless otherwise stated. siRNA oligo 5, which targets the 3’UTR of NPHP5 mRNA, was used to deplete endogenous NPHP5 in cilia rescue experiments. The siRNAs for Cep290 and CP110 silencing were previously described (12).

Induction of Primary Cilia

RPE-1 or ARPE-19 cells transfected with siRNA were brought to quiescence by serum starvation for 48–72 hr. Cells were examined for well-established primary cilium markers such as acetylated tubulin, glutamylated tubulin, IFT88 or Gli2.

Cell Cycle Synchronization and *Fluorescence-Activated Cell Sorting* **Analysis**

Cells were fixed in 95% ethanol at 4^{o}C for at least 1 hr and were subsequently incubated with 0.1 mg/ml RNase A in PBS at 37^{o}C for 30 min. After centrifugation and removal of supernatant, cells were stained with 50 ug/ml propidium iodide at 4^{o}C for 30 min. Samples of 100,000 cells were analyzed with a FACScalibur flow cytometer and CellQuest and FlowJo cell cycle analysis software.

Far Western Blotting and *In Vitro* Binding Assay

For Far Western blotting, membrane was incubated in AC buffer (0.1 M NaCl, 20 mM Tris/pH 7.5, 1 mM EDTA/pH 8, 0.05% Tween 20, 3% milk, 1 mM DTT, 10% glycerol) containing 6 M guanidine-HCl for 30 min at 22^{o}C, followed by AC buffer with 3 M guanidine-HCl for 30 min. at 22^{o}C, AC buffer with 0.1 M guanidine-HCl for 30 min. at 4^{o}C, and AC buffer only for 1 hr at 4^{o}C. After blocking with 3% milk for 1 h at 22^{o}C, membrane

was incubated with purified GST-NPHP5(469-598) bait protein in binding buffer (0.1 M NaCl, 20 mM Tris/pH 7.5, 0.5 mM EDTA/pH 8, 0.1% Tween 20, 3% milk, 1mM DTT, 10% glycerol) overnight at 4^{o}C. Bait protein was detected by anti-GST conjugated to HRP (GenScript). For *in vitro* binding, bacterially purified NPHP5-His mixed with purified GST or calmodulin (Cedarlane) at 4^{o}C for 1h was incubated with HisPur cobalt resin (Thermo Scientific) at 4^{o}C for another hour. After extensive washing with equilibration buffer (50mM $NaPO_4$, 300mM NaCl, 10mM imidazole/pH 7.4), bound proteins were analyzed by SDS-PAGE and immunoblotting.

Statistical Analysis

The statistical significance of the difference between two means was determined by using a two-tailed Student's *t* test. Briefly, the means and standard deviations of two data sets were determined in order to generate a *t* value. The *t* value was used in conjunction with the degrees of freedom to obtain a *p* value. Differences were considered significant when $p<0.01$.

Acknowledgements

We thank all members of the Tsang laboratory for constructive advice. We thank N. Al-Bader and H. Ling for assistance with cloning and anti-NPHP5 antibody generation, respectively. We thank E. Nigg and A. Merdes for providing antibodies, and K. Lee, J. Adelman, J.F. Cote and B. Dynlacht for providing plasmids. W.Y.T. was a Canadian Institutes of Health Research New Investigator and a Fonds de recherche Santé Junior 1 Research Scholar. This work was supported by the Canadian Institutes of Health Research (IC1-111427 and MOP-115033 to W.Y.T.).

Conflict of Interest

The authors have no conflicts of interest to declare.

Addendum 1er article

Rôles de NPHP5 et CEP290 dans les organismes ciliés

NPHP5 est une protéine conservée chez les vertébrés avec de nombreux orthologues notamment chez la souris, le chien, ou le poisson zèbre. NPHP5 est localisée au niveau des centrosomes dans divers tissus dont le rein ou dans les cils des photorécepteurs de la rétine et elle interagit entre autre avec CEP290 (15, 19-21, 38). La déplétion de NPHP5 chez le poisson zèbre par morpholinos entraine la formation de kystes rénaux, la dégénérescence de la rétine et des anomalies cérébrales. Ces symptômes sont semblables à ceux observés chez les patients humains ayant des mutations dans NPHP5 (15-19). Il faut noter qu'à ce jour, aucun modèle de souris pour NPHP5 n'est disponible.

CEP290 est une protéine également très conservée au cours de l'évolution avec de nombreux orthologues. Chez *Chlamydomonas reinhardtii*, organisme unicellulaire, CEP290 est localisée au niveau de la zone de transition entre le corps basal du flagelle et l'axonème. Plus précisément, CEP290 se situe au niveau des connecteurs entre la membrane et les microtubules. Une perte de CEP290 entraine des défauts aux niveaux de ces connecteurs ainsi qu'un contenu anormal en protéines comme les complexes IFT dans le flagelle (39). Chez les vertébrés comme le poisson zèbre, la souris ou l'homme, CEP290 est localisée au niveau des centrosomes, des satellites péricentriolaires, des cils dans les photorécepteurs et dans les boutons dendritiques des neurones olfactifs. Une inhibition de CEP290 par ARN interférence, morpholinos ou mutations, entraine des phénotypes au niveau des reins, des rétines et du cerveau (12, 19, 20, 40). Les fonctions de CEP290 se sont donc complexifiées au cours de l'évolution tout en gardant la fonction initiale au niveau des cils. Les nouvelles fonctions de CEP290 peuvent s'expliquer par la localisation diversifiée de CEP290 chez les vertébrés ainsi qu'un nombre plus important de partenaires potentiels.

Études pharmacologiques

Pour les expériences pharmacologiques, nous avons utilisé dix drogues ciblant cinq protéines impliquées dans la ciliogénèse. FAK Inhibitor 14 et PF573228 (PF) sont deux inhibiteurs de la kinase d'adhésion focale (FAK). Ils inhibent l'autophosphorylation de FAK sur le résidu Tyr397, ce qui perturbe l'adhésion focale et bloque la migration cellulaire dépendante de l'intégrine sans bloquer la croissance cellulaire (41-43). Cytochalasine D (CytoD) et Latrunculine B (LatB) sont des inhibiteurs de la polymérisation de l'actine. CytoD se lie aux filaments d'actine et inhibe toute polymérisation ultérieure tandis que LatB empêche la formation de filament d'actine en séquestrant l'actine G dans la cellule (36, 44, 45). CK548 et CK636 agissent sur la protéine Arp3 (Actin-related protein 3) qui est impliquée dans la polymérisation de l'actine ramifiée (branched actin). CK548 s'insère dans le noyau hydrophobique de Arp3 ce qui entraine un changement de conformation et bloque la formation du complexe Arp2/3. CK636 se lie directement au complexe préformé Arp2/3 et inhibe sa capacité à polymériser l'actine (46-48). Oleyloxyethyl phosphorylcholine (OPC) et CAY10590 agissent sur la phospholipase sécrétée A2 (PLA_2). Ces drogues restaurent le trafic vésiculaire vers les cils ainsi que le recyclage des endosomes qui sont altérés par PLA_2 (49-51). Enfin, embelin et TPEN se lient et inhibent la protéine XIAP (X-linked inhibitor of apoptosis). XIAP est connue pour son rôle dans la régulation de l'apoptose mais récemment de nouvelles fonctions, notamment dans l'ubiquitination, ont été mises en évidence (52-56).

Lorsque NPHP5 ou CEP290 sont inhibées par ARN interférence, on observe une diminution drastique du nombre de cellules ciliées ainsi qu'un défaut de migration du centrosome. CytoD, LatB et PF sont les plus efficaces pour rétablir la formation des cils dans les deux cas. Ces drogues sont impliquées dans la stabilité du cytosquelette d'actine, le trafic vésiculaire et la migration cellulaire. Il est reconnu que le transport de protéines et la migration du centrosome vers la membrane cellulaire sont des étapes nécessaires à la ciliogénèse. On peut donc imaginer que ces évènements se situent en aval de l'action de NPHP5 et CEP290 et qu'une modulation des protéines impliquées permet de sauver la formation des cils si NPHP5 et CEP290 sont inhibées.

Prenant en compte la localisation de ces deux protéines, on peut penser qu'elles sont impliquées dans la modulation du cytosquelette d'actine et le transport protéique lorsque les cellules entrent en quiescence. Cela confirme aussi que NPHP5 et CEP290 seraient impliquées dans la même voie de signalisation et ce à une étape précoce de la ciliogénèse.

Lorsque IFT88 est inhibée, la formation des cils est affectée mais pas la migration du centrosome. De manière intéressante, CytoD, CK548 et l'inhibiteur de FAK sont les plus efficaces pour rétablir la ciliogénèse. Ces drogues sont elles aussi impliquées dans la formation/stabilité du cytosquelette d'actine dont l'actine ramifiée, le trafic de protéines et la migration cellulaire. Ces résultats sont consistant avec les fonctions connues de IFT88. En effet, IFT88 est une protéine impliquée dans le transport de cargos dans les cils ainsi que la stabilité des microtubules au niveau des centrosomes (57-59).

References

1 Brito, D.A., Gouveia, S.M. and Bettencourt-Dias, M. (2012) Deconstructing the centriole: structure and number control. *Current opinion in cell biology*, **24**, 4-13.

2 Nigg, E.A. and Stearns, T. (2011) The centrosome cycle: Centriole biogenesis, duplication and inherent asymmetries. *Nat Cell Biol*, **13**, 1154-1160.

3 Ishikawa, H. and Marshall, W.F. (2011) Ciliogenesis: building the cell's antenna. *Nat Rev Mol Cell Biol*, **12**, 222-234.

4 Avasthi, P. and Marshall, W.F. (2012) Stages of ciliogenesis and regulation of ciliary length. *Differentiation*, **83**, S30-42.

5 Pedersen, L.B., Veland, I.R., Schroder, J.M. and Christensen, S.T. (2008) Assembly of primary cilia. *Developmental dynamics : an official publication of the American Association of Anatomists*, **237**, 1993-2006.

6 Hildebrandt, F., Benzing, T. and Katsanis, N. (2011) Ciliopathies. *N Engl J Med*, **364**, 1533-1543.

7 Bettencourt-Dias, M., Hildebrandt, F., Pellman, D., Woods, G. and Godinho, S.A. (2011) Centrosomes and cilia in human disease. *Trends Genet*, **27**, 307-315.

8 Sayer, J.A., Otto, E.A., O'Toole, J.F., Nurnberg, G., Kennedy, M.A., Becker, C., Hennies, H.C., Helou, J., Attanasio, M., Fausett, B.V. *et al.* (2006) The centrosomal protein nephrocystin-6 is mutated in Joubert syndrome and activates transcription factor ATF4. *Nat Genet*, **38**, 674-681.

9 Coppieters, F., Lefever, S., Leroy, B.P. and De Baere, E. (2010) CEP290, a gene with many faces: mutation overview and presentation of CEP290base. *Hum Mutat*, **31**, 1097-1108.

10 Valente, E.M., Silhavy, J.L., Brancati, F., Barrano, G., Krishnaswami, S.R., Castori, M., Lancaster, M.A., Boltshauser, E., Boccone, L., Al-Gazali, L. *et al.* (2006) Mutations in

CEP290, which encodes a centrosomal protein, cause pleiotropic forms of Joubert syndrome. *Nat Genet*, **38**, 623-625.
11 Kim, J., Krishnaswami, S.R. and Gleeson, J.G. (2008) CEP290 interacts with the centriolar satellite component PCM-1 and is required for Rab8 localization to the primary cilium. *Human molecular genetics*, **17**, 3796-3805.
12 Tsang, W.Y., Bossard, C., Khanna, H., Peranen, J., Swaroop, A., Malhotra, V. and Dynlacht, B.D. (2008) CP110 suppresses primary cilia formation through its interaction with CEP290, a protein deficient in human ciliary disease. *Dev Cell*, **15**, 187-197.
13 Graser, S., Stierhof, Y.D., Lavoie, S.B., Gassner, O.S., Lamla, S., Le Clech, M. and Nigg, E.A. (2007) Cep164, a novel centriole appendage protein required for primary cilium formation. *J Cell Biol*, **179**, 321-330.
14 Spektor, A., Tsang, W.Y., Khoo, D. and Dynlacht, B.D. (2007) Cep97 and CP110 suppress a cilia assembly program. *Cell*, **130**, 678-690.
15 Otto, E.A., Loeys, B., Khanna, H., Hellemans, J., Sudbrak, R., Fan, S., Muerb, U., O'Toole, J.F., Helou, J., Attanasio, M. *et al.* (2005) Nephrocystin-5, a ciliary IQ domain protein, is mutated in Senior-Loken syndrome and interacts with RPGR and calmodulin. *Nature genetics*, **37**, 282-288.
16 Otto, E.A., Helou, J., Allen, S.J., O'Toole, J.F., Wise, E.L., Ashraf, S., Attanasio, M., Zhou, W., Wolf, M.T. and Hildebrandt, F. (2008) Mutation analysis in nephronophthisis using a combined approach of homozygosity mapping, CEL I endonuclease cleavage, and direct sequencing. *Human mutation*, **29**, 418-426.
17 Stone, E.M., Cideciyan, A.V., Aleman, T.S., Scheetz, T.E., Sumaroka, A., Ehlinger, M.A., Schwartz, S.B., Fishman, G.A., Traboulsi, E.I., Lam, B.L. *et al.* (2011) Variations in NPHP5 in patients with nonsyndromic leber congenital amaurosis and Senior-Loken syndrome. *Arch Ophthalmol*, **129**, 81-87.
18 Estrada-Cuzcano, A., Koenekoop, R.K., Coppieters, F., Kohl, S., Lopez, I., Collin, R.W., De Baere, E.B., Roeleveld, D., Marek, J., Bernd, A. *et al.* (2011) IQCB1 mutations in patients with leber congenital amaurosis. *Invest Ophthalmol Vis Sci*, **52**, 834-839.
19 Schafer, T., Putz, M., Lienkamp, S., Ganner, A., Bergbreiter, A., Ramachandran, H., Gieloff, V., Gerner, M., Mattonet, C., Czarnecki, P.G. *et al.* (2008) Genetic and physical interaction between the NPHP5 and NPHP6 gene products. *Hum Mol Genet*, **17**, 3655-3662.
20 Chang, B., Khanna, H., Hawes, N., Jimeno, D., He, S., Lillo, C., Parapuram, S.K., Cheng, H., Scott, A., Hurd, R.E. *et al.* (2006) In-frame deletion in a novel centrosomal/ciliary protein CEP290/NPHP6 perturbs its interaction with RPGR and results in early-onset retinal degeneration in the rd16 mouse. *Hum Mol Genet*, **15**, 1847-1857.
21 Sang, L., Miller, J.J., Corbit, K.C., Giles, R.H., Brauer, M.J., Otto, E.A., Baye, L.M., Wen, X., Scales, S.J., Kwong, M. *et al.* (2011) Mapping the NPHP-JBTS-MKS protein network reveals ciliopathy disease genes and pathways. *Cell*, **145**, 513-528.
22 Luo, X., He, Q., Huang, Y. and Sheikh, M.S. (2005) Cloning and characterization of a p53 and DNA damage down-regulated gene PIQ that codes for a novel calmodulin-binding IQ motif protein and is up-regulated in gastrointestinal cancers. *Cancer research*, **65**, 10725-10733.
23 Otto, E.A., Hurd, T.W., Airik, R., Chaki, M., Zhou, W., Stoetzel, C., Patil, S.B., Levy, S., Ghosh, A.K., Murga-Zamalloa, C.A. *et al.* (2010) Candidate exome capture identifies mutation of SDCCAG8 as the cause of a retinal-renal ciliopathy. *Nat Genet*, **42**, 840-850.

24 Kim, J., Lee, J.E., Heynen-Genel, S., Suyama, E., Ono, K., Lee, K., Ideker, T., Aza-Blanc, P. and Gleeson, J.G. (2010) Functional genomic screen for modulators of ciliogenesis and cilium length. *Nature*, **464**, 1048-1051.
25 Dawe, H.R., Smith, U.M., Cullinane, A.R., Gerrelli, D., Cox, P., Badano, J.L., Blair-Reid, S., Sriram, N., Katsanis, N., Attie-Bitach, T. *et al.* (2007) The Meckel-Gruber Syndrome proteins MKS1 and meckelin interact and are required for primary cilium formation. *Human molecular genetics*, **16**, 173-186.
26 Chaki, M., Hoefele, J., Allen, S.J., Ramaswami, G., Janssen, S., Bergmann, C., Heckenlively, J.R., Otto, E.A. and Hildebrandt, F. (2011) Genotype-phenotype correlation in 440 patients with NPHP-related ciliopathies. *Kidney Int*, **80**, 1239-1245.
27 Wang, X., Wang, H., Cao, M., Li, Z., Chen, X., Patenia, C., Gore, A., Abboud, E.B., Al-Rajhi, A.A., Lewis, R.A. *et al.* (2011) Whole-exome sequencing identifies ALMS1, IQCB1, CNGA3, and MYO7A mutations in patients with Leber congenital amaurosis. *Hum Mutat*, **32**, 1450-1459.
28 Otto, E.A., Ramaswami, G., Janssen, S., Chaki, M., Allen, S.J., Zhou, W., Airik, R., Hurd, T.W., Ghosh, A.K., Wolf, M.T. *et al.* (2011) Mutation analysis of 18 nephronophthisis associated ciliopathy disease genes using a DNA pooling and next generation sequencing strategy. *J Med Genet*, **48**, 105-116.
29 Fahim, A.T., Bowne, S.J., Sullivan, L.S., Webb, K.D., Williams, J.T., Wheaton, D.K., Birch, D.G. and Daiger, S.P. (2011) Allelic heterogeneity and genetic modifier loci contribute to clinical variation in males with X-linked retinitis pigmentosa due to RPGR mutations. *PLoS One*, **6**, e23021.
30 Kobayashi, T., Tsang, W.Y., Li, J., Lane, W. and Dynlacht, B.D. (2011) Centriolar kinesin Kif24 interacts with CP110 to remodel microtubules and regulate ciliogenesis. *Cell*, **145**, 914-925.
31 Gakovic, M., Shu, X., Kasioulis, I., Carpanini, S., Moraga, I. and Wright, A.F. (2011) The role of RPGR in cilia formation and actin stability. *Hum Mol Genet*, **20**, 4840-4850.
32 Stowe, T.R., Wilkinson, C.J., Iqbal, A. and Stearns, T. (2012) The centriolar satellite proteins Cep72 and Cep290 interact and are required for recruitment of BBS proteins to the cilium. *Molecular biology of the cell*, **23**, 3322-3335.
33 Lopes, C.A., Prosser, S.L., Romio, L., Hirst, R.A., O'Callaghan, C., Woolf, A.S. and Fry, A.M. (2011) Centriolar satellites are assembly points for proteins implicated in human ciliopathies, including oral-facial-digital syndrome 1. *J Cell Sci*, **124**, 600-612.
34 Singla, V., Romaguera-Ros, M., Garcia-Verdugo, J.M. and Reiter, J.F. (2010) Ofd1, a human disease gene, regulates the length and distal structure of centrioles. *Dev Cell*, **18**, 410-424.
35 Hard, T. and Lendel, C. (2012) Inhibition of amyloid formation. *J Mol Biol*, **421**, 441-465.
36 Wakatsuki, T., Schwab, B., Thompson, N.C. and Elson, E.L. (2001) Effects of cytochalasin D and latrunculin B on mechanical properties of cells. *Journal of cell science*, **114**, 1025-1036.
37 Schultze, A. and Fiedler, W. (2010) Therapeutic potential and limitations of new FAK inhibitors in the treatment of cancer. *Expert Opin Investig Drugs*, **19**, 777-788.
38 Guyon, R., Pearce-Kelling, S.E., Zeiss, C.J., Acland, G.M. and Aguirre, G.D. (2007) Analysis of six candidate genes as potential modifiers of disease expression in canine XLPRA1, a model for human X-linked retinitis pigmentosa 3. *Mol Vis*, **13**, 1094-1105.

39 Craige, B., Tsao, C.C., Diener, D.R., Hou, Y., Lechtreck, K.F., Rosenbaum, J.L. and Witman, G.B. (2010) CEP290 tethers flagellar transition zone microtubules to the membrane and regulates flagellar protein content. *The Journal of cell biology*, **190**, 927-940.
40 Garcia-Gonzalo, F.R., Corbit, K.C., Sirerol-Piquer, M.S., Ramaswami, G., Otto, E.A., Noriega, T.R., Seol, A.D., Robinson, J.F., Bennett, C.L., Josifova, D.J. *et al.* (2011) A transition zone complex regulates mammalian ciliogenesis and ciliary membrane composition. *Nature genetics*, **43**, 776-784.
41 Hochwald, S.N., Nyberg, C., Zheng, M., Zheng, D., Wood, C., Massoll, N.A., Magis, A., Ostrov, D., Cance, W.G. and Golubovskaya, V.M. (2009) A novel small molecule inhibitor of FAK decreases growth of human pancreatic cancer. *Cell cycle*, **8**, 2435-2443.
42 Golubovskaya, V.M., Nyberg, C., Zheng, M., Kweh, F., Magis, A., Ostrov, D. and Cance, W.G. (2008) A small molecule inhibitor, 1,2,4,5-benzenetetraamine tetrahydrochloride, targeting the y397 site of focal adhesion kinase decreases tumor growth. *J Med Chem*, **51**, 7405-7416.
43 Slack-Davis, J.K., Martin, K.H., Tilghman, R.W., Iwanicki, M., Ung, E.J., Autry, C., Luzzio, M.J., Cooper, B., Kath, J.C., Roberts, W.G. *et al.* (2007) Cellular characterization of a novel focal adhesion kinase inhibitor. *The Journal of biological chemistry*, **282**, 14845-14852.
44 Nightingale, T.D., White, I.J., Doyle, E.L., Turmaine, M., Harrison-Lavoie, K.J., Webb, K.F., Cramer, L.P. and Cutler, D.F. (2011) Actomyosin II contractility expels von Willebrand factor from Weibel-Palade bodies during exocytosis. *The Journal of cell biology*, **194**, 613-629.
45 Ostlund, R.E., Jr., Leung, J.T. and Hajek, S.V. (1980) Regulation of microtubule assembly in cultured fibroblasts. *The Journal of cell biology*, **85**, 386-391.
46 Nolen, B.J., Tomasevic, N., Russell, A., Pierce, D.W., Jia, Z., McCormick, C.D., Hartman, J., Sakowicz, R. and Pollard, T.D. (2009) Characterization of two classes of small molecule inhibitors of Arp2/3 complex. *Nature*, **460**, 1031-1034.
47 Zhou, K., Muroyama, A., Underwood, J., Leylek, R., Ray, S., Soderling, S.H. and Lechler, T. (2013) Actin-related protein2/3 complex regulates tight junctions and terminal differentiation to promote epidermal barrier formation. *Proceedings of the National Academy of Sciences of the United States of America*, **110**, E3820-3829.
48 Kwon, K.W., Park, H. and Doh, J. (2013) Migration of T cells on surfaces containing complex nanotopography. *PloS one*, **8**, e73960.
49 Antonopoulou, G., Magrioti, V., Stephens, D., Constantinou-Kokotou, V., Dennis, E.A. and Kokotos, G. (2008) Synthesis of 2-oxoamides based on sulfonamide analogs of gamma-amino acids and their activity on phospholipase A2. *J Pept Sci*, **14**, 1111-1120.
50 Balestrieri, B. and Arm, J.P. (2006) Group V sPLA2: classical and novel functions. *Biochim Biophys Acta*, **1761**, 1280-1288.
51 Gijs, H.L., Willemarck, N., Vanderhoydonc, F., Khan, N.A., Dehairs, J., Derua, R., Waelkens, E., Taketomi, Y., Murakami, M., Agostinis, P. *et al.* (2015) Primary cilium suppression by SREBP1c involves distortion of vesicular trafficking by PLA2G3. *Mol Biol Cell*, **26**, 2321-2332.
52 Hyun, H.J., Sohn, J.H., Ha, D.W., Ahn, Y.H., Koh, J.Y. and Yoon, Y.H. (2001) Depletion of intracellular zinc and copper with TPEN results in apoptosis of cultured human retinal pigment epithelial cells. *Invest Ophthalmol Vis Sci*, **42**, 460-465.

53 Chimienti, F., Seve, M., Richard, S., Mathieu, J. and Favier, A. (2001) Role of cellular zinc in programmed cell death: temporal relationship between zinc depletion, activation of caspases, and cleavage of Sp family transcription factors. *Biochem Pharmacol*, **62**, 51-62.
54 Galban, S. and Duckett, C.S. (2010) XIAP as a ubiquitin ligase in cellular signaling. *Cell Death Differ*, **17**, 54-60.
55 Nikolovska-Coleska, Z., Xu, L., Hu, Z., Tomita, Y., Li, P., Roller, P.P., Wang, R., Fang, X., Guo, R., Zhang, M. *et al.* (2004) Discovery of embelin as a cell-permeable, small-molecular weight inhibitor of XIAP through structure-based computational screening of a traditional herbal medicine three-dimensional structure database. *J Med Chem*, **47**, 2430-2440.
56 Ahn, K.S., Sethi, G. and Aggarwal, B.B. (2007) Embelin, an inhibitor of X chromosome-linked inhibitor-of-apoptosis protein, blocks nuclear factor-kappaB (NF-kappaB) signaling pathway leading to suppression of NF-kappaB-regulated antiapoptotic and metastatic gene products. *Mol Pharmacol*, **71**, 209-219.
57 Berbari, N.F., Sharma, N., Malarkey, E.B., Pieczynski, J.N., Boddu, R., Gaertig, J., Guay-Woodford, L. and Yoder, B.K. (2013) Microtubule modifications and stability are altered by cilia perturbation and in cystic kidney disease. *Cytoskeleton (Hoboken)*, **70**, 24-31.
58 Delaval, B., Bright, A., Lawson, N.D. and Doxsey, S. (2011) The cilia protein IFT88 is required for spindle orientation in mitosis. *Nat Cell Biol*, **13**, 461-468.
59 Jiang, L., Wei, Y., Ronquillo, C.C., Marc, R.E., Yoder, B.K., Frederick, J.M. and Baehr, W. (2015) Heterotrimeric kinesin-2 (KIF3) mediates transition zone and axoneme formation of mouse photoreceptors. *The Journal of biological chemistry*, **290**, 12765-12778.

Figure Legends

Figure 1. NPHP5 localizes to the distal region of centrioles and is cell cycle regulated.
(**A**) RPE-1 cells in different stages of the cell cycle were processed for immunofluorescence with anti-NPHP5 (red) and anti-centrin (green) antibodies. DNA was stained with DAPI (blue). (**B**) U2OS cells transiently transfected with plasmid expressing Flag-Plk4 to induce simultaneous production of multiple procentrioles adjoining a single parental centriole were stained with antibodies against NPHP5 (red) and Flag or centrin (green). (**C**) Quiescent RPE-1 cells were processed for immunofluorescence with anti-NPHP5 (red) and anti-glutamylated tubulin (GT335) or anti-acetylated tubulin (Ac-tub) (green) antibodies. DNA was stained with DAPI (blue). (**D**) RPE-1 cells were processed for immunofluorescence with anti-NPHP5 (red) and anti-CP110, anti-Cep290, anti-Cep164, anti-Sas-6 or anti-C-Nap-1 (green) antibodies. DNA was stained with DAPI (blue).

Figure 2. RNAi-mediated suppression of NPHP5 inhibits an early step of cilia formation.
(**A**) RPE-1 cells were transfected with control (NS) or NPHP5 siRNAs and processed for immunofluorescence with anti-NPHP5 (red) and anti-centrin (green) antibodies. DNA was stained with DAPI (blue). (**B**) Extracts from RPE-1, U2OS or HEK293 cells transfected with control (NS) or NPHP5 siRNAs, or transfected with plasmid expressing full-length Flag-NPHP5 were probed by Western blotting with anti-NPHP5 antibody. α-tubulin was used as a loading control. (**C**) RPE-1 cells transfected with control (NS) or NPHP5 siRNAs, induced to quiescence, and stained with antibodies against NPHP5 (red) and glutamylated tubulin (GT335), and with DAPI (blue) (pictures).

The percentages of cycling (left graph) and quiescent (right graph) RPE-1 cells with primary cilia were determined using glutamylated tubulin (GT335), acetylated tubulin (Ac-tub), IFT88 or Gli2 as ciliary markers. (**D**) The percentages of cycling (left graph) and quiescent (right graph) RPE-1 cells stained positive for the proliferative marker Ki67 were determined. (**E**) RPE-1 cells transfected with control (NS) or NPHP5 siRNAs, induced to quiescence, and stained with antibodies against NPHP5 (red) and glutamylated tubulin (GT335, green), and with DAPI (blue). Fluorescent images were merged with corresponding differential interference contrast images. The distance from the center of the nucleus to the centrosome was measured and indicated by a white arrowed line (pictures). The percentages of control (NS), NPHP5, Cep290 or IFT88 siRNA-treated quiescent RPE-1 cells having a nucleus-to-centrosome distance of <7 μm and >7 μm were determined (graph). In (**C-E**), the average of 2-3 independent experiments is shown. Error bars represent standard errors. At least 100 cells for each siRNA condition were scored each time. *$p<0.01$ compared with NS.

Figure 3. NPHP5 interacts with Cep290 and CaM and possesses distinct functional domains.

(**A**) Western blotting of endogenous Cep290, NPHP5 and CaM after immunoprecipitation from HEK293 extracts with anti-NPHP5, anti-Cep290 or anti-Flag (control) antibodies. IN denotes input. (**B**) Flag (control), full-length (FL) or the indicated fragments and mutants of Flag-tagged NPHP5 were expressed in HEK293 cells and immunoprecipitated from lysates. Flag-NPHP5, Cep290 and CaM were detected after western blotting the resulting immunoprecipitates. IN indicates input. An asterisk denotes a band corresponding to the expected recombinant protein.

(**C-D**) Summary of the results of *in vivo* binding, centrosomal localization and cilia rescue experiments using NPHP5 truncation, deletion and single-point mutants. FL, Δ and ND denote full-length, deletion and not determined, respectively. A putative coiled coil domain is located at amino acid residues 340-371, while three putative IQ CaM-binding motifs reside at residues 300-328, 391-410 and 420-437. Further mapping results are shown in Figure 5.

Figure 4. NPHP5 interaction with Cep290 is crucial for cilia formation.

(**A**) Western blotting of Cep290 and NPHP5 in HEK293 cells treated with control (NS), NPHP5 or Cep290 siRNAs. α-tubulin was used as a loading control. (**B**) RPE-1 cells transfected with control (NS), NPHP5 or Cep290 siRNAs were stained with antibodies against NPHP5 or Cep290 (red) and centrin (green), and with DAPI (blue). Identical results were also obtained in HEK293 cells. (**C**) The percentages of transfected, cycling RPE-1 cells showing proper recombinant protein localization to centrosomes, relative to full-length, were determined using centrin as a centrosomal marker. Control denotes expression of an irrelevant Flag-tagged protein. FL denotes full-length. (**D**) The percentages of transfected, quiescent and NPHP5 siRNA-depleted ARPE-19 cells expressing primary cilia were determined using acetylated tubulin as a marker. Note that NPHP5 siRNA oligo 5 was used. Control denotes expression of an irrelevant Flag-tagged protein. FL denotes full-length. In (**C-D**), at least 75 transfected cells were scored for each construct, and average data obtained from three independent experiments is shown. Error bars represent standard errors. *$p<0.01$ compared with FL.

Figure 5. NPHP5 interaction with CaM prevents aggregate formation.

(**A**) Flag (control), full-length (FL) or the indicated mutants of Flag-tagged NPHP5 were expressed in HEK293 cells and immunoprecipitated from lysates. Flag-NPHP5, Cep290 and CaM were detected after western blotting the resulting immunoprecipitates. IN indicates input. (**B**) Summary of the results of *in vivo* binding, centrosomal localization and cilia rescue experiments using NPHP5 truncation, deletion and single-point mutants. FL, Δ and ND denote full-length, deletion and not determined, respectively. (**C**) The percentages of transfected, quiescent and NPHP5 siRNA-depleted ARPE-19 cells expressing primary cilia were determined using acetylated tubulin as a marker. Note that NPHP5 siRNA oligo 5 was used. Control denotes expression of an irrelevant Flag-tagged protein. FL denotes full-length. (**D**) The percentages of transfected, cycling RPE-1 cells possessing recombinant protein aggregates were determined using Flag as a marker. Control denotes expression of an irrelevant Flag-tagged protein. FL denotes full-length. In (**C-D**), at least 75 transfected cells were scored for each construct, and average data obtained from three independent experiments is shown. Error bars represent standard errors. *$p<0.01$ compared with FL.

Figure 6. Pathogenic *NPHP5* mutations abolish protein interaction with Cep290, induce protein mis-localization and inhibit cilia formation.

(**A**) Summary of the results of *in vivo* binding, centrosomal localization and cilia rescue experiments using NPHP5 disease-causing mutants. FL, fs and X denote full-length, frameshift and termination, respectively. Known pathogenic mutations causing SLS and LCA are indicated by inverted triangles. Disease phenotypes associated with F142fsX146, R332X, R461X, R502X and H506fsX518 mutations are indicated.

(**B**) Full-length (FL) or the indicated mutants of Flag-tagged NPHP5 were expressed in HEK293 cells and immunoprecipitated from lysates. Flag-NPHP5, Cep290 and CaM were detected after western blotting the resulting immunoprecipitates. IN indicates input. An asterisk denotes a band corresponding to the expected recombinant protein. (**C**) The percentages of transfected, cycling RPE-1 cells showing proper recombinant protein localization to centrosomes, relative to full-length, were determined using centrin as a centrosomal marker. FL denotes full-length. (**D**) The percentages of transfected, quiescent and NPHP5 siRNA-depleted ARPE-19 cells expressing primary cilia were determined using acetylated tubulin as a marker. Note that NPHP5 siRNA oligo 5 was used. FL denotes full-length. In (**C-D**), at least 75 transfected cells were scored for each construct, and average data obtained from three independent experiments is shown. Error bars represent standard errors. *$p<0.01$ compared with FL.

Figure 7. Inhibition of negative regulators of the ciliogenic pathway restores cilia formation in the absence of NPHP5.

(**A**) A table summarizing proteins known to inhibit ciliogenesis and their corresponding biological functions, along with drugs known to target these proteins. (**B**) The percentages of control (NS), NPHP5, CP110 or double siRNA-treated cycling RPE-1 cells with primary cilia were determined using glutamylated tubulin as a marker. (**C**) The percentages of control (NS), NPHP5, Cep290 or IFT88 siRNA-treated cycling RPE-1 cells exposed to drugs and possessing primary cilia were determined using glutamylated tubulin as a marker. In (**B-C**), at least 75 transfected cells were scored for each siRNA condition, and average data obtained from three independent experiments is shown. Error bars represent standard errors. In (**B**), *$p<0.01$ compared with NPHP5 knockdown. In (**C**), *$p<0.01$ compared with NS.

Supplemental figure legends

Figure S1. NPHP5 is a stable intrinsic component of centrosomes.

(**A**) RPE-1 cells treated with or without 10 μM nocodazole for 1 hr to induce microtubule de-polymerization were processed for immunofluorescence with anti-NPHP5 (red) and anti-α-tubulin or anti-γ-tubulin (green) antibodies. DNA was stained with DAPI (blue). (**B**) RPE-1 cells transfected with control (NS) or five individual NPHP5 siRNAs (Oligo 1 to 5) were stained with antibodies against NPHP5 (red) and centrin (green), and with DAPI (blue). (**C**) ARPE-19, HEK293 or U2OS cells transfected with control (NS) or NPHP5 siRNAs were stained with antibodies against NPHP5 (red) and centrin (green), and with DAPI (blue). (**D**) RPE-1 cells transfected with control (NS) or NPHP5 siRNAs were stained with three different anti-NPHP5 antibodies (Santa Cruz, Abcam, IRCM2, red) and anti-centrin (green) antibodies, and with DAPI (blue). Ab denotes antibody.

Figure S2. RNAi-mediated suppression of NPHP5 does not affect several aspects of centrosome function or cell cycle progression.

(**A**) The percentages of cells with the indicated number of centrin dots in control (NS) and NPHP5-depleted cells were determined. (**B**) The percentages of cells with the indicated number of γ-tubulin dots in control (NS) and NPHP5-depleted cells were determined. (**C**) The percentages of cells with well-separated centrin dots in control (NS) and NPHP5-depleted cells were determined. (**D**) The mitotic indices of control (NS) and NPHP5-depleted cells were determined. In (**A-D**), at least 100 transfected cells were scored for each siRNA condition, and average data obtained from two independent experiments is shown. Error bars represent standard errors.

(**E**) FACS analysis of cycling RPE-1 cells treated with control (NS) or NPHP5 siRNAs for 72 hrs. (**F**) RPE-1 cells transfected with control (NS) or NPHP5 siRNAs and stained with antibodies against glutamylated tubulin (GT335, red) and Rab11a or NPHP5 (green), and with DAPI (blue).

Figure S3. Mapping of the NPHP5-binding domain of Cep290 and direct association between NPHP5 and Cep290.

(**A**) Flag (control), full-length (FL) or the indicated fragments of Flag-tagged Cep290 were expressed along with full-length GFP-tagged NPHP5 in HEK293 cells and immunoprecipitated from lysates with anti-Flag beads. Flag-Cep290, GFP-NPHP5 and CaM were detected after western blotting the resulting immunoprecipitates. IN indicates input. An asterisk denotes a band corresponding to the expected recombinant protein. (**B**) Summary of the results of *in vivo* binding and centrosomal localization experiments using Cep290 truncation mutants. FL denotes full-length. (**C**) Flag (control) or two indicated fragments of Flag-tagged Cep290 were expressed in HEK293 cells and immunoprecipitated from lysates. Immunoprecipitates were subjected to SDS-PAGE and transferred onto a membrane. Proteins were denatured, re-natured, incubated with purified GST-NPHP5(469-598) and detected with anti-GST-HRP antibodies (Far-Western blot, left). Membrane was subsequently stripped and re-probed with anti-Flag antibodies (Western blot, right) Solid and dashed arrows indicate the positions of Flag-Cep290(580-1695) and Flag-Cep290(2037-2479) recombinant proteins, respectively.

Figure S4. Localization of recombinant wild type and mutant NPHP5 to centrosomes.
RPE-1 cells transiently transfected with plasmid expressing full-length (FL) or mutant Flag-NPHP5 were stained with antibodies against Flag (red) and centrin (green), and with DAPI (blue).

Figure S5. NPHP5 directly interacts with CaM and crippled interaction induces NPHP5 self-aggregation without affecting protein localization to the centrosome.
(**A**) Flag (control) or full-length Flag-tagged NPHP5 (1-598) was expressed in HEK293T cells and immunoprecipitated from lysates supplemented with either none, $CaCl_2$ ($+Ca^{2+}$) or EGTA ($-Ca^{2+}$). Flag-NPHP5, Cep290 and CaM were detected after Western blotting the resulting immunoprecipitates. IN indicates input. (**B**) The indicated recombinant proteins were expressed in HEK293 cells and immunoprecipitated from lysates with anti-Flag beads. Flag-CaM, GFP-NPHP5 and Cep290 were detected after Western blotting the resulting immunoprecipitates. IN indicates input. CaM1234 denotes a CaM mutant that no longer binds Ca^{2+}. (**C**) Western blot detection of NPHP5-His, CaM and GST after mixing purified full-length His-tagged NPHP5 protein with purified CaM or GST and binding to cobalt resin. IN denotes input. (**D**) RPE-1 cells transiently transfected with plasmid expressing full-length (FL) or mutant Flag-tagged NPHP5 were stained with antibodies against Flag (red) and centrin, γ-tubulin, CP110 or Cep290 (green), and with DAPI (blue). Punctate foci or blobs were significantly noticeable in cells expressing ΔIQ123, I393N and ΔIQ12.

Figure S6. Pathogenic *NPHP5* mutations induce protein mis-localization and inhibit cilia formation.

(**A**) RPE-1 cells transiently transfected with plasmid expressing full-length (FL) or mutant Flag-NPHP5 were stained with antibodies against Flag (red) and centrin (green), and with DAPI (blue). (**B**) ARPE-19 cells transfected with NPHP5 siRNAs (oligo 5) and plasmid expressing full-length (FL) or mutant Flag-tagged NPHP5, induced to quiescence, were stained with antibodies against Flag (red) and acetylated-tubulin (Ac-tub) (green), and with DAPI (blue).

Figure S7. Inhibition of negative regulators of the ciliogenic pathway restores cilia formation in NPHP5-deficient cells.

(A) RPE-1 cells transfected with control (NS), NPHP5 or Cep290 siRNAs and exposed to cytochalasin D or latrunculin B were stained with antibodies against NPHP5 (red) and glutamylated tubulin (GT335, green), and with DAPI (blue). (**B**) ARPE-19 cells transfected with NPHP5 siRNAs (oligo 5) and plasmid expressing full-length (FL) or mutant Flag-tagged NPHP5, induced to quiescence and exposed to cytochalasin D, were stained with antibodies against Flag (red) and acetylated-tubulin (Ac-tub) (green), and with DAPI (blue).

Figures

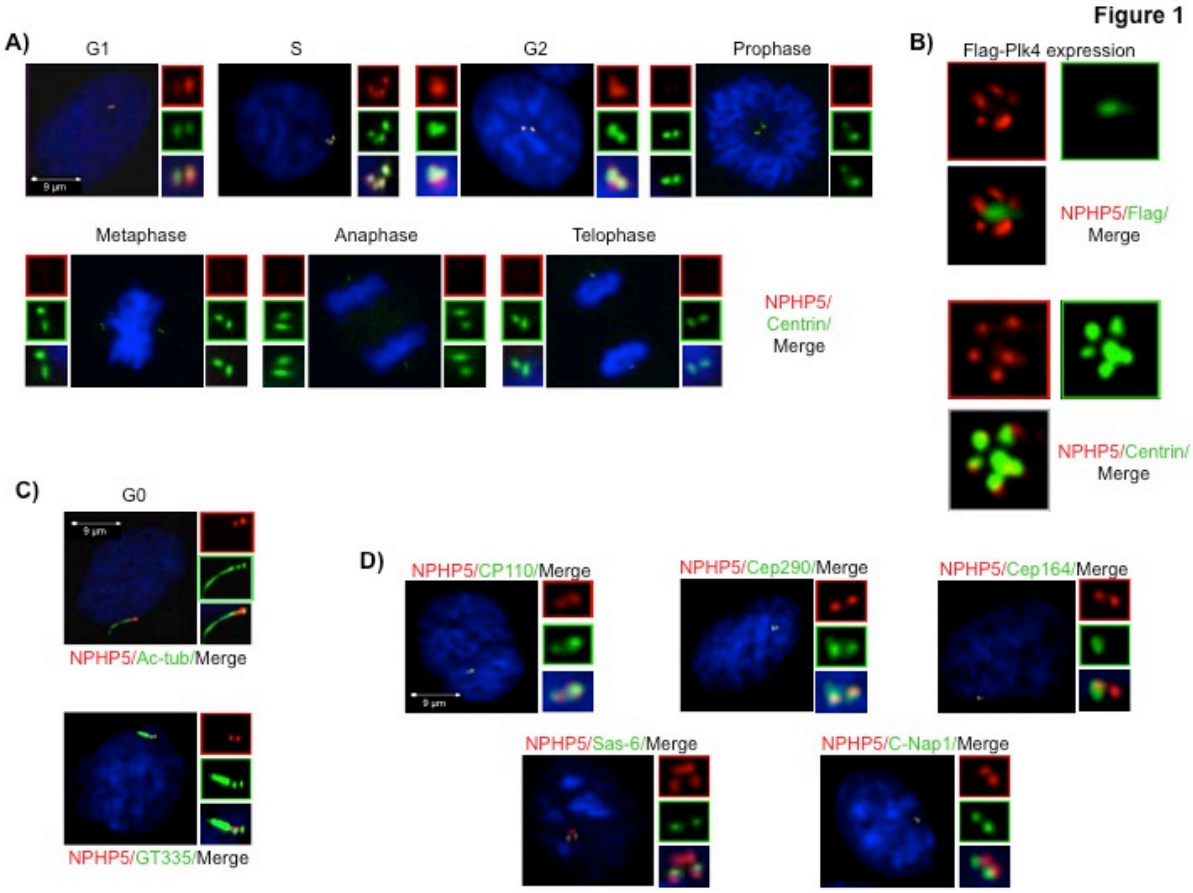

Figure 1. NPHP5 localizes to the distal region of centrioles and is cell cycle regulated.

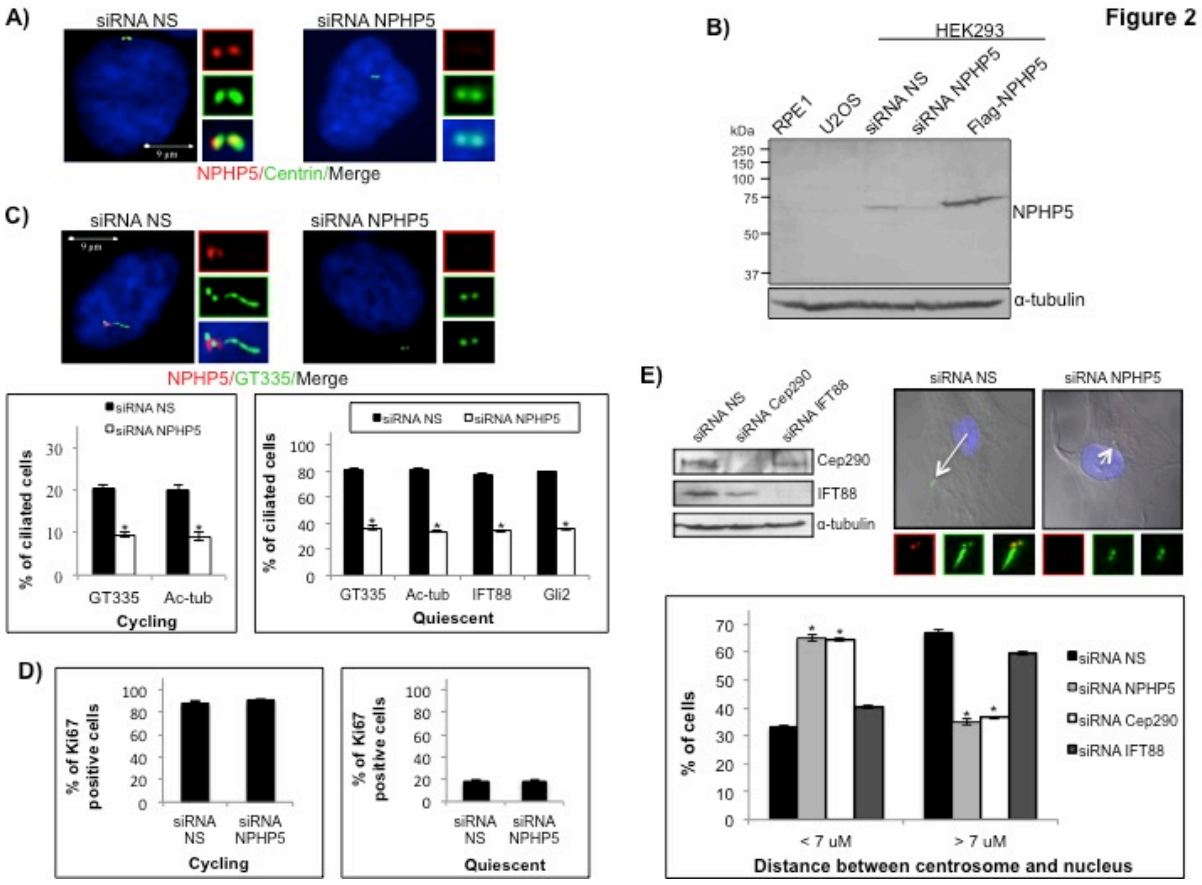

Figure 2. RNAi-mediated suppression of NPHP5 inhibits an early step of cilia formation.

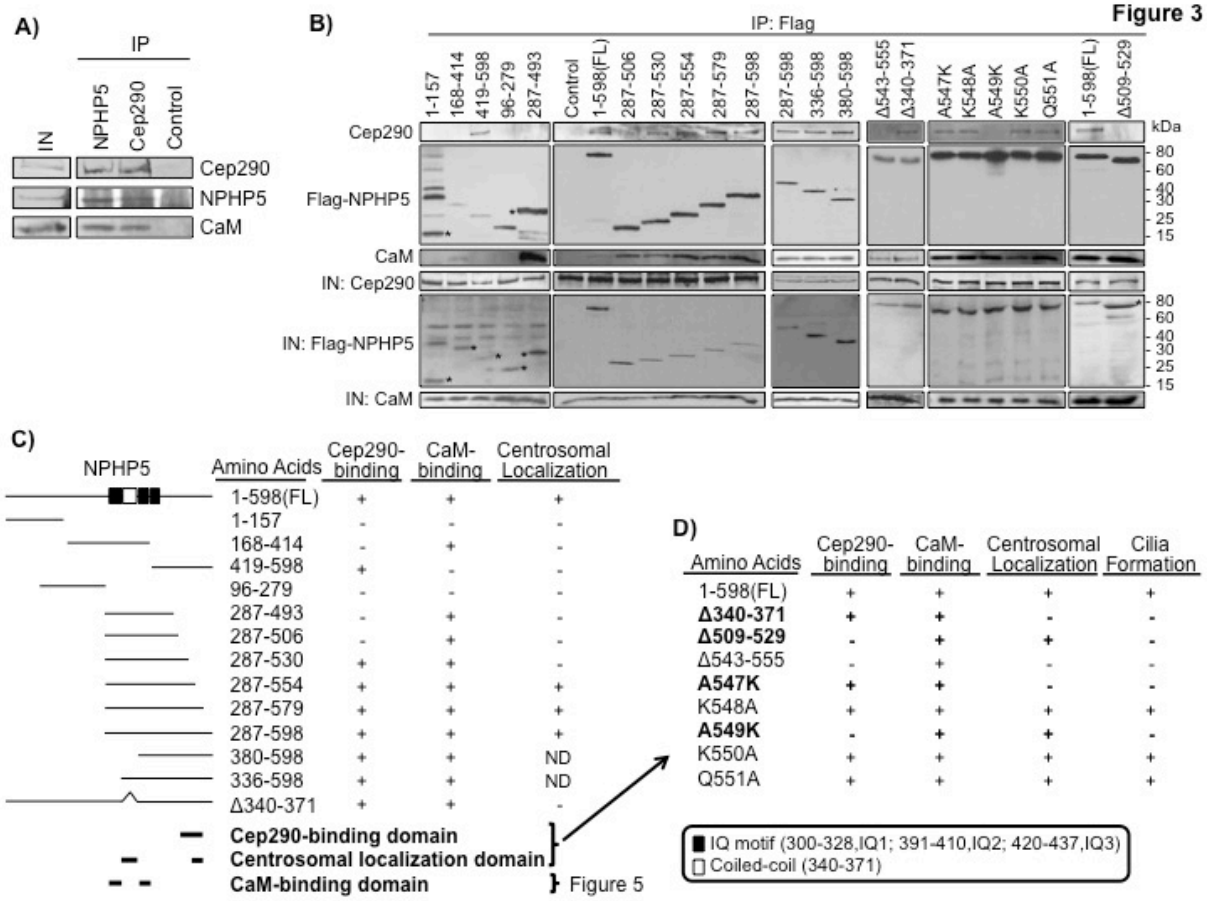

Figure 3. NPHP5 interacts with Cep290 and CaM and possesses distinct functional domains.

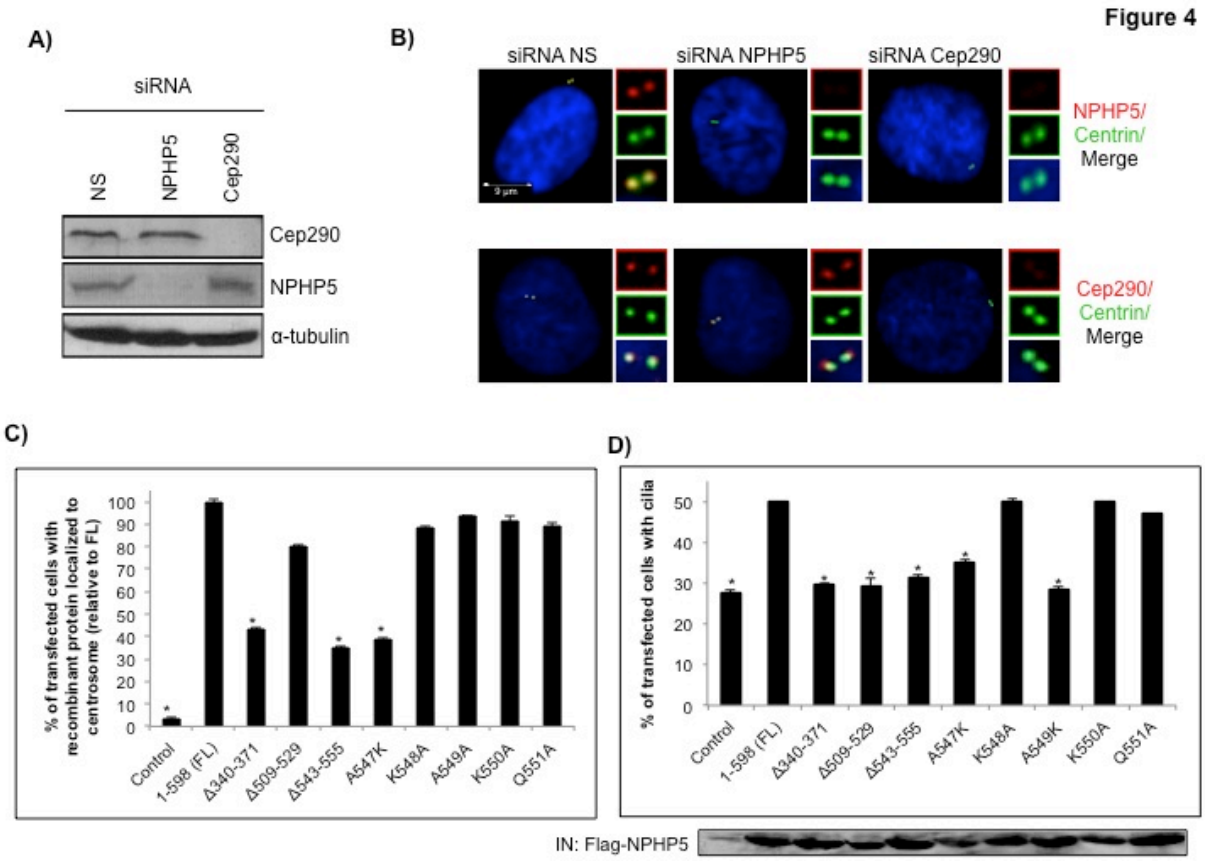

Figure 4. NPHP5 interaction with Cep290 is crucial for cilia formation.

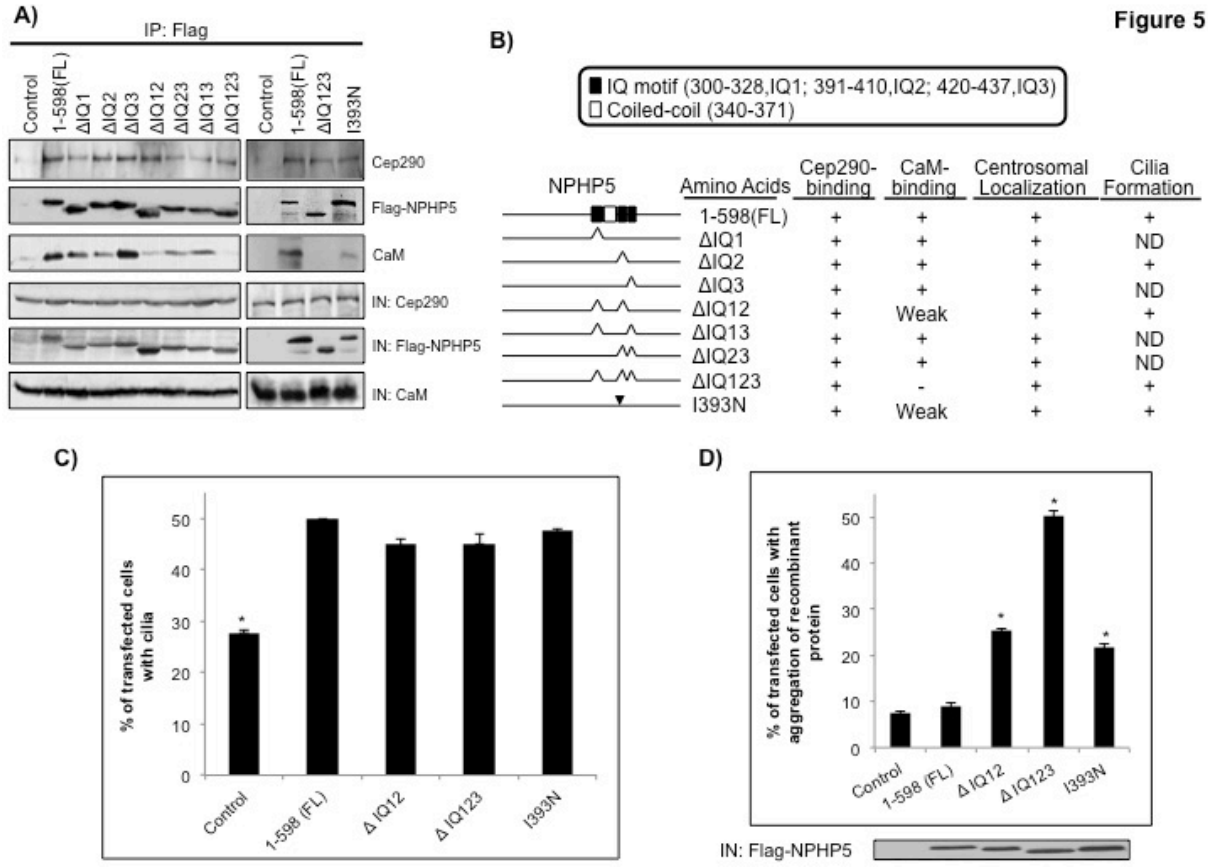

Figure 5. NPHP5 interaction with CaM prevents aggregate formation.

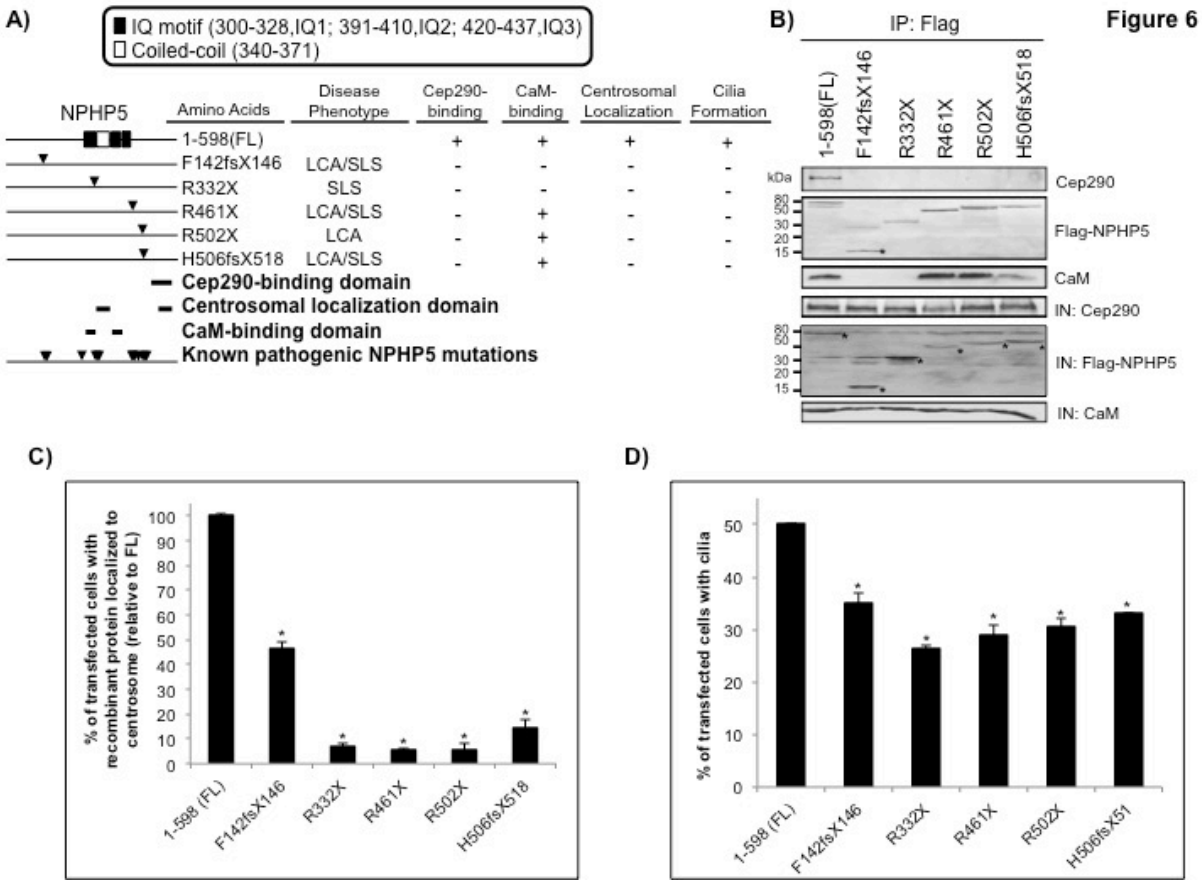

Figure 6. Pathogenic *NPHP5* mutations abolish protein interaction with Cep290, induce protein mis-localization and inhibit cilia formation.

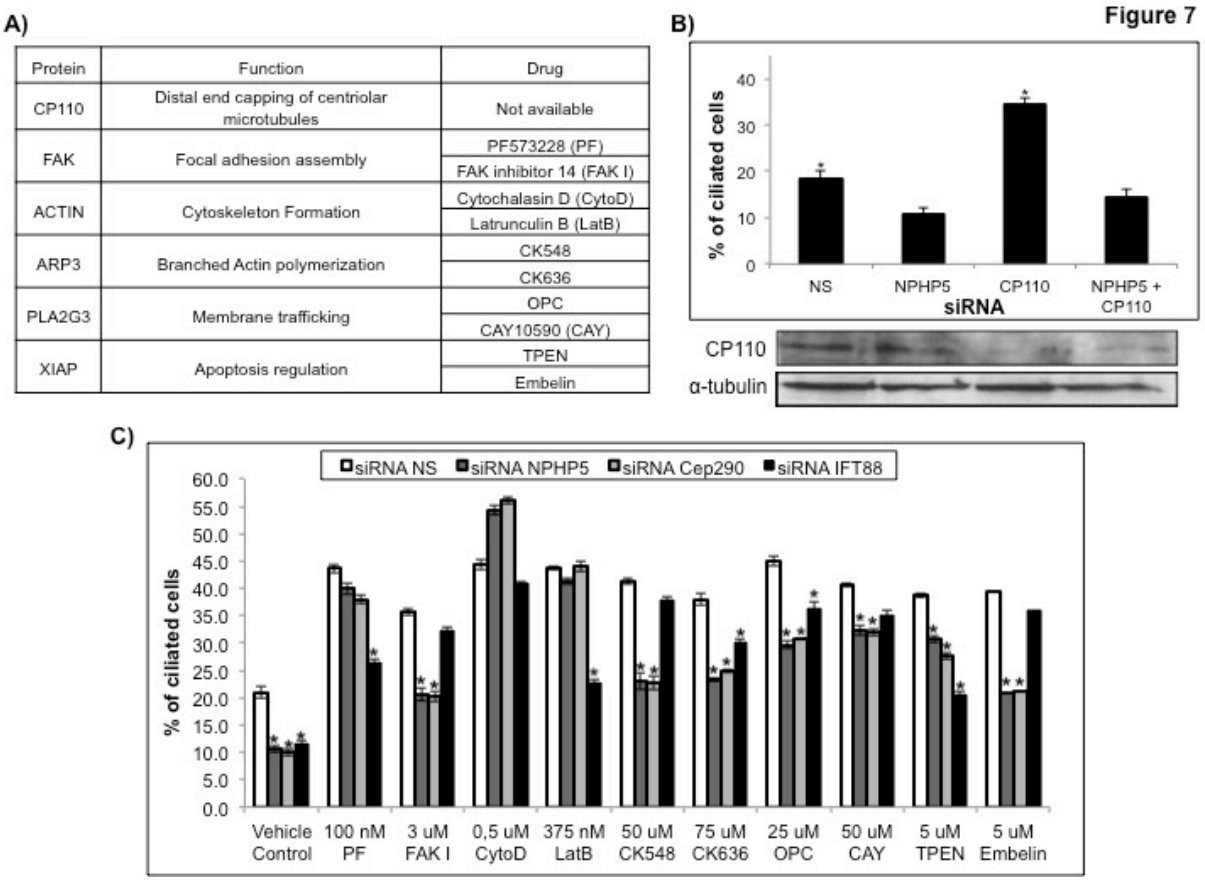

Figure 7. Inhibition of negative regulators of the ciliogenic pathway restores cilia formation in the absence of NPHP5.

Supplemental figures

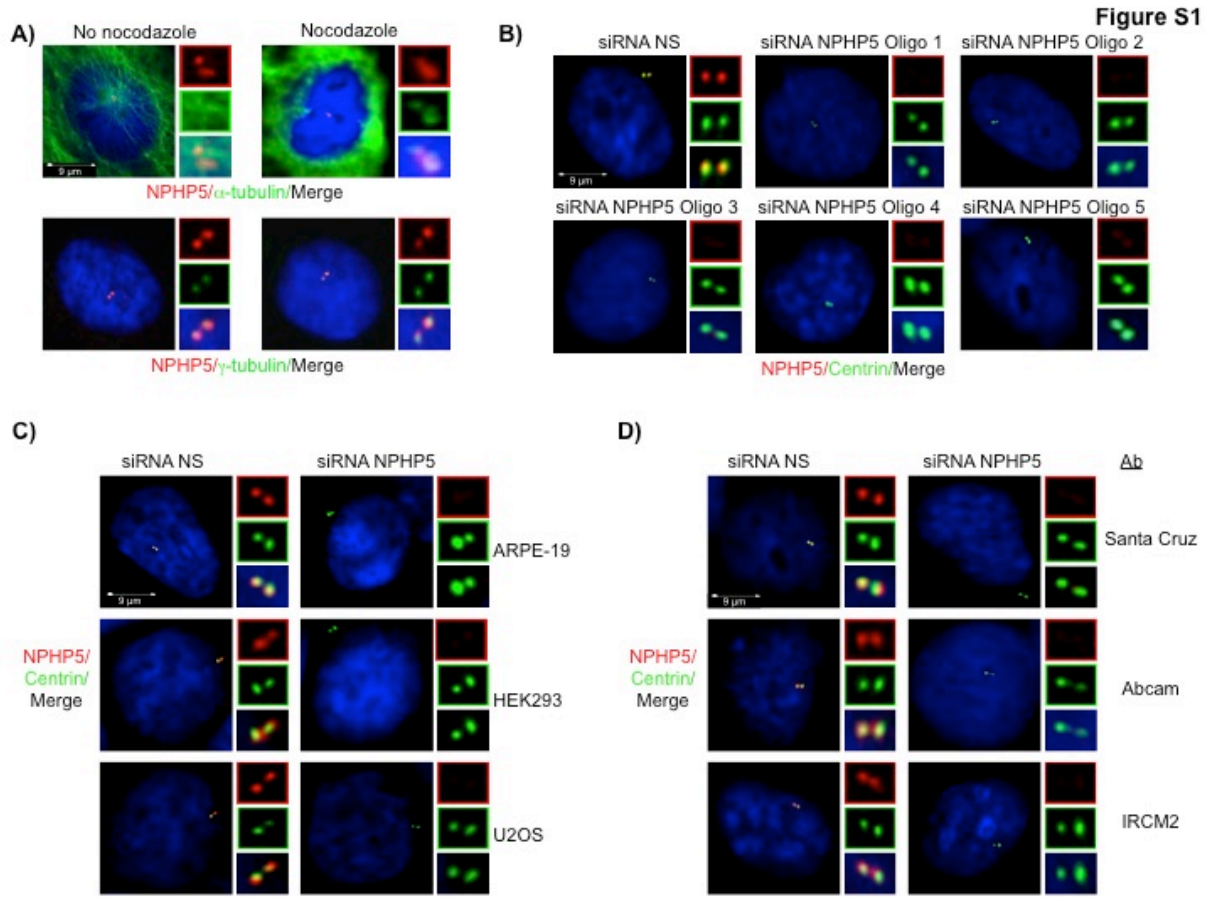

Figure S1. NPHP5 is a stable intrinsic component of centrosomes.

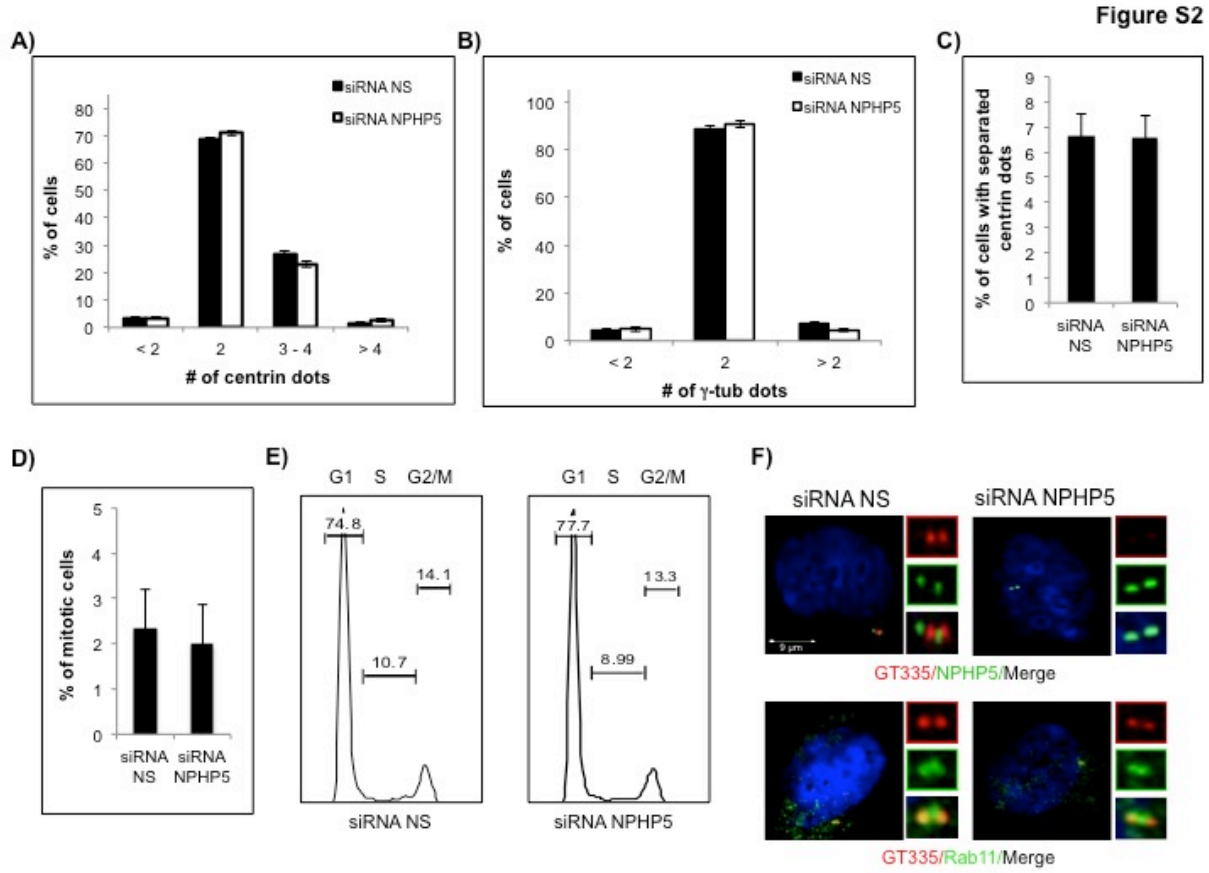

Figure S2. RNAi-mediated suppression of NPHP5 does not affect several aspects of centrosome function or cell cycle progression.

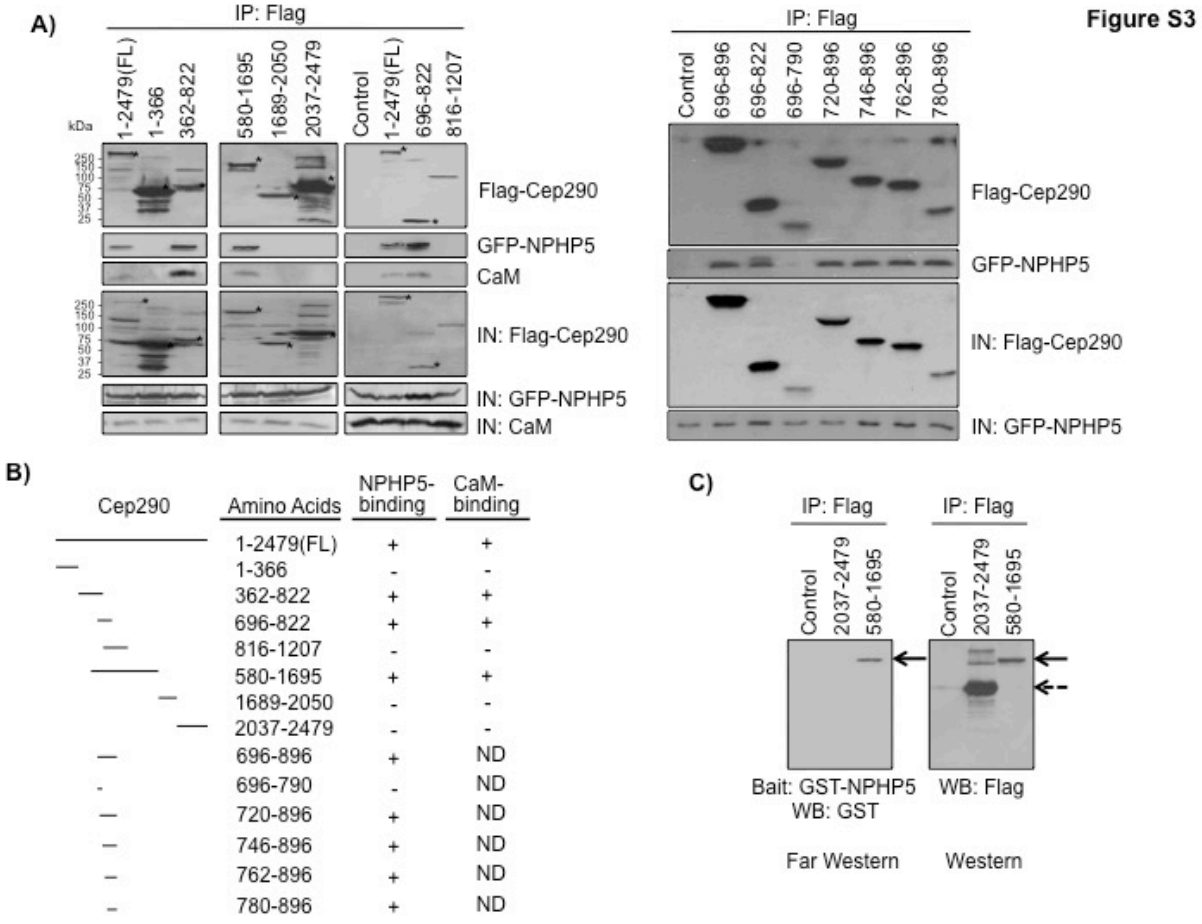

Figure S3. Mapping of the NPHP5-binding domain of Cep290 and direct association between NPHP5 and Cep290.

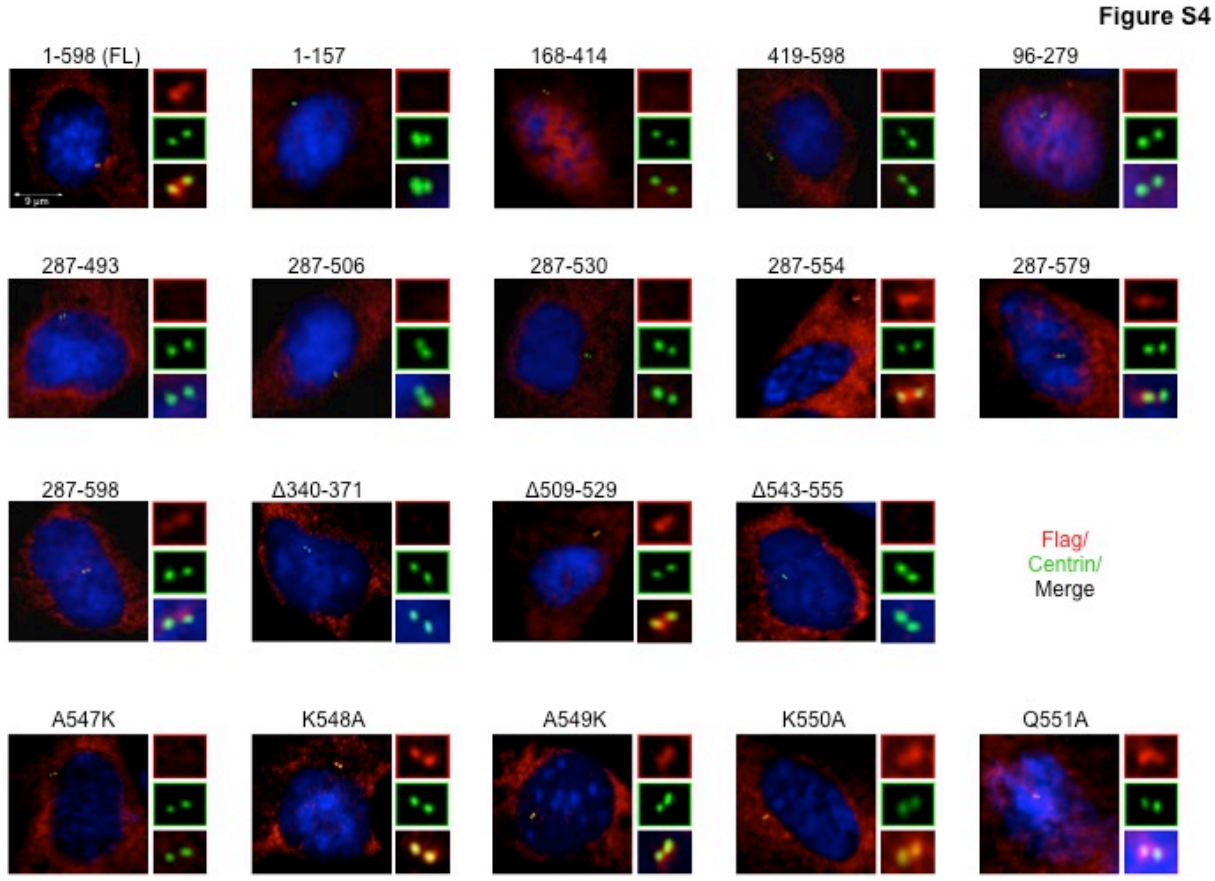

Figure S4. Localization of recombinant wild type and mutant NPHP5 to centrosomes.

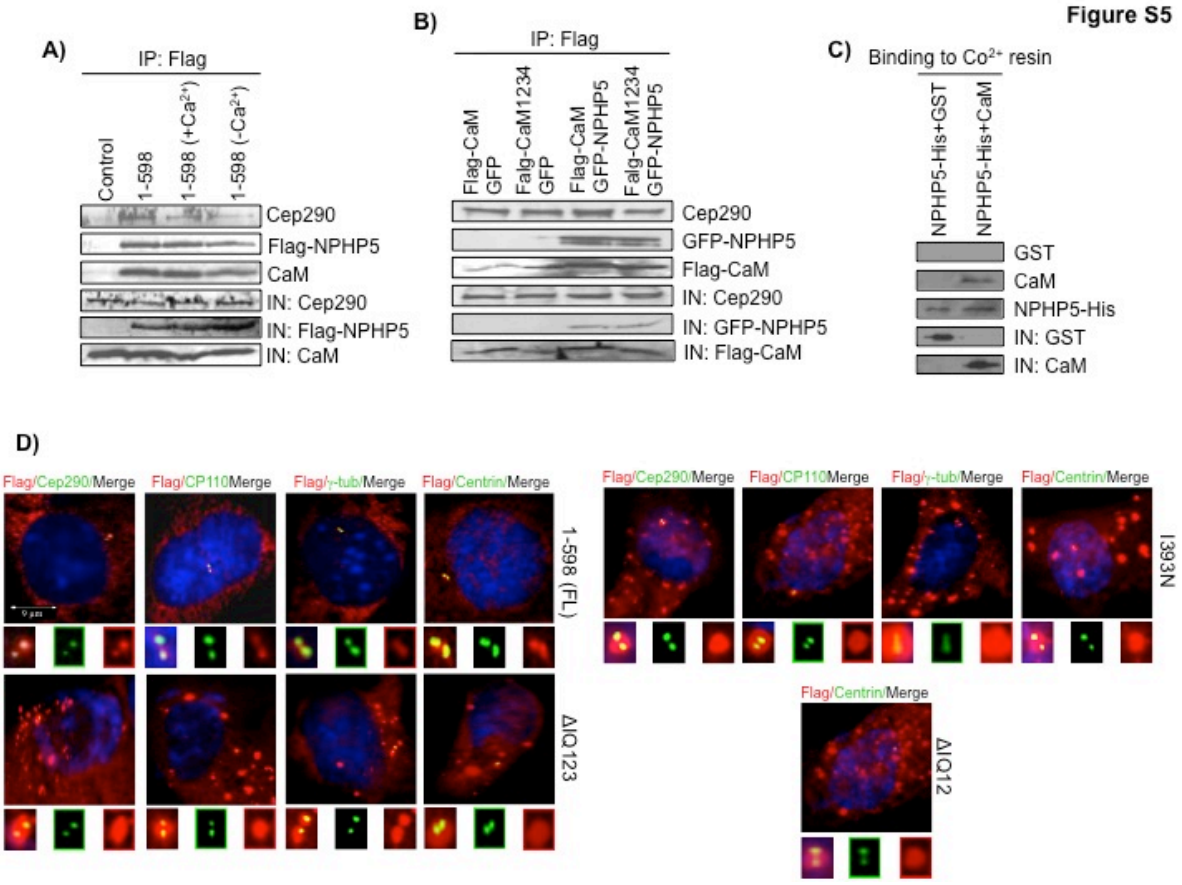

Figure S5. NPHP5 directly interacts with CaM and crippled interaction induces NPHP5 self-aggregation without affecting protein localization to the centrosome.

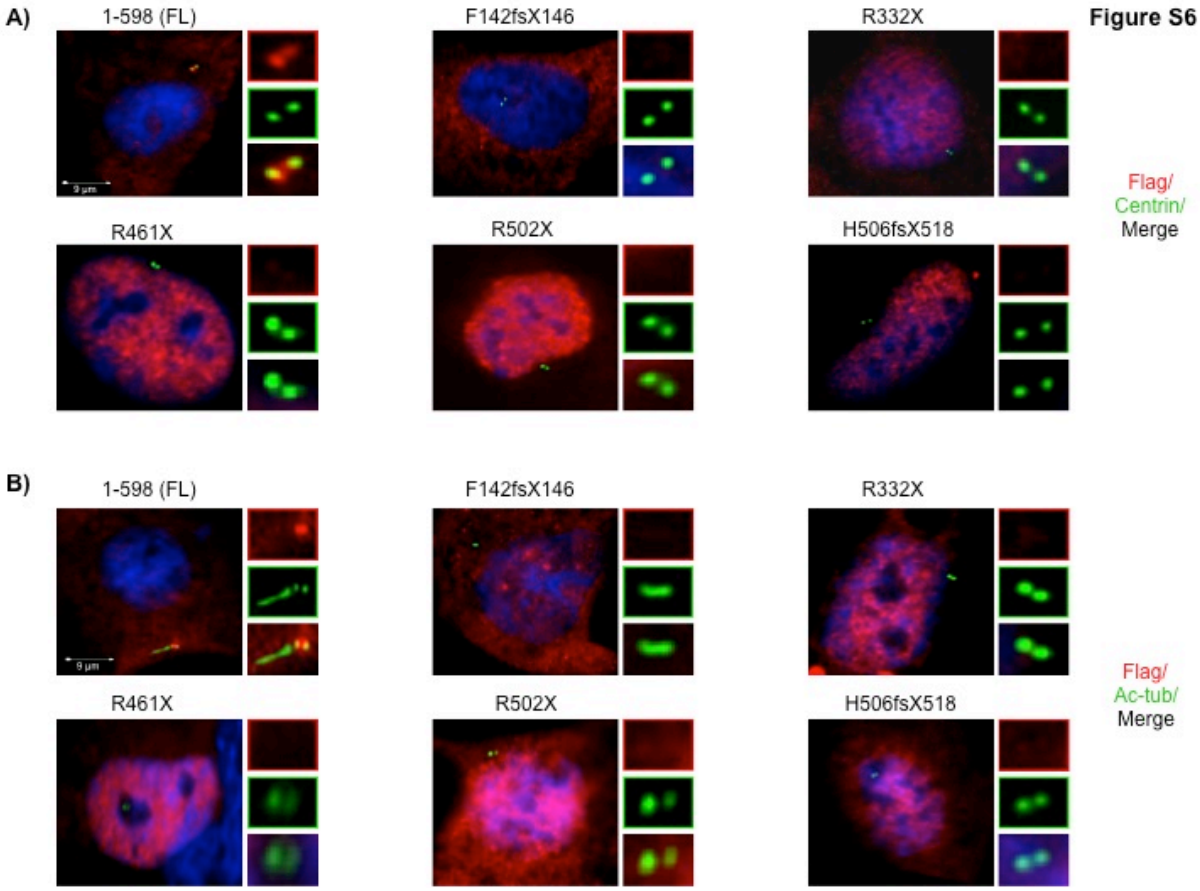

Figure S6. Pathogenic *NPHP5* mutations induce protein mis-localization and inhibit cilia formation.

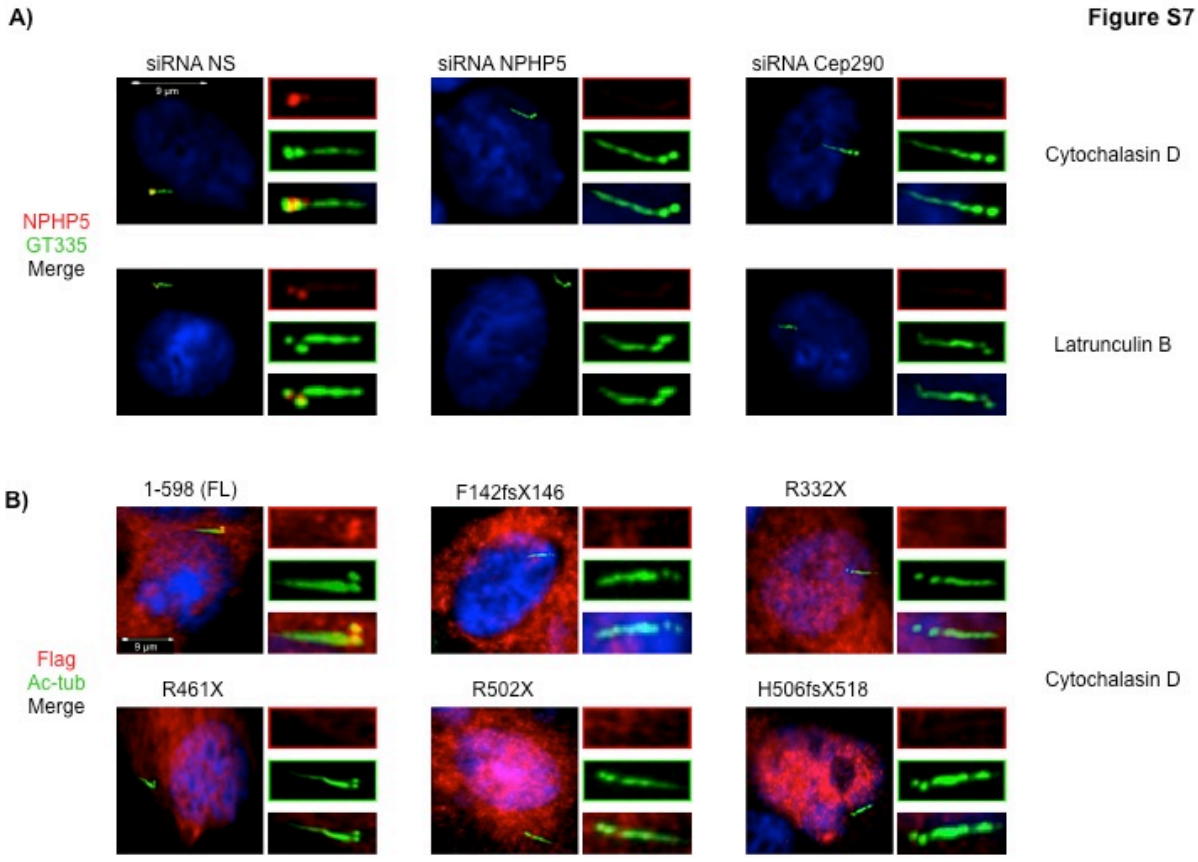

Figure S7. Inhibition of negative regulators of the ciliogenic pathway restores cilia formation in NPHP5-deficient cells.

Article 2 : Nephrocystin Proteins NPHP5 and Cep290 Regulate BBSome Integrity, Ciliary Trafficking and Cargo Delivery

Marine Barbelanne[1,2], Delowar Hossain[1,3], David Puth Chan[1], Johan Peränen[4] and William Y. Tsang[1,2,3,*]

[1] Institut de recherches cliniques de Montréal, 110 avenue des Pins Ouest, Montréal, Québec H2W 1R7, Canada

[2] Faculté de Médecine, Université de Montréal, Montréal, Québec H3C 3J7, Canada

[3] Division of Experimental Medicine, McGill University, Montréal, Québec H3A 1A3, Canada

[4] Institute of Biotechnology, University of Helsinki, Helsinki, 00014, Finland

Short title: Physical and functional interaction between NPHP5, Cep290 and BBSome

Contributions de M.B. : Toutes les expériences sauf clonage, size exclusion chromatography et WB des figures 1A, C ; 2A-C; 3A et 6C. Créations de toutes les figures/tables et participation dans l'interprétation des résultats et l'écriture du manuscrit.

Abstract

Proper functioning of cilia, hair-like structures responsible for sensation and locomotion, requires nephrocystin-5 (NPHP5) and a multi-subunit complex called the Bardet-Biedl syndrome (BBS)ome, but their precise relationship is not understood. The BBSome is involved in the trafficking of membrane cargos to cilia. While it is known that a loss of any single subunit prevents ciliary trafficking of the BBSome and its cargos, the mechanisms underlying ciliary entry of this complex are not well characterized. Here, we report that a transition zone protein, NPHP5 contains two separate BBS-binding sites and interacts with the BBSome to mediate its integrity. Depletion of NPHP5, or expression of NPHP5 mutant missing one binding site, specifically leads to dissociation of BBS2 and BBS5 from the BBSome and loss of ciliary BBS2 and BBS5 without compromising the ability of the other subunits to traffic into cilia. Depletion of Cep290, another transition zone protein that directly binds to NPHP5, causes additional dissociation of BBS8 and loss of ciliary BBS8. Furthermore, delivery of BBSome cargos, smoothened, VPAC2 and Rab8a, to the ciliary compartment is completely disabled in the absence of single BBS subunits, but is selectively impaired in the absence of NPHP5 or Cep290. These findings define a new role of NPHP5 and Cep290 in controlling integrity and ciliary trafficking of the BBSome, which in turn impinge on the delivery of ciliary cargo.

Introduction

In animal cells, centrioles are composed of nine sets of microtubule triplets and constitute the core of centrosomes, essential organelles that modulate various cellular processes including cell division, cell cycle progression, aging, cell morphology, polarity and motility(1, 2). A pair of centrioles, termed the mother and daughter centrioles, recruit an amorphous mass of protein called the pericentriolar matrix (PCM) which is responsible for microtubule nucleation and anchoring(3, 4). In quiescent cells, mother centrioles, but not daughter centrioles, transform into basal bodies and become competent to template cilia, hair-like protuberances that possess sensory and/or motility functions(5-7). Regardless of functionality, every cilium is made up of an axoneme, the microtubular backbone, surrounded by a ciliary membrane that is continuous with the plasma membrane. Cilia malfunction is increasingly recognized as a major cause of ciliary diseases or ciliopathies, a heterogeneous group of genetic disorders affecting many parts of the body, including the kidney, eye, liver and brain(8, 9). Clinically distinct disorders often display overlapping phenotypes, but the molecular basis of this overlap is not fully understood and remains an open question.

Bardet-Biedl Syndrome (BBS) is a ciliopathy characterized by retinal degeneration, renal failure, obesity, diabetes, male infertility, polydactyly, and cognitive impairment(10, 11). To date, 19 genes had been identified as disease loci, and the majority encode products that are essential for the formation and proper functioning of a multi-subunit complex called the BBSome. The BBSome is comprised of eight distinct BBS subunits (BBS1, BBS2, BBS4, BBS5, BBS7, BBS8, BBS9 and BBIP10/BBS18) and its assembly occurs in several stages(12, 13).

In brief, three chaperonin-like subunits, BBS6, BBS10 and BBS12 first bind to and stabilize BBS7, leading to the generation of an assembly intermediate known as the BBSome core which consists of BBS2, BBS7 and BBS9(14, 15). Subsequent incorporation of peripheral subunits BBS1, BBS5, BBS8, and finally BBS4, to the core completes its transformation to the holo-complex(15). BBS4 is also known to interact with BBIP10, although it is not certain when and how the latter is integrated into the BBSome(13). BBSome subunits possess domains known to mediate protein-protein interactions. BBS1, BBS2, BBS7 and BBS9 contain β-propeller domains. BBS4 and BBS8 contain solenoid or tetratricopeptide repeat domains, while BBIP10 possesses two alpha helices. In contrast, BBS5 contains pleckstrin homology domains, binds to phosphoinositides, and is believed to be the only BBSome subunit in direct contact with the ciliary membrane(12). Recently, BBS3/ARL6, an Arf-like GTPase, is shown to be a major effector of the BBSome. BBS3 recruits the BBSome to the membrane, wherein it assembles a coat that selectively sorts membrane cargos to cilia(16). In the nematode *Caenorhabditis elegans*, the BBSome regulates the assembly of intraflagellar transport (IFT) particles(17), a multi-subunit complex responsible for transporting the BBSome and its associated cargos into and out of the ciliary compartment(18). Unlike the BBSome which is generally not required for cilia assembly(13, 19), the IFT complex controls the bidirectional motility along the axoneme that is essential for the formation, maintenance and function of cilia.

Despite our knowledge of the BBSome, the precise mechanisms by which its ciliary trafficking is regulated remain enigmatic. Previous studies have demonstrated that all BBSome subunits are essential for BBSome assembly, and only a fully assembled holo-complex can gain entry to the ciliary compartment(20-22).

Ciliary entry requires the passage of the BBSome through a special region between the basal body and the axoneme called the transition zone, which acts as a permeability barrier to control the entry and exit of ciliary proteins(23). The transition zone contains several multi-subunit complexes including Cep290/NPHP5(24-26), NPHP1/NPHP4/NPHP8(24, 27, 28), MKS(27, 29, 30) and nucleoporin(31); however, the precise manner in which these complexes function remains shrouded in mystery. Here, we established a previously unknown connection between the BBSome and NPHP5, a transition zone protein whose deficiency is associated with ciliopathies. We demonstrated that NPHP5 and its binding partner Cep290, another transition zone protein, modulate not only BBSome integrity, but also trafficking of the holo-complex and its associated cargos into the cilium.

Results

NPHP5 interacts with the BBSome through two distinct binding sites

NPHP5 is a ciliopathy protein localized to the distal ends of centrioles, including the ciliary base(24, 25). Pathogenic mutations in the *NPHP5* gene render the resulting protein non-functional(25) and cause two ciliary diseases, Leber congenital amaurosis (LCA; retinal degeneration) and Senior-Løken syndrome (SLS; retinal degeneration and renal failure)(32-35). Because LCA and SLS share overlapping clinical manifestations with BBS, we hypothesize that NPHP5 and BBS proteins could interact to regulate cilia homeostasis. Thus, the ability of NPHP5 to associate with the first twelve BBS subunits was examined.

We immunoprecipitated recombinant, N-terminal tagged NPHP5 (Flag-NPHP5) from HEK293 cell extracts and found that it interacts with all GFP-tagged BBSome subunits BBS1, BBS2, BBS4, BBS7 and BBS8 except BBS5 (Figure 1a). No or weak co-immunoprecipitation was observed between NPHP5 and non-BBSome subunits, including an Arf-like GTPase BBS3, chaperonin-like BBS proteins BBS6, BBS10 and BBS12, and an E3 ubiquitin ligase BBS11(36) (Figure 1a). Similar results were obtained when a C-terminal tagged NPHP5 (NPHP5-Flag) was used instead of Flag-NPHP5 (Figure S1a) or when immunoprecipitations were performed in a less stringent lysis buffer designed to emulate physiological conditions (150 mM salt, pH 7.4) (Figure S1b). Since every BBSome subunit apart from BBS5 associates with NPHP5, we wondered whether the position and/or size of the tag on BBS5 or NPHP5 interfere(s) with binding. We co-expressed Flag-BBS5 or BBS5-Flag and GFP-NPHP5 or NPHP5-GFP, performed anti-Flag immunoprecipitations, and confirmed that recombinant NPHP5 and BBS5 interact in all possible combinations (Figure 1b). Notably, NPHP5 may bind to the N-terminal region of BBS5, since recombinant NPHP5 interacted strongly with BBS5-Flag but poorly with Flag-BBS5 (Figure 1b), and did not interact at all with GFP-BBS5 (Figures 1a and S1a-b). Moreover, no interaction was observed between GFP-NPHP5 and non-BBSome subunits BBS3-Flag, BBS6-Flag or BBS10-Flag (Figure S1c), suggesting that NPHP5 specifically associates with the holo-complex. To provide further proof that NPHP5 interacts with the BBSome, endogenous NPHP5, BBS2, BBS4, BBS5 and BBS8 co-fractionated in a discrete protein complex at ~500 kDa (Figures 1c and 6c), which is in close agreement with the reported molecular weight of the BBSome(12). In addition, antibodies against BBS2 or BBS5 co-precipitated NPHP5, along with known NPHP5-interacting proteins, Cep290 and calmodulin (CaM) (Figure 1d and (25, 26, 33, 37)).

An *in situ* proximity ligation assay (PLA) designed to detect interaction at a distance below 40nm(38) also revealed an association of NPHP5 with BBSome subunits (Table 1 and Figure 4; see below). Given that some BBSome subunits are efficiently co-immunoprecipitated with, and physically closer to, NPHP5 than others (Figures 1, 4, S1 and Table 1), these data together suggest that NPHP5 interacts with the holo-complex through certain subunits. Moreover, NPHP5 most likely forms a complex with the BBSome, Cep290 and CaM.

Next, we sought to map the BBSome-binding domain(s) of NPHP5 by expressing a series of epitope-tagged NPHP5 truncation mutants and BBSome subunits and examining their ability to co-immunoprecipitate in cell extracts. We found that there are two distinct BBSome-binding sites, one at the N-terminal region and the other at the C-terminal region (Figure 2a). Further mapping studies revealed that the first 157 residues (1-157) and the last 68 residues (530-598) of NPHP5 are critical for binding (Figures 2b-d).

During the course of our mapping studies, an unexpected and reproducible phenomenon was noticed with regard to the specificity of the two BBSome-binding sites of NPHP5. We found that BBS1 interacted more strongly with a N-terminal fragment of NPHP5 (1-287), encompassing the N-terminal BBSome-binding site, than full-length (1-598) or a C-terminal fragment of NPHP5 (287-598) (Figure 2a). Likewise, two other N-terminal fragments of NPHP5 (1-157 and 1-332) also exhibited a stronger interaction with BBS1 compared to full-length NPHP5 (data not shown). Conversely, BBS9 bound more robustly to 287-598 than 1-598 or 1-287 (Figure 2a). BBS2, BBS4, BBS5 and BBS7 mostly interacted with the C-terminal BBSome-binding site, since they bound equally well to 1-598 and 287-598 but poorly to 1-287 (Figure 2a).

BBS8, meanwhile, bound to 1-598, 1-287 and 287-598 with similar affinity (Figure 2a). Our data suggest that the N-terminal site, when present alone and/or acting independently, may preferentially bind BBS1, whereas the C-terminal site is favorably occupied by BBS9 and several other subunits.

NPHP5 interacts with the BBSome independently of its associated partner, Cep290

We had previously demonstrated that residues 509-529 and 549 of NPHP5 are critical for binding to Cep290(25). Given that Cep290 interacts with the BBSome(39) and that the Cep290- and the C-terminal BBSome-binding sites are mapped to the C-terminal region of NPHP5, we determined if these two sites overlap, and whether NPHP5 and Cep290 could associate with the BBSome independently of each other. First, we showed that a C-terminal fragment of NPHP5 (Flag-NPHP5(287-598)) containing only one BBSome-binding site interacted with Cep290 and the BBSome (Figure 3a). In contrast, the same fragment carrying a point mutation (Flag-NPHP5(287-598A549K)) or a deletion (Flag-NPHP5(287-598Δ509-529)) known to disrupt Cep290 binding still associated with the BBSome (Figure 3a). Second, antibodies against BBS2 and BBS5 co-precipitated endogenous NPHP5 in extracts specifically depleted of Cep290 (Figure 3b). Likewise, the same antibodies co-precipitated Cep290 in extracts depleted of NPHP5 (Figure 3c). Taken together, our findings suggest that NPHP5 and Cep290 can independently bind to the BBSome.

NPHP5 and Cep290 interact with the BBSome in non-ciliated and ciliated cells

A number of studies showed that BBS proteins are localized to centrosomes and cilia(12, 13, 16, 17, 22, 40-46). Since NPHP5 and the BBSome interact, we therefore examined the localization of these proteins in greater detail by performing immunofluorescence experiments to co-stain NPHP5 with BBSome subunits in proliferating (non-ciliated) and quiescent (ciliated) human retinal pigmented epithelial (RPE-1) cells. We found that NPHP5 staining partially overlapped with every subunit at the centrosome/ciliary base (Figures S2a-b). Of note, BBSome subunits generally exhibited weak staining at the centrosome in proliferating cells but accumulated at the cilium in quiescent cells (Figures S2a-b). Thus, it is conceivable that when cilia have yet to form, the BBSome complex may be present in minute amounts and is not fully assembled. Because ciliary accumulation of the BBSome coincides with ciliogenesis and because the BBSome has to pass through the transition zone at the ciliary base prior to entry into cilia, we asked whether NPHP5 at the centrosome/ciliary base could interact with the BBSome in proliferating and quiescent cells. *In situ* PLA was used to identify endogenous interaction between NPHP5 and BBSome subunits and to access how close these two entities are in space. To validate assay specificity, we first visualized the interaction between NPHP5 and Cep290, which is known to be direct (24, 25). Both proteins are also shown to localize to the distal ends of centrioles/ciliary base during interphase and quiescence (25, 47, 48). We observed strong PLA signals in proliferating and quiescent cells when anti-NPHP5 and anti-Cep290 antibodies were used (Figure 4a and Table 1).

These signals substantially overlapped with a centrosomal marker, γ-tubulin, suggesting that NPHP5 and Cep290 interact at the centrosome/ciliary base under all conditions (Figure 4a). Negligible signal was detected when one or more antibodies were omitted, or when anti-NPHP5 antibody was mixed with an irrelevant antibody (Figure 4a). *In situ* PLAs performed using proximity probes against NPHP5 and different BBSome subunits revealed that NPHP5 interacts with, and/or is in close proximity to, every BBSome subunit (Figure 4b and Table 1). PLA signal intensity varies between different NPHP5/subunit combinations and between proliferative and quiescence states for a given combination. Notably, the NPHP5/BBS4 combination in quiescent cells yielded the strongest signal (Figure 4b and Table 1). PLA signals of varying intensity were likewise detected when antibodies against Cep290 and BBSome subunits were combined. Overall, these signals tended to be weaker than those of NPHP5/BBSome subunits (Figure 4c and Table 1), suggesting that Cep290 may be physically further from the BBSome than NPHP5. Interestingly, a strong PLA signal was also reported for the Cep290/BBS4 combination in quiescent cells (Figure 4c and Table 1). Since NPHP5 interacts with Cep290 and the BBSome, contains two BBSome-binding sites with different subunit specificities, and is in close proximity to different subunits depending on proliferation status, our data suggest that NPHP5 and Cep290 could control some aspects of BBSome function.

NPHP5 and Cep290 control BBSome integrity and ciliary trafficking

In an effort to reveal the biological relevance of the interaction between NPHP5 and the BBSome, we performed reciprocal depletion of NPHP5 and two BBS subunits, BBS2 and BBS5, using small-interfering RNAs (siRNAs) in HEK293, RPE-1 and ARPE-19 cells.

Depletion of BBS2 or BBS5 had no effect on the levels and localization of NPHP5 (Figures S3a-b), and likewise, ablation of NPHP5 did not alter the levels of BBS2, BBS4 or BBS5 (Figure 5a). We and others have previously shown that although siRNA depletion of NPHP5 greatly compromises ciliogenesis(24, 25), cilia can still form in cells where the silencing is not as efficient. Remarkably, we found that a loss of NPHP5 specifically affects ciliary localization of BBS2 and BBS5 without affecting other BBSome subunits (BBS1, BBS4, BBS7, BBS8, BBS9 and BBIP10) and BBS3 in cells that have retained their cilia (Figures 5b-c). In particular, BBS5 was no longer detected at the cilium, whereas BBS2 was either completely absent from, or confined to a proximal region of, the cilium (Figures 5b-d), reminiscent of the so-called inversin compartment or EvC zone(49-51). Of note, proximal ciliary confinement of BBS2 was not due to shortened cilia, since cilia length (as judged by staining of three different ciliary markers, detyrosinated tubulin, glutamylated tubulin and IFT88) was unaffected in NPHP5-depleted cells (Figure 5b and 5d). Furthermore, depletion of NPHP5 did not result in enhanced staining or accumulation of other BBSome subunits (BBS1, BBS4, BBS7, BBS8, BBS9 and BBIP10) at the cilium (Figure 5b), suggesting that this protein, unlike BBS17 or AZI1(22, 52), is not a negative regulator of BBSome ciliary trafficking. Next, we conducted rescue experiments in which we expressed full-length NPHP5 (1-598) or a NPHP5 mutant lacking the N-terminal BBSome-binding site (287-598) in quiescent cells depleted of endogenous NPHP5, using a siRNA oligo that targets the 3'UTR of NPHP5 mRNA.

We found that although 1-598 and 287-598 both localize to centrosomes, the two phenotypes associated with NPHP5 depletion, namely, loss of ciliary BBS2/BBS5 and proximal ciliary staining of BBS2, were largely rescued by 1-598 but not 287-598 expression (Figures 6a and 6b). These results suggest that NPHP5-binding to the BBSome is crucial for BBSome integrity and ciliary trafficking of certain subunits.

The mis-localization of BBS2 and BBS5 provoked by NPHP5 depletion strongly suggests that these two subunits are separated from the rest of the BBSome. To examine this possibility, we noticed that in size exclusion chromatography, BBS2, BBS4, BBS5 and BBS8 peak at around fractions 7-9 (~500 kDa) in control cells (Figure 6c)(12, 22). In NPHP5-depleted cells, however, a significant amount of BBS2 and BBS5 was found in early fractions (fractions 5-6) (Figure 6c), indicating that these two subunits co-fractionate in a high molecular weight complex distinct from the BBSome. The overall size of the remaining BBSome is expected to decrease after losing two critical subunits, and indeed, we reproducibly detected a shift of BBS4 and BBS8 to lower molecular weight fractions (fractions 9-11) in NPHP5-depleted cells, but not in control cells (Figure 6c). Importantly, we also demonstrated that while endogenous BBS1, BBS2, BBS5 and BBS8 co-immunoprecipitated with GFP-BBS4 in control extracts, only BBS1 and BBS8 were co-immunoprecipitated in the absence of NPHP5 (Figure 6d). Taken together, our data suggest the existence of a BBSome sub-complex, devoid of BBS2 and BBS5, which retains the capacity to traffic into cilia.

Since Cep290 docks NPHP5 at the centrosome/ciliary base and is required for ciliogenesis(24, 25, 53), we surmise that ablation of Cep290 should phenocopy NPHP5 loss of function.

Depletion of Cep290 indeed prevented ciliary localization of BBS2 and BBS5, in addition to restricting BBS2 to the proximal region of cilia in a subpopulation of ciliated cells (Figures 5b-d). Interestingly, ciliary localization of BBS8 was also abolished, a result consistent with previous work(54), whereas the remaining BBSome subunits (BBS1, BBS4, BBS7, BBS9 and BBIP10) and BBS3 were efficiently targeted to the cilium (Figures 5b-c). Furthermore, GFP-BBS4 associated with BBS1 but not with BBS2, BBS5 or BBS8 in Cep290-depleted cells (Figure 6d), suggesting that BBS2, BBS5 and BBS8 disintegrate and are no longer in a complex with BBS1/BBS4. To ascertain that the BBS8 phenotype is direct consequence of Cep290 loss and that suppression of Cep290 indirectly affects BBS2/BBS5, we performed rescue experiments in which we expressed full-length NPHP5 (1-598) in quiescent cells depleted of endogenous Cep290. We found that exclusion of BBS2/BBS5 from cilia and proximal ciliary confinement of BBS2 were largely rescued, whereas loss of ciliary BBS8 was not (Figures 7a and 7b). Finally, we showed that the phenotype induced by NPHP5 or Cep290 loss is unique, since ciliary entry of the BBSome or any single subunit, including BBS2, BBS4, BBS5, BBIP10, BBS8(22) and BBS9(22), was precluded in BBS2- or BBS5-depleted cells (Figure S3c). Considered together, our data suggest that NPHP5 maintains association of BBS2 and BBS5 with the BBSome, while Cep290 keeps BBS8 glued to the complex. In the absence of NPHP5 or Cep290, the BBSome is missing some subunits, and yet its trafficking to cilia is not compromised. Since only a holo-BBSome enters cilia(20-22), we reason that NPHP5 and Cep290 may perform an additional gatekeeping function to restrain entry of a malformed BBSome into cilia.

To assess the potential role of NPHP5 and Cep290 as a gatekeeper, we sought to determine if their inactivation triggers gross malformation of the transition zone at the ciliary base. We found that two components of the NPHP1/NPHP4/NPHP8 complex, NPHP1 and NPHP8, and two components of the MKS complex, TCTN1 and MKS3, were efficiently recruited to the ciliary base in NPHP5- or Cep290-depleted cells (Figure 7c). In addition, no aberrant accumulation of two IFT subunits, IFT43 and IFT88 at the ciliary tip, indicative of impaired retrograde transport, was observed (Figure 7d). Likewise, there was no apparent loss of ciliary IFT43 or IFT88 (Figure 7d), suggesting that anterograde transport is not compromised. Moreover, depletion of NPHP5 or Cep290 did not affect ciliary trafficking or accumulation of most BBSome subunits (Figures 5b-c). These data suggest that the transition zone is not grossly malformed, and ciliary content is not substantially altered. Therefore, it appears that these two proteins specifically regulate ciliary trafficking of the BBSome.

Loss of NPHP5 or Cep290 partially impairs ciliary targeting of BBSome cargoes

Next, we asked whether a malformed BBSome induced by a loss of NPHP5 or Cep290 could impinge on ciliary trafficking of its cargos. We hypothesize that such BBSome sub-complex is proficient in delivering some, but not all cargos to cilia. In mammals, the BBSome is known to traffic a subset of cargos, including G protein-coupled receptors smoothened (Smo), melanin-concentrating hormone receptor 1 (MCHR1), somatostatin receptor 3 (SSTR3), vasoactive intestinal peptide receptor 2 (VPAC2) and dopamine receptor 1 (D1R) into and/or out of cilia(16, 22, 55-59). In addition, this complex cooperates with the GTPase Rab8a to regulate vesicular trafficking and ciliary membrane biogenesis(12).

Although previously reported in other cell lines and tissues (58, 59), we were unable to detect endogenous MCHR1 or SSTR3 at the cilium or abnormal accumulation of ciliary D1R caused by depletion of BBS proteins in quiescent RPE-1 cells. Nevertheless, endogenous VPAC2 and Rab8a were localized to the centrosome and cilium, and although Smo was not detectable in unstimulated cells, it exhibited strong ciliary accumulation in response to a Smo agonist in quiescent RPE-1 cells (Figure 8a). We first confirmed earlier reports(22, 57) by showing that ciliary localization of Smo in response to stimulation, along with ciliary localization of VPAC2, was greatly diminished in cells depleted of BBS proteins (Figure 8a). Ablation of BBS proteins also abolished ciliary targeting of Rab8a (Figure 8a), consistent with the notion that this GTPase is a downstream effector of the BBSome. In contrast, centrosomal targeting of VPAC2 or Rab8a remained unaffected, suggesting that the BBSome may play a more prominent role in cargo delivery to cilia than cargo loading (Figure 8a). In NPHP5 or Cep290-depleted cells, ciliary Smo was also dramatically reduced but was never confined to the proximal region of cilia (Figure 8a), reminiscent of BBS5 mis-localization. Since BBS5 and Smo are known to interact(22), our data strongly suggest that a loss of ciliary BBS5 impairs Smo trafficking to cilia. Remarkably, we found that ciliary trafficking of VPAC2 remained unaffected upon suppression of NPHP5 or Cep290, whereas depletion of Cep290, but not NPHP5, resulted in exclusion of Rab8a from the ciliary membrane (Figure 8a). Centrosomal targeting of Rab8a, on the other hand, remains unaffected. Thus, despite losing BBS2 and BBS5, the BBSome sub-complex owing to NPHP5 loss can still undergo ciliary trafficking and deliver Rab8a and VPAC2 to cilia. In the absence of Cep290, the BBSome sub-complex lacks BBS2, BBS5 and BBS8, and our data suggest that an additional loss of BBS8 leads to defective trafficking of Rab8a to cilia.

Discussion

In recent years, cilia have become a topic of intense research interest because of their role in different signaling pathways and human disease. The BBSome is a multi-subunit complex required for proper cilia function, and defects in any one subunit can have detrimental consequences on complex formation and/or function, giving rise to disease(10, 12, 22). Therefore, current efforts focus on understanding how this complex is assembled and trafficked into cilia, and how it delivers cargos into the ciliary compartment. In order for the BBSome to gain access to cilia, it has to transit through a control barrier called the transition zone located at the ciliary base(23). The transition zone houses several protein complexes, including the Cep290/NPHP5 complex(24-26), whose function is incompletely understood. Here, we demonstrated for the first time that NPHP5 interacts with, and is located in close proximity to, every subunit of the BBSome, suggesting that NPHP5 associates with the holo-complex. We further showed that NPHP5 exists in a complex with Cep290 and the BBSome. Thus, these data add another layer of complexity to protein interaction network at the ciliary base, since NPHP5 is known to directly interact with Cep290(24, 25), while Cep290 interacts with BBS4(39).

How exactly does NPHP5/Cep290 modulate the function of the BBSome, or vice versa? Our data strongly suggest that NPHP5 and Cep290 specifically regulate BBSome integrity. In the absence of NPHP5 or Cep290, the BBSome sub-complex is missing at least two subunits, BBS2 and BBS5. Since BBS2 is an early and essential player in BBSome assembly(15), it is difficult to envisage how this sub-complex, or for that matter the BBSome core, is formed without BBS2.

Depletion of NPHP5 does not impinge on the levels or localization of BBS2 at the centrosome/ciliary base (Figure 5a and data not shown), suggesting that BBSome assembly, which probably takes place in this location, is not affected. Although we cannot rule out the possibility that the BBSome is assembled at another sub-cellular compartment, such process would still require BBS2. We propose that the BBSome is either partially formed or not formed in non-ciliated cells, and its assembly could only take place at full throttle at the centrosome/ciliary base during cilia formation. At this critical juncture, protein interactions between different BBSome subunits are highly dynamic and are presumed to be broken and formed readily, with NPHP5/Cep290 serving as the glue to keep certain subunits together. It is currently unknown whether the holo-complex is first formed and a subset of subunits subsequently falls apart, or whether the sub-complex represents a late assembly intermediate. Further studies are needed to distinguish these two possibilities.

In addition to BBSome integrity, a number of our observations suggest that NPHP5 and Cep290 could act as a gatekeeper to specifically control entry of the BBSome to cilia. First, the transition zone does not appear to be not grossly malformed in the absence of NPHP5 or Cep290, and further structural analysis will be needed to unequivocally prove that the transition zone maintains its normal architecture. Second, depletion of NPHP5 or Cep290 does not affect anterograde and retrograde IFT. Third, with the exception of a subset of BBSome subunits, ciliary content of several other ciliary proteins tested remains normal. Forth, ciliary trafficking of BBSome cargos due to NPHP5 or Cep290 loss is partially impaired.

In this regard, Cep290 has been postulated to form a diffusion barrier between the cilium and the cytoplasm, based on studies that it associates with a cohort of proteins at the transition zone, localizes to Y-shaped linkers that connect the axoneme to the ciliary membrane, and directly binds to membranes and microtubules(30, 60-62). The gatekeeping role of NPHP5/Cep290 is also consistent with the idea that only the holo-BBSome can traffic into cilia under normal conditions (Figure 8b). When NPHP5/Cep290 is missing, a compromised gate mistakenly allows the malformed BBSome and a subset of associated cargos to enter cilia (Figure 8b). On the contrary, the malformed sub-complex provoked by depletion of any single BBS subunit is always incompetent to undergo ciliary trafficking, since ciliary entry is restricted by NPHP5/Cep290 at the transition zone (Figure 8b).

In addition to being present at the transition zone(24, 30, 31, 48, 60-62), Cep290 is known to localize to centriolar satellites(46, 47) where it may facilitate the relocalization of BBS4 from the satellites to the cilium(54). This relocalization event is thought to be crucial for ciliary recruitment of BBS8 and possibly other BBSome subunits(54). Indeed, a previous report has shown that depletion of Cep290 diminishes ciliary localization of BBS4 and BBS8 in RPE-1 cells that are still able to form cilia(54). We also reported a loss of ciliary BBS8 here; however, we did not observe an impairment of ciliary BBS4 upon Cep290 knockdown. We speculate that this discrepancy may be due to efficiency of RNA silencing and/or detection of endogenous (our present study) versus recombinant BBS4(54). Further studies will be needed to examine the relative contribution of the two pools of Cep290 (transition zone and satellites) to BBSome ciliary trafficking. It is important to note that unlike Cep290, NPHP5 is not recruited to centriolar satellites (data not shown).

The BBSome is thought to deliver specific membrane cargos to cilia(13, 19). However, the majority of BBSome cargos have not been identified, and how different cargos are tethered to the holo-complex for transport is not known. We propose that different BBSome subunits tether a unique set of cargos to the complex for delivery to the ciliary compartment (Figure 8b). In support of this, Smo is a BBSome cargo that interacts with BBS5(22), and we have shown here that a loss of ciliary BBS5 and Smo can be triggered by ablation of NPHP5, Cep290 or BBS proteins. Likewise, the BBSome sub-complex induced by NPHP5 (or Cep290) depletion is able to promote ciliary trafficking of VPAC2 despite missing BBS2/BBS5 (and BBS8), raising the possibility that the remaining subunit(s) BBS1, BBS4, BBS7, BBS9 and/or BBIP10 tether(s) VPAC2 to the BBSome. Moreover, since a loss of ciliary BBS8 correlates with impaired trafficking of Rab8a to cilia, Rab8a may preferentially bind to BBS8. Further analysis will be needed to identify additional cargoes that are uniquely associated with each individual subunit.

Previously, it was shown that depletion of NPHP5 or Cep290 has no effect on hedgehog (Hh) signaling in osteoblasts(24). This result appears to contradict our findings that ciliary Smo, a key component of the Hh pathway, is reduced in NPHP5- or Cep290-depleted retinal epithelial cells. We speculate that NPHP5/Cep290 could function differently in different cell/tissue types. Since mutations in NPHP5/Cep290 often give rise to renal and retinal failure, these two proteins may specifically be involved in Hh signaling in these cell/tissue types. Indeed, abnormal Hh signaling has recently been reported in kidneys from Cep290 mutant mice(63), and it would be interesting to determine if such abnormality also contributes to retinal failure.

Materials and Methods

Cell Culture and Plasmids

Human ARPE-19, hTERT-RPE-1 and HEK293 cells were grown in DMEM supplemented with 10% FBS at 37°C in a humidified 5% CO2 atmosphere. To generate Flag-tagged NPHP5 fusion proteins, human NPHP5 cDNA fragments encoding residues 1-287, 157-332, 287-598(A549K), 287-598(Δ509-529) were amplified by PCR using Phusion High-Fidelity DNA Polymerase (New England Biolabs) and sub-cloned into mammalian expression vector pCBF-Flag. Human NPHP5 cDNA was also sub-cloned into mammalian vector pFlag-C-CMV to generate NPHP5-Flag. Other Flag-NPHP5 constructs were previously described(25). To generate GFP-tagged NPHP5 protein, human NPHP5 cDNAs were sub-cloned into mammalian vector pEGFP-C1 or pEGFP-N1. To generate GFP-BBS proteins, human BBS cDNAs (BBS1 to BBS12) were sub-cloned into mammalian vector pEGFP-C1. Human BBS cDNAs were also sub-cloned into mammalian vector pFlag-CMV5 or pFlag-C-CMV to generate Flag-BBS or BBS-Flag. All constructs were verified by DNA sequencing.

Antibodies

Antibodies used in this study included anti-NPHP5(25), anti-Rab8a(64), anti-Cep290 (Bethyl Laboratories), anti-centrin, anti-detyrosinated tubulin, anti-BBS4, anti-BBIP10 (Millipore), anti-BBS1, anti-BBS2, anti-BBS3, anti-BBS4, anti-BBS7, anti-BBS9, anti-Cep290, anti-γ-tubulin-FITC, anti-VPAC2, anti-NPHP1 (Santa Cruz), anti-α-tubulin, anti-acetylated tubulin, anti-BBS8, anti-Flag, anti-GFP, anti-γ-tubulin, anti-NPHP8, anti-IFT43 (Sigma-Aldrich), anti-glutamylated tubulin GT335 (Invitrogen), anti-IFT88, anti-BBS5, anti-TCTN1, anti-MKS3 (ProteinTech), anti-Smoothened, anti-CaM and anti-NPHP5 (Abcam). Specificity of antibodies against BBS1, BBS2, BBS4, BBS5 and BBS7 is presented in Figures S3 and S4.

Immunoprecipitation, Immunoblotting, and Immunofluorescence Microscopy

Cells were lysed with ELB buffer (50 mM HEPES/pH 7.4, 250 mM NaCl (or 150 mM NaCl as indicated), 5 mM EDTA/pH 8, 0.1% NP-40, 1 mM DTT, 0.5 mM PMSF, 2 μg/ml leupeptin, 2 μg aprotinin, 10 mM NaF, 50 mM β-glycerophosphate and 10% glycerol) at 4°C for 30 minutes and extracted proteins were recovered in the supernatant after centrifugation at 16,000g. For immunoprecipitation, 2 mg of the resulting supernatant was incubated with an appropriate antibody at 4°C for 1 hour and collected using protein A- or G-Sepharose. The resin was washed with lysis buffer, and bound proteins were analyzed by SDS-PAGE and immunoblotting with primary antibodies and horseradish peroxidase (HRP)-conjugated secondary antibodies (VWR). 100μg of lysate was typically loaded into the input (IN) lane. For experiments involving recombinant protein expression, Flag-tagged and/or GFP-tagged constructs were (co-)transfected into HEK293 cells, and cells were harvested 48–72 hours after transfection. Anti-Flag M2 beads (Sigma-Aldrich) or anti-GFP coupled to protein G-Sepharose were used for immunoprecipitations. For indirect immunofluorescence, cells were grown on glass coverslips, fixed with cold methanol or 4% paraformaldehyde, and permeabilized with 1% Triton X-100/PBS. Slides were blocked with 3% BSA in 0.1% Triton X-100/PBS prior to incubation with primary antibodies. Secondary antibodies used were Cy3-, Cy5- or Alexa488- conjugated donkey anti-mouse, anti-rat or anti-rabbit IgG (Jackson Immunolabs and Molecular Probes). Cells were then stained with DAPI, and slides were mounted, observed, and photographed using a Leitz DMRB (Leica) microscope (100×, NA 1.3) equipped with a Retiga EXi cooled camera. For ciliary staining, cells were pre-fixed in 0.4% paraformaldehyde for 5 minutes at 37°C, extracted with 0.5% Triton X-100 in PHEM buffer (60 mM PIPES, 25 mM HEPES, 10 mM EGTA, 2 mM $MgCl_2$, pH 6.9) for 2 minutes at

37°C, and washed with PBS before proceeding with the normal protocol. To detect ciliary Smo, cells were treated with 1 μM purmorphamine (Abcam), a Smo agonist, for 24 hours at 37°C prior to indirect immunofluorescence. Cilia length was determined using the Matlab software.

***In situ* proximity ligation assay (PLA)**

Duolink *in situ* PLA kit (Sigma) was used following manufacturer's instruction. Proliferating or quiescent RPE-1 cells grown on glass coverslips were fixed and permeabilized according to the normal immunoflourescence protocol. After pre-incubation with a blocking reagent for 1 hour, samples were incubated with two primary antibodies raised in different host species (rabbit, mouse or goat) for 1 hour at room temperature. Following this, samples were washed in Duolink Wash Buffer A twice at room temperature. PLA anti-mouse/goat MINUS probe and anti-rabbit/mouse PLUS probe were then applied to samples in a preheated humidity chamber for 1 hour at 37°C. Samples were washed in Wash Buffer A twice for 5 minutes, incubated with the Duolink Ligation Stock for 30 minutes at 37°C, washed in Wash Buffer A twice for 2 minutes, incubated with the Duolink Amplification Stock for 100 minutes at 37°C, washed in Wash Buffer B twice for 10 minutes, incubated with anti-γ-tubulin-FITC for 45 minutes, and washed in Wash Buffer B once for 5 minutes. Finally, slides were mounted with the Duolink Mounting Medium with DAPI. ImageJ (v1.43 m; Rasband, W.S., ImageJ, US National Institutes of Health, Bethesda, MD, USA) was used to quantify the PLA signal of each image. The PLA signal was assigned an arbitrary range of 0 to 1.00 (no signal, 0-0.25; weak signal, 0.26-0.50; medium signal, 0.51-0.75; strong signal, 0.76-1.00) and normalized according to the PLA signal of NPHP5/Cep290 pair, which had a value of 1.00.

RNA Interference

Transfection of siRNAs was performed using siImporter (Millipore) per manufacturer's instructions. siRNAs for Cep290, NPHP5 and the non-specific control were previously described(25). Smartpool siRNAs against human BBS1, BBS2, BBS4, BBS5 and BBS7 were obtained from Thermo Fisher Scientific.

Induction of Primary Cilia

RPE-1 or ARPE-19 cells were brought to quiescence by serum starvation for 48–72 hours and examined for cilia markers such as detyrosinated tubulin or glutamylated tubulin. ~80-90% of cells formed cilia under this condition as opposed to ~10% when cells were proliferating.

Size exclusion chromatography

2 mg of cell extract was chromatographed (ÄKTA FPLC; GE Healthcare) over a Superose-6 10/300 GL column (GE Healthcare). 1 ml fractions were collected, TCA precipitated and analyzed by SDS-PAGE. The column was calibrated with Gel Filtration Standard (Bio-Rad) containing a mixture of molecular weight markers from 17 to 670 kDa.

Acknowledgements

We thank all members of the Tsang laboratory for constructive advice. W.Y.T. was a Canadian Institutes of Health Research New Investigator and a Fonds de recherche Santé Junior 1 Research Scholar. This work was supported by the Canadian Institutes of Health Research (MOP-115033 to W.Y.T.) and the IRCM (Emmanuel Triassi scholarship to M.B).

Conflict of Interest

The authors have no conflicts of interest to declare.

References

1 Bornens, M. (2012) The centrosome in cells and organisms. *Science*, **335**, 422-426.

2 Hossain, D. and Tsang, W.Y. (2013) Centrosome dysfunction and senescence: coincidence or causality? *Aging Sci.*, **1**, 113.

3 Nigg, E.A. and Stearns, T. (2011) The centrosome cycle: Centriole biogenesis, duplication and inherent asymmetries. *Nat Cell Biol*, **13**, 1154-1160.

4 Debec, A., Sullivan, W. and Bettencourt-Dias, M. (2010) Centrioles: active players or passengers during mitosis? *Cell Mol Life Sci*, **67**, 2173-2194.

5 Kim, S. and Dynlacht, B.D. (2013) Assembling a primary cilium. *Curr Opin Cell Biol*, **25**, 506-511.

6 Avasthi, P. and Marshall, W.F. (2012) Stages of ciliogenesis and regulation of ciliary length. *Differentiation*, **83**, S30-42.

7 Tsang, W.Y. and Dynlacht, B.D. (2013) CP110 and its network of partners coordinately regulate cilia assembly. *Cilia*, **2**, 9.

8 Nigg, E.A. and Raff, J.W. (2009) Centrioles, centrosomes, and cilia in health and disease. *Cell*, **139**, 663-678.

9 Hildebrandt, F., Benzing, T. and Katsanis, N. (2011) Ciliopathies. *N Engl J Med*, **364**, 1533-1543.

10 Daniels, A.B., Sandberg, M.A., Chen, J., Weigel-DiFranco, C., Fielding Hejtmancic, J. and Berson, E.L. (2012) Genotype-phenotype correlations in Bardet-Biedl syndrome. *Arch Ophthalmol*, **130**, 901-907.

11 Zaghloul, N.A. and Katsanis, N. (2009) Mechanistic insights into Bardet-Biedl syndrome, a model ciliopathy. *J Clin Invest*, **119**, 428-437.

12 Nachury, M.V., Loktev, A.V., Zhang, Q., Westlake, C.J., Peranen, J., Merdes, A., Slusarski, D.C., Scheller, R.H., Bazan, J.F., Sheffield, V.C. *et al.* (2007) A core complex of BBS proteins cooperates with the GTPase Rab8 to promote ciliary membrane biogenesis. *Cell*, **129**, 1201-1213.

13 Loktev, A.V., Zhang, Q., Beck, J.S., Searby, C.C., Scheetz, T.E., Bazan, J.F., Slusarski, D.C., Sheffield, V.C., Jackson, P.K. and Nachury, M.V. (2008) A BBSome subunit links ciliogenesis, microtubule stability, and acetylation. *Dev Cell*, **15**, 854-865.

14 Seo, S., Baye, L.M., Schulz, N.P., Beck, J.S., Zhang, Q., Slusarski, D.C. and Sheffield, V.C. (2010) BBS6, BBS10, and BBS12 form a complex with CCT/TRiC family chaperonins and mediate BBSome assembly. *Proc Natl Acad Sci U S A*, **107**, 1488-1493.

15 Zhang, Q., Yu, D., Seo, S., Stone, E.M. and Sheffield, V.C. (2012) Intrinsic protein-protein interaction-mediated and chaperonin-assisted sequential assembly of stable bardet-biedl syndrome protein complex, the BBSome. *J Biol Chem*, **287**, 20625-20635.

16 Jin, H., White, S.R., Shida, T., Schulz, S., Aguiar, M., Gygi, S.P., Bazan, J.F. and Nachury, M.V. (2010) The conserved Bardet-Biedl syndrome proteins assemble a coat that traffics membrane proteins to cilia. *Cell*, **141**, 1208-1219.

17 Wei, Q., Zhang, Y., Li, Y., Zhang, Q., Ling, K. and Hu, J. (2012) The BBSome controls IFT assembly and turnaround in cilia. *Nat Cell Biol*, **14**, 950-957.

18 Kozminski, K.G., Johnson, K.A., Forscher, P. and Rosenbaum, J.L. (1993) A motility in the eukaryotic flagellum unrelated to flagellar beating. *Proc Natl Acad Sci U S A*, **90**, 5519-5523.

19 Mykytyn, K., Mullins, R.F., Andrews, M., Chiang, A.P., Swiderski, R.E., Yang, B., Braun, T., Casavant, T., Stone, E.M. and Sheffield, V.C. (2004) Bardet-Biedl syndrome type 4 (BBS4)-null mice implicate Bbs4 in flagella formation but not global cilia assembly. *Proc Natl Acad Sci U S A*, **101**, 8664-8669.

20 Blacque, O.E., Li, C., Inglis, P.N., Esmail, M.A., Ou, G., Mah, A.K., Baillie, D.L., Scholey, J.M. and Leroux, M.R. (2006) The WD repeat-containing protein IFTA-1 is required for retrograde intraflagellar transport. *Mol Biol Cell*, **17**, 5053-5062.

21 Lechtreck, K.F., Johnson, E.C., Sakai, T., Cochran, D., Ballif, B.A., Rush, J., Pazour, G.J., Ikebe, M. and Witman, G.B. (2009) The Chlamydomonas reinhardtii BBSome is an IFT cargo required for export of specific signaling proteins from flagella. *J Cell Biol*, **187**, 1117-1132.

22 Seo, S., Zhang, Q., Bugge, K., Breslow, D.K., Searby, C.C., Nachury, M.V. and Sheffield, V.C. (2011) A novel protein LZTFL1 regulates ciliary trafficking of the BBSome and Smoothened. *PLoS Genet*, **7**, e1002358.

23 Reiter, J.F., Blacque, O.E. and Leroux, M.R. (2012) The base of the cilium: roles for transition fibres and the transition zone in ciliary formation, maintenance and compartmentalization. *EMBO Rep*, **13**, 608-618.

24 Sang, L., Miller, J.J., Corbit, K.C., Giles, R.H., Brauer, M.J., Otto, E.A., Baye, L.M., Wen, X., Scales, S.J., Kwong, M. *et al.* (2011) Mapping the NPHP-JBTS-MKS protein network reveals ciliopathy disease genes and pathways. *Cell*, **145**, 513-528.

25 Barbelanne, M., Song, J., Ahmadzai, M. and Tsang, W.Y. (2013) Pathogenic NPHP5 mutations impair protein interaction with Cep290, a prerequisite for ciliogenesis. *Hum Mol Genet*, **22**, 2482-2494.

26 Schafer, T., Putz, M., Lienkamp, S., Ganner, A., Bergbreiter, A., Ramachandran, H., Gieloff, V., Gerner, M., Mattonet, C., Czarnecki, P.G. *et al.* (2008) Genetic and physical interaction between the NPHP5 and NPHP6 gene products. *Hum Mol Genet*, **17**, 3655-3662.

27 Williams, C.L., Li, C., Kida, K., Inglis, P.N., Mohan, S., Semenec, L., Bialas, N.J., Stupay, R.M., Chen, N., Blacque, O.E. *et al.* (2011) MKS and NPHP modules cooperate to establish basal body/transition zone membrane associations and ciliary gate function during ciliogenesis. *J Cell Biol*, **192**, 1023-1041.

28 Awata, J., Takada, S., Standley, C., Lechtreck, K.F., Bellve, K.D., Pazour, G.J., Fogarty, K.E. and Witman, G.B. (2014) Nephrocystin-4 controls ciliary trafficking of membrane and large soluble proteins at the transition zone. *J Cell Sci*.

29 Chih, B., Liu, P., Chinn, Y., Chalouni, C., Komuves, L.G., Hass, P.E., Sandoval, W. and Peterson, A.S. (2012) A ciliopathy complex at the transition zone protects the cilia as a privileged membrane domain. *Nat Cell Biol*, **14**, 61-72.

30 Garcia-Gonzalo, F.R., Corbit, K.C., Sirerol-Piquer, M.S., Ramaswami, G., Otto, E.A., Noriega, T.R., Seol, A.D., Robinson, J.F., Bennett, C.L., Josifova, D.J. *et al.* (2011) A transition zone complex regulates mammalian ciliogenesis and ciliary membrane composition. *Nat Genet*, **43**, 776-784.

31 Kee, H.L., Dishinger, J.F., Blasius, T.L., Liu, C.J., Margolis, B. and Verhey, K.J. (2012) A size-exclusion permeability barrier and nucleoporins characterize a ciliary pore complex that regulates transport into cilia. *Nat Cell Biol*, **14**, 431-437.

32 Otto, E.A., Helou, J., Allen, S.J., O'Toole, J.F., Wise, E.L., Ashraf, S., Attanasio, M., Zhou, W., Wolf, M.T. and Hildebrandt, F. (2008) Mutation analysis in nephronophthisis using a combined approach of homozygosity mapping, CEL I endonuclease cleavage, and direct sequencing. *Hum Mutat*, **29**, 418-426.

33 Otto, E.A., Loeys, B., Khanna, H., Hellemans, J., Sudbrak, R., Fan, S., Muerb, U., O'Toole, J.F., Helou, J., Attanasio, M. *et al.* (2005) Nephrocystin-5, a ciliary IQ domain protein, is mutated in Senior-Loken syndrome and interacts with RPGR and calmodulin. *Nat Genet*, **37**, 282-288.

34 Stone, E.M., Cideciyan, A.V., Aleman, T.S., Scheetz, T.E., Sumaroka, A., Ehlinger, M.A., Schwartz, S.B., Fishman, G.A., Traboulsi, E.I., Lam, B.L. *et al.* (2011) Variations in NPHP5 in patients with nonsyndromic leber congenital amaurosis and Senior-Loken syndrome. *Arch Ophthalmol*, **129**, 81-87.

35 Estrada-Cuzcano, A., Koenekoop, R.K., Coppieters, F., Kohl, S., Lopez, I., Collin, R.W., De Baere, E.B., Roeleveld, D., Marek, J., Bernd, A. *et al.* (2011) IQCB1 mutations in patients with leber congenital amaurosis. *Invest Ophthalmol Vis Sci*, **52**, 834-839.

36 Chiang, A.P., Beck, J.S., Yen, H.J., Tayeh, M.K., Scheetz, T.E., Swiderski, R.E., Nishimura, D.Y., Braun, T.A., Kim, K.Y., Huang, J. *et al.* (2006) Homozygosity mapping with SNP arrays identifies TRIM32, an E3 ubiquitin ligase, as a Bardet-Biedl syndrome gene (BBS11). *Proc Natl Acad Sci U S A*, **103**, 6287-6292.

37 Luo, X., He, Q., Huang, Y. and Sheikh, M.S. (2005) Cloning and characterization of a p53 and DNA damage down-regulated gene PIQ that codes for a novel calmodulin-binding IQ motif protein and is up-regulated in gastrointestinal cancers. *Cancer Res*, **65**, 10725-10733.

38 Soderberg, O., Gullberg, M., Jarvius, M., Ridderstrale, K., Leuchowius, K.J., Jarvius, J., Wester, K., Hydbring, P., Bahram, F., Larsson, L.G. *et al.* (2006) Direct observation of individual endogenous protein complexes in situ by proximity ligation. *Nat Methods*, **3**, 995-1000.

39 Zhang, Y., Seo, S., Bhattarai, S., Bugge, K., Searby, C.C., Zhang, Q., Drack, A.V., Stone, E.M. and Sheffield, V.C. (2014) BBS mutations modify phenotypic expression of CEP290-related ciliopathies. *Hum Mol Genet*, **23**, 40-51.

40 Wiens, C.J., Tong, Y., Esmail, M.A., Oh, E., Gerdes, J.M., Wang, J., Tempel, W., Rattner, J.B., Katsanis, N., Park, H.W. *et al.* (2010) Bardet-Biedl syndrome-associated small GTPase ARL6 (BBS3) functions at or near the ciliary gate and modulates Wnt signaling. *J Biol Chem*, **285**, 16218-16230.

41 Dawe, H.R., Smith, U.M., Cullinane, A.R., Gerrelli, D., Cox, P., Badano, J.L., Blair-Reid, S., Sriram, N., Katsanis, N., Attie-Bitach, T. *et al.* (2007) The Meckel-Gruber Syndrome

proteins MKS1 and meckelin interact and are required for primary cilium formation. *Hum Mol Genet*, **16**, 173-186.

42 Shah, A.S., Farmen, S.L., Moninger, T.O., Businga, T.R., Andrews, M.P., Bugge, K., Searby, C.C., Nishimura, D., Brogden, K.A., Kline, J.N. *et al.* (2008) Loss of Bardet-Biedl syndrome proteins alters the morphology and function of motile cilia in airway epithelia. *Proc Natl Acad Sci U S A*, **105**, 3380-3385.

43 Ansley, S.J., Badano, J.L., Blacque, O.E., Hill, J., Hoskins, B.E., Leitch, C.C., Kim, J.C., Ross, A.J., Eichers, E.R., Teslovich, T.M. *et al.* (2003) Basal body dysfunction is a likely cause of pleiotropic Bardet-Biedl syndrome. *Nature*, **425**, 628-633.

44 Kim, J.C., Badano, J.L., Sibold, S., Esmail, M.A., Hill, J., Hoskins, B.E., Leitch, C.C., Venner, K., Ansley, S.J., Ross, A.J. *et al.* (2004) The Bardet-Biedl protein BBS4 targets cargo to the pericentriolar region and is required for microtubule anchoring and cell cycle progression. *Nat Genet*, **36**, 462-470.

45 Kim, J.C., Ou, Y.Y., Badano, J.L., Esmail, M.A., Leitch, C.C., Fiedrich, E., Beales, P.L., Archibald, J.M., Katsanis, N., Rattner, J.B. *et al.* (2005) MKKS/BBS6, a divergent chaperonin-like protein linked to the obesity disorder Bardet-Biedl syndrome, is a novel centrosomal component required for cytokinesis. *J Cell Sci*, **118**, 1007-1020.

46 Kim, J., Krishnaswami, S.R. and Gleeson, J.G. (2008) CEP290 interacts with the centriolar satellite component PCM-1 and is required for Rab8 localization to the primary cilium. *Hum Mol Genet*, **17**, 3796-3805.

47 Chang, B., Khanna, H., Hawes, N., Jimeno, D., He, S., Lillo, C., Parapuram, S.K., Cheng, H., Scott, A., Hurd, R.E. *et al.* (2006) In-frame deletion in a novel centrosomal/ciliary protein CEP290/NPHP6 perturbs its interaction with RPGR and results in early-onset retinal degeneration in the rd16 mouse. *Hum Mol Genet*, **15**, 1847-1857.

48 Tsang, W.Y., Bossard, C., Khanna, H., Peranen, J., Swaroop, A., Malhotra, V. and Dynlacht, B.D. (2008) CP110 suppresses primary cilia formation through its interaction with CEP290, a protein deficient in human ciliary disease. *Dev Cell*, **15**, 187-197.

49 Shiba, D., Yamaoka, Y., Hagiwara, H., Takamatsu, T., Hamada, H. and Yokoyama, T. (2009) Localization of Inv in a distinctive intraciliary compartment requires the C-terminal ninein-homolog-containing region. *J Cell Sci*, **122**, 44-54.

50 Shiba, D., Manning, D.K., Koga, H., Beier, D.R. and Yokoyama, T. (2010) Inv acts as a molecular anchor for Nphp3 and Nek8 in the proximal segment of primary cilia. *Cytoskeleton (Hoboken)*, **67**, 112-119.

51 Dorn, K.V., Hughes, C.E. and Rohatgi, R. (2012) A Smoothened-Evc2 complex transduces the Hedgehog signal at primary cilia. *Dev Cell*, **23**, 823-835.

52 Chamling, X., Seo, S., Searby, C.C., Kim, G., Slusarski, D.C. and Sheffield, V.C. (2014) The centriolar satellite protein AZI1 interacts with BBS4 and regulates ciliary trafficking of the BBSome. *PLoS Genet*, **10**, e1004083.

53 Graser, S., Stierhof, Y.D., Lavoie, S.B., Gassner, O.S., Lamla, S., Le Clech, M. and Nigg, E.A. (2007) Cep164, a novel centriole appendage protein required for primary cilium formation. *J Cell Biol*, **179**, 321-330.

54 Stowe, T.R., Wilkinson, C.J., Iqbal, A. and Stearns, T. (2012) The centriolar satellite proteins Cep72 and Cep290 interact and are required for recruitment of BBS proteins to the cilium. *Mol Biol Cell*, **23**, 3322-3335.

55 Zhang, Q., Seo, S., Bugge, K., Stone, E.M. and Sheffield, V.C. (2012) BBS proteins interact genetically with the IFT pathway to influence SHH-related phenotypes. *Hum Mol Genet*, **21**, 1945-1953.

56 Berbari, N.F., Lewis, J.S., Bishop, G.A., Askwith, C.C. and Mykytyn, K. (2008) Bardet-Biedl syndrome proteins are required for the localization of G protein-coupled receptors to primary cilia. *Proc Natl Acad Sci U S A*, **105**, 4242-4246.

57 Soetedjo, L., Glover, D.A. and Jin, H. (2013) Targeting of vasoactive intestinal peptide receptor 2, VPAC2, a secretin family G-protein coupled receptor, to primary cilia. *Biol Open*, **2**, 686-694.

58 Domire, J.S., Green, J.A., Lee, K.G., Johnson, A.D., Askwith, C.C. and Mykytyn, K. (2011) Dopamine receptor 1 localizes to neuronal cilia in a dynamic process that requires the Bardet-Biedl syndrome proteins. *Cell Mol Life Sci*, **68**, 2951-2960.

59 Zhang, Q., Nishimura, D., Vogel, T., Shao, J., Swiderski, R., Yin, T., Searby, C., Carter, C.S., Kim, G., Bugge, K. *et al.* (2013) BBS7 is required for BBSome formation and its absence in mice results in Bardet-Biedl syndrome phenotypes and selective abnormalities in membrane protein trafficking. *J Cell Sci*, **126**, 2372-2380.

60 Craige, B., Tsao, C.C., Diener, D.R., Hou, Y., Lechtreck, K.F., Rosenbaum, J.L. and Witman, G.B. (2010) CEP290 tethers flagellar transition zone microtubules to the membrane and regulates flagellar protein content. *J Cell Biol*, **190**, 927-940.

61 Drivas, T.G., Holzbaur, E.L. and Bennett, J. (2013) Disruption of CEP290 microtubule/membrane-binding domains causes retinal degeneration. *J Clin Invest*, **123**, 4525-4539.

62 Gorden, N.T., Arts, H.H., Parisi, M.A., Coene, K.L., Letteboer, S.J., van Beersum, S.E., Mans, D.A., Hikida, A., Eckert, M., Knutzen, D. *et al.* (2008) CC2D2A is mutated in Joubert syndrome and interacts with the ciliopathy-associated basal body protein CEP290. *Am J Hum Genet*, **83**, 559-571.

63 Hynes, A.M., Giles, R.H., Srivastava, S., Eley, L., Whitehead, J., Danilenko, M., Raman, S., Slaats, G.G., Colville, J.G., Ajzenberg, H. *et al.* (2014) Murine Joubert syndrome reveals Hedgehog signaling defects as a potential therapeutic target for nephronophthisis. *Proc Natl Acad Sci U S A*, **111**, 9893-9898.

64 Peranen, J., Auvinen, P., Virta, H., Wepf, R. and Simons, K. (1996) Rab8 promotes polarized membrane transport through reorganization of actin and microtubules in fibroblasts. *J Cell Biol*, **135**, 153-167.

Figure legends

Figure 1. NPHP5 interacts with the BBSome.

(**a**) Flag-NPHP5 and the indicated GFP proteins were co-expressed in HEK293 cells, and lysates were immunoprecipitated with an anti-Flag antibody. The resulting immunoprecipitates were Western blotted with anti-Flag or anti-GFP antibodies. IN, input. (**b**) The indicated N-terminal or C-terminal tagged recombinant NPHP5 or BBS5 proteins were co-expressed in HEK293 cells, and lysates were immunoprecipitated with an anti-Flag antibody. The resulting immunoprecipitates were Western blotted with anti-Flag or anti-GFP antibodies. IN, input. (**c**) HEK293 cell extract was chromatographed on a Superose-6 gel filtration column, and the resulting fractions were Western blotted with indicated antibodies. Estimated molecular weights are indicated. IN, input; F, fraction. (**d**) Western blotting of endogenous Cep290, NPHP5, BBS2, BBS5 and CaM after immunoprecipitation of HEK293 cell extracts with anti-Flag (control), anti-BBS2 or anti-BBS5 antibodies. IN, input.

Figure 2. NPHP5 possesses two distinct BBSome-binding sites.

(**a**) Left panel: Flag (control), Flag-tagged full-length NPHP5 (1-598) or the indicated fragments of Flag-tagged NPHP5 were co-expressed with the indicated GFP-BBS proteins in HEK293 cells, and lysates were immunoprecipitated with an anti-Flag antibody.

Flag-NPHP5 and GFP-BBS were detected after western blotting the resulting immunoprecipitates. IN, input. Right panel: GFP (control), GFP-tagged full-length NPHP5 (1-598) or the indicated fragments of GFP-tagged NPHP5 were co-expressed with BBS5-Flag in HEK293 cells, and lysates were immunoprecipitated with an anti-Flag antibody. BBS5-Flag and GFP-NPHP5 were detected after western blotting the resulting immunoprecipitates. IN, input. (**b-c**) Flag (control) or the indicated fragments of Flag-tagged NPHP5 were co-expressed with the indicated GFP-BBS proteins in HEK293 cells, and lysates were immunoprecipitated with an anti-Flag antibody. Flag-NPHP5 and GFP-BBS were detected after western blotting the resulting immunoprecipitates. IN, input. (**d**) Summary of the results of *in vivo* binding experiments. Known domains of NPHP5 (centrosomal localization, CaM-binding and Cep290-binding domains) are indicated as in (189). Each fragment used for the study takes into account the position of these domains so that a given domain is not prematurely truncated. +, interaction; -, no interaction; ND, not determined.

Figure 3. NPHP5 and Cep290 bind to the BBSome independently of each other.

(**a**) Flag (control) or the indicated fragments and mutants of Flag-tagged NPHP5 were co-expressed with the indicated GFP-BBS proteins in HEK293 cells, and lysates were immunoprecipitated with an anti-Flag antibody. Flag-NPHP5, GFP-BBS and endogenous Cep290 were detected after western blotting the resulting immunoprecipitates. IN, input. (**b-c**) Western blotting of endogenous Cep290, NPHP5, BBS2 and BBS5 after immunoprecipitation of HEK293 cell extracts with anti-Flag (control), anti-BBS2 or anti-BBS5 antibodies. Extracts were transfected with control (siNSp), NPHP5 (siNPHP5) or Cep290 (siCep290) siRNAs prior to immunoprecipitation. IN, input.

Figure 4. NPHP5/Cep290 interaction with the BBSome in ciliated and non-ciliated cells.
(**a**) *In situ* PLA using antibodies against NPHP5 and Cep290 was performed to visualize protein-protein interaction (PLA signal in red) in proliferating (non-ciliated) and quiescent (ciliated) RPE-1 cells. Cells were co-stained with γ-tubulin (green) to visualize the centrosome. No PLA signal was detected when one or both antibodies were missing, or when an NPHP5 antibody was combined with an irrelevant antibody, glutamylated tubulin (GT335). No Ab, no antibody. (**b-c**) *In situ* PLAs using the indicated combinations of antibodies were performed to visualize protein-protein interaction (PLA signal in red) in proliferating (non-ciliated) and quiescent (ciliated) RPE-1 cells. Cells were co-stained with γ-tubulin (green) to visualize the centrosome.

Figure 5. Depletion of NPHP5 or Cep290 impairs ciliary localization of a subset of BBSome subunits.
(**a**) Western blotting of Cep290, BBS2, BBS4, BBS5 and NPHP5 in HEK293 cells treated with control (siNSp), NPHP5 (siNPHP5) or Cep290 (siCep290) siRNAs. α-tubulin was used as loading control. (**b**) RPE-1 cells transfected with control (siNSp), NPHP5 (siNPHP5) or Cep290 (siCep290) siRNAs and induced to quiescence were stained with the indicated combinations of antibodies. Detyr-tub, detyrosinated tubulin; GT335, polyglutamylated tubulin. (**c**) The percentages of quiescent RPE-1 cells showing BBS staining along the entire length of cilia were determined using detyrosinated tubulin or GT335 as a ciliary marker. (**d**) (Top) The percentages of quiescent RPE-1 cells showing BBS2 staining along the proximal region of cilia were determined. (Bottom) Cilia length was measured with different markers (BBS2, detyrosinated tubulin, polyglutamylated tubulin and IFT88).

In (**c–d**), at least 100 cells were counted and/or measured per siRNA condition, and error bars represent average of three independent experiments.

Figure 6. NPHP5 and Cep290 regulate BBSome integrity.

(**a**) ARPE-19 cells transfected with control siRNA (siNSp) or siRNA targeting NPHP5 3'UTR (siNPHP5) and plasmid expressing an irrelevant Flag-tagged protein (control), full-length Flag-NPHP5 (1-598) or a C-terminal fragment of Flag-tagged NPHP5 (287-598) lacking a BBSome-binding site, induced to quiescence, were stained with antibodies against Flag (green), detyrosinated-tubulin or GT335 (blue), and BBS2, BBS4 or BBS5 (red). (**b**) (Top) The percentages of quiescent cells with ciliary BBS2, BBS4 or BBS5 staining were determined using either detyrosinated tubulin or GT335 as a ciliary marker. At least 100 transfected cells were counted per condition, and error bars represent average of three independent experiments. (Bottom left) Western blotting of Flag, with α-tubulin used as loading control. (Bottom right) Cells were processed for immunofluorescence and stained with anti-NPHP5 (red) antibody. (**c**) Extract from control (siNSp) or NPHP5 siRNA-depleted (siNPHP5) HEK293 cells was chromatographed on a Superose-6 gel filtration column, and the resulting fractions were Western blotted with indicated antibodies. Estimated molecular weights are indicated. IN, input; F, fraction. (**d**) GFP or GFP-BBS4 were expressed in HEK293 cells treated with control (siNSp), NPHP5 (siNPHP5) or Cep290 (siCep290) siRNAs and immunoprecipitated from lysates. Endogenous (*) and recombinant BBS4 (**), along with endogenous BBS1, BBS2, BBS5 and BBS8 were detected after western blotting the resulting immunoprecipitates. Western blotting of NPHP5 and Cep290 were performed to monitor knockdown efficiency. IN, input. α-tubulin was used as loading control.

Figure 7. Cep290 regulates the BBSome integrity and depletion of NPHP5 or Cep290 does not impair the localization of transition zone proteins.

(**a**) ARPE-19 cells transfected with control (siNSp) or Cep290 (siCep290) siRNA and plasmid expressing an irrelevant Flag-tagged protein (control) or full-length Flag-NPHP5 (1-598), induced to quiescence, were stained with antibodies against Flag (green), detyrosinated-tubulin or GT335 (blue), and BBS2, BBS5 or BBS8 (red). (**B**) (Left) The percentages of quiescent cells with ciliary BBS2, BBS5 or BBS8 staining were determined using either detyrosinated tubulin or GT335 as a ciliary marker. At least 100 transfected cells were counted per condition, and error bars represent average of three independent experiments. (Right) Western blotting of Flag and Cep290. α-tubulin was used as loading control. (**c-d**) RPE-1 cells transfected with control (NSp), NPHP5 (siNPHP5) or Cep290 (siCep290) siRNAs and induced to quiescence were stained with the indicated antibodies.

Figure 8. Depletion of NPHP5 or Cep290 partially disrupts ciliary trafficking of BBSome cargos.

(**a**) (Left) RPE-1 cells transfected with control (NSp), NPHP5 (siNPHP5), Cep290 (siCep290), BBS2 (siBBS2) or BBS5 (siBBS5) siRNAs, induced to quiescence, were stained with antibodies against Smo, VPAC2 or Rab8a (red) and GT335 (green). In the case of Smo, cells were treated with a Smo agonist prior to immunofluorescence. (Top right) The percentage of quiescent cells with ciliary Smo, untreated (unstimulated) or treated with a Smo agonist (stimulated), was determined using GT335 as a ciliary marker. (Bottom right) The fold decrease in the percentage of cells with ciliary Smo, VPAC2 or Rab8a was determined using GT335 as a ciliary marker. At least 100 cells were scored per condition, and error bars represent average of three independent experiments.

(**b**) Model illustrating the roles of NPHP5 and Cep290 in BBSome homeostasis. (I) NPHP5 and Cep290 at the ciliary base serve two purposes: they regulate BBSome integrity and form a diffusion barrier that allows the selective passage of the holo-complex into the cilium. Although NPHP5 and Cep290 interact with multiple subunits, their interaction with BBS4/BBS8 is shown for the sake of simplicity. (II) In the absence of NPHP5, BBS2 and BBS5 dissociate from the BBSome, and BBS5 is completely mis-localized from the cilium. A fraction of BBS2 exhibits similar mis-localization pattern, whereas another fraction is confined to the proximal region of the cilium through an undefined mechanism. A faulty barrier permits the BBSome sub-complex to traffic into the cilium. Ciliary trafficking of Smo is impaired, since this cargo normally interacts with BBS5. (III) A loss of Cep290 induces NPHP5 mis-localization and promotes further dissociation of BBS8 from the BBSome; yet this sub-complex is also allowed to undergo ciliary trafficking. Rab8a ciliary trafficking is additionally impaired, but its centrosomal localization is unaffected. (IV and V) In contrast, a loss of any single BBS subunit, irrespective of its effects on BBSome assembly, is excluded from the cilium due to an intact barrier created by NPHP5/Cep290. Inactivation of BBS2 is known to destabilize BBS7 and prevents early BBSome assembly, whereas inactivation of BBS5 has minor impact on assembly(188, 211). As a consequence, Smo, Rab8a and VPAC2 are unable to enter the ciliary compartment, and Rab8a and VPAC2 remain at the centrosome. We speculate that Rab8a is transported into the cilium by tethering to BBS8, whereas ciliary trafficking of VPAC2 likely requires interaction with BBS1, BBS4, BBS7, BBS9 and/or BBIP10. The interaction between VPAC2 and BBS1 is shown for simplicity.

Supplemental figure legends

Figure S1. NPHP5 binds to the BBSome.

(**a**) NPHP5-Flag and the indicated GFP proteins were expressed in HEK293 cells, and lysates were immunoprecipitated with an anti-Flag antibody. The resulting immunoprecipitates were Western blotted with anti-Flag or anti-GFP antibodies. IN, input. (**b**) Same as in Figure 1a except that lysis buffer contained 150 mM NaCl. (**c**) GFP-NPHP5 and the indicated Flag proteins were expressed in HEK293 cells, and lysates were immunoprecipitated with an anti-Flag antibody. The resulting immunoprecipitates were Western blotted with anti-Flag or anti-GFP antibodies. IN, input.

Figure S2. Co-localization studies of NPHP5 and BBSome subunits.

(**a-b**) Proliferating (non-ciliated) or quiescent (ciliated) RPE-1 cells were processed for immunofluorescence with anti-NPHP5 (red) and anti-BBS1, BBS2, BBS4, BBS5, BBS7, BBS8, BBS9 or BBIP10 (green) antibodies.

Figure S3. Depletion of BBS2 or BBS5 disrupts trafficking of the BBSome to cilia but does not affect localization or protein levels of NPHP5.

(**a**) RPE-1 cells transfected with control (siNSp), BBS2 (siBBS2) or BBS5 (siBBS5) siRNAs, induced to quiescence, were processed for immunofluorescence with anti-NPHP5, anti-BBS2 or anti-BBS5 (red) and anti-detyrosinated tubulin or GT335 (green) antibodies. DNA was stained with DAPI (blue). (**b**) Western blotting of BBS2, BBS5 or NPHP5 in HEK293 cells treated with control (siNSp), BBS2 (siBBS2) or BBS5 (siBBS5) siRNAs. α-tubulin was used as loading control.

(**c**) RPE-1 cells transfected with control (siNSp), BBS2 (siBBS2) or BBS5 (siBBS5) siRNAs, induced to quiescence, were stained with the indicated BBS antibodies (red) and antibodies against detyrosinated tubulin or GT335 (green).

Figure S4. Specificity of antibodies against BBS1, BBS4 and BBS7.

(**a**) RPE-1 cells transfected with control (siNSp), BBS1 (siBBS1), BBS4 (siBBS4) or BBS7 (siBBS7) siRNAs, induced to quiescence, were processed for immunofluorescence with anti-BBS1, anti-BBS4 or anti-BBS7 (red) and anti-detyrosinated tubulin or GT335 (green) antibodies. DNA was stained with DAPI (blue). (**b**) Western blotting of BBS1 or BBS4 in HEK293 cells treated with control (siNSp), BBS1 (siBBS1) or BBS4 (siBBS4) siRNAs. α-tubulin was used as loading control.

Figures

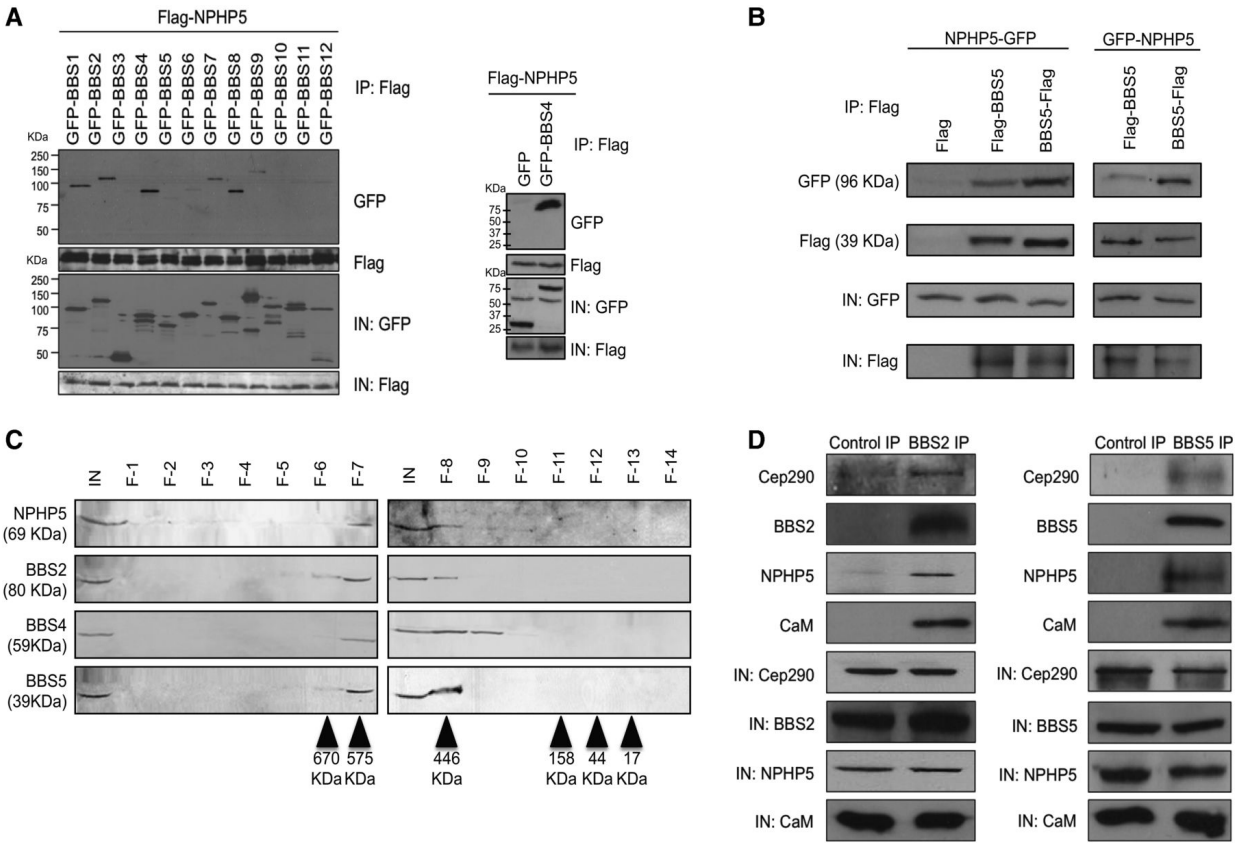

Figure 1. NPHP5 interacts with the BBSome.

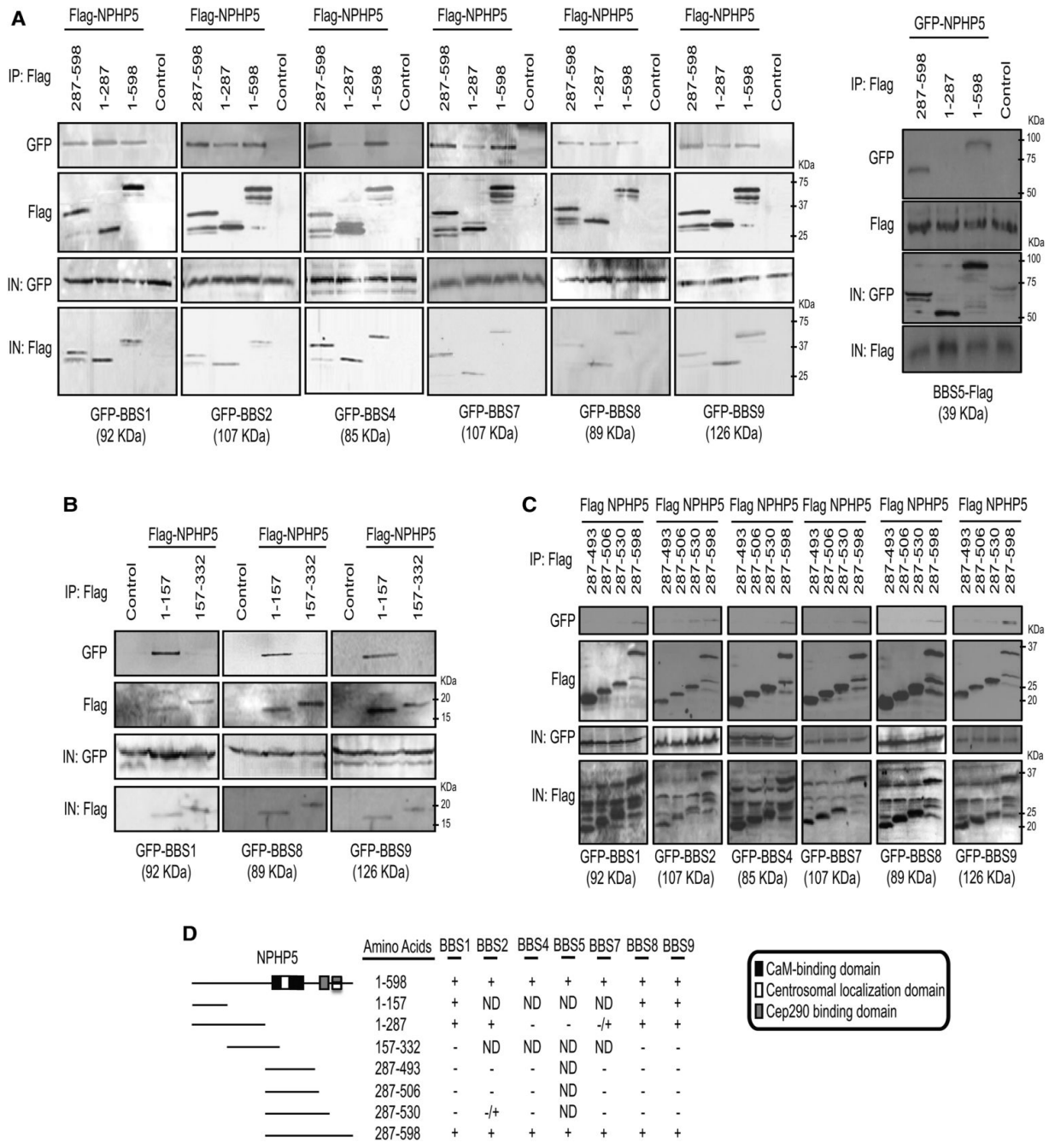

Figure 2. NPHP5 possesses two distinct BBSome-binding sites.

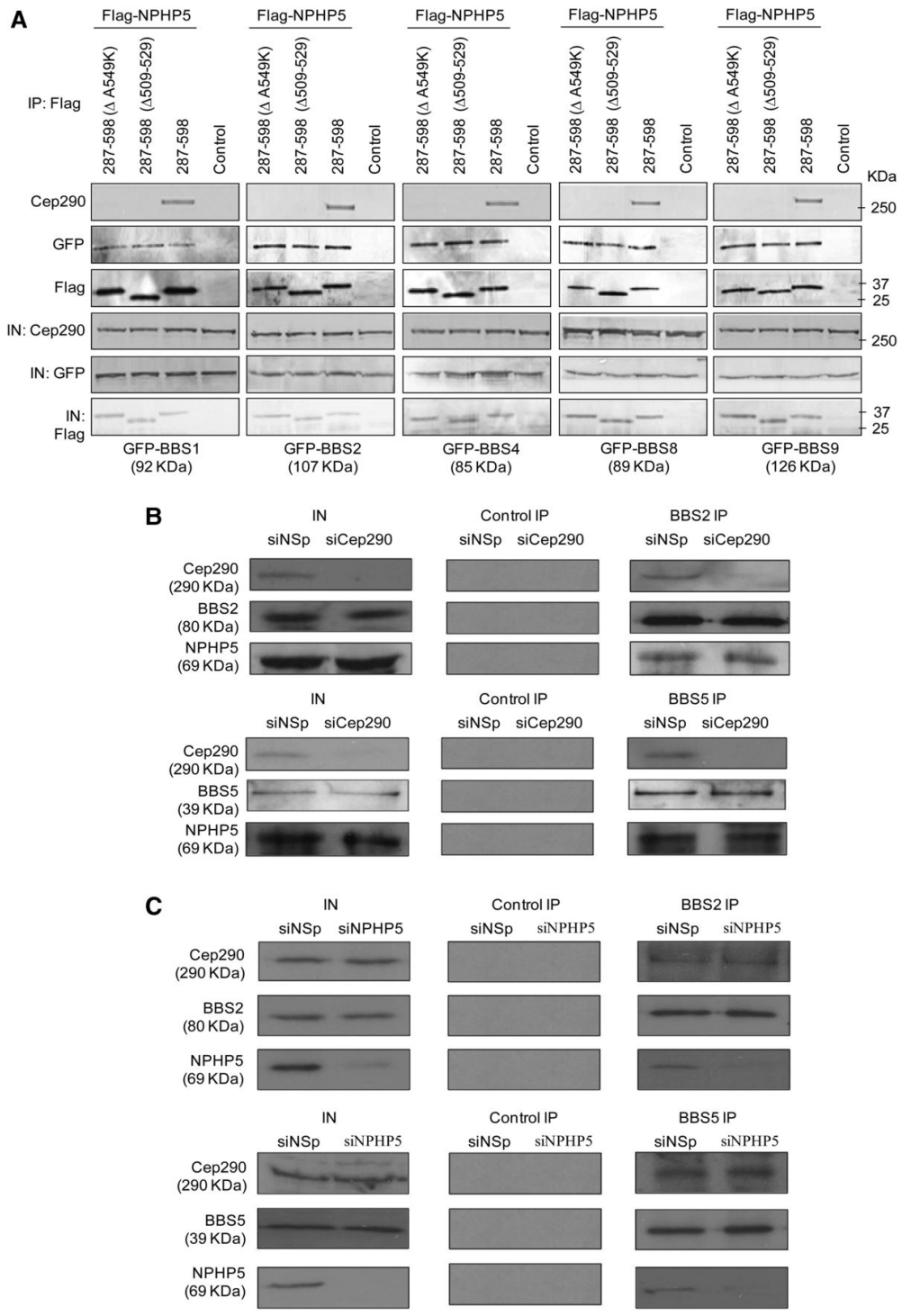

Figure 3. NPHP5 and Cep290 bind to the BBSome independently of each other.

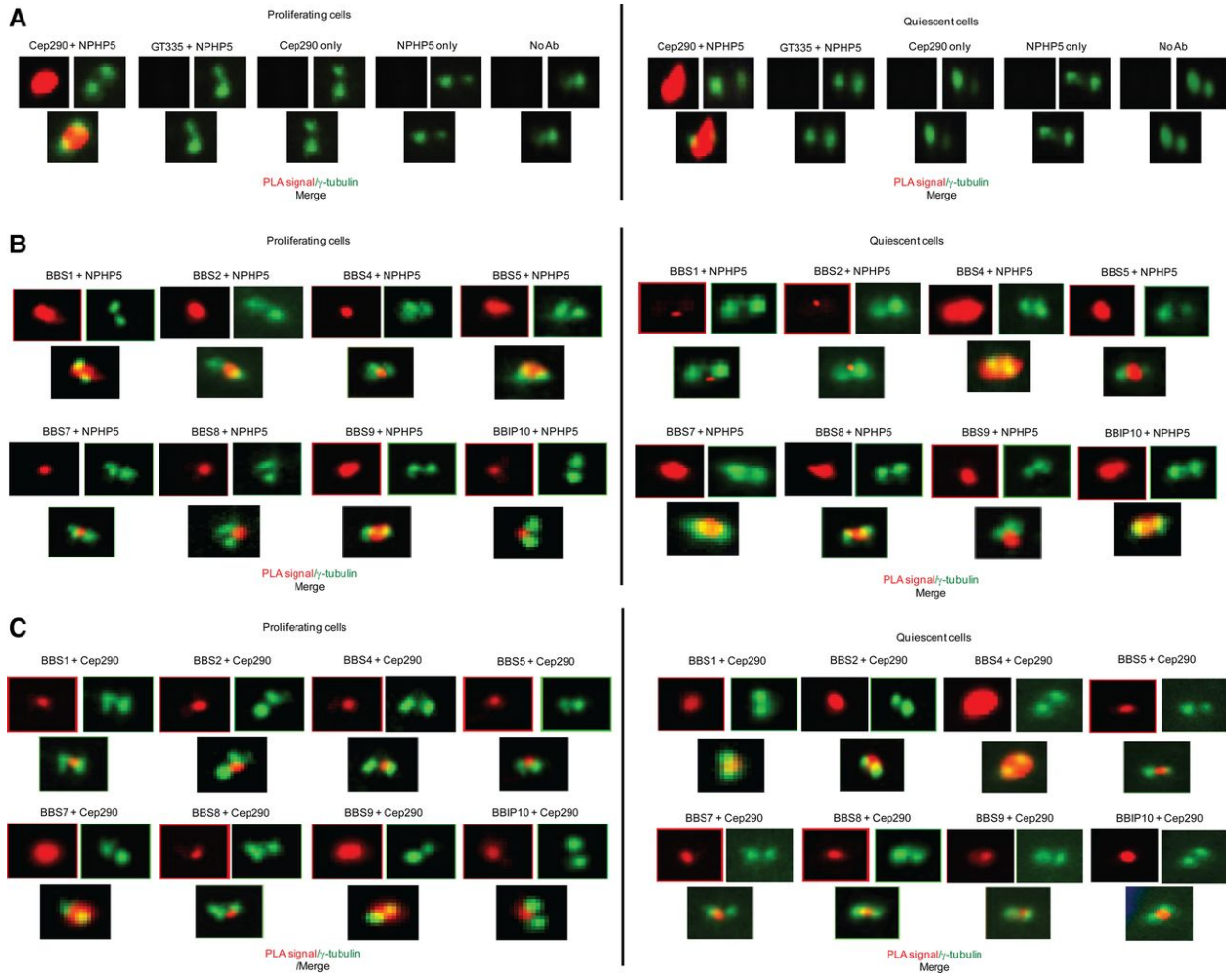

Figure 4. NPHP5/Cep290 interaction with the BBSome in ciliated and non-ciliated cells.

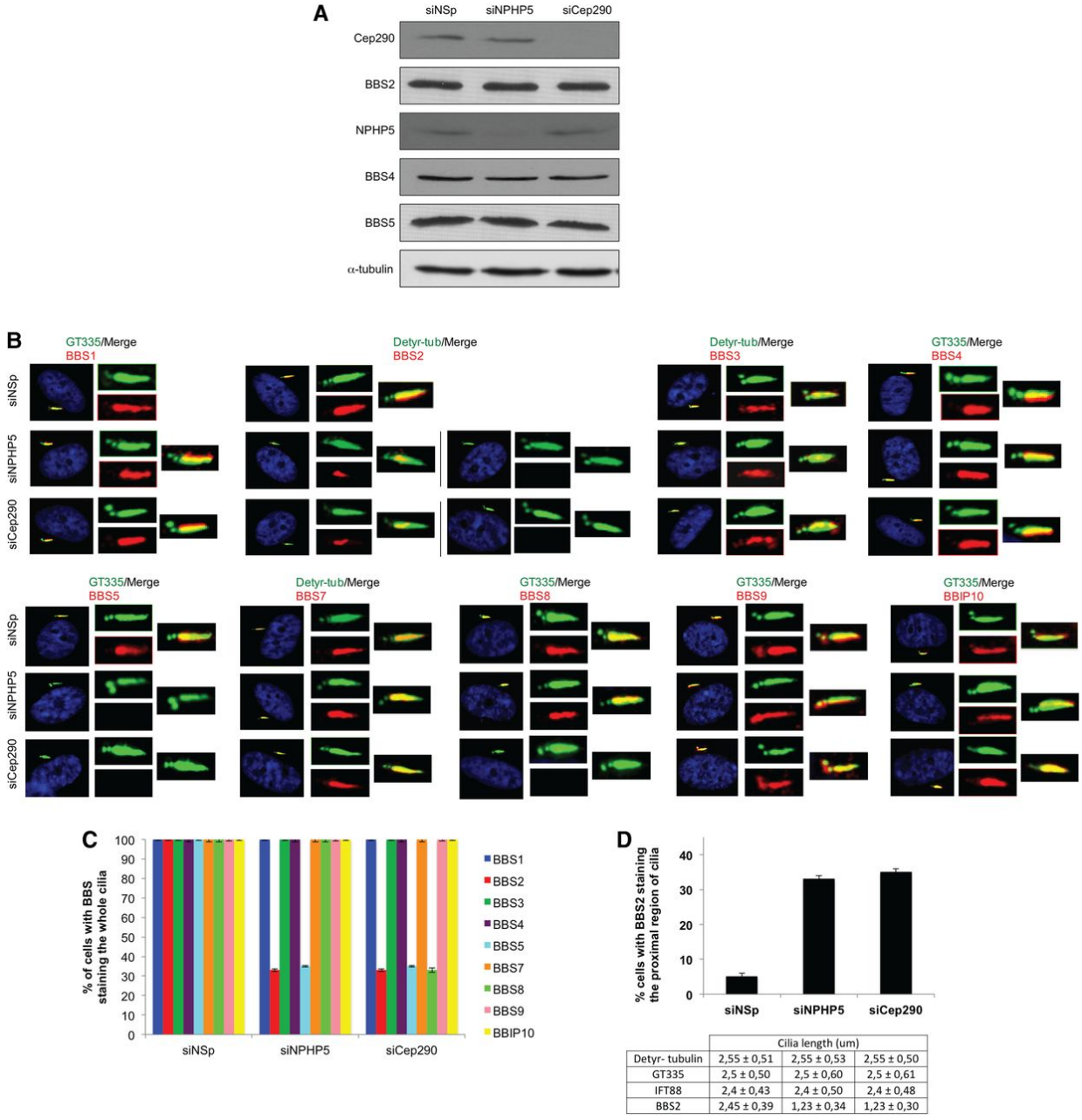

	Cilia length (um)		
Detyr- tubulin	2,55 ± 0,51	2,55 ± 0,53	2,55 ± 0,50
GT335	2,5 ± 0,50	2,5 ± 0,60	2,5 ± 0,61
IFT88	2,4 ± 0,43	2,4 ± 0,50	2,4 ± 0,48
BBS2	2,45 ± 0,39	1,23 ± 0,34	1,23 ± 0,30

Figure 5. Depletion of NPHP5 or Cep290 impairs ciliary localization of a subset of BBSome subunits.

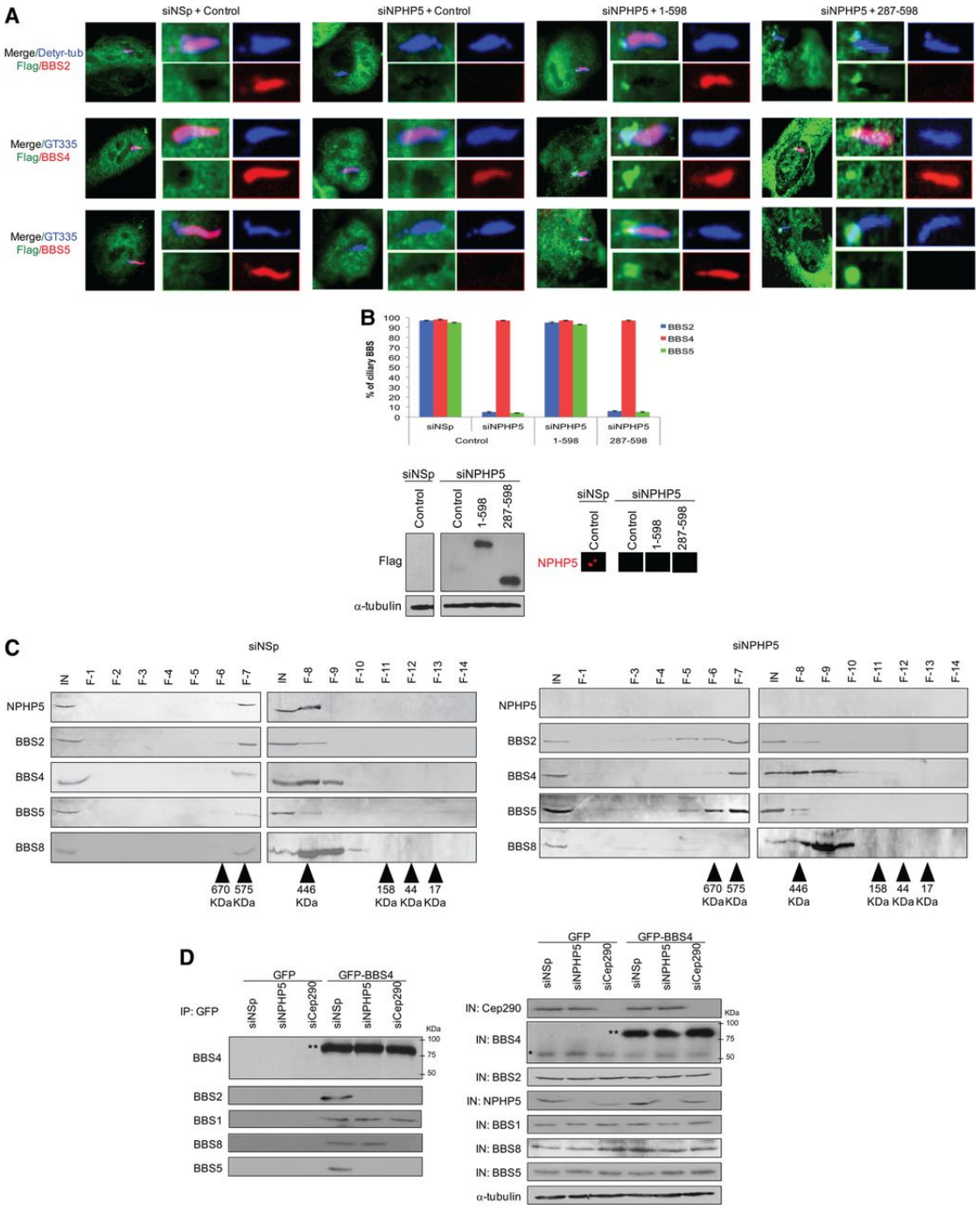

Figure 6. NPHP5 and Cep290 regulate BBSome integrity.

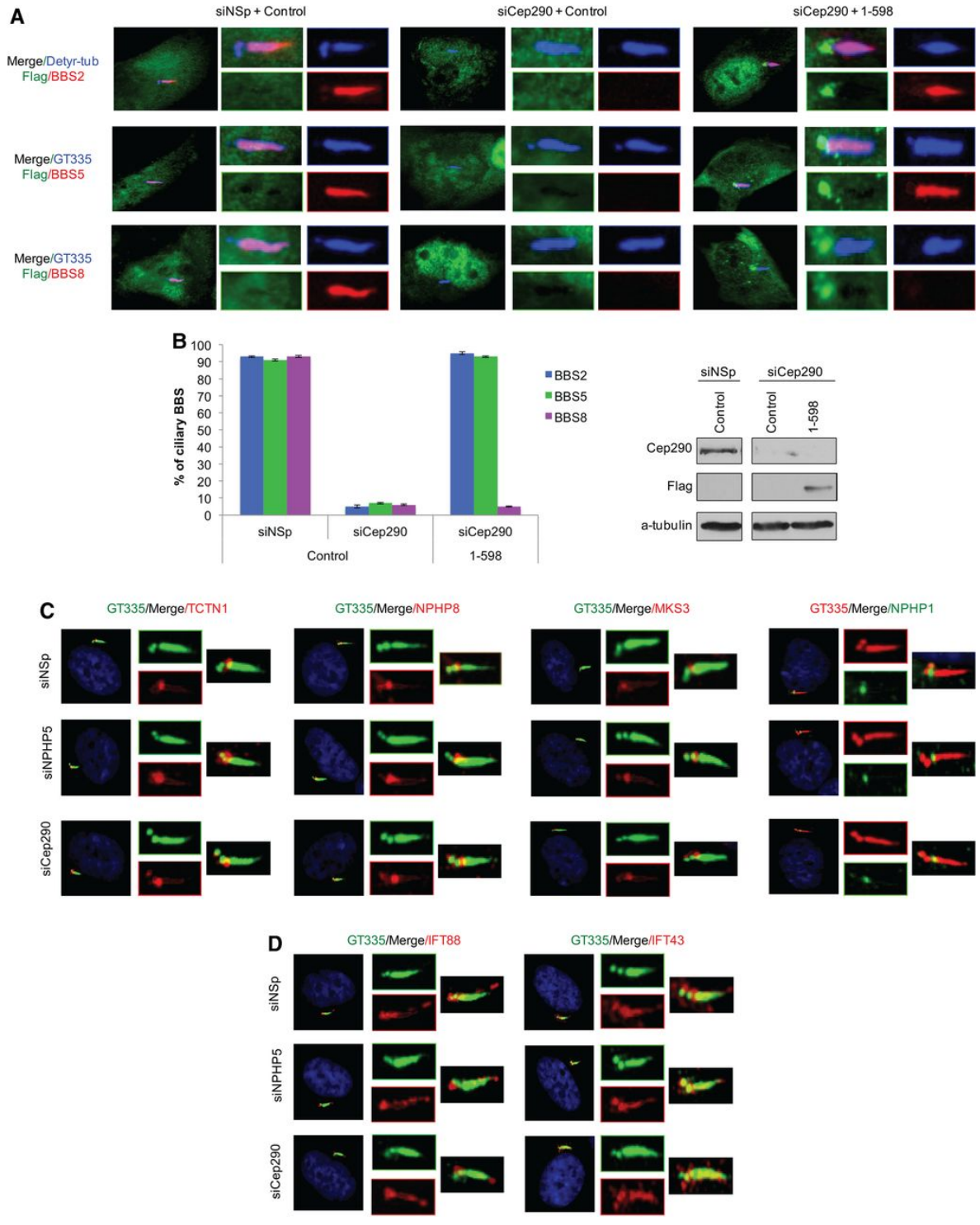

Figure 7. Cep290 regulates the BBSome integrity and depletion of NPHP5 or Cep290 does not impair the localization of transition zone proteins.

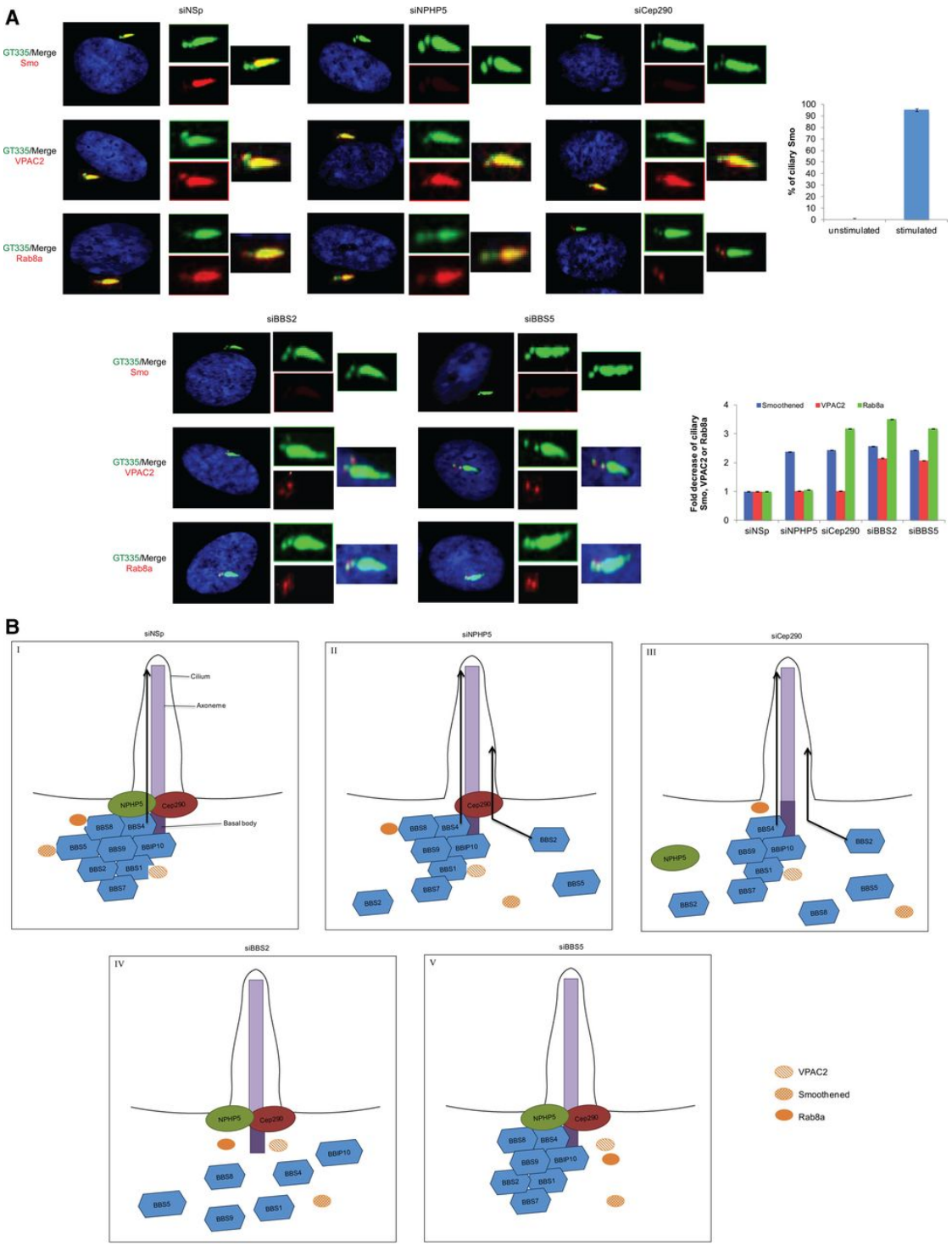

Figure 8. Depletion of NPHP5 or Cep290 partially disrupts ciliary trafficking of BBSome cargos.

Supplemental figures

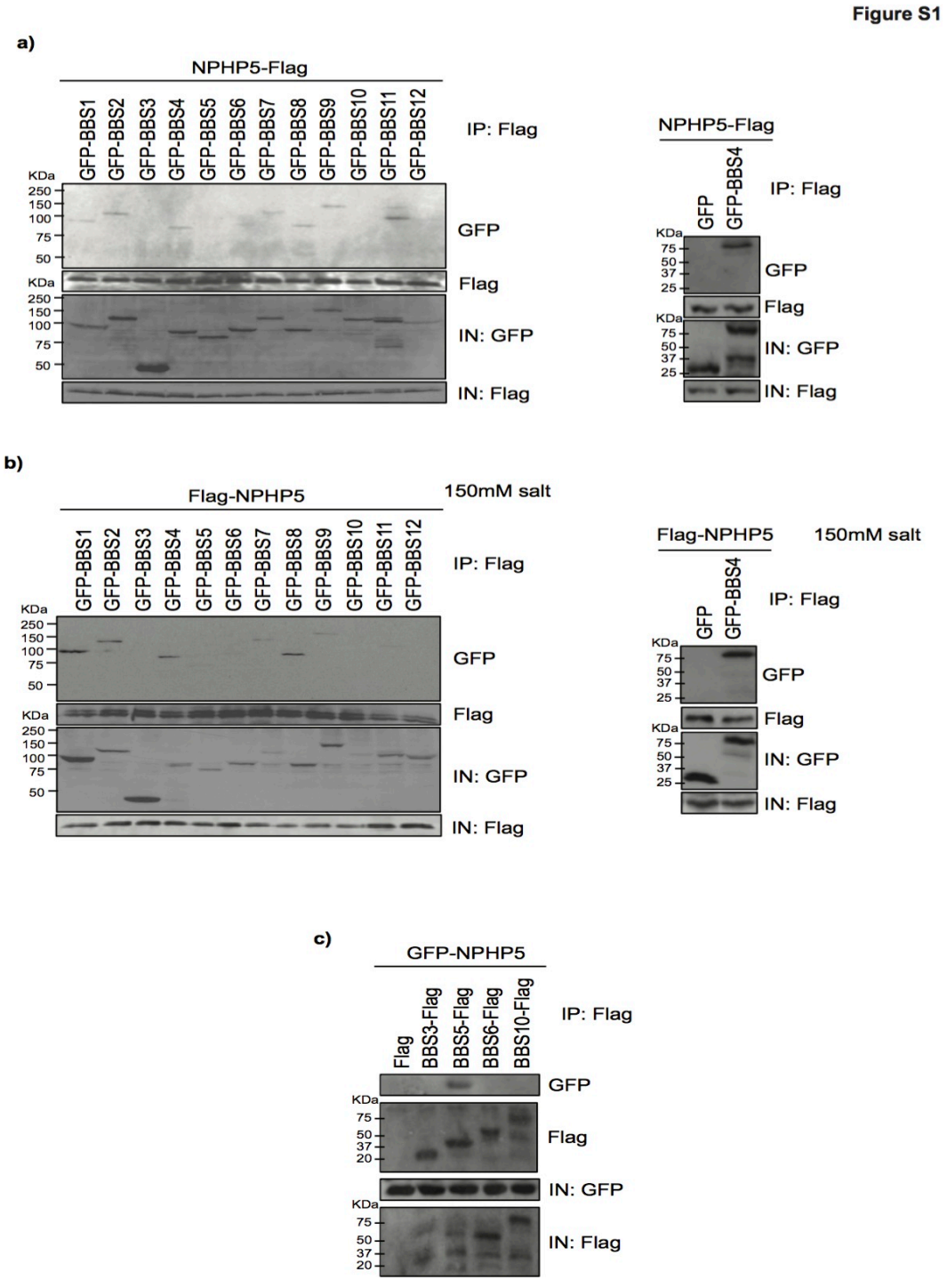

Figure S1. NPHP5 binds to the BBSome.

Figure S2

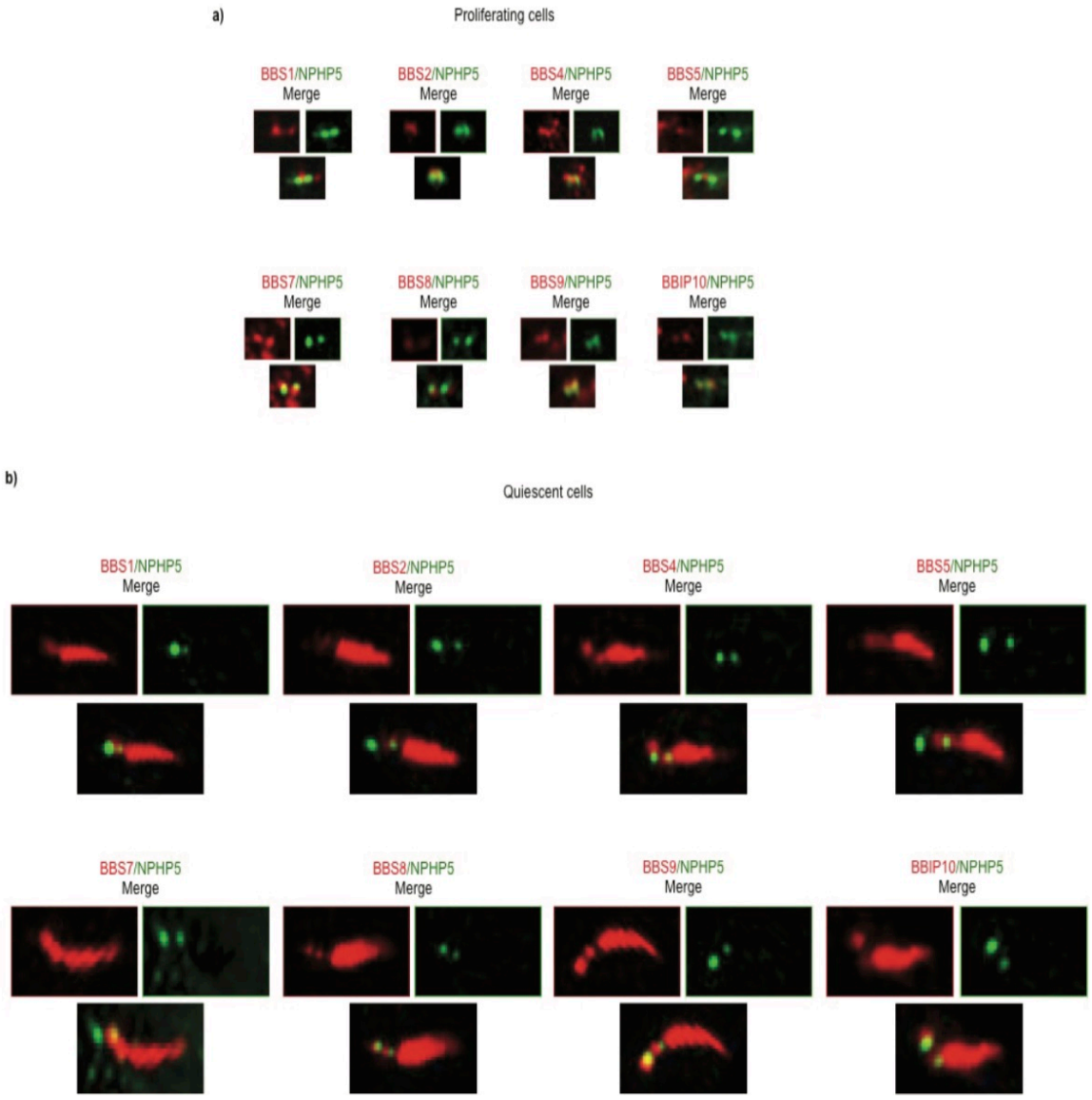

Figure S2. Co-localization studies of NPHP5 and BBSome subunits.

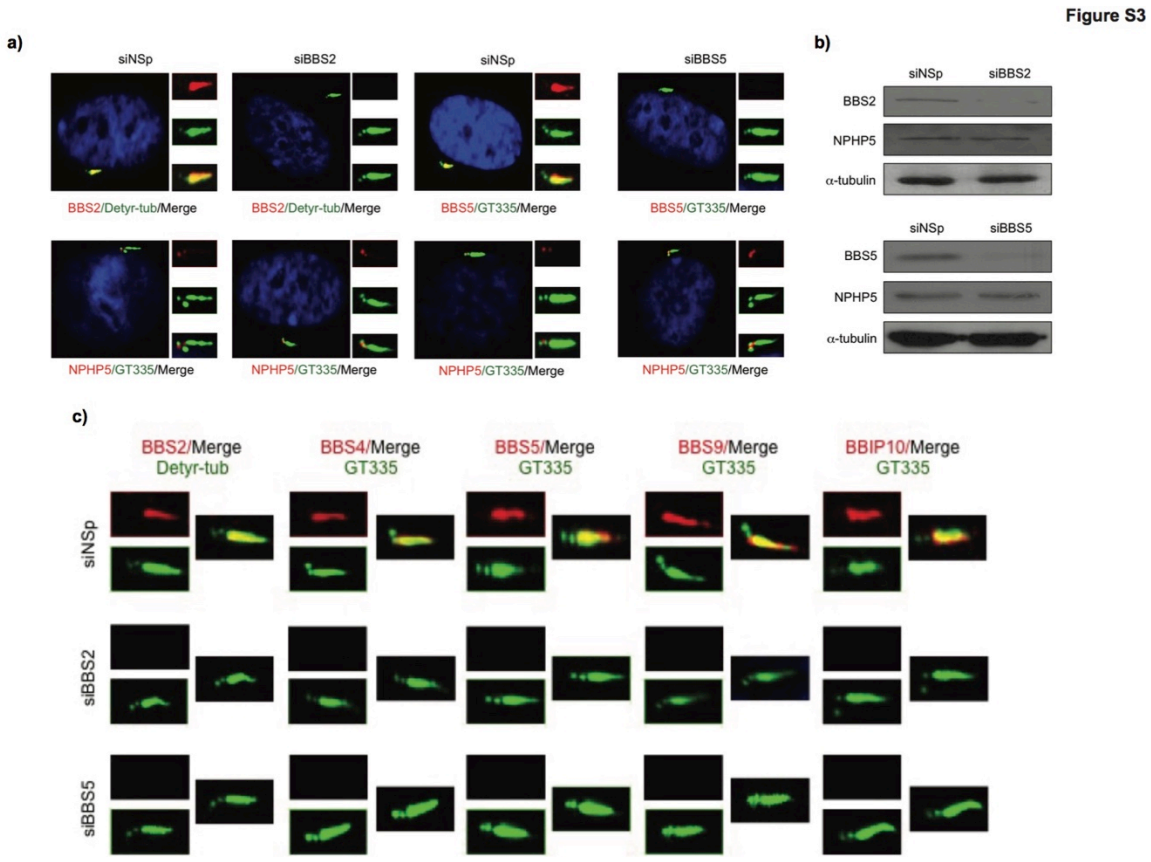

Figure S3. Depletion of BBS2 or BBS5 disrupts trafficking of the BBSome to cilia but does not affect localization or protein levels of NPHP5.

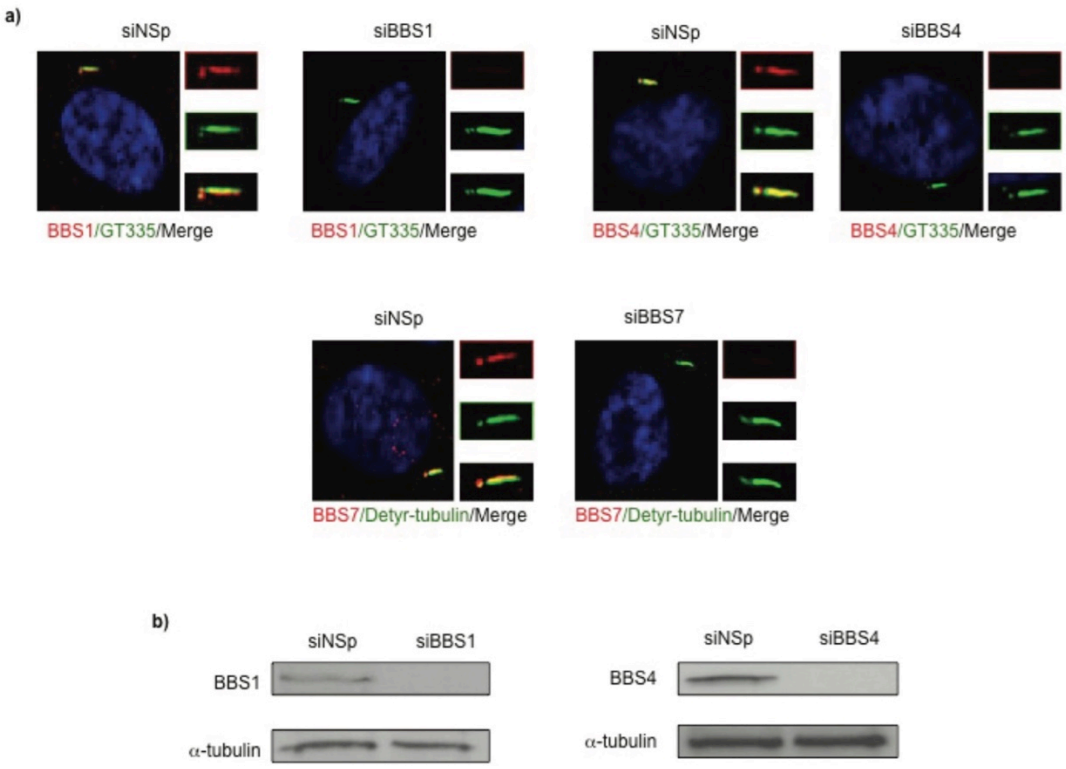

Figure S4. Specificity of antibodies against BBS1, BBS4 and BBS7.

Table

% cells	Proliferating (PLA signal intensity)				Quiescent (PLA signal intensity)			
	no	weak	medium	strong	no	weak	medium	strong
NPHP5 + BBS1	2	6	60	32	46	50	4	0
NPHP5 + BBS2	3	15	75	7	12	76	12	0
NPHP5 + BBS4	14	78	8	0	0	6	16	78
NPHP5 + BBS5	2	10	62	26	4	42	54	0
NPHP5 + BBS7	42	50	8	0	6	18	74	2
NPHP5 + BBS8	10	84	6	0	2	38	58	2
NPHP5 + BBS9	8	42	48	2	0	10	66	24
NPHP5 + BBIP10	16	82	2	0	6	20	72	2

% cells	Proliferating (PLA signal intensity)				Quiescent (PLA signal intensity)			
	no	weak	medium	strong	no	weak	Medium	strong
Cep290 + BBS1	46	52	2	0	48	50	2	0
Cep290 + BBS2	12	76	12	0	4	46	48	2
Cep290 + BBS4	46	50	4	0	0	6	14	80
Cep290 + BBS5	48	50	2	0	47	50	3	0
Cep290 + BBS7	8	44	46	2	47	53	0	0
Cep290 + BBS8	48	50	2	0	46	50	4	0
Cep290 + BBS9	4	10	54	32	10	46	42	2
Cep290 + BBIP10	48	50	2	0	9	42	48	1
Cep290 + NPHP5	0	6	24	70	0	2	16	82

Table 1

PLA signals generated from *in situ* PLAs using the indicated combinations of antibodies were quantitated and normalized. The percentages of proliferating (non-ciliated) or quiescent (ciliated) RPE-1 cells possessing no, weak, medium and strong signal for each antibody combination were determined.

Article 3 : Opposing Post-Translational Modifications Regulate Cep76 Function to Suppress Centriole Amplification

Marine Barbelanne[1,2], Andrea Chiu[1], Jin Qian[1] and William Y. Tsang[1,2,3,*]

[1] Institut de recherches cliniques de Montréal, 110 avenue des Pins Ouest, Montréal, Québec H2W 1R7, Canada

[2] Faculté de Médecine, Université de Montréal, Montréal, Québec H3C 3J7, Canada

[3] Division of Experimental Medicine, McGill University, Montréal, Québec H3A 1A3, Canada

Keywords: CDK2, cyclin A, Cep76, centriole amplification, phosphorylation, acetylation, cancer

Contributions de M.B. : Toutes les expériences sauf clonage, WB des figures 1A-C et figures S1, S8 et S9. Créations de toutes les figures/tables et participation dans l'interprétation des résultats et l'écriture du manuscrit.

Abstract

Centrioles are critical for many cellular processes including cell division and cilia assembly. The number of centrioles within a cell is under strict control, and deregulation of centriole copy number is a hallmark of cancer. The molecular mechanisms that halt centriole amplification have not been fully elucidated. Here, we found that centrosomal protein of 76 kDa (Cep76), previously shown to restrain centriole amplification, interacts with cyclin-dependent kinase 2 (CDK2) and is a bona fide substrate of this kinase. Cep76 is preferentially phosphorylated by cyclin A/CDK2 at a single site S83, and this event is crucial to suppress centriole amplification in S phase. A novel Cep76 mutation S83C identified in a cancer patient fails to prevent centriole amplification. Mechanistically, Cep76 phosphorylation inhibits activation of polo-like kinase 1 (Plk1), thereby blocking premature centriole disengagement and subsequent amplification. Cep76 can also be acetylated, and enforced acetylation at K279 dampens the protein's ability to inhibit amplification and precludes S83 phosphorylation. Acetylation of Cep76 normally occurs in G2 phase and correlates with loss of protein function. Our data suggest that temporal changes in posttranslational modifications of Cep76 during the cell cycle regulate its capacity to suppress centriole amplification, and its deregulation may contribute to malignancy.

Introduction

Centrosomes are well-known for their role in cell division (1). They are composed of a pair of centrioles surrounded by a pericentriolar matrix from which microtubules emanate and elongate. A single centrosome present in G1 phase of the cell cycle undergoes duplication in S phase. The duplicated centrosomes, once separated, establish the mitotic spindle at the onset of mitosis, ensuring faithful segregation of chromosomes into daughter cells. Centrosome duplication, like DNA replication, occurs once and only once per cell cycle and is under stringent control (2). Too few or too many centrosomes could jeopardize cell division, leading to cancer development (3). Indeed, centrosome amplification has been documented in many types of cancers (4-6) and is thought to be an important contributor to malignant transformation (5, 7-9) owing to its capacity to induce chromosome mis-segregation and cell invasion (10, 11). It is therefore of paramount importance to decipher the poorly understood mechanisms governing the fidelity of centrosome duplication.

Cyclin-dependent kinase 2 (CDK2) is a critical regulator of the cell cycle associated with cancer development. Although CDK2 is dispensable for viability in mice (12, 13) and its loss can be compensated by CDK1 (14), chemical genetics reveals a requirement of this kinase in cell cycle progression and cell proliferation (15). CDK2 also regulates centrosome duplication (16-19) by phosphorylating several key centrosomal substrates. Centrosome duplication begins when nucleophosmin/B23, a protein that associates with unduplicated centrosomes, dissociates from this organelle upon CDK2 phosphorylation (20). CDK2 phosphorylates Mps1 and CP110, two centrosomal proteins essential for duplication and amplification (21, 22). Furthermore, CDK2 cooperates with polo-like kinase 4 to regulate centrosome amplification, although the two proteins do not appear to interact (23, 24).

Elegant studies using knockout mouse embryonic fibroblasts have demonstrated that whereas CDK2 is not required for normal centrosome duplication, it is needed for amplification (25, 26). Thus, current evidence favors the notion that CDK2 activity supports centrosome duplication/amplification. It is not entirely clear if CDK2 substrates always exert a positive effect on duplication/amplification, since a complete set of centrosomal CDK2 substrates have not been identified (27).

Centrosomal protein of 76 kDa (Cep76) was originally identified as a novel component of the centrosome using mass spectrometry-based proteomics (28). Previous studies indicate that this protein plays a pivotal role in restraining centriole amplification (29). A loss of Cep76 induces accumulation of supernumerary centrioles primarily during S phase (29). In addition, ectopic expression of Cep76 specifically suppresses centriole and centrosome amplification induced by hydroxyurea (HU), a drug that inhibits S phase progression and promotes multiple rounds of centriole duplication (29, 30). Interestingly, Cep76 protein levels peak in S phase (29), coinciding with elevated CDK2 activity and centriole duplication (31). The relationship between Cep76 and CDK2, if any, is unknown. Moreover, precisely how Cep76 suppresses centriole amplification at a mechanistic level has not been characterized.

Results

Cep76 preferentially interacts with cyclin A/CDK2

In an effort to identify potential upstream and downstream regulators of Cep76, we performed a proteomic screen for components of Cep76-containing complexes. Two centrosomal proteins, CP110 and Cep97, previously shown to interact with Cep76 were found (29), confirming the success of the screen. In addition, we identified CDK2, an S/G2 phase CDK (32, 33), as a novel Cep76-interacting partner from two independent experiments. To determine whether Cep76 and CDK2 interact in cells, we transfected a plasmid expressing HA-CDK2 in HEK293 cells, performed immunoprecipitations with anti-HA antibody, and showed that both HA-CDK2 and endogenous Cep76 were co-precipitated (Figure 1A). When Flag-Cep76 was expressed, endogenous CDK2 was likewise detected in Flag-Cep76 immunoprecipitates (Figure 1B). Flag-Cep76 specifically associated with CDK2 but not with other CDKs, including CDK1, CDK4 and CDK6, involved in cell cycle progression (Figure 1B). CDK2 is known to pair with cyclin E in late G1 and cyclin A in S/G2 phase (32), and we found that Flag-Cep76 interacts with cyclin A only (Figure 1B). The interaction between Cep76 and cyclin A was confirmed in other cell lines including U2OS and Saos-2 (Figure 1C and data not shown). Endogenous Cep76, cyclin A and CDK2 also interacted with each other (Figure 1D). Furthermore, *in vitro* binding experiments using purified proteins revealed that while Cep76 associates weakly with cyclin E/CDK2, it binds strongly to cyclin A/CDK2 (Figure 1E), in close agreement with our immunoprecipitation results (Figure 1B). Taken together, these findings suggest that Cep76 preferentially interacts with cyclin A/CDK2.

Cep76 is phosphorylated by cyclin A/CDK2 at a single site S83

Cyclin/CDKs are known to phosphorylate substrates possessing the consensus sequence (S/T)-P (34-36). Sequence analysis of Cep76 revealed the presence of four putative consensus phosphorylation sites (Figure 2A). To determine whether Cep76 is a cyclin/CDK substrate, we first immunoprecipitated Flag-Cep76 from HEK293 cells, excised the band corresponding to the recombinant protein from a SDS-PAGE gel, and analyzed phosphorylation by mass spectrometry. In three independent experiments, we reproducibly detected phosphorylation of one single amino acid, serine 83 (S83) (Figure 2B), which overlaps with one of the four predicted CDK consensus sites of Cep76 (Figure 2A). Phosphorylation on S83 can be attenuated by the addition of a CDK inhibitor roscovitine (Figure S1), indicating that Cep76 is phosphorylated by CDK *in vivo*. Next, we performed *in vitro* kinase assays using purified cyclin/CDK and Cep76 and asked if the former directly phosphorylates the latter. In accordance with earlier results that Cep76 strongly interacts with cyclin A/CDK2, this protein is robustly phosphorylated by cyclin A/CDK2 (Figure 2C). Cyclin E/CDK2, on the other hand, exhibited negligible kinase activity on Cep76 (Figure 2C). In comparison, a known cyclin/CDK substrate histone H1 and a non-substrate NPHP5 are good and poor substrate for both kinases, respectively (Figure 2C). Moreover, we generated two Cep76 phosphorylation site mutants, one in which S83 was mutated to alanine (S83A) and the other in which all four putative CDK consensus sites were mutated to alanine (S83AT3335AS558AS615A; quadruple mutant), and tested their ability to undergo cyclin A/CDK2-dependent phosphorylation. We found that phosphorylation of S83A was drastically reduced compared to wild type protein, and the extent of diminution was comparable to the quadruple mutant (Figure 2D).

The failure of cyclin A/CDK2 to phosphorylate mutant proteins is not a consequence of impaired binding, since wild type, S83A and the quadruple mutant bound equally well to the kinase (Figure 2E). S83, therefore, appears to be the only CDK consensus site that becomes phosphorylated by cyclin A/CDK2.

In addition to CDK consensus sites, a number of cyclin/CDK substrates possess KXL/RXL motifs known to facilitate interactions with cyclins, especially cyclin A, allowing for efficient substrate-kinase interaction and substrate phosphorylation (37-39). Cep76 contains nine putative KXL/RXL motifs (Figures 2A and S2A) and exhibits preferential binding to cyclin A (Figures 1B and 1E); thus, we sought to examine the potential role of these motifs in mediating interaction with cyclin A. We mutated each of the nine KXL/RXL motifs individually by replacing arginine and leucine with alanine (AXA mutants, Figure S2A), and found that these mutants are still able to interact with cyclin A (Figure S2B). A limited set of double and triple AXA mutants were tested and they could also bind cyclin A (data not shown). Furthermore, AXA mutant proteins appeared to be fully functional, since they localized to the centrosome and were able to suppress centriole amplification (Figures S2C and S3; see below for functional assays). From these results, we conclude that other determinants apart from the KXL/RXL motifs are likely responsible for the interaction between Cep76 and cyclin A.

Phosphorylation of Cep76 suppresses centriole amplification in S phase

To assess the functional significance of Cep76 phosphorylation, we conducted rescue experiments in which we introduced recombinant wild type Cep76 or the S83A mutant in U2OS cells depleted of endogenous Cep76, using a siRNA oligo that targets the 3'UTR of Cep76 mRNA. A phosphomimetic mutant S83E was also tested in the same assay. A loss of Cep76 specifically leads to the production of supernumerary centrioles in S phase (29), and we indeed confirmed an earlier report that Cep76 depletion led to a 3-4 fold increase in the number of cells with >4 centriolar CP110 dots or >2 dots of C-Nap1 which stains the proximal ends of mother and daughter centrioles (Figures 3A-B and data not shown). Remarkably, this phenotype was rescued by wild type Cep76 and S83E, but not S83A mutant expression (Figures 3A-B, S4A and data not shown), despite comparable levels of protein expression (Figure 3C). Furthermore, both S83A and S83E mutants were properly localized to the centrosome (Figure 3B). These data suggest that the phosphomimetic mutant is functional and that phosphorylation at S83 is critical for Cep76 to suppress centriole amplification.

In addition, we tested the ability of wild type Cep76, S83A and S83E mutants to suppress HU-induced centriole amplification. The percentages of HU-treated control cells possessing >4 CP110 (centriolar) dots and >2 γ-tubulin (centrosomal) dots were ~30-35% and ~35-40%, respectively. These percentages dropped to ~5-15% and ~10-15% in HU-treated cells expressing wild type Cep76 or the S83E mutant (Figures 4A-B and S4B), indicating that either protein inhibits amplification. In contrast, expression of the S83A mutant in HU-arrested cells did not suppress amplification, since the percentages of cells with >4 CP110 dots and >2 γ-tubulin dots (~34% and 33%, respectively) were similar to control (Figures 4A-B).

Finally, we verified that wild type Cep76, S83A and S83E proteins were expressed at similar levels (Figure 4C). Our rescue experiments and HU overduplication assay altogether revealed that phosphorylation of Cep76 at S83 prevents centriole amplification in S phase.

Significance of Cep76 phosphorylation in human cancer

Since Cep76 is critical for protection against centriole amplification, a hallmark of cancer cells, a loss of protein function may cause a predisposition to cancer. A database search for somatic mutations in human cancer uncovered the Cep76 S83C mutation, identified in one of 307 cases of cervical squamous cell carcinoma and endocervical adenocarcinoma. It is currently unknown whether the mutation is present in one or both gene copies. The S83C mutation destroys a CDK2 phosphorylation site, and accordingly, we predicted that it would cripple protein function. Indeed, mutant S83C protein was unable to suppress centriole amplification induced by HU (Figures 5A-C) or depletion of Cep76 (Figures S5A-B).

Mechanism underlying suppression of centriole amplification by Cep76

We sought to address the mechanism by which Cep76 prevents centriole amplification. Because CDK2 promotes centriole amplification (16-19) and certain CDK2 substrates are known to regulate the kinase (40-42), we first asked whether the activity of cyclin A/CDK2 is inhibited by Cep76. Cyclin A/CDK2 activity was monitored using histone H1 as a substrate in the presence of the S83A or S83E mutant, neither of which is phosphorylated by the kinase (Figure 2D). Excessive amounts of S83A or S83E did not substantially modulate cyclin A/CDK2 kinase activity towards histone H1 (Figure 5D), suggesting that Cep76 is not an inhibitor of cyclin A/CDK2.

Next, we examined if Cep76 regulates targeting of the kinase to the centrosome and hence, its ability to phosphorylate centrosomal substrates. Although CDK2 and cyclin A were both reported to be associated with centrosomes (43-46), depletion of Cep76 slightly influenced the centrosomal amount of cyclin A and CDK2 (Figures S6A-B). Thus, Cep76 has minimal effect on the abundance and activity of cyclin A/CDK2 at the centrosome.

Centriole disengagement is a prerequisite for a new round of duplication (47) and reduplication induced by HU (48). We therefore asked if Cep76 suppresses amplification by restraining centriole disengagement. Centriole disengagement was determined by examining the spacing of CP110/γ-tubulin dots and the ratio of CP110 to γ-tubulin dots. When the two centrioles are engaged, two closely spaced CP110 dots are associated with a single γ-tubulin dot and a 2:1 ratio of CP110:γ-tubulin is expected. Centriole disengagement causes centrioles to move further apart, and in this scenario, each CP110 dot is associated with a single γ-tubulin dot and a 1:1 ratio of CP110:γ-tubulin is expected. We noticed a 2:1 ratio, but rarely a 1:1 ratio, of CP110:γ-tubulin dots in HU-treated cells expressing wild type Cep76 or S83E (Figure 5E). In striking contrast, a 1:1 ratio of CP110:γ-tubulin dots was frequently observed in a subpopulation of HU-treated control cells or cells expressing S83A which have not undergone amplification (Figure 5E). In addition, we found that activated polo-like kinase 1 (Plk1) or Plk1-pT210, reportedly associated with disengaged centrioles in HU-treated control cells (48), is present at centrioles in HU-treated cells expressing S83A only (Figure 5F). From these results, we conclude that Cep76 inhibits centriole disengagement and consequently amplification by blocking Plk1 activation at the centrosome.

To further interrogate the relationship between Cep76 and Plk1, we found that centriole amplification due to loss of Cep76 can be prevented by the addition of a Plk1 inhibitor BI 2536 (Figure S7A). Moreover, while centriole amplification is suppressed by enforced expression of Cep76 in HU-treated cells, this phenotype can be overridden by co-expression of constitutively active Plk1 (Plk1-T210D) (Figure S7B). Taken together, these data suggest that Cep76 inhibits Plk1 at the centrosome.

Acetylation of Cep76 at K279 cannot suppress centriole amplification

So far, we have demonstrated that phosphorylation at S83 is crucial for Cep76 function in S phase. Because protein function is often controlled by different types of posttranslational modification (PTM) (49), we first examined if Cep76 could be regulated by other modifications. A recent proteomic study identified lysine 279 (K279) as an acetylation site on Cep76 (50), although its biological relevance is unknown. To determine if Cep76 is acetylated, we immunoprecipitated Cep76 and showed that the endogenous protein is highly acetylated when cells were treated with a histone deacetylase inhibitor trichostatin A (TSA) (Figure 6A). Likewise, reciprocal immunoprecipitations with an anti-acetyl-lysine antibody revealed a marked increase in endogenous Cep76 acetylation upon TSA treatment (Figure 6B). Acetylation of recombinant Flag-Cep76 could also be detected (Figures S8A-B). We subsequently confirmed that acetylation takes place at K279, since an acetylation site mutant in which K279 was mutated to an arginine (K279R) exhibited considerably less acetylation compared to wild type protein (Figure 6C). Next, we asked if acetylation impacts Cep76 function.

For this purpose, the ability of the acetylmimetic mutant K279Q, along with K279R, to suppress centriole amplification was investigated. We found that centriole overduplication induced by depletion of Cep76 or prolonged HU treatment was suppressed by K279R but not K279Q expression (Figures 6D-E). Both mutants localize to the centrosome and showed similar levels of protein expression compared to wild type protein (Figure 6F and data not shown). Thus, Cep76 can be acetylated at K279, and acetylation likely dampens the protein's capacity to suppress centriole amplification.

To gain molecular insight into why the K279R but not the K279Q mutant is proficient in suppressing centriole amplification and to explore the possibility of PTM crosstalk, we determined whether these mutant proteins could be phosphorylated by cyclin A/CDK2 *in vitro*. In sharp contrast to K279Q, the K279R mutant was robustly phosphorylated, reaching a level comparable to wild type protein (Figure 6G). Importantly, phosphorylation of K279R appears to occur on S83, since the S83AK279R double mutant exhibited markedly reduced phosphorylation (Figure 6G). The functionality of the K279R mutant is likewise dependent on S83, since the S83AK279R mutant could no longer suppress HU-induced amplification (Figures 6E-F). Remarkably, we found that the S83EK279Q double mutant, similar to the K279Q single mutant, was also unable to suppress centriole amplification induced by HU (Figures 6E-F), indicating that K279 acetylation alone is sufficient to override the effect of S83 phosphorylation and turn off Cep76. Considered together, our data suggest that acetylation at K279 negatively regulates Cep76 by limiting protein activity and S83 phosphorylation.

Temporal changes in Cep76 PTMs correlate with protein function

Next, we examined when phosphorylation and acetylation of Cep76 occur in the cell cycle. For analysis of protein phosphorylation, the abundance of S83 phosphopeptide was quantitatively determined by mass spectrometric analysis of Cep76 protein immuno-purified from synchronized cells. These experiments revealed that S83 phosphorylation increases from G1 to S but decreases thereafter (Figure 7A). Likewise, when we immunoprecipitated Flag-Cep76 from synchronized cells and Western blotted the resulting immunoprecipitates with anti-phosphoserine antibody, we found that phosphorylation is highly enriched in S phase (Figure S9). Thus, S83 phosphorylation appears to coincide with Cep76 function during S phase. For analysis of protein acetylation, we expressed Flag-Cep76 in synchronized cells and showed that the protein is more highly acetylated in G2 compared to other cell cycle phases (Figure 7B). Fittingly, Cep76 failed to inhibit centriole amplification induced by RO 3306 (Figures 7C-E), a small molecule inhibitor that triggers prolonged arrest in G2 phase and repeated rounds of centriole duplication (48, 51, 52). In these cells, both centriole disengagement and centrosomal Plk1-pT210 staining were observed (Figures 7F-G). As a further proof that acetylation of Cep76 in G2 phase leads to a loss of protein function, we found that Cep76 could not prevent centriole amplification induced by doxorubicin (DOX) (Figure 7H), a radiomimetic drug that induces G2 arrest (52). Our findings suggest that acetylation of Cep76 in G2 phase renders the protein unable to function.

Discussion

Centriole duplication is a highly orchestrated process that occurs once per cell cycle. Deregulated duplication often leads to amplification, a hallmark of cancer cells (5). Because centriole amplification is believed to be an early event in tumorigenesis (5, 7-9), it is essential to identify the players that control the duplication process and examine their relevance to cancer development. CDK2 has emerged as a master regulator of duplication. However, much remains to be studied about how CDK2 controls this process, in part because a complete set of centrosomal CDK2 substrates have not been identified. Here, we uncovered a link between CDK2 and Cep76, a protein that limits centriole duplication to once per cell cycle (29), and demonstrated that the latter is a bona fide substrate of the former. To our knowledge, Cep76 is the first CDK2 substrate known to negatively regulate centriole amplification, since a small handful of substrates identified to date promote duplication and amplification in a positive manner.

Several centrosomal proteins, including Cep76, origin recognition complex 1 (ORC1), minichromosome maintenance 5 (MCM5), RNA-binding motif protein 14 (RBM14) and CDC14 are reported to suppress centriole amplification without affecting normal duplication (29, 53-57). Their mechanisms of action, however, have not been fully deciphered. While MCM5 and ORC1 associate with both cyclin E and cyclin A, only ORC1 inhibits cyclin/CDK2 activity. CDC14 dephosphorylates certain CDK substrates and may counteract CDK-mediated phosphorylation of centrosomal substrates (58, 59). RBM14 has no connection to CDK2; it suppresses the assembly of centriolar protein complexes that would lead to the formation of extra centrioles. Unlike the aforementioned proteins, Cep76 is a CDK2 substrate, and its phosphorylation by CDK2 is required to suppress centriole amplification.

Although CDK2 can impinge on Cep76 function, the converse is not true, since Cep76 does not substantially affect the activity or localization of the kinase. Instead, our data revealed that Cep76 phosphorylation blocks Plk1 activity, thereby preventing premature centriole disengagement and amplification. Thus, the mechanism by which Cep76 suppresses centriole amplification appears to be unique.

Centriole disengagement is known to require the activities of Plk1 and the anaphase-promoting complex (APC) (52, 60, 61). Although either activity alone is sufficient to disengage centrioles, the extent to which they contribute to this intricate process remains unclear. We showed that Cep76 can prevent centriole disengagement and amplification in S phase but not in G2 phase. Thus, it is possible that HU-induced centriole disengagement is more highly dependent on Plk1 which can be easily overcome by Cep76 expression, whereas RO 3306- and DOX-induced disengagement is less dependent on Plk1. In support of this, we found that expression of a constitutively active Cep76 mutant S83EK279R, which retains the ability to block Plk1 activation at the centrosome, cannot suppress centriole amplification in RO 3306-treated cells (Figure S10). Another possibility is that Cep76 could specifically function in S phase and not in G2 phase. The two possibilities are not mutually exclusive.

Our data suggest that the function of Cep76 is modulated in a temporal manner during the cell cycle by two different types of PTM. Since Cep76 protein levels and cyclin/CDK2 activity peak in S phase and coincides with centriole duplication (29, 60, 61), we envision that this protein is phosphorylated and becomes activated by cyclin A/CDK2 in S phase to control the fidelity of duplication. Disruption of S83 phosphorylation, such as the phosphorylation site mutation S83A and the S83C mutation found in human cancer, compromises protein function.

Once duplication is completed, Cep76 becomes acetylated at K279 in G2 phase. Acetylation of Cep76 serves to block S83 phosphorylation and to directly inhibit protein function possibly by relieving Plk1 from inhibition (Figures 6 and S10). It is uncertain how acetylation prevents protein phosphorylation. The K279Q mutant can still bind cyclin A/CDK2 (data not shown), suggesting that acetylation does not affect the interaction between the substrate and the kinase. Instead, acetylation of Cep76 may enhance its binding to a phosphatase which can promote dephosphorylation at S83, in a manner similar to the effect of acetylation on glycogen phosphorylase phosphorylation (62). As several phosphatases were identified in our proteomic screen for Cep76-interacting partners (data not shown), experiments are currently underway to determine if any of these could interact with Cep76.

In conclusion, we established that CDK2-mediated phosphorylation of a novel centrosomal substrate Cep76 is required to block centriole amplification in S phase. We also demonstrated the significance of a functional crosstalk between phosphorylation and acetylation. These results raise the intriguing possibility that deregulation of Cep76 might be linked to cancer risk.

Materials and Methods

Cell culture and plasmids

U2OS, Saos-2 and HEK293 cells (American Type Culture Collection) were grown in DMEM supplemented with 5% FBS at 37°C in a humidified 5% CO2 atmosphere. A plasmid expressing human recombinant Flag-Cep76 protein, pCDEF3-Flag-Cep76, was described previously (29). The following Cep76 mutations (S83C, S83A, S83E, S83AT335AS558AS615A, K279R, K279Q, S83AK279R, S83EK279Q, S83EK279R, AXA12-14, AXA54-56, AXA67-69, AXA106-108, AXA325-327, AXA331-333, AXA448-450, AXA533-535, AXA541-543) were introduced into full-length cDNA by employing a two-step PCR mutagenesis strategy and sub-cloned into pCDEF3-Flag. All constructs were verified by DNA sequencing. Myc-cyclin A and CDK2-HA plasmids were obtained from J. Archambault, and myc-Plk1-T210D was obtained from Addgene.

Antibodies

Antibodies used in this study included anti-HA (sc-7392), anti-myc (sc-40), anti-CDK2 (sc-163), anti-CDK1 (sc-954), anti-CDK4 (sc-4601), anti-CDK6 (sc-177), anti-cyclin A (sc-751), anti-cyclin E (sc-481), anti-C-Nap1 (sc-1358) (Santa Cruz); anti-α-tubulin (T5168), anti-Flag (F7425), anti-γ-tubulin (T3559) (Sigma); anti-acetyl lysine (#9441; Cell Signaling); anti-phosphoserine (05-1000X; Millipore); anti-Plk1-pT210 (ab39068; Abcam) and anti-CP110 (A301-344A) and anti-Cep76 (A302-326A) (Bethyl Laboratories)

Mass spectrometric identification of Cep76 associated proteins and phosphorylation sites

To identify Cep76-interacting proteins, Flag-Cep76 was expressed in HEK293 and U2OS cells and immunoprecipitated with anti-Flag agarose beads (Sigma) for 2 hours at 4^{o}C. Bounded proteins were eluted with Flag peptide for 30 minutes, and the resultant eluates were precipitated with trichloroacetic acid and fractionated by SDS-PAGE. Six gel slices containing polypeptides were excised after Coomassie staining and subjected to proteolytic digestion mass spectrometric analysis. Analyses were performed at the Harvard Taplin Mass Spectrometry facility and the mass spectrometry core facility from IRCM by micro-capillary LC/MS/MS. For the identification of phosphorylation sites, cells were treated with 100 nM calyculin A for 30 min before lysis, and the lysis buffer contained 10 mM sodium fluoride, 0.2 mM sodium orthovanadate and 50mM β-glycerophosphate. A gel slice corresponding to Flag-Cep76 was excised. LC-MS peptide quantitation was performed by manual integration of the extracted ion chromatogram of each peptide using Qual Browser/Xcalibur version 2.2 (ThermoFisher Scientific).

Immunoprecipitation, immunoblotting, and immunofluorescence microscopy

Immunoprecipitation, immunoblotting and immunofluorescence were performed as described (63, 64). Densitometric analyses were performed with the ImageJ software (v1.43m, US National Institutes of Health) using the gel analysis and label peaks tools. ImageJ was also used to quantify the Plk1-pT210 signal at centrosomes.

Centrosome overduplication assay, cell cycle synchronization and FACS analysis

Cells were treated with 2mM HU (Sigma), 15 μM RO 3306 (Sigma) or 0.1 μM DOX (Santa Cruz) for 48 hours. The drug concentration and treatment time were optimized to minimize toxicity and to obtain the largest number of cells with overduplicated centrosomes. For cell cycle synchronization, G1, S, G2 and M phase cells were obtained by treating cells for 24 hours with 0.4 mM mimosine, 2 mM HU and release for 4 hours, 15 μM RO 3306, and 40ng/ml nocodazole, respectively. Cell cycle distribution was confirmed by fluorescence-activated cell sorting as described previously (64).

RNA interference

Transfection of siRNAs was performed using siImporter (Millipore) as per manufacturer's instructions. The 21-nucleotide siRNA sequence for the non-specific control was 5'-AATTCTCCGAACGTGTCACGT-3'. The 21-nucleotide siRNA sequences for Cep76 were 5'-GAGCGTACAACAAGTATATTT-3' and 5'-AATCACAATCTGGCTTGAATGTT-3' (for targeting the 3'UTR region) (Dharmacon).

Production of recombinant proteins

Purified and active cyclin A/CDK2 and cyclin E/CDK2 were obtained from Millipore. Flag-Cep76 wild type or mutant, or Flag-NPHP5, was expressed in U2OS cells, lysed and incubated with anti-Flag beads for 2 hours. Beads were washed twice with ELB buffer containing 500mM NaCl and proteins were eluted with Flag peptide. A small sample was run on a gel and Coomassie stained to assess protein purity. We determined that our Flag-Cep76 or Flag-NPHP5 protein was at least 90% pure.

In vitro binding assay

1 μg of purified Flag-Cep76 protein was mixed with 1 μg of purified cyclin A/CDK2 or cyclin E/CDK2 at 4°C for 1h, followed by incubation with anti-Flag agarose beads at 4°C for 2h. After extensive washing with ELB buffer, bound proteins were analyzed by SDS-PAGE and immunoblotting.

In vitro kinase assay

The ADP-Glo™ kinase assay (Promega) was used for the *in vitro* kinase assay. The assay was carried out as per manufacturer's instructions in a 96-well plate in kinase buffer (40 mM Tris pH 7.5, 20 mM $MgCl_2$, 0.1% BSA) containing 100 ng of active cyclin A/CDK2 or cyclin E/CDK2, 1 μg of purified Flag-Cep76, histone H1 or Flag-NPHP5, and 1.25 μl of 1 mM ATP (Promega). The signal was quantitated using the GloMax 96 Microplate Luminometer (Promega). For the kinase inhibition assay, histone H1 was used as a substrate for cyclin A/CDK2 and increasing amounts of purified Flag-76 mutant protein S83A or S83E were then added to the reaction.

Statistical analysis

Experiments were performed at minimum of two to three times. Graphs were generated in Microsoft Excel. Error bars represent standard error of the mean.

Conflict of Interest

The authors declare no conflict of interest.

Acknowledgements

We thank all members of the Tsang laboratory for constructive advice, E. Gomes and J. Song for assistance with cloning, and Ross Tomaino and Denis Faubert for assistance with mass spectrometry. W.Y.T. is a Canadian Institutes of Health Research New Investigator and a Fonds de recherche Santé Junior 1 Research Scholar. This work was supported by the Canadian Institutes of Health Research (MOP-115033 to W.Y.T.) and the Natural Sciences and Engineering Research Council of Canada.

References

1. Bornens M. The centrosome in cells and organisms. Science. 2012;335(6067):422-6.
2. Nigg EA, Stearns T. The centrosome cycle: Centriole biogenesis, duplication and inherent asymmetries. Nat Cell Biol. 2011;13(10):1154-60.
3. Nigg EA, Raff JW. Centrioles, centrosomes, and cilia in health and disease. Cell. 2009;139(4):663-78.
4. Lingle WL, Lutz WH, Ingle JN, Maihle NJ, Salisbury JL. Centrosome hypertrophy in human breast tumors: implications for genomic stability and cell polarity. Proceedings of the National Academy of Sciences of the United States of America. 1998;95(6):2950-5.
5. Chan JY. A clinical overview of centrosome amplification in human cancers. International journal of biological sciences. 2011;7(8):1122-44.
6. Pihan GA, Purohit A, Wallace J, Knecht H, Woda B, Quesenberry P, et al. Centrosome defects and genetic instability in malignant tumors. Cancer Res. 1998;58(17):3974-85.
7. Duensing S, Lee LY, Duensing A, Basile J, Piboonniyom S, Gonzalez S, et al. The human papillomavirus type 16 E6 and E7 oncoproteins cooperate to induce mitotic defects and genomic instability by uncoupling centrosome duplication from the cell division cycle. Proceedings of the National Academy of Sciences of the United States of America. 2000;97(18):10002-7.
8. Lingle WL, Barrett SL, Negron VC, D'Assoro AB, Boeneman K, Liu W, et al. Centrosome amplification drives chromosomal instability in breast tumor development. Proceedings of the National Academy of Sciences of the United States of America. 2002;99(4):1978-83.
9. Pihan GA, Wallace J, Zhou Y, Doxsey SJ. Centrosome abnormalities and chromosome instability occur together in pre-invasive carcinomas. Cancer Res. 2003;63(6):1398-404.
10. Ganem NJ, Godinho SA, Pellman D. A mechanism linking extra centrosomes to chromosomal instability. Nature. 2009;460(7252):278-82.
11. Godinho SA, Picone R, Burute M, Dagher R, Su Y, Leung CT, et al. Oncogene-like induction of cellular invasion from centrosome amplification. Nature. 2014;510(7503):167-71.
12. Berthet C, Aleem E, Coppola V, Tessarollo L, Kaldis P. Cdk2 knockout mice are viable. Current biology : CB. 2003;13(20):1775-85.
13. Ortega S, Prieto I, Odajima J, Martin A, Dubus P, Sotillo R, et al. Cyclin-dependent kinase 2 is essential for meiosis but not for mitotic cell division in mice. Nature genetics. 2003;35(1):25-31.
14. Santamaria D, Barriere C, Cerqueira A, Hunt S, Tardy C, Newton K, et al. Cdk1 is sufficient to drive the mammalian cell cycle. Nature. 2007;448(7155):811-5.
15. Merrick KA, Wohlbold L, Zhang C, Allen JJ, Horiuchi D, Huskey NE, et al. Switching Cdk2 on or off with small molecules to reveal requirements in human cell proliferation. Mol Cell. 2011;42(5):624-36.
16. Hinchcliffe EH, Li C, Thompson EA, Maller JL, Sluder G. Requirement of Cdk2-cyclin E activity for repeated centrosome reproduction in Xenopus egg extracts. Science. 1999;283(5403):851-4.
17. Lacey KR, Jackson PK, Stearns T. Cyclin-dependent kinase control of centrosome duplication. Proceedings of the National Academy of Sciences of the United States of America. 1999;96(6):2817-22.

18. Meraldi P, Lukas J, Fry AM, Bartek J, Nigg EA. Centrosome duplication in mammalian somatic cells requires E2F and Cdk2-cyclin A. Nat Cell Biol. 1999;1(2):88-93.
19. Matsumoto Y, Hayashi K, Nishida E. Cyclin-dependent kinase 2 (Cdk2) is required for centrosome duplication in mammalian cells. Current biology : CB. 1999;9(8):429-32.
20. Okuda M, Horn HF, Tarapore P, Tokuyama Y, Smulian AG, Chan PK, et al. Nucleophosmin/B23 is a target of CDK2/cyclin E in centrosome duplication. Cell. 2000;103(1):127-40.
21. Fisk HA, Winey M. The mouse Mps1p-like kinase regulates centrosome duplication. Cell. 2001;106(1):95-104.
22. Chen Z, Indjeian VB, McManus M, Wang L, Dynlacht BD. CP110, a cell cycle-dependent CDK substrate, regulates centrosome duplication in human cells. Developmental cell. 2002;3(3):339-50.
23. Habedanck R, Stierhof YD, Wilkinson CJ, Nigg EA. The Polo kinase Plk4 functions in centriole duplication. Nat Cell Biol. 2005;7(11):1140-6.
24. Korzeniewski N, Zheng L, Cuevas R, Parry J, Chatterjee P, Anderton B, et al. Cullin 1 functions as a centrosomal suppressor of centriole multiplication by regulating polo-like kinase 4 protein levels. Cancer Res. 2009;69(16):6668-75.
25. Duensing A, Liu Y, Tseng M, Malumbres M, Barbacid M, Duensing S. Cyclin-dependent kinase 2 is dispensable for normal centrosome duplication but required for oncogene-induced centrosome overduplication. Oncogene. 2006;25(20):2943-9.
26. Adon AM, Zeng X, Harrison MK, Sannem S, Kiyokawa H, Kaldis P, et al. Cdk2 and Cdk4 regulate the centrosome cycle and are critical mediators of centrosome amplification in p53-null cells. Molecular and cellular biology. 2010;30(3):694-710.
27. Errico A, Deshmukh K, Tanaka Y, Pozniakovsky A, Hunt T. Identification of substrates for cyclin dependent kinases. Adv Enzyme Regul. 2010;50(1):375-99.
28. Andersen JS, Wilkinson CJ, Mayor T, Mortensen P, Nigg EA, Mann M. Proteomic characterization of the human centrosome by protein correlation profiling. Nature. 2003;426(6966):570-4.
29. Tsang WY, Spektor A, Vijayakumar S, Bista BR, Li J, Sanchez I, et al. Cep76, a centrosomal protein that specifically restrains centriole reduplication. Developmental cell. 2009;16(5):649-60.
30. Balczon R, Bao L, Zimmer WE, Brown K, Zinkowski RP, Brinkley BR. Dissociation of centrosome replication events from cycles of DNA synthesis and mitotic division in hydroxyurea-arrested Chinese hamster ovary cells. The Journal of cell biology. 1995;130(1):105-15.
31. Rosenblatt J, Gu Y, Morgan DO. Human cyclin-dependent kinase 2 is activated during the S and G2 phases of the cell cycle and associates with cyclin A. Proceedings of the National Academy of Sciences of the United States of America. 1992;89(7):2824-8.
32. Harper JW, Adams PD. Cyclin-dependent kinases. Chem Rev. 2001;101(8):2511-26.
33. Malumbres M. Cyclin-dependent kinases. Genome Biol. 2014;15(6):122.
34. Nigg EA. The substrates of the cdc2 kinase. Semin Cell Biol. 1991;2(4):261-70.
35. Moreno S, Nurse P. Substrates for p34cdc2: in vivo veritas? Cell. 1990;61(4):549-51.
36. Nigg EA. Cellular substrates of p34(cdc2) and its companion cyclin-dependent kinases. Trends in cell biology. 1993;3(9):296-301.

37. Adams PD, Sellers WR, Sharma SK, Wu AD, Nalin CM, Kaelin WG, Jr. Identification of a cyclin-cdk2 recognition motif present in substrates and p21-like cyclin-dependent kinase inhibitors. Molecular and cellular biology. 1996;16(12):6623-33.
38. Chen J, Saha P, Kornbluth S, Dynlacht BD, Dutta A. Cyclin-binding motifs are essential for the function of p21CIP1. Molecular and cellular biology. 1996;16(9):4673-82.
39. Zhu L, Harlow E, Dynlacht BD. p107 uses a p21CIP1-related domain to bind cyclin/cdk2 and regulate interactions with E2F. Genes & development. 1995;9(14):1740-52.
40. Sheaff RJ, Groudine M, Gordon M, Roberts JM, Clurman BE. Cyclin E-CDK2 is a regulator of p27Kip1. Genes & development. 1997;11(11):1464-78.
41. Tsang WY, Wang L, Chen Z, Sanchez I, Dynlacht BD. SCAPER, a novel cyclin A-interacting protein that regulates cell cycle progression. The Journal of cell biology. 2007;178(4):621-33.
42. Tsang WY, Dynlacht BD. Double identity of SCAPER: a substrate and regulator of cyclin A/Cdk2. Cell cycle. 2008;7(6):702-5.
43. Pascreau G, Eckerdt F, Churchill ME, Maller JL. Discovery of a distinct domain in cyclin A sufficient for centrosomal localization independently of Cdk binding. Proceedings of the National Academy of Sciences of the United States of America. 2010;107(7):2932-7.
44. Pagano M, Pepperkok R, Verde F, Ansorge W, Draetta G. Cyclin A is required at two points in the human cell cycle. The EMBO journal. 1992;11(3):961-71.
45. De Boer L, Oakes V, Beamish H, Giles N, Stevens F, Somodevilla-Torres M, et al. Cyclin A/cdk2 coordinates centrosomal and nuclear mitotic events. Oncogene. 2008;27(31):4261-8.
46. Nishimura T, Takahashi M, Kim HS, Mukai H, Ono Y. Centrosome-targeting region of CG-NAP causes centrosome amplification by recruiting cyclin E-cdk2 complex. Genes Cells. 2005;10(1):75-86.
47. Tsou MF, Stearns T. Mechanism limiting centrosome duplication to once per cell cycle. Nature. 2006;442(7105):947-51.
48. Loncarek J, Hergert P, Khodjakov A. Centriole reduplication during prolonged interphase requires procentriole maturation governed by Plk1. Current biology : CB. 2010;20(14):1277-82.
49. Yang XJ, Seto E. Lysine acetylation: codified crosstalk with other posttranslational modifications. Mol Cell. 2008;31(4):449-61.
50. Zhao S, Xu W, Jiang W, Yu W, Lin Y, Zhang T, et al. Regulation of cellular metabolism by protein lysine acetylation. Science. 2010;327(5968):1000-4.
51. Vassilev LT, Tovar C, Chen S, Knezevic D, Zhao X, Sun H, et al. Selective small-molecule inhibitor reveals critical mitotic functions of human CDK1. Proceedings of the National Academy of Sciences of the United States of America. 2006;103(28):10660-5.
52. Douthwright S, Sluder G. Link between DNA damage and centriole disengagement/reduplication in untransformed human cells. J Cell Physiol. 2014;229(10):1427-36.
53. Wu J, Cho HP, Rhee DB, Johnson DK, Dunlap J, Liu Y, et al. Cdc14B depletion leads to centriole amplification, and its overexpression prevents unscheduled centriole duplication. The Journal of cell biology. 2008;181(3):475-83.
54. Hemerly AS, Prasanth SG, Siddiqui K, Stillman B. Orc1 controls centriole and centrosome copy number in human cells. Science. 2009;323(5915):789-93.

55. Ferguson RL, Maller JL. Cyclin E-dependent localization of MCM5 regulates centrosome duplication. Journal of cell science. 2008;121(Pt 19):3224-32.
56. Ferguson RL, Pascreau G, Maller JL. The cyclin A centrosomal localization sequence recruits MCM5 and Orc1 to regulate centrosome reduplication. Journal of cell science. 2010;123(Pt 16):2743-9.
57. Shiratsuchi G, Takaoka K, Ashikawa T, Hamada H, Kitagawa D. RBM14 prevents assembly of centriolar protein complexes and maintains mitotic spindle integrity. The EMBO journal. 2015;34(1):97-114.
58. Li L, Ljungman M, Dixon JE. The human Cdc14 phosphatases interact with and dephosphorylate the tumor suppressor protein p53. The Journal of biological chemistry. 2000;275(4):2410-4.
59. Ovejero S, Ayala P, Bueno A, Sacristan MP. Human Cdc14A regulates Wee1 stability by counteracting CDK-mediated phosphorylation. Mol Biol Cell. 2012;23(23):4515-25.
60. Pagano M, Pepperkok R, Lukas J, Baldin V, Ansorge W, Bartek J, et al. Regulation of the cell cycle by the cdk2 protein kinase in cultured human fibroblasts. The Journal of cell biology. 1993;121(1):101-11.
61. Tsai LH, Lees E, Faha B, Harlow E, Riabowol K. The cdk2 kinase is required for the G1-to-S transition in mammalian cells. Oncogene. 1993;8(6):1593-602.
62. Zhang T, Wang S, Lin Y, Xu W, Ye D, Xiong Y, et al. Acetylation negatively regulates glycogen phosphorylase by recruiting protein phosphatase 1. Cell Metab. 2012;15(1):75-87.
63. Barbelanne M, Hossain D, Chan DP, Peranen J, Tsang WY. Nephrocystin proteins NPHP5 and Cep290 regulate BBSome integrity, ciliary trafficking and cargo delivery. Hum Mol Genet. 2014.
64. Barbelanne M, Song J, Ahmadzai M, Tsang WY. Pathogenic NPHP5 mutations impair protein interaction with Cep290, a prerequisite for ciliogenesis. Hum Mol Genet. 2013;22(12):2482-94.

Figure Legends

Figure 1

Cep76 interacts with cyclin A/CDK2. (**A**) HA (control) or CDK2-HA was expressed in HEK293 cells and immunoprecipitated from lysate with an anti-HA antibody. The resulting immunoprecipitates were Western blotted with anti-HA or anti-Cep76 antibodies. IN, input. (**B**) Flag (control) or Flag-Cep76 were expressed in HEK293 cells and immunoprecipitated with anti-Flag beads. Immunoprecipitates were Western blotted with the indicated antibodies. IN, input. (**C**) Flag or Flag-Cep76 and myc or myc-cyclin A were co-expressed in U2OS cells and Flag proteins were immunoprecipitated. Flag-Cep76 and myc-cyclin A were detected after western blotting the resulting immunoprecipitates. IN, input. (**D**) Western blotting of endogenous Cep76, CDK2 and Cyclin A after immunoprecipitation of U2OS cell extracts with anti-Flag (control), anti-Cep76, anti-CDK2 or anti-Cyclin A antibodies. IN, input. (**E**) Purified Flag-tagged Cep76 protein was mixed with purified cyclin A/CDK2 (left lane), cyclin E/CDK2 (right lane) or an irrelevant protein (middle lane). Proteins were immunoprecipitated with anti-Flag beads, followed by Western blotting of Flag, CDK2, cyclin A and cyclin E. IN, input.

Figure 2

Cyclin A/CDK2 phosphorylates Cep76 at S83. (**A**) Amino acid sequence of human Cep76. Putative cyclin-binding motifs (KXL/RXL) and CDK2 phosphorylation sites (SP/TP) are bold and underlined, respectively. Numbers denote amino acid positions. (**B**) Detection of phosphorylated residues by mass spectrometry. (**C**) *In vitro* kinase assays using purified Cep76 (Cep76 FL), NPHP5 or Histone H1 and purified cyclin A/CDK2 or cyclin E/CDK2. RLU, relative light units. Error bars represent standard errors. (**D**) *In vitro* kinase assays using

Cep76 wild type (Cep76 FL), mutant S83A, S83E or S83AT335AS558AS615A protein and cyclin A/CDK2. (**E**) Purified Flag-tagged Cep76 protein (Cep76 FL) or mutant protein (Cep76 S83A or Cep76 S83AT335AS558AS615A) was mixed with purified cyclin A/CDK2. Proteins were immunoprecipitated with anti-Flag beads, followed by Western blotting of Flag, CDK2 and cyclin A. IN, input.

Figure 3

Ectopic expression of Cep76 or a phosphomimetic mutant rescues centriole amplification induced by loss of endogenous Cep76. (**A**) U2OS cells transfected with control siRNA (siNSp) or siRNA targeting Cep76 3'UTR (siCep76) and plasmid expressing an irrelevant Flag-tagged protein (control), Flag-Cep76 wild type (Cep76 FL) or mutant (Cep76 S83A or Cep76 S83E). The percentages of transfected cells with >4 centrioles were determined by using CP110 as a marker. At least 75 transfected cells were scored per condition, and average of three independent experiments is shown. Error bars represent standard errors. (**B**) Cells were stained with DAPI (blue) and antibodies against Flag (red) and CP110 (green). (**C**) (Bottom) Western blotting of Cep76 in U2OS cells treated with control siRNA (siNSp) or siRNA targeting Cep76 3'UTR and (top) of Flag in U2OS cells transfected with the indicated siRNA oligos and plasmids expressing the indicated Flag-tagged proteins. α-tubulin was used as a loading control.

Figure 4

Ectopic expression of Cep76 or a phosphomimetic mutant suppresses HU-induced centriole amplification. U2OS cells were transiently transfected with plasmid expressing an irrelevant

Flag-tagged protein (control), Flag-Cep76 wild type (Cep76 FL) or mutant (Cep76 S83A or Cep76 S83E) and either left untreated or treated with HU. (**A**) The percentages of transfected cells with >4 CP110 or >2 γ-tubulin dots were determined. At least 75 transfected cells were scored per condition, and average of three independent experiments is shown. Error bars represent standard errors. (**B**) Cells were stained with DAPI (blue) and antibodies against Flag (red) and CP110 or γ-tubulin (green). (**C**) Western blotting of Flag in U2OS cells expressing the indicated Flag-tagged proteins. α-tubulin was used as a loading control.

Figure 5

Characterization of a cancer-associated Cep76 S83C mutation and the mechanism that suppresses centriole amplification. (**A**) U2OS cells were transfected with plasmid expressing an irrelevant Flag-tagged protein (control), Flag-Cep76 wild type (Cep76 FL) or disease mutant (Cep76 S83C) and either left untreated or treated with HU. The percentages of transfected cells with >2 γ-tubulin dots were determined. (**B**) Cells were stained with DAPI (blue) and antibodies against Flag (red) and γ-tubulin (green). (**C**) Western blotting of Flag in U2OS cells expressing the indicated Flag-tagged proteins. α-tubulin was used as a loading control. (**D**) *In vitro* kinase assay with purified histone H1 as a substrate and cyclin A/CDK2 as a kinase. Increasing amounts of purified Cep76 were added to reactions. RLU, relative light units. (**E, F**) U2OS cells were transfected with plasmid expressing an irrelevant Flag-tagged protein (control), Flag-Cep76 wild type (Cep76 FL) or mutant (Cep76 S83A or Cep76 S83E) and either left untreated or treated with HU. (**E**) (Left) Cells were stained with antibodies against Flag (green), CP110 (red) and γ-tubulin (blue). (Right) The percentages of transfected cells with disengaged centrioles were determined. (**F**) (Left) Cells were stained with

antibodies against Flag (green), Plk1-pT210 (red) and γ-tubulin (blue). (Right) The percentages of transfected cells with Plk1-pT210 at centrosomes and the fluorescence intensities of centrosomal Plk1-pT210 were measured. In (**A**, **E** and **F**), at least 75 transfected cells were scored per condition, and average of two independent experiments is shown. Error bars represent standard errors.

Figure 6

Enforced acetylation of Cep76 at K279 abrogates the protein's ability to suppress centriole amplification. (**A**) U2OS cells were either left untreated or treated with TSA. Endogenous Cep76 was immunoprecipitated with an anti-Cep76 antibody, and the resulting immunoprecipitates were Western blotted with antibodies against acetyl-lysine and Cep76. IN, input. (**B**) Same as (**A**), except that endogenous proteins were immunoprecipitated with an anti-acetyl-lysine antibody. The resulting immunoprecipitates were Western blotted with an anti-Cep76 antibody. IN, input. Densitometric analyses were performed with ImageJ. (**C**) Flag-Cep76 wild type (Cep76 FL) or mutant (Cep76 K279R) protein expressed in U2OS cells were immunoprecipitated with an anti-acetyl-lysine antibody. The resulting immunoprecipitates were Western blotted with an anti-Flag antibody. IN, input. (**D**) U2OS cells transfected with control siRNA (siNSp) or siRNA targeting Cep76 3'UTR (siCep76) and plasmid expressing an irrelevant Flag-tagged protein (control), Flag-Cep76 wild type (Cep76 FL) or mutant (Cep76 K279R or Cep76 K279Q). The percentages of transfected cells with >4 CP110 dots were determined. (**E**) U2OS cells were transfected with plasmid expressing an irrelevant Flag-tagged protein (control), Flag-Cep76 wild type (Cep76 FL) or mutant (Cep76 K279R, K279Q, S83AK279R or S83EK279Q) and either left untreated or treated with HU.

The percentages of transfected cells with (left) >4 CP110 or (right) >2 γ-tubulin dots were determined. (**F**) Western blotting of Flag in U2OS cells expressing the indicated Flag-tagged proteins. α-tubulin was used as a loading control. (**G**) *In vitro* kinase assays using purified Cep76 wide type (Cep76 FL), mutant K279R, K279Q or S83AK279R protein and cyclin A/CDK2. In (**D** and **E**), at least 75 transfected cells were scored per condition, and average of three independent experiments is shown. Error bars represent standard errors.

Figure 7

Temporal changes in Cep76 PTMs in the cell cycle correlate with protein function. (**A**) Mass spectrometric quantitation of S83 phosphopeptides from asynchronous (AS) and synchronized U2OS cells expressing Flag-Cep76. (**B**) Acetylated proteins from asynchronous (AS) and synchronized U2OS cells expressing Flag-tagged Cep76 were immunoprecipitated with an anti-acetyl-lysine antibody, and the resulting immunoprecipitates were Western blotted with an anti-Flag antibody. IN, input. (**C**) U2OS cells were transfected with plasmid expressing an irrelevant Flag-tagged protein (control) or Flag-Cep76 wild type (Cep76 FL) and either left untreated or treated with RO 3306. The percentages of transfected cells with (left) >4 CP110 or (right) >2 γ-tubulin dots were determined. (**D**) Western blotting of Flag in U2OS cells expressing the indicated Flag-tagged proteins. α-tubulin was used as a loading control. (**E**) Cells were stained with DAPI (blue) and antibodies against Flag (red) and CP110 or γ-tubulin (green). (**F, G**) U2OS cells were transfected with plasmid expressing an irrelevant Flag-tagged protein (control) or Flag-Cep76 wild type (Cep76 FL) and either left untreated or treated with RO 3306. (Top) Cells were stained with antibodies against Flag (green), γ-tubulin (blue) and (**F**) CP110 or (**G**) Plk1-pT210 (red). (Bottom) (**F**) The percentages of transfected cells with

disengaged centrioles or (**G**) Plk1-pT210 at centrosomes were determined and (**G**) the fluorescence intensities of centrosomal Plk1-pT210 were quantitated. (**H)** U2OS cells were transfected with plasmid expressing an irrelevant Flag-tagged protein (control) or Flag-Cep76 wild type (Cep76 FL) and either left untreated or treated with DOX. (Top) Cells were stained with antibodies against Flag (green), CP110 (red) and γ-tubulin (blue). (Bottom) The percentages of transfected cells with >4 CP110 dots were determined. In (**C, F, G** and **H**), at least 75 transfected cells were scored per condition, and average of three independent experiments is shown. Error bars represent standard errors.

Supplemental figures legends

Figure S1

CDK inhibition attenuates S83 phosphorylation. Mass spectrometric quantitation of S83 phosphopeptides from Flag-Cep76 expressing U2OS cells grown asynchronously (AS) or synchronized with HU and released into S phase in the absence (S) or presence of roscovitine (S+roscovitine).

Figure S2

Cep76 AXA mutants bind cyclin A and are functional. (**A**) Schematic representation of AXA mutants of Cep76. (**B**) Flag (control), Flag-Cep76 wild type (FL) or AXA mutants were expressed in U2OS cells and immunoprecipitated from lysates with anti-Flag beads. The resulting immunoprecipitates were Western blotted with anti-Flag and cyclin A antibodies. IN, input. (**C**) The percentages of transfected U2OS cells with (top) >4 CP110 or (bottom) >2 γ-tubulin dots were determined. At least 75 transfected cells were scored per condition, and average of three independent experiments is shown. Error bars represent standard errors.

Figure S3

Cep76 AXA mutants suppress HU-induced centriole amplification. U2OS cells transfected with the indicated plasmids and either left untreated or treated with HU were stained with DAPI (blue) and antibodies against Flag (red) and γ-tubulin (green). Control denotes expression of an irrelevant Flag-tagged protein.

Figure S4

A ~1.5 fold overexpression of Flag-Cep76 is sufficient to rescue centriole amplification induced by loss of Cep76 or HU treatment. (**A**) U2OS cells were transfected with control siRNA (siNSp) or siRNA targeting Cep76 3'UTR and the indicated amounts of plasmid expressing Flag-Cep76. (Top) Western blotting of endogenous and recombinant Cep76 using an anti-Cep76 antibody. α-tubulin was used as a loading control. (Bottom) The percentages of transfected cells with >4 CP110 dots were determined. (**B**) U2OS cells expressing increasing amounts of Flag-Cep76 were either left untreated or treated with HU. (Top) Western blotting of endogenous and recombinant Cep76 using an anti-Cep76 antibody. α-tubulin was used as a loading control. (Bottom) The percentages of transfected cells with >4 CP110 dots were determined. In (**A** and **B**), at least 75 transfected cells were scored per condition, and average of three independent experiments is shown. Error bars represent standard errors. Densitometric analyses were performed with ImageJ.

Figure S5

A cancer-associated Cep76 S83C mutation is unable to suppress centriole amplification. U2OS cells transfected with control siRNA (siNSp) or siRNA targeting Cep76 3'UTR (siCep76) and plasmid expressing an irrelevant Flag-tagged protein (control), Flag-Cep76 wild type (Cep76 FL) or mutant (Cep76 S83C). (**A**) The percentages of transfected cells with >4 CP110 dots were determined. At least 75 transfected cells were scored per condition, and average of three independent experiments is shown. Error bars represent standard errors. (**B**) Cells were stained with DAPI (blue) and antibodies against Flag (red) and CP110 (green).

Figure S6

Cep76 slightly but not dramatically affects CDK2 and Cyclin A localization to the centrosome. (**A**) Fluorescence intensity of endogenous CDK2 at the centrosome was measured in U2OS cells transfected with control siRNA (siNSp) or Cep76 siRNA. **(B**) Fluorescence intensity of endogenous cyclin A at the centrosome was measured in U2OS cells transfected with control siRNA (siNSp) or Cep76 siRNA. In (**A** and **B**), at least 75 transfected cells were scored per condition, and average of three independent experiments is shown. Error bars represent standard errors.

Figure S7

Cep76 antagonizes Plk1 function to suppress centriole amplification. (**A**) (Left) U2OS cells were transfected with control siRNA (siNSp) or Cep76 siRNA and either left untreated or treated with BI 2536. The percentages of transfected cells with >4 centrin dots were determined. (Right) Cells were stained with DAPI (blue) and antibodies against Cep76 (red) and centrin (green). (**B**) U2OS cells transfected with plasmids expressing Flag and Myc, Flag-Cep76 and Myc, or Flag-Cep76 and constitutively active Plk1 (Myc-Plk1-T210D), were either left untreated or treated with HU. The percentages of transfected cells with >4 CP110 dots were determined. (**A-B**) At least 75 transfected cells were scored per condition, and average of three independent experiments is shown. Error bars represent standard errors.

Figure S8

Flag-Cep76 is acetylated *in vivo*. (**A**) U2OS cells expressing Flag-tagged Cep76 were either left untreated or treated with TSA. Recombinant proteins were immunoprecipitated with anti-Flag beads, and the resulting immunoprecipitates were Western blotted with anti-acetyl-lysine and Flag antibodies. IN, input. (**B**) Same as (**A**), except that proteins were immunoprecipitated with an anti-acetyl-lysine antibody. The resulting immunoprecipitates were Western blotted with an anti-Flag antibody. IN, input. Densitometric analyses were performed with ImageJ.

Figure S9

Cep76 is highly phosphorylated in S phase. Flag-Cep76 expressed in asynchronous (AS) or synchronized U2OS cells were immunoprecipitated with an anti-Flag antibody, and the resulting immunoprecipitates were Western blotted with anti-Flag and anti-phosphoserine antibodies. IN, input.

Figure S10

Acetylation of Cep76 relieves Plk1 from inhibition but is insufficient to prevent centriole amplification induced by RO 3306. U2OS cells were transfected with plasmid expressing an irrelevant Flag-tagged protein (control), Flag-Cep76 wild type (Cep76 FL) or mutant (S83E, S83EK279Q and S83EK279R) and either left untreated or treated with RO 3306. The percentages of transfected cells with (top) >4 CP110 dots or (bottom) Plk1-pT210 at centrosomes were determined. At least 75 transfected cells were scored per condition, and average of two independent experiments is shown. Error bars represent standard errors.

Figures

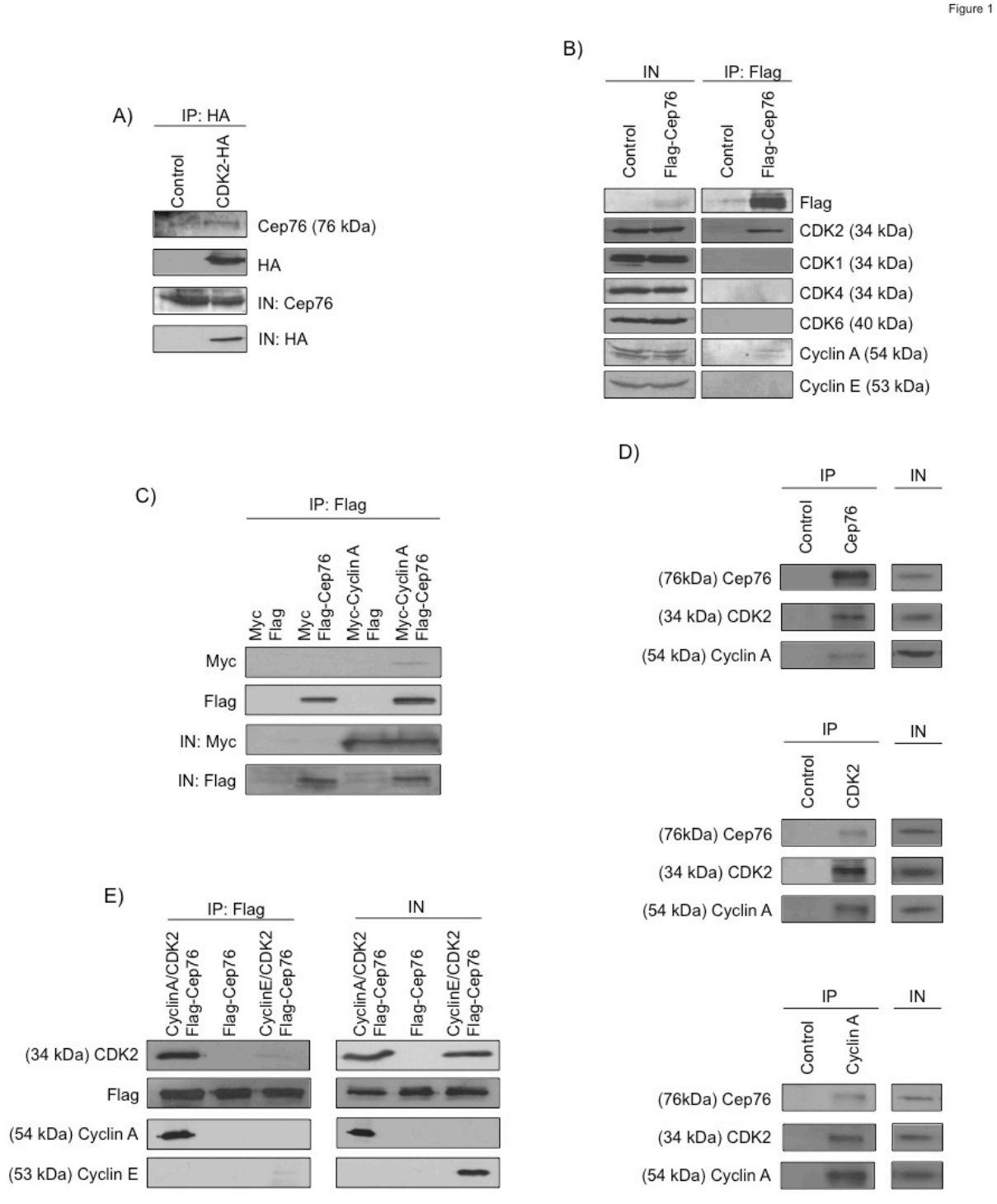

Figure 1. Cep76 interacts with cyclin A/CDK2.

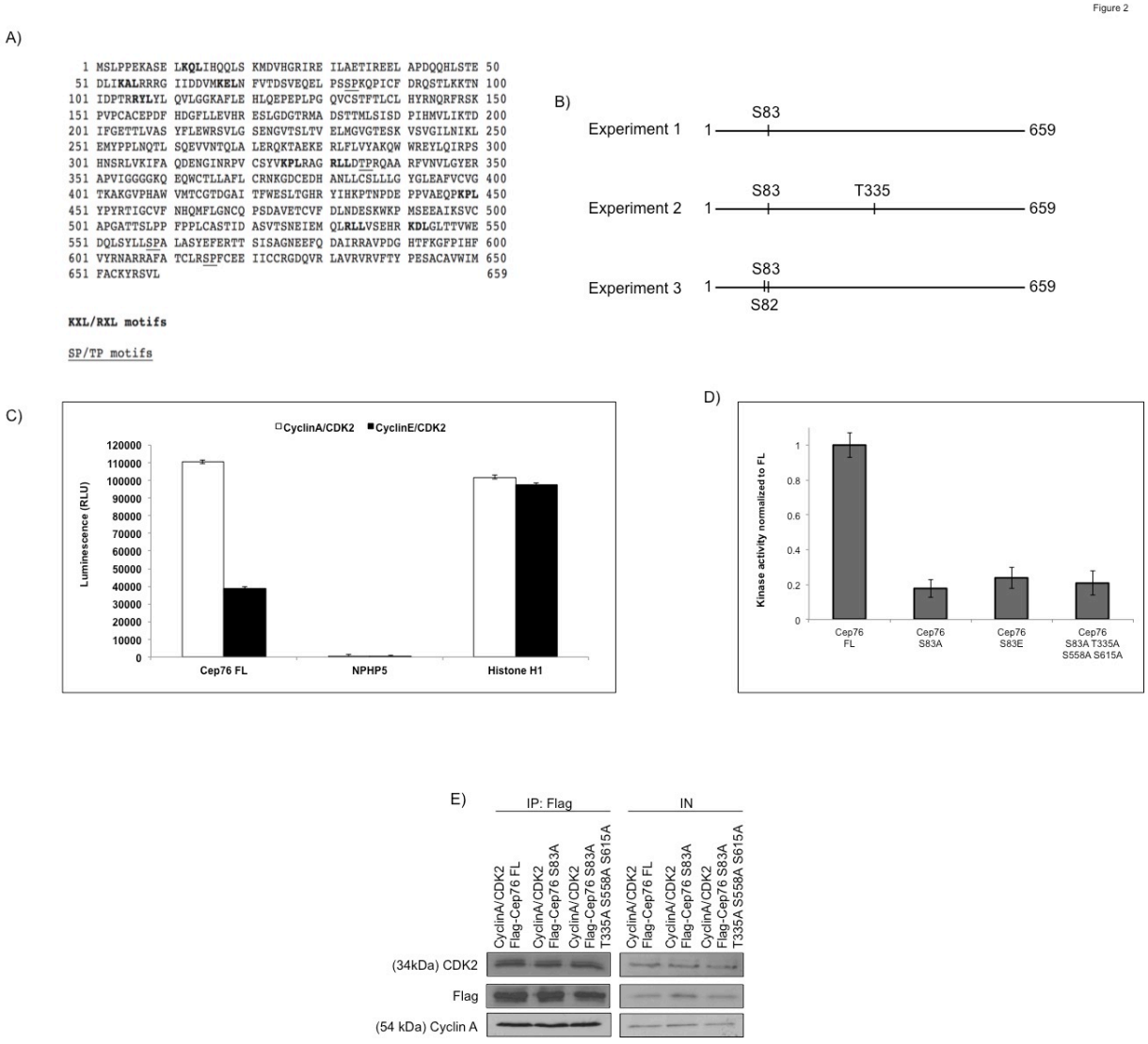

Figure 2. Cyclin A/CDK2 phosphorylates Cep76 at S83.

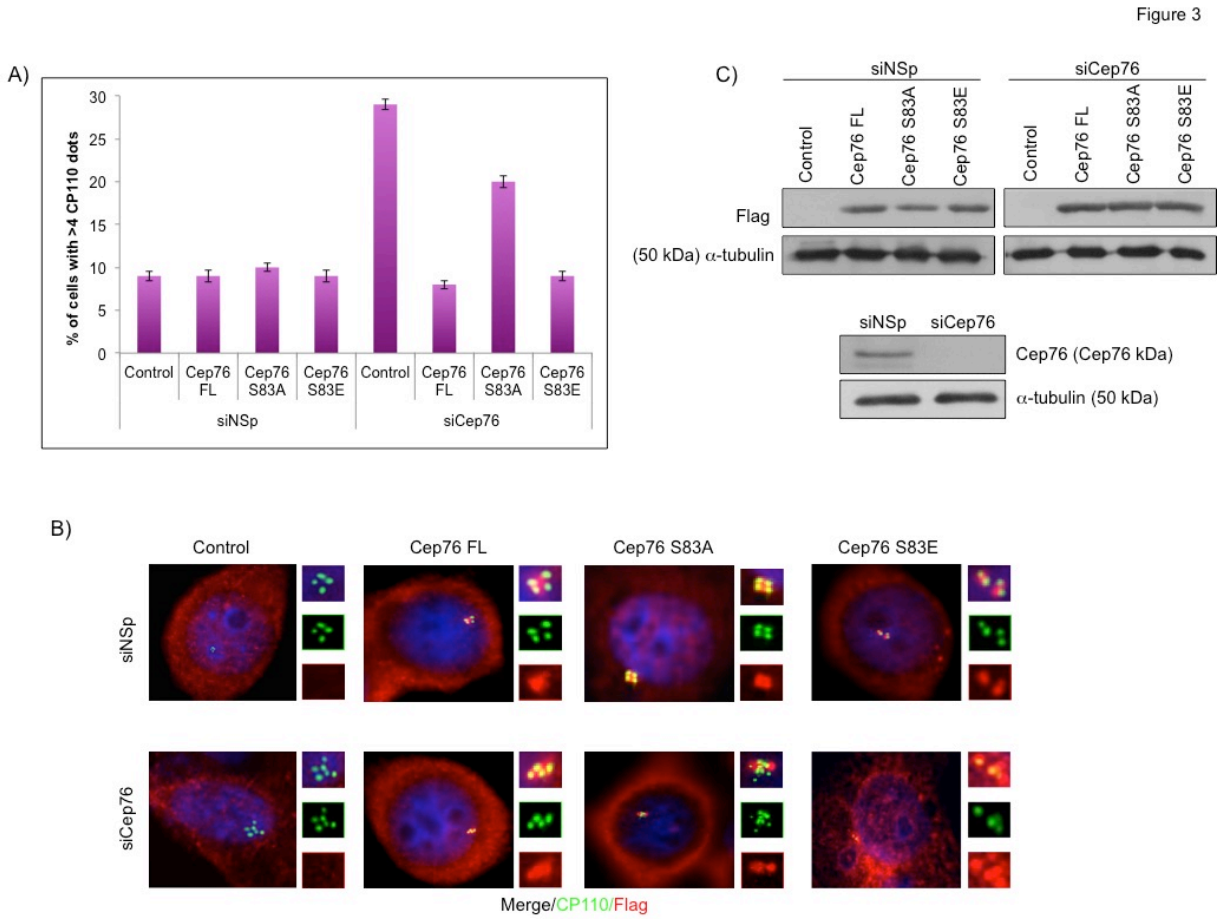

Figure 3. Ectopic expression of Cep76 or a phosphomimetic mutant rescues centriole amplification induced by loss of endogenous Cep76.

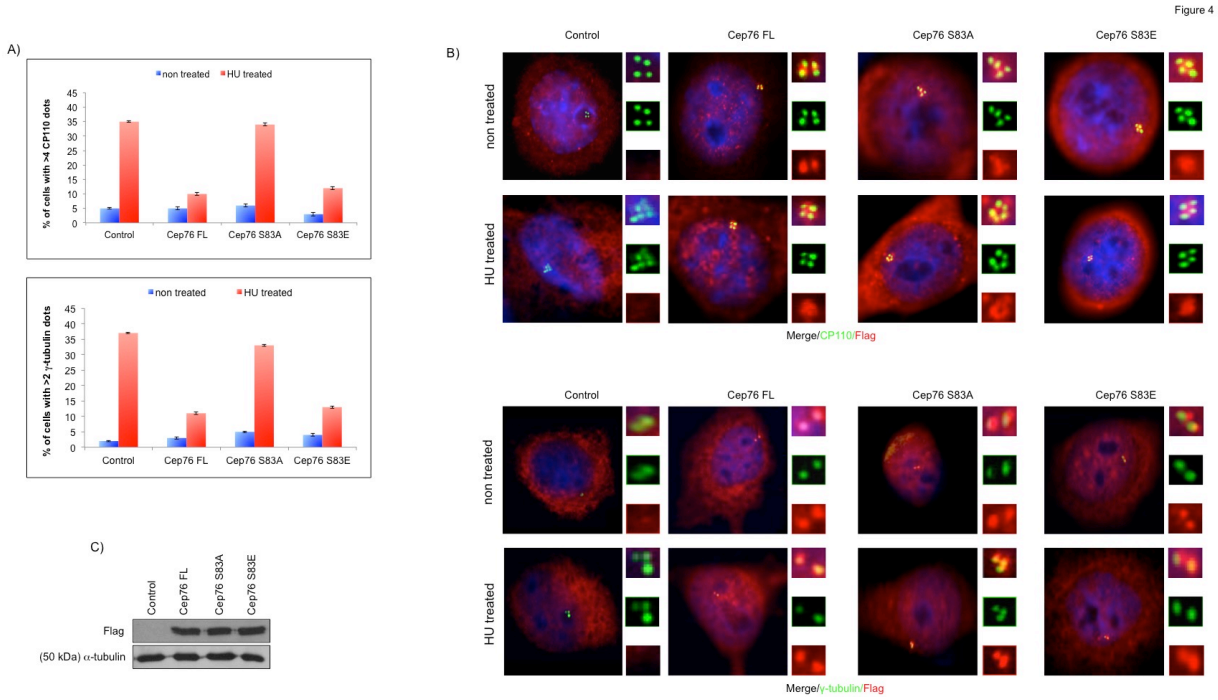

Figure 4. Ectopic expression of Cep76 or a phosphomimetic mutant suppresses HU-induced centriole amplification.

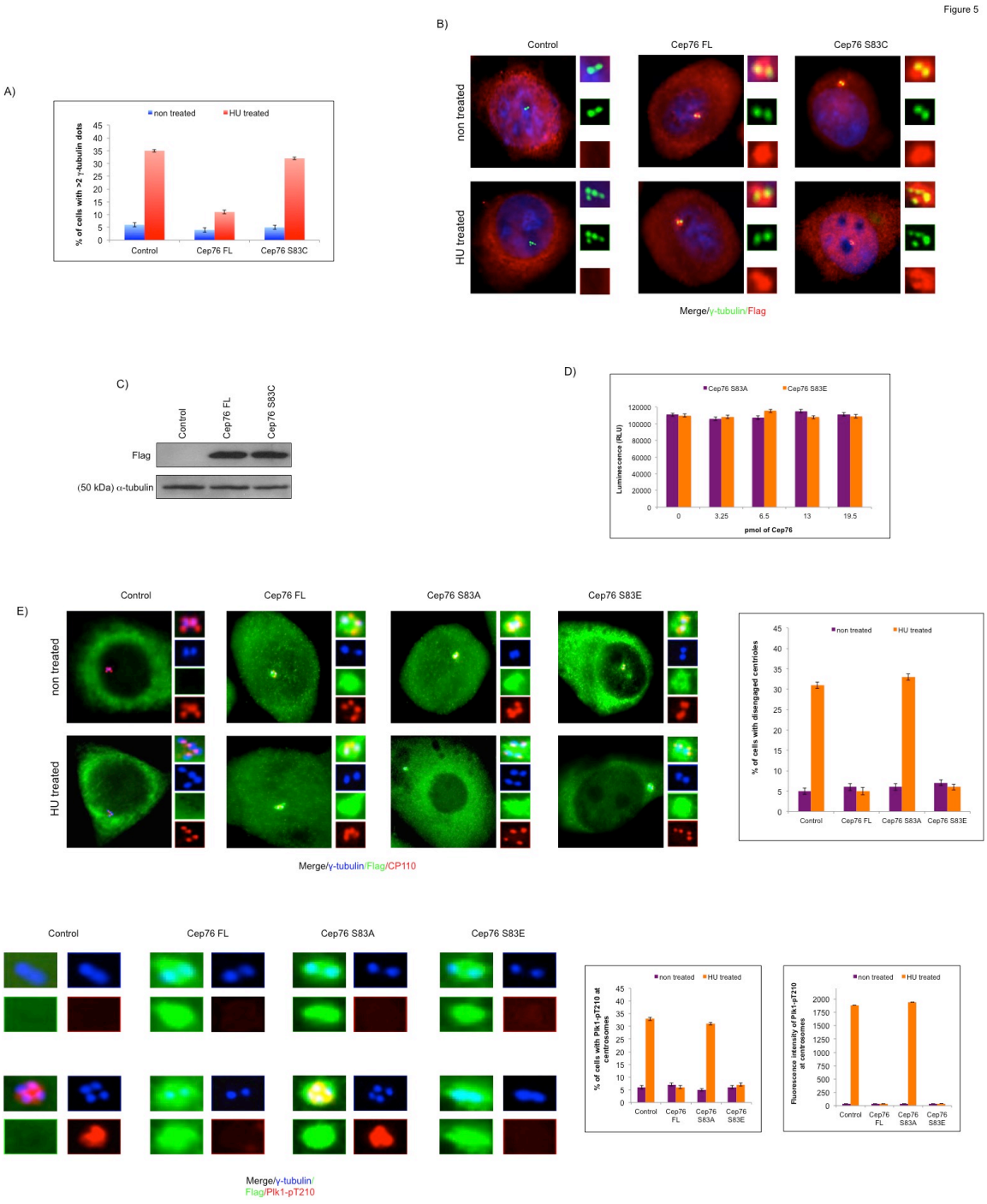

Figure 5. Characterization of a cancer-associated Cep76 S83C mutation and the mechanism that suppresses centriole amplification.

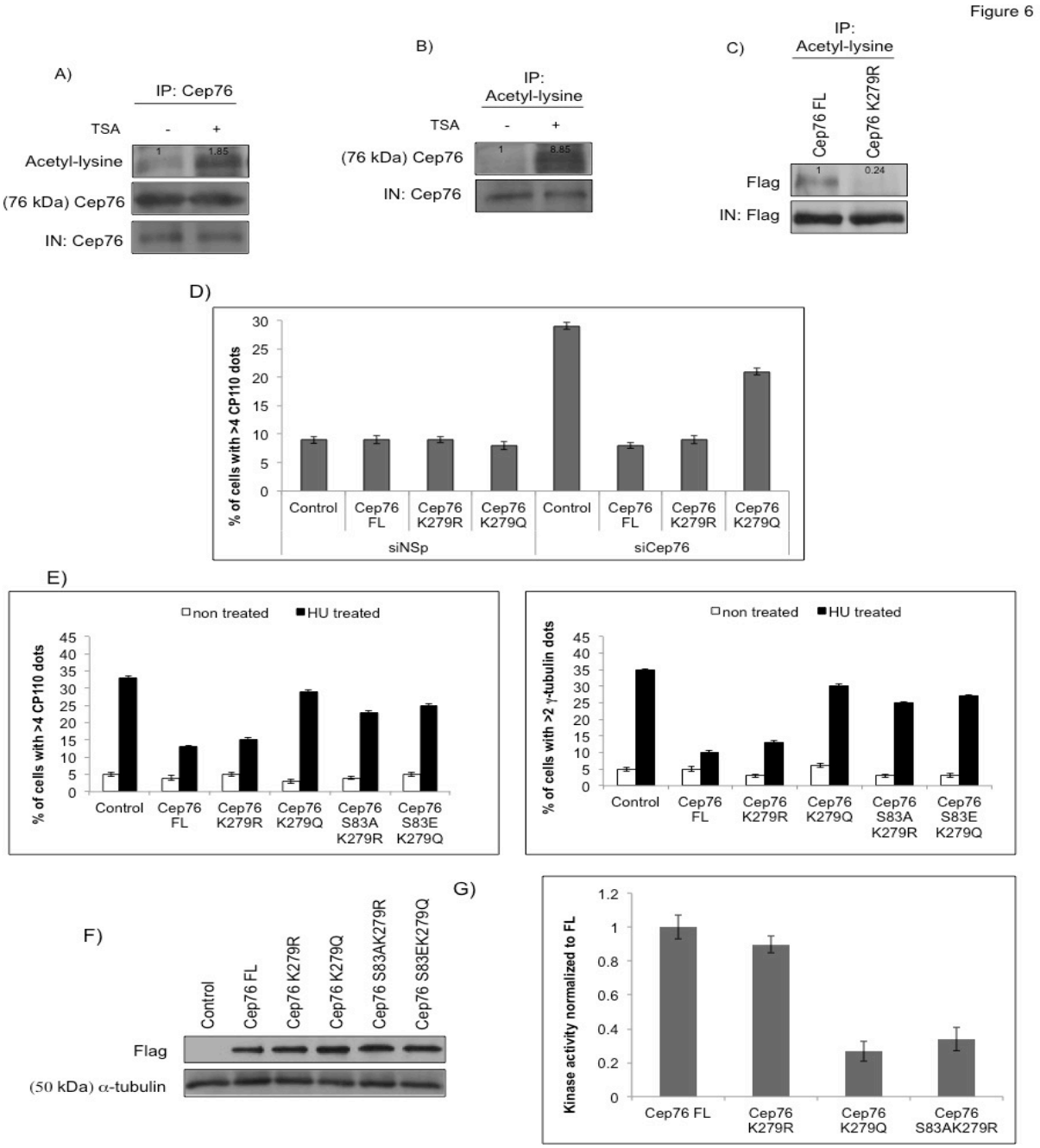

Figure 6. Enforced acetylation of Cep76 at K279 abrogates the protein's ability to suppress centriole amplification.

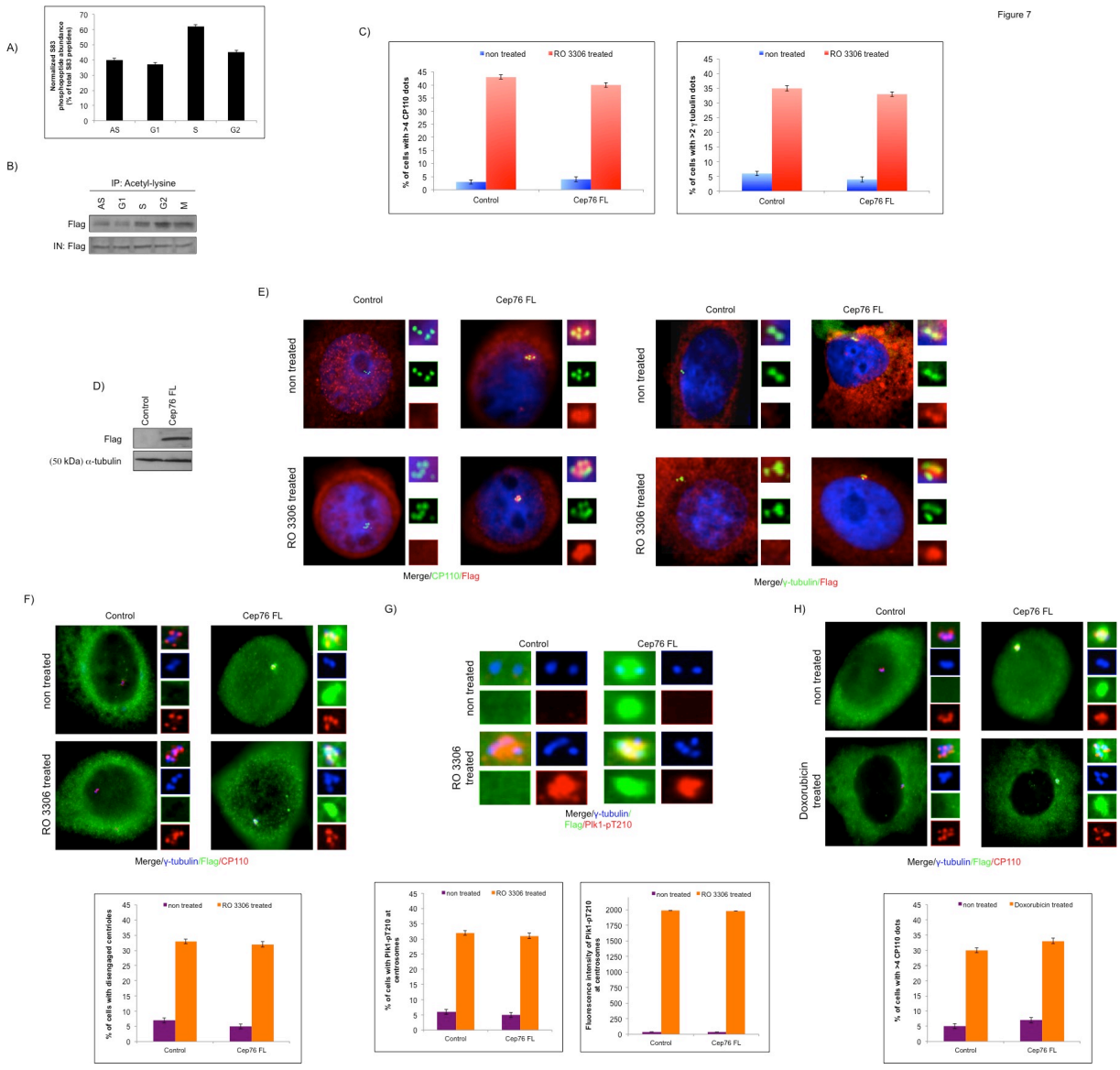

Figure 7. Temporal changes in Cep76 PTMs in the cell cycle correlate with protein function..

Supplemental figures

Figure S1

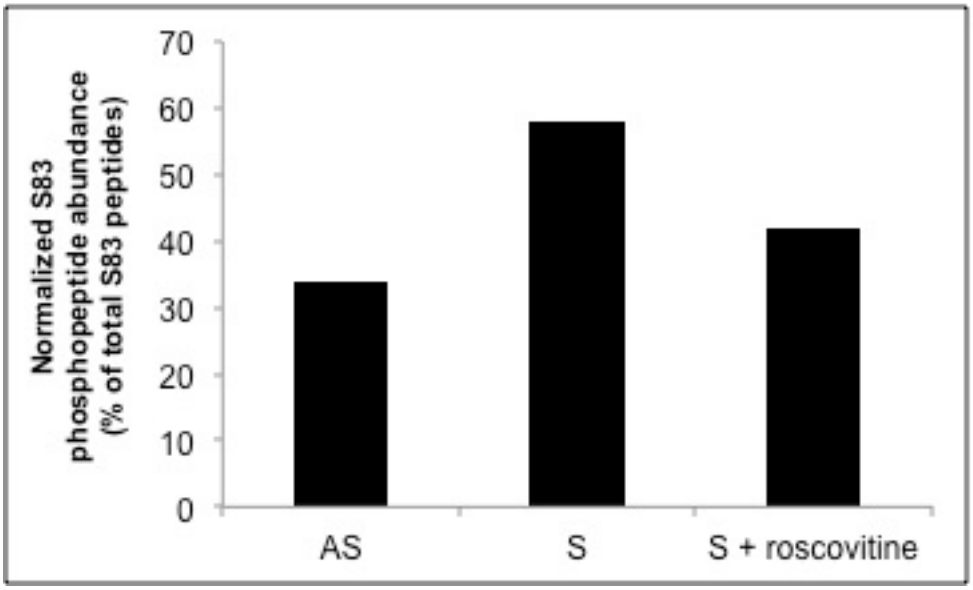

Figure S1. CDK inhibition attenuates S83 phosphorylation.

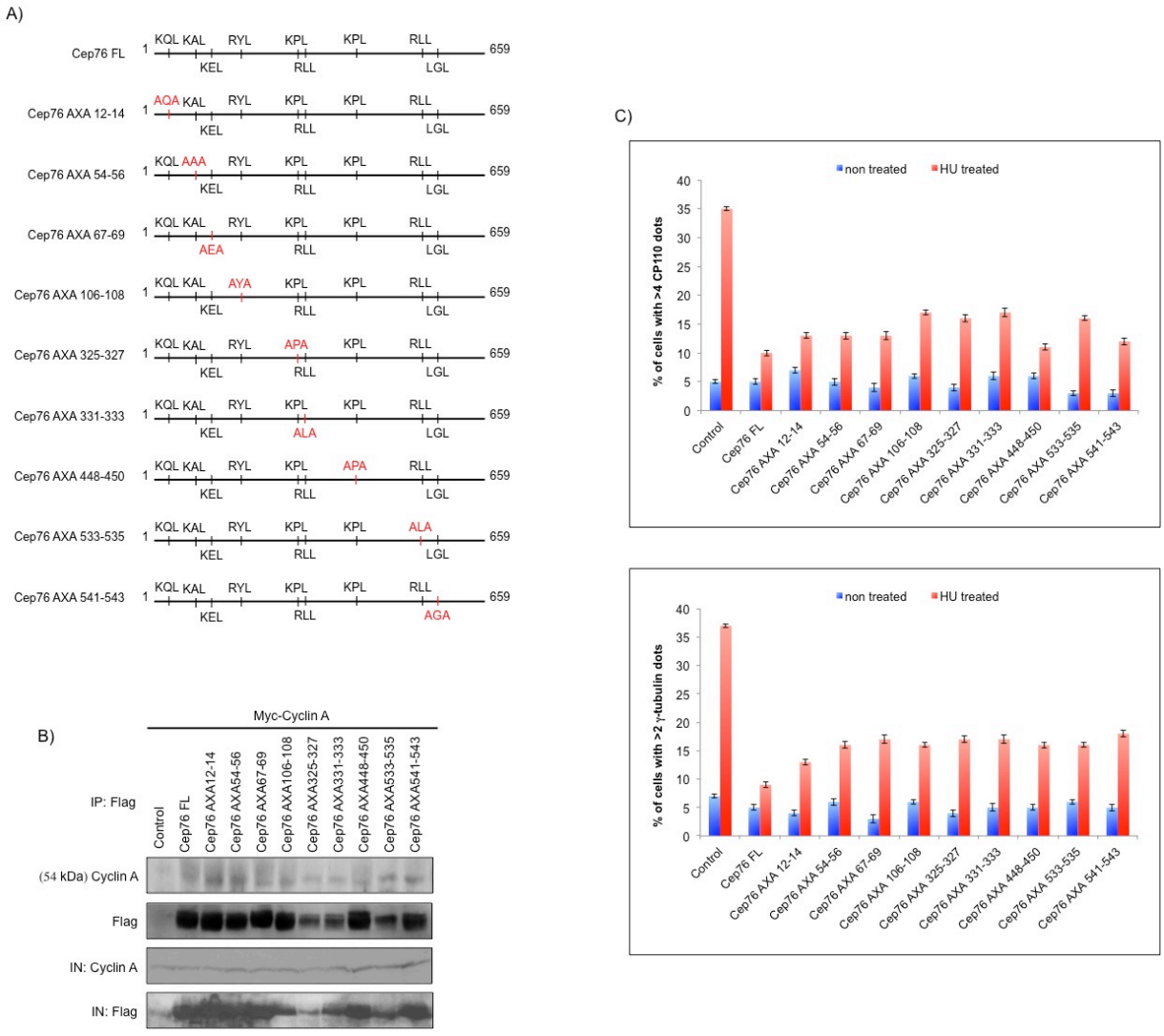

Figure S2. Cep76 AXA mutants bind cyclin A and are functional.

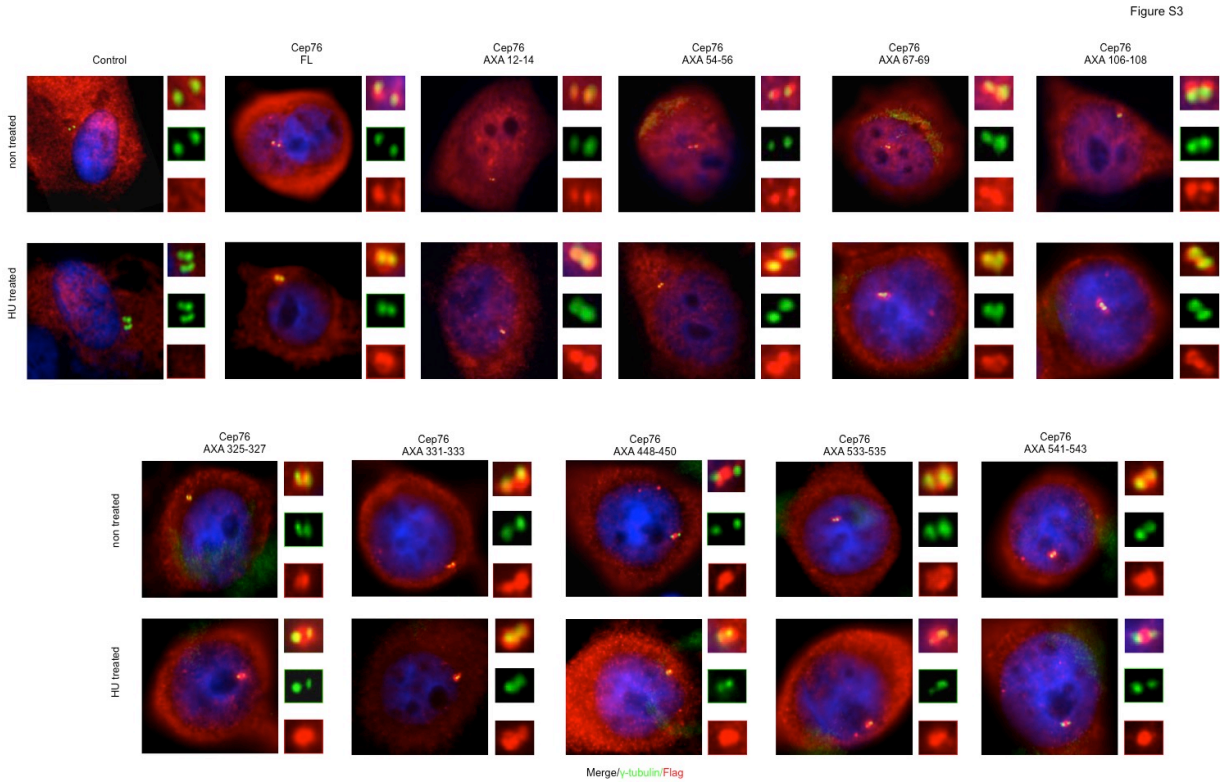

Figure S3. Cep76 AXA mutants suppress HU-induced centriole amplification.

Figure S4

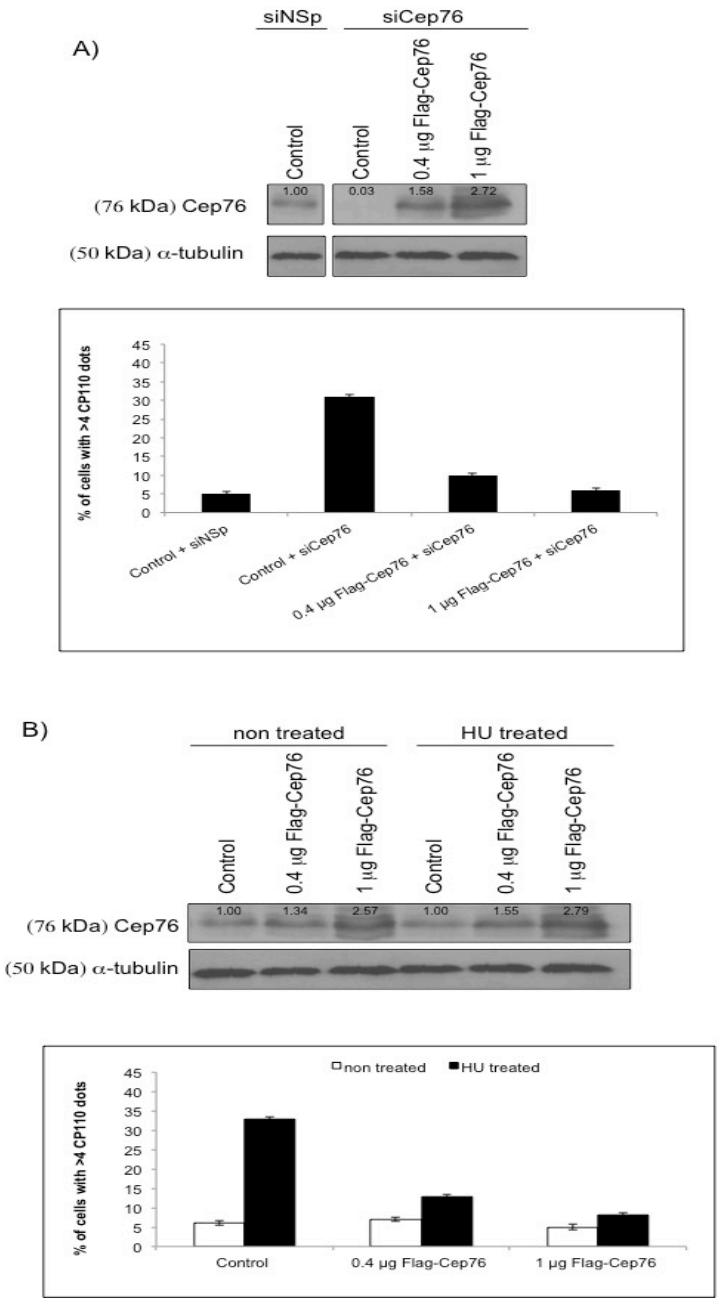

Figure S4. A ~1.5 fold overexpression of Flag-Cep76 is sufficient to rescue centriole amplification induced by loss of Cep76 or HU treatment.

Figure S5

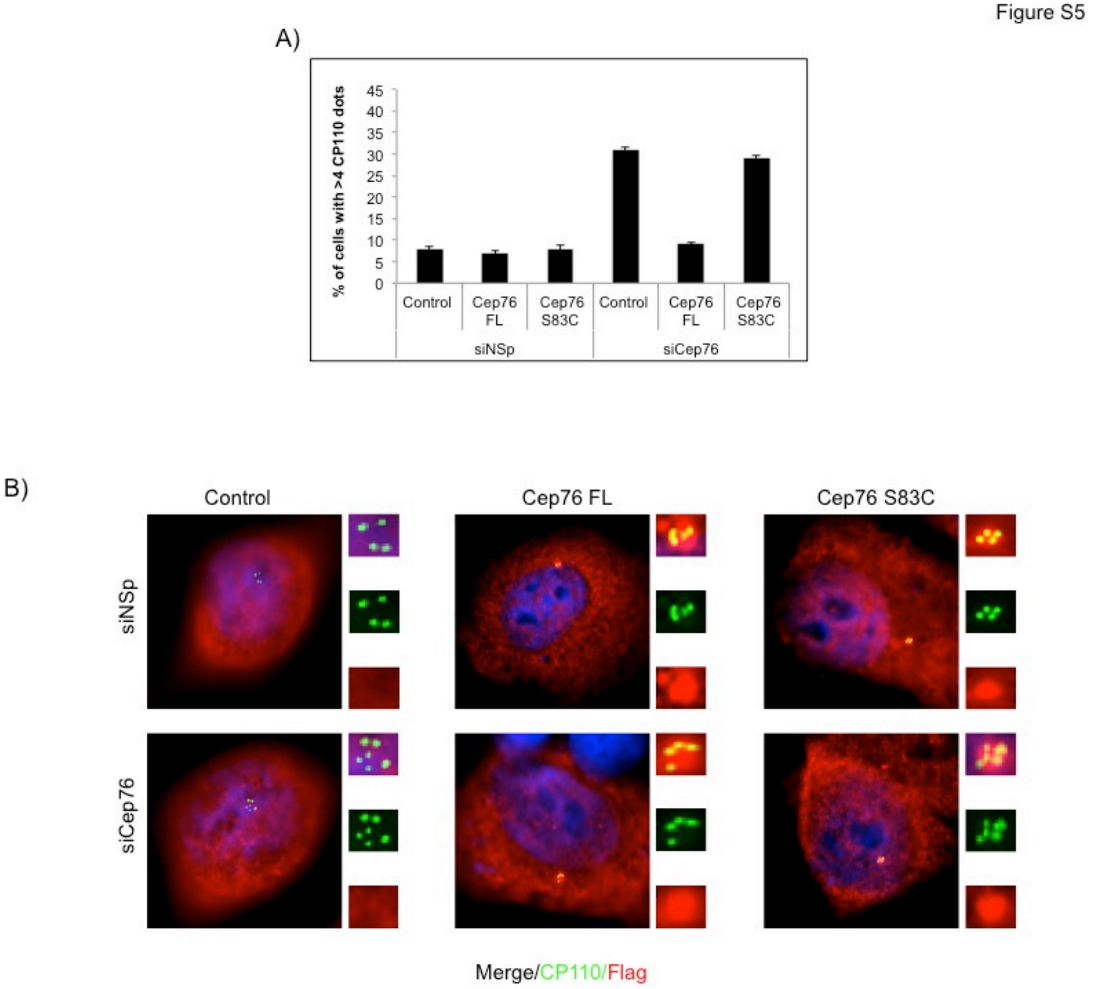

Figure S5. A cancer-associated Cep76 S83C mutation is unable to suppress centriole amplification.

Figure S6

A)

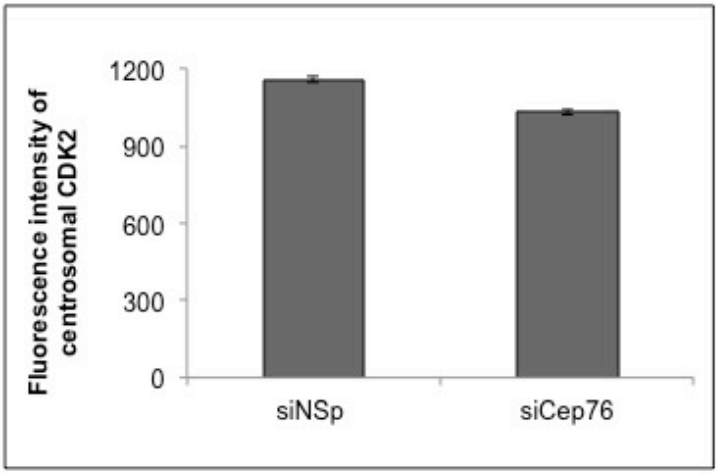

B)

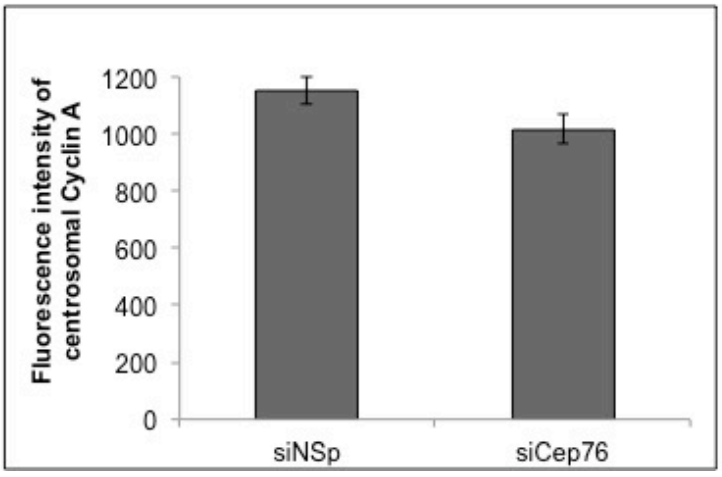

Figure S6. Cep76 slightly but not dramatically affects CDK2 and Cyclin A localization to the centrosome.

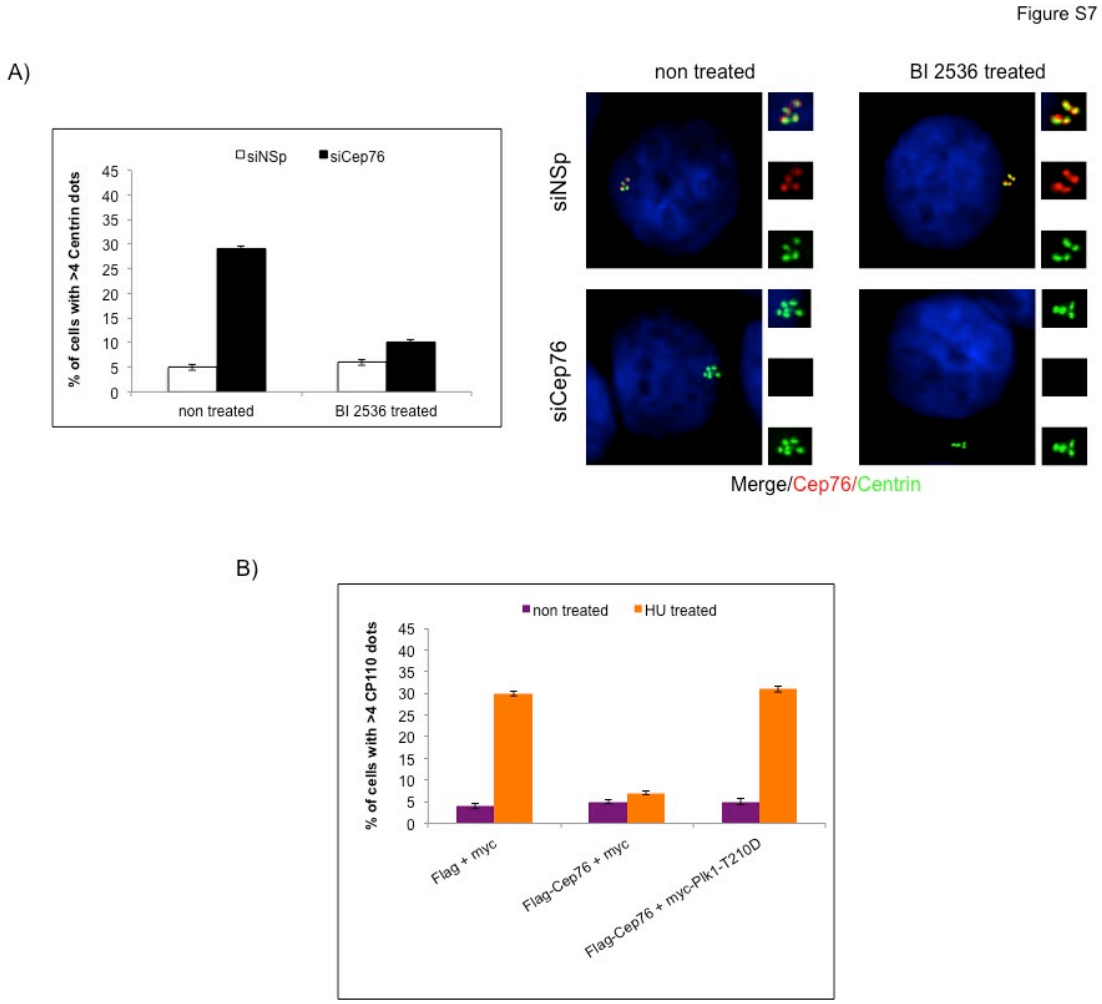

Figure S7. Cep76 antagonizes Plk1 function to suppress centriole amplification.

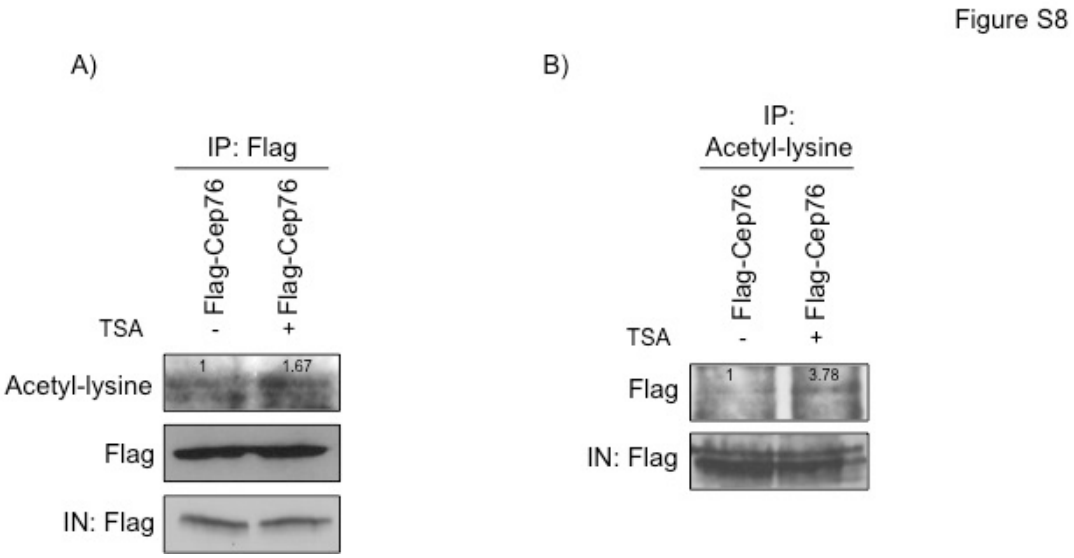

Figure S8. Flag-Cep76 is acetylated *in vivo*.

Figure S9

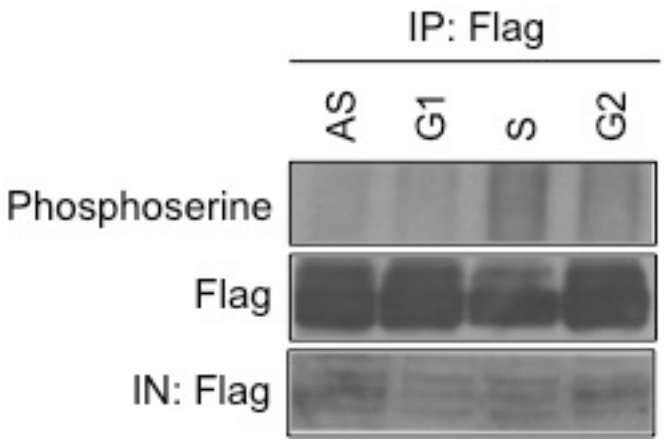

Figure S9. Cep76 is highly phosphorylated in S phase.

Figure S10

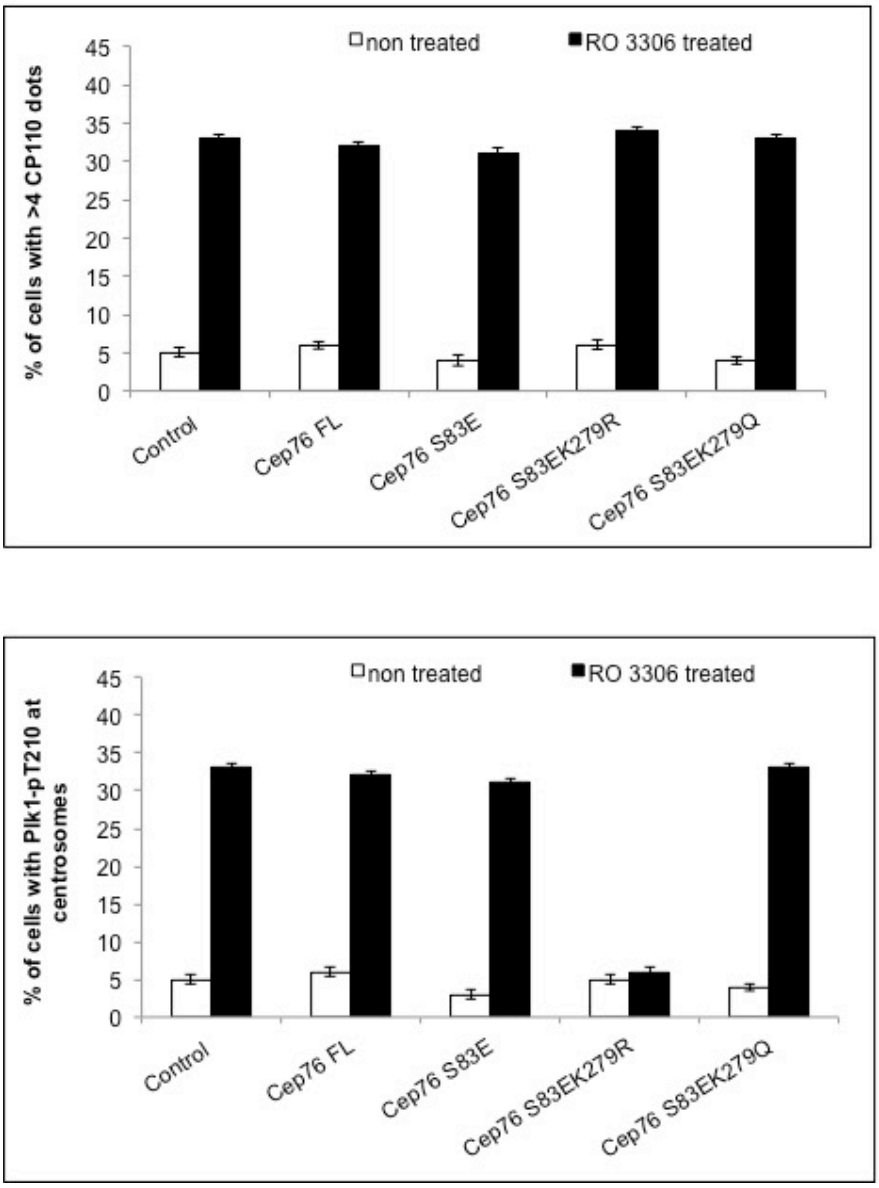

Figure S10. Acetylation of Cep76 relieves Plk1 from inhibition but is insufficient to prevent centriole amplification induced by RO 3306.

Table

Protéines	Nombre de peptides
ACTA2	361
ACTB	389
AHNAK	2057
ALMS1	165
CAD	18
CALU	15
CAPZB	24
CCDC88A	11
CCT2	27
CCT3	16
CEP170	13
CEP76	2663
CEP97	47
CGN	11
CLTC	63
CP110	52
CUL3	14
DAPK3	16
DARS	19
DBN1	22
DDX21	23
DHX15	16

Protéines	Nombre de peptides
GAPDH	29
HNRNPA2B	25
HNRNPUL1	27
HSP90AA1	17
HSP90AB3P	23
HSP90B1	15
HSPA1A	33
HSPA5	51
HSPA8	141
HSPA9	50
KCTD10	42
KIAA0586	46
KIAA1217	53
KIF11	145
KPNB1	32
LIMA1	22
LUZP1	145
MAP3K7	15
MARS	13
MVP	27
MYH10	33
MYH9	67

Protéines	Nombre de peptides
PABPC1	33
PKM	32
PLEC	72
POTEKP	31
PPL	30
PRDX1	27
RANBP2	164
RANGAP1	57
RBBP8	18
RCC1	14
RPL13	57
RPS3	26
SEC16A	63
SPTAN1	74
SPTBN1	56
STK38	84
SYNM	64
TAB1	21
TFG	47
TUBA1A	116
TUBB1	30
UBAP2	56

Table 1.

Non-exhaustive list of proteins detected in the mass spectrometry experiment. Proteins considered as ‘‘hits " are those whose number of peptides in the Cep76 sample is at least greater than 10 and the number of peptides in the control sample is close or equal to 0.

Addendum

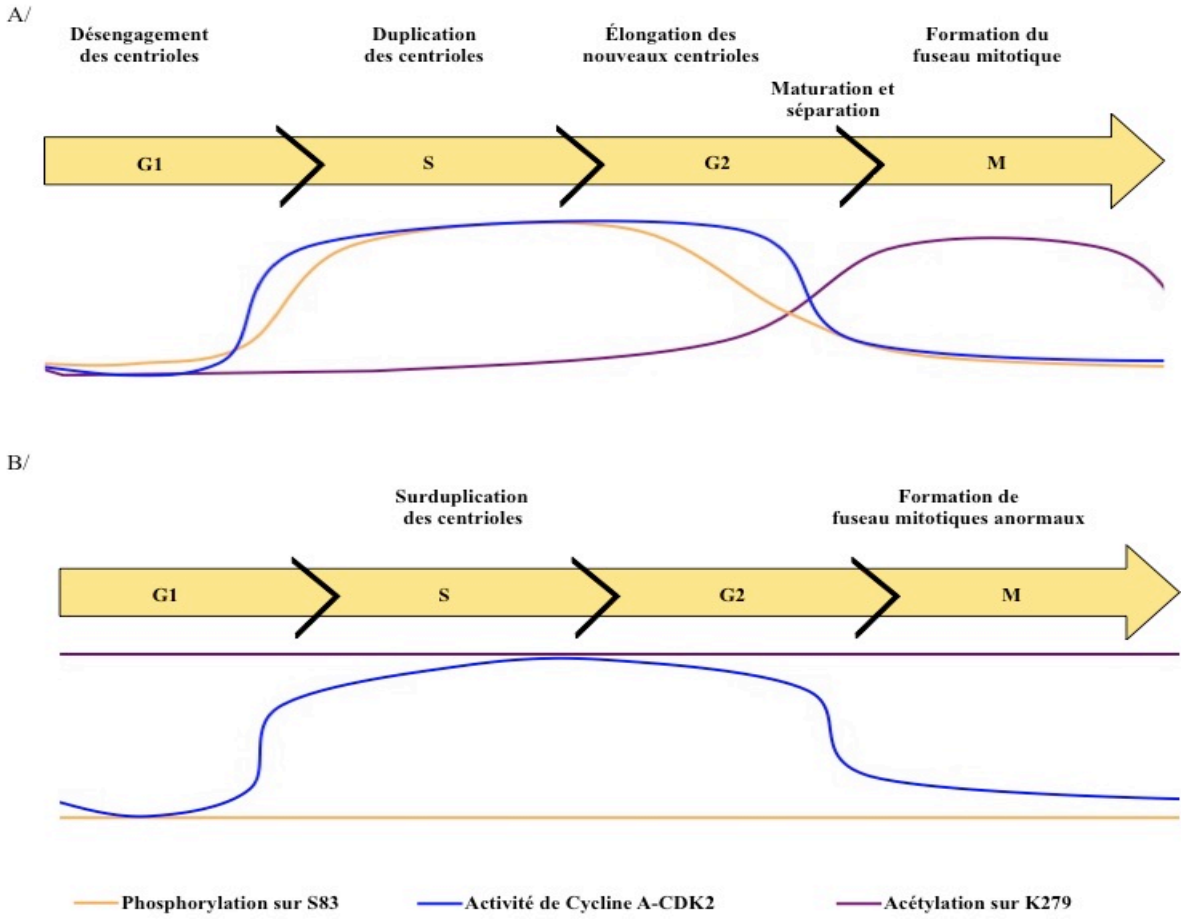

Résumé schématique.

A/ Lors d'un cycle cellulaire normal, Cep76 se lie au complexe CDK2/Cyclin A en phase S et G2 où la protéine sera phosphorylée sur le résidu S83. Cette activation de Cep76 permet un contrôle du cycle de duplication des centrioles et une progression du cycle cellulaire normale. Cep76 devient acétylée sur le résidu K279 en fin de phase G2 et M pour inhiber sa fonction.B/ Lorsque Cep76 est constitutivement acétylée sur le résidu K279 ou perd sa phosphorylation sur le résidu S83, la protéine devient non fonctionnelle et entraine une sur-duplication des centrioles en phase S. Ce dérèglement du cycle des centrosomes peut alors provoquer des mitoses aberrantes.

Conclusion

Les centrosomes sont des organelles essentielles au bon fonctionnement de nombreux processus cellulaires comme la polarité, l'adhésion, la mitose ou la ciliogénèse. Des défauts dans leur structure ou leur fonction peuvent amener des problèmes majeurs et des maladies comme les cancers ou les ciliopathies. Ceci explique l'importance d'étudier cette organelle et de décortiquer les éléments essentiels pour sa formation et sa fonction. Lors de mon doctorat, je me suis concentrée sur deux nouvelles protéines centrosomales : NPHP5 et Cep76.

NPHP5

Localisation et ciliogénèse

Dans un premier temps, nous avons cherché à caractériser la localisation précise de NPHP5 au cours du cycle cellulaire. Par immunofluorescence (IF) indirecte, nous avons démontré que la protéine se situe dans la partie distale des centrioles tout au long de l'interphase avant de disparaître en mitose. NPHP5 est également présente à la base du cil dans les cellules quiescentes. Ensuite, pour étudier la fonction de NPHP5 aux centrosomes, nous avons utilisé une approche d'ARN interférence pour inhiber transitoirement la protéine dans les cellules. Cette délétion n'affecte pas la progression du cycle cellulaire ou du cycle des centrosomes. En revanche, l'absence de NPHP5 entraine un blocage de la ciliogénèse dans la majorité des cellules, que ce soit à l'état prolifératif ou de quiescence. La localisation de NPHP5 dans la partie distale des centrioles pourrait donc avoir un rôle majeur dans la fonction de la protéine au cours de la ciliogénèse. Comme mentionné dans l'introduction, les appendices distaux et sub-distaux du centriole mère, ou corps basal, sont essentiels à la formation des cils.

Il serait donc très intéressant de pouvoir étudier de manière plus fine la localisation de NPHP5 dans la partie distale des centrioles pour mieux comprendre son rôle dans la formation des cils. En utilisant les techniques de microscopie électronique et immunomarquage, plusieurs groupes ont déjà analysé la localisation de protéines dans des cellules fixées et/ou dans des centrosomes purifiés avec grand succès (193-197). En employant les mêmes approches, nous pourrions étudier le lien entre la localisation de NPHP5 et les appendices distaux/sub-distaux des centrosomes. La microscopie électronique à transmission a également été utilisée à mainte reprise pour caractériser la structure détaillée d'organelles comme les centrosomes ou les cils (198-202). Nous pourrions alors étudier la structure des cils/centrosomes dans les cellules contrôles versus celles où NPHP5 est inhibé. Cela pourrait nous aider à déterminer à quel stade de la ciliogénèse NPHP5 est impliquée. Des expériences sont actuellement en cours pour élucider ces questions.

NPHP5 et ses partenaires

Par la suite, nous nous sommes intéressés aux partenaires de NPHP5 et leur influence dans ses fonctions.

Cep290 est une protéine centrosomale aussi impliquée dans les ciliopathies et sa liaison à NPHP5 s'avère essentielle à la formation de cils dans les cellules tant quiescentes que prolifératives. Toutefois, il est important de noter que les phénotypes cliniques associés à des défauts de Cep290 sont plus diversifiés que ceux associés à des défauts de NPHP5 (150, 203). Cette différence pourrait provenir d'un profil d'expression divergent de ces deux protéines dans les tissus mais aussi du fait que Cep290 est également localisée au niveau de structures appelées satellites, contrairement à NPHP5 (152, 153, 204).

La calmoduline est une protéine ubiquitaire capable de s'associer aux ions calcium présents dans le milieu cellulaire. Un grand nombre de protéines qui se lient à la calmoduline sont incapables de se lier eux-mêmes au calcium, et utilisent la calmoduline comme un capteur de calcium et transducteur de signal pour moduler leur fonction (205-207).

NPHP5 se lie à la calmoduline par trois sites distincts et cette liaison est importe pour empêcher l'auto-agrégation de NPHP5. Bien que ces agglomérats ne semblent pas gêner la localisation de NPHP5 ou la ciliogénèse en elle-même ; il est connu que l'accumulation de protéines en agrégats peut conduire à la formation de fibres amyloïdes et à une neuro-dégénération (207-209). De plus amples expériences sont donc nécessaires pour délier le rôle potentiel de NPHP5 dans la formation de ces fibres et la sévérité des maladies neuro-dégénératives comme la rétinite pigmentaire, au niveau de l'œil (210, 211).

De manière plus générale, il serait intéressant de rechercher d'autres partenaires éventuels de NPHP5 par spectrométrie de masse (SDM) ainsi que des modifications post-traductionnelles comme l'ubiquitination ou la phosphorylation. Cela permettrait de mieux comprendre comment NPHP5 est elle-même régulée au cours du cycle cellulaire mais aussi comment elle module des voies de signalisations dans les cellules. Par exemple, une simple approche par IF avec un anticorps phospho-spécifique ou encore de la microscopie en temps réel nous aiderait à suivre les modifications post-traductionnelles au cours du cycle cellulaire ainsi que la localisation de la protéine. De même, la technique de PLA (proximity ligation assay) pourrait être utilisée pour valider de nouveaux partenaires de NPHP5 avant une étude plus approfondie. Certaines expériences sont en cours de réalisation et des résultats sont attendus sous peu.

NPHP5 et ses différents domaines fonctionnels

Afin de mieux comprendre les différentes interactions de NPHP5 avec ses partenaires ainsi que leur rôle dans sa fonction, la prochaine étape évidente a été de discerner les différents domaines de la protéine. Pour cela, nous avons utilisé une série de délétions ou mutations pour créer diverses protéines tronquées et analyser leur localisation ou leur liaison aux partenaires, par IF et immunoprécipitation-western blot (IP-WB) respectivement. En utilisant ces techniques, j'ai montré que Cep290 se lie à la partie C-terminale de NPHP5 tandis que la calmoduline se lie sur la partie centrale de la protéine.

De façon intéressante, la séquence de localisation au centrosome se situe dans la partie C-terminale extrême de NPHP5 et chevauche le domaine de liaison à Cep290. L'hypothèse était donc que Cep290 recrutait NPHP5 au niveau des centrosomes, ce que suggéraient également les résultats d'IF après traitement par siRNA (NPHP5 est absent des centrosomes si Cep290 est inhibé mais l'inverse n'est pas vrai). Toutefois, parmi les divers mutants créés, quatre étaient capables de lier Cep290 mais exclu du centrosome alors que deux se localisaient au centrosome mais étaient incapables de lier Cep290. Une explication possible pour ses résultats serait qu'un énième facteur à ce jour inconnu soit responsable du recrutement de NPHP5 aux centrosomes où celle ci pourrait alors se lier à Cep290. Encore une fois, des expériences de SDM permettraient éventuellement d'identifier de nouveaux partenaires de NPHP5 dont ce facteur inconnu.

NPHP5 et drogues pharmacologiques

Les résultats précédents ont permis de distinguer NPHP5 comme étant un régulateur positif de la ciliogénèse, et ce à un stade précoce. Cela veut dire qu'une modulation des protéines en aval de NPHP5 serait potentiellement capable de corriger les défauts de ciliogénèse dus à la défaillance de NPHP5. Plusieurs étapes de la formation du cil sont essentielles dont la dépolymérisation de l'actine, le trafic à la membrane ou encore la perte de l'adhésion focale. Ces étapes sont souvent contrôlées par des régulateurs négatifs de la ciliogénèse comme la kinase d'adhésion focale (FAK), la protéine apparentée à l'actine 3 (ARP3), la phospholipase sécrétée A2 groupe 3 (PLA2G3) ou l'inhibiteur d'apoptose associé à l'X (XIAP) (212-216). En utilisant des drogues ciblant ces diverses protéines, nous avons pu observer un sauvetage drastique du phénotype causé par la déplétion de NPHP5 avec trois d'entre elles. En effet, la cytochalasine D, la latruculine B et le composé PF573228 sont capables de rétablir une ciliogénèse normale dans les cellules dépourvues de NPHP5 ou exprimant différents mutants de la protéine. La cytochalasine D et la latruculine B sont des drogues qui inhibent la polymérisation du cytosquelette d'actine tandis que le composé PF573228 est un inhibiteur compétitif de FAK.

Ces résultats laissent donc penser que NPHP5 pourrait être impliqué dans un de ces processus et des études plus poussées sont donc nécessaires. Par exemple, des expériences d'IP-WB ou de PLA permettraient de vérifier la liaison potentielle entre NPHP5 et l'actine monomérique ou les protéines impliquées dans l'adhésion focale. Des expérimentations par chromatographie d'exclusion de taille pourraient aussi déterminer le rôle de NPHP5 dans la formation et/ou le maintien des complexes d'adhésion focale. Ces résultats serviraient à élucider en partie les mécanismes moléculaires impliqués dans la ciliogénèse et pourraient aider au développement de nouvelles cibles thérapeutiques.

NPHP5 et le BBSome

Dans le deuxième article, nous avons étudié le rôle de NPHP5 dans l'assemblage et le trafic du complexe BBSome dans le cil. Nous nous sommes intéressé au syndrome de Bardet-Biedl pour deux raisons principales. La première est que la néphronophtise (NPHP) et le syndrome de Bardet-Biedl (BBS) sont des ciliopathies qui partagent des caractéristiques cliniques communes. La deuxième est que NPHP5 est localisée au niveau de la zone de transition à la base du cil. Cette zone de transition sert de barrière de diffusion où l'entrée de complexes protéiques comme le BBSome est contrôlée de manière précise afin de moduler la ciliogénèse et le transport intra-flagellaire (TIF) (126, 146, 174, 185). J'ai démontré que NPHP5 interagit avec les différentes sous-unités du BBSome via deux sites situés au niveau C-terminal et N-terminal respectivement. Cette liaison est indépendante de Cep290 et se produit tant dans les cellules quiescentes qu'en prolifération. De manière intéressante, nous avons montré que l'inhibition de NPHP5 ou de CEP290 conduit à la dissociation de trois sous-unités du BBSome (BBS2, BBS5 et BBS8) formant alors un sous-complexe dont la capacité de migration dans le cil n'est pas compromise. BBS2 étant une des premières sous-unités essentielles à la formation du BBSome entier (217), il est difficile de concevoir la formation stable d'un sous complexe en absence de cette protéine.

Une première hypothèse plausible serait que le BBSome soit immature ou pas du tout formé dans les cellules en prolifération mais que dès l'induction de la quiescence, les différentes sous-unités s'assemblent au niveau de la base du cil. Une deuxième hypothèse serait que le complexe entier se forme dans les cellules en prolifération mais qu'une fois assemblées certaines sous-unités ne soient plus essentielles à son maintien. En utilisant des techniques comme la chromatographie à exclusion de taille ou PLA, il serait possible de différentier ces deux possibilités et ainsi étudier de façon plus poussée les mécanismes moléculaires impliqués dans la stabilité du BBSome.

Les résultats précédents ont également mis en valeur un rôle de ''gardiens'' pour NPHP5 et Cep290 au niveau de la zone de transition. En effet, si les deux protéines sont présentes, seuls les BBSomes complètement formés circulent dans le cil; mais en cas de déplétion de NPHP5 ou Cep290, les sous-complexes alors formés peuvent tout de même entrer dans le cil. Il est important de noter que dans le cas d'une déplétion de NPHP5 ou Cep290, les transports antérograde et rétrograde ainsi que le recrutement de protéines essentielles à la formation de la zone de transition ne paraissent pas altérés. Il semblerait donc que le rôle de NPHP5 et Cep290 soit particulier au BBSome. Pour confirmer que la zone de transition est réellement intacte lors de l'inhibition de NPHP5 ou Cep290, des analyses structurales par microscopie électronique ou microscopie super-résolution seraient primordiales. Des études en microscopie en temps réel pour contrôler le TIF seraient aussi nécessaires.

Pour finir, nous avons montré que la déplétion de NPHP5 ou Cep290, en raison de la perte de certaines sous-unités, provoque un défaut dans le TIF de certains cargos par le BBSome. En effet, un des rôles connus du BBSome est de transporter des protéines membranaires vers le cil pour permettre la transduction de signal de diverses voies de signalisation (174, 178, 179, 185, 218). Par exemple, l'inhibition de NPHP5 ou Cep290 entraine respectivement une perte de Smoothened (Smo) ou de Rab8a au niveau du cil. Toutefois, tous les cargos ne sont pas encore connus à ce jour ni comment ou par quelle sous-unité chacun est transporté au niveau du cil. Il serait donc intéressant de déterminer, par IP-SDM, les différents cargos associés à chaque sous-unité du BBSome. Il faut aussi souligner le fait que la perte de Smo après déplétion de NPHP5 semble être spécifique à certains tissus.

En effet, dans les cellules osseuses ostéoblastes, l'inhibition de NPHP5 n'affecte pas la voie de signalisation de Smo (146) contrairement à ce que j'ai montré dans les cellules épithéliales de la rétine. Il est donc important d'étudier l'importance de NPHP5 dans différents tissus, notamment dans la rétine et le rein, les deux organes affectés lors de néphronophtise. Ces connaissances pourraient ouvrir la porte à des approches thérapeutiques beaucoup plus ciblées en cas de maladie.

Cep76

Cep76 et le complexe CDK2/CYCLINE A

De manière à identifier les régulateurs potentiels de Cep76, plusieurs expériences de SDM ont été réalisées. La kinase CDK2 a ainsi été identifiée comme partenaire de Cep76, résultat qui a été confirmé par IP-WB et expérience de liaison *in vitro*. De manière intéressante, ces mêmes techniques ont permis de montrer que Cep76 s'associait préférentiellement avec la CYCLINE A qui forme un complexe avec CDK2 en phase S du cycle cellulaire (24, 28). Ces résultats suggéraient que Cep76 était un substrat de CDK2 en phase S. Pour vérifier cette hypothèse, nous avons premièrement validé par SDM les sites de phosphorylation sur Cep76. Le site S83 a été identifié lors de trois expériences indépendantes. Il est important de souligner aussi que le site S83 correspond à un site consensus de phosphorylation par les CDK (219, 220). Deuxièmement, nous avons confirmé par des tests kinase *in vitro* que le complexe CDK2/CYCLINE A phosphoryle directement Cep76 à la position S83. En parallèle, nous avons aussi étudié la liaison de Cep76 avec la CYCLINE A. Bien que cette interaction ait été confirmée, nous n'avons pu déterminer le ou les site(s) de liaison entre Cep76 et la CYCLINE A. En effet, même en mutant les motifs RXL/KXL, connus pour être les motifs de liaison aux cyclines, Cep76 pouvait toujours se lier à la CYCLINE A.

Ces résultats suggèrent que d'autres motifs/sites sont impliqués dans cette interaction. Il serait donc intéressant de faires des expériences d'IP-WB avec divers mutants et fragments de Cep76 pour essayer de mieux caractériser cette liaison.

Cep76 et amplification des centrioles en phase S

Afin de mieux comprendre l'importance de la phosphorylation de Cep76 sur le site S83, nous avons effectué des expériences de sauvetage en surexprimant soit la protéine sauvage soit différents mutants de phosphorylation dans des cellules contrôles, traitées avec siRNA contre Cep76 ou avec la drogue hydroxyurée (HU, arrêt en phase S). Les résultats obtenus montrent que Cep76 doit être phosphorylée spécifiquement au site S83 pour supprimer une surduplication des centrioles en phase S du cycle cellulaire. Toutefois, lorsque les cellules étaient traitées avec les drogues RO3306 ou doxorubicine pour stopper le cycle cellulaire en phase G2, Cep76 n'était plus capable de supprimer la surduplication des centrioles. Cela suggère que Cep76 est impliquée spécifiquement en phase S du cycle cellulaire, phase où la protéine est la plus abondante et fonctionnelle. On peut donc imaginer l'existence de points de contrôle au niveau des centrosomes, tout comme les points de contrôle du cycle cellulaire, qui permettrait de vérifier le bon déroulement de la duplication des centrioles à chaque phase du cycle. Ces points de contrôle seraient alors régulés par des protéines ou voies de signalisation spécifiques à chaque phase, Cep76 étant une des protéines spécifiquement impliquées au niveau de la phase S.

Cep76 et son mécanisme d'action

Afin d'élucider par quel(s) mécanisme(s) Cep76 empêche l'amplification des centrioles, nous avons en premier vérifié si la protéine pouvait elle même contrôler la fonction de CDK2. En utilisant la phosphorylation de l'histone H1 comme marqueur de l'activité kinase de CDK2, nous avons démontré que Cep76, sauvage ou muté au site S83, n'est pas un inhibiteur de CDK2. Ensuite, nos résultats d'IF ont montré que Cep76 n'influence pas la localisation centrosomale de CDK2 ou de la CYCLINE A. La séparation des centrioles est une phase primordiale pour la duplication des centrosomes et est associée à l'activation de la kinase PLK1 au centrosome (68, 221). Nous avons donc vérifié par IF quel était le rôle de Cep76 à cette étape. Nos résultats montrent que Cep76 empêche la séparation des centrioles, en phase S, en bloquant la phosphorylation activatrice de PLK1 au site T210 au niveau des centrosomes. Nous avons donc mis à jour un nouveau mécanisme spécifique à Cep76 dans le contrôle du cycle des centrosomes.

Cep76 et acétylation au site K279

Par la suite, nous voulions savoir si Cep76 subissait d'autres modifications post-traductionnelles (MPT). En effet, il a déjà été montré qu'une protéine est souvent contrôlée par plusieurs MPT pour réguler sa fonction (222). Une analyse protéomique a récemment mis en évidence l'acétylation de Cep76 au site K279 (223) et nos expériences d'IP-WB ont confirmé ce résultat. Dans le but d'étudier la fonction de cette acétylation, nous avons créé deux mutants opposés de Cep76 : une perte d'acétylation et une acétylation constante. L'analyse par IF et WB de ces mutants a montré que l'acétylation de Cep76 diminue sa capacité à contrôler l'amplification des centrosomes en phase S. Pour comprendre comment l'acétylation de Cep76 module son activité, nous avons ensuite étudié la possibilité de diaphonie avec la phosphorylation au site S83.

En utilisant des essais kinase *in vitro*, de l'IF et des WB nous avons montré que l'acétylation de Cep76 au site K279 est nécessaire et suffisante pour inhiber sa phosphorylation au site S83, et par conséquent son activité au niveau des centrosomes, et qu'elle est maximale en phase G2. Bien que l'acétylation de Cep76 a été confirmée, la protéine acétyletranférase responsable n'est pas connue à ce jour. Il serait donc important de faire des expériences de SDM pour identifier des candidats puis les valider par IP-WB ou avec des test d'acétylation *in vitro*. Ces résultats permettraient de mieux comprendre les mécanismes impliqués dans le contrôle de la fonction de Cep76 mais pourraient également être de nouvelles cibles thérapeutiques.

De manière plus générale, il serait intéressant de pouvoir suivre le statut de phosphorylation au site S83 ou d'acétylation au site K279 de Cep76 au cours du cycle cellulaire. La création d'anticorps phospho-spécifique ou acétyl-spécifique pour ces deux sites serait alors nécessaire pour ces expériences. Ces anticorps seraient aussi des outils puissants pour étudier de manière plus précise les mécanismes régulant Cep76 et sa fonction au niveau des centrosomes.

Cep76 et cancer

Un nombre anormal de centrosomes dans la cellule est caractéristique d'un développement tumoral (55, 97-99) et comme Cep76 est impliquée dans le contrôle de l'amplification des centrosomes, on peut imaginer un lien de cause à effet. Une recherche dans les bases de données de patients atteints de cancer a mis en évidence la mutation S83C (ICGC data portal). Cette mutation a été identifiée chez une patiente atteinte d'un carcinome épidermoïde du col utérin. Par IF, nous avons pu démontrer que cette mutation rend la protéine non fonctionnelle et permet donc une surduplication des centrosomes. Cela met en évidence un caractère potentiellement pathogène de la mutation et pourrait être une cause plutôt qu'une conséquence du cancer. Toutefois, cette mutation n'a été détectée que chez une patiente et des études plus poussées sont donc nécessaires dans cette direction.

Il serait également intéressant d'étudier d'autres types de cancer pour savoir si le rôle de Cep76 est spécifique à certains tissus/types cellulaires ou s'il est limité au carcinome épidermoïde du col utérin.

En conclusion, cette thèse a répondu à des questions importantes menant à une meilleure compréhension des centrosomes dans des conditions tant physiologiques que pathologiques. Nous avons mis en évidence un rôle essentiel de NPHP5 dans la formation des cils primaires et dans le développement de maladies comme la néphronophtise ou le syndrome de Bardet-Biedl. De plus, nos résultats concernant Cep76 mettent en valeur la participation cruciale de Cep76 au contrôle du cycle des centrosomes et à la formation de certains cancers. Ces résultats permettent une meilleure compréhension des mécanismes moléculaires qui se déroulent aux centrosomes et ces nouvelles découvertes peuvent contribuer à répondre aux défis actuels dans le développement de nouvelles thérapies en cas de maladies.

Bibliographie

1 Schafer, K.A. (1998) The cell cycle: a review. *Veterinary pathology*, **35**, 461-478.

2 Cooper, G. (2000) *The Cell: A Molecular Approach. 2nd edition*. Sinauer Associates.

3 Zhu, L. and Skoultchi, A.I. (2001) Coordinating cell proliferation and differentiation. *Current opinion in genetics & development*, **11**, 91-97.

4 Li, V.C., Ballabeni, A. and Kirschner, M.W. (2012) Gap 1 phase length and mouse embryonic stem cell self-renewal. *Proceedings of the National Academy of Sciences of the United States of America*, **109**, 12550-12555.

5 Miller, J.P., Yeh, N., Vidal, A. and Koff, A. (2007) Interweaving the cell cycle machinery with cell differentiation. *Cell cycle*, **6**, 2932-2938.

6 Malumbres, M. and Barbacid, M. (2001) To cycle or not to cycle: a critical decision in cancer. *Nature reviews. Cancer*, **1**, 222-231.

7 Hitomi, M. and Stacey, D.W. (2001) Ras-dependent cell cycle commitment during G2 phase. *FEBS letters*, **490**, 123-131.

8 Takeda, D.Y. and Dutta, A. (2005) DNA replication and progression through S phase. *Oncogene*, **24**, 2827-2843.

9 Das-Bradoo, S.B., A. (2010), in press.

10 Bruce Alberts, A.J., Julian Lewis, Martin Raff, Keith Roberts, Peter Walter. (2007) *Molecular Biology of the Cell*. Garland Science.

11 Hirano, T. (2015) Chromosome Dynamics during Mitosis. *Cold Spring Harbor perspectives in biology*, **7**.

12 Nath, S., Ghatak, D., Das, P. and Roychoudhury, S. (2015) Transcriptional control of mitosis: deregulation and cancer. *Frontiers in endocrinology*, **6**, 60.

13 Reber, S. and Hyman, A.A. (2015) Emergent Properties of the Metaphase Spindle. *Cold Spring Harbor perspectives in biology*, **7**.

14 Tanenbaum, M.E. and Medema, R.H. (2010) Mechanisms of centrosome separation and bipolar spindle assembly. *Developmental cell*, **19**, 797-806.

15 Vermeulen, K., Van Bockstaele, D.R. and Berneman, Z.N. (2003) The cell cycle: a review of regulation, deregulation and therapeutic targets in cancer. *Cell proliferation*, **36**, 131-149.

16 Hernandez-Verdun, D. (2011) Assembly and disassembly of the nucleolus during the cell cycle. *Nucleus*, **2**, 189-194.

17 Smith, L.D. and Ecker, R.E. (1971) The interaction of steroids with Rana pipiens Oocytes in the induction of maturation. *Developmental biology*, **25**, 232-247.

18 Nurse, P. (1975) Genetic control of cell size at cell division in yeast. *Nature*, **256**, 547-551.

19 Hartwell, L.H., Culotti, J. and Reid, B. (1970) Genetic control of the cell-division cycle in yeast. I. Detection of mutants. *Proceedings of the National Academy of Sciences of the United States of America*, **66**, 352-359.

20 Evans, T., Rosenthal, E.T., Youngblom, J., Distel, D. and Hunt, T. (1983) Cyclin: a protein specified by maternal mRNA in sea urchin eggs that is destroyed at each cleavage division. *Cell*, **33**, 389-396.

21 Hadwiger, J.A., Wittenberg, C., Richardson, H.E., de Barros Lopes, M. and Reed, S.I. (1989) A family of cyclin homologs that control the G1 phase in yeast. *Proceedings of the National Academy of Sciences of the United States of America*, **86**, 6255-6259.
22 Nash, R., Tokiwa, G., Anand, S., Erickson, K. and Futcher, A.B. (1988) The WHI1+ gene of Saccharomyces cerevisiae tethers cell division to cell size and is a cyclin homolog. *The EMBO journal*, **7**, 4335-4346.
23 Sherr, C.J. (1993) Mammalian G1 cyclins. *Cell*, **73**, 1059-1065.
24 Girard, F., Strausfeld, U., Fernandez, A. and Lamb, N.J. (1991) Cyclin A is required for the onset of DNA replication in mammalian fibroblasts. *Cell*, **67**, 1169-1179.
25 Jackson, P.K., Chevalier, S., Philippe, M. and Kirschner, M.W. (1995) Early events in DNA replication require cyclin E and are blocked by p21CIP1. *The Journal of cell biology*, **130**, 755-769.
26 Knoblich, J.A., Sauer, K., Jones, L., Richardson, H., Saint, R. and Lehner, C.F. (1994) Cyclin E controls S phase progression and its down-regulation during Drosophila embryogenesis is required for the arrest of cell proliferation. *Cell*, **77**, 107-120.
27 Ohtsubo, M., Theodoras, A.M., Schumacher, J., Roberts, J.M. and Pagano, M. (1995) Human cyclin E, a nuclear protein essential for the G1-to-S phase transition. *Molecular and cellular biology*, **15**, 2612-2624.
28 Pagano, M., Pepperkok, R., Verde, F., Ansorge, W. and Draetta, G. (1992) Cyclin A is required at two points in the human cell cycle. *The EMBO journal*, **11**, 961-971.
29 Strausfeld, U.P., Howell, M., Descombes, P., Chevalier, S., Rempel, R.E., Adamczewski, J., Maller, J.L., Hunt, T. and Blow, J.J. (1996) Both cyclin A and cyclin E have S-phase promoting (SPF) activity in Xenopus egg extracts. *Journal of cell science*, **109 (Pt 6)**, 1555-1563.
30 Zindy, F., Lamas, E., Chenivesse, X., Sobczak, J., Wang, J., Fesquet, D., Henglein, B. and Brechot, C. (1992) Cyclin A is required in S phase in normal epithelial cells. *Biochemical and biophysical research communications*, **182**, 1144-1154.
31 Nakayama, Y. and Yamaguchi, N. (2013) Role of cyclin B1 levels in DNA damage and DNA damage-induced senescence. *International review of cell and molecular biology*, **305**, 303-337.
32 Lindqvist, A., Rodriguez-Bravo, V. and Medema, R.H. (2009) The decision to enter mitosis: feedback and redundancy in the mitotic entry network. *The Journal of cell biology*, **185**, 193-202.
33 Fung, T.K. and Poon, R.Y. (2005) A roller coaster ride with the mitotic cyclins. *Seminars in cell & developmental biology*, **16**, 335-342.
34 Gavet, O. and Pines, J. (2010) Progressive activation of CyclinB1-Cdk1 coordinates entry to mitosis. *Developmental cell*, **18**, 533-543.
35 Brown, N.R., Korolchuk, S., Martin, M.P., Stanley, W.A., Moukhametzianov, R., Noble, M.E. and Endicott, J.A. (2015) CDK1 structures reveal conserved and unique features of the essential cell cycle CDK. *Nature communications*, **6**, 6769.
36 Fisher, D., Krasinska, L., Coudreuse, D. and Novak, B. (2012) Phosphorylation network dynamics in the control of cell cycle transitions. *Journal of cell science*, **125**, 4703-4711.
37 Kim, S. and Yu, H. (2011) Mutual regulation between the spindle checkpoint and APC/C. *Seminars in cell & developmental biology*, **22**, 551-558.

38 van Leuken, R., Clijsters, L. and Wolthuis, R. (2008) To cell cycle, swing the APC/C. *Biochim Biophys Acta*, **1786**, 49-59.
39 Oakes, V., Wang, W., Harrington, B., Lee, W.J., Beamish, H., Chia, K.M., Pinder, A., Goto, H., Inagaki, M., Pavey, S. *et al.* (2014) Cyclin A/Cdk2 regulates Cdh1 and claspin during late S/G2 phase of the cell cycle. *Cell cycle*, **13**, 3302-3311.
40 Reed, S.I. (2003) Ratchets and clocks: the cell cycle, ubiquitylation and protein turnover. *Nature reviews. Molecular cell biology*, **4**, 855-864.
41 Willems, A.R., Schwab, M. and Tyers, M. (2004) A hitchhiker's guide to the cullin ubiquitin ligases: SCF and its kin. *Biochim Biophys Acta*, **1695**, 133-170.
42 Donzelli, M. and Draetta, G.F. (2003) Regulating mammalian checkpoints through Cdc25 inactivation. *EMBO reports*, **4**, 671-677.
43 Maya, R., Balass, M., Kim, S.T., Shkedy, D., Leal, J.F., Shifman, O., Moas, M., Buschmann, T., Ronai, Z., Shiloh, Y. *et al.* (2001) ATM-dependent phosphorylation of Mdm2 on serine 395: role in p53 activation by DNA damage. *Genes & development*, **15**, 1067-1077.
44 Thornton, T.M. and Rincon, M. (2009) Non-classical p38 map kinase functions: cell cycle checkpoints and survival. *International journal of biological sciences*, **5**, 44-51.
45 Ito, K., Hirao, A., Arai, F., Takubo, K., Matsuoka, S., Miyamoto, K., Ohmura, M., Naka, K., Hosokawa, K., Ikeda, Y. *et al.* (2006) Reactive oxygen species act through p38 MAPK to limit the lifespan of hematopoietic stem cells. *Nature medicine*, **12**, 446-451.
46 Bartek, J. and Lukas, J. (2003) Chk1 and Chk2 kinases in checkpoint control and cancer. *Cancer cell*, **3**, 421-429.
47 Kitagawa, R., Bakkenist, C.J., McKinnon, P.J. and Kastan, M.B. (2004) Phosphorylation of SMC1 is a critical downstream event in the ATM-NBS1-BRCA1 pathway. *Genes & development*, **18**, 1423-1438.
48 Bartek, J., Lukas, C. and Lukas, J. (2004) Checking on DNA damage in S phase. *Nature reviews. Molecular cell biology*, **5**, 792-804.
49 Karlsson-Rosenthal, C. and Millar, J.B. (2006) Cdc25: mechanisms of checkpoint inhibition and recovery. *Trends in cell biology*, **16**, 285-292.
50 Rothblum-Oviatt, C.J., Ryan, C.E. and Piwnica-Worms, H. (2001) 14-3-3 binding regulates catalytic activity of human Wee1 kinase. *Cell growth & differentiation : the molecular biology journal of the American Association for Cancer Research*, **12**, 581-589.
51 Cleveland, D.W., Mao, Y. and Sullivan, K.F. (2003) Centromeres and kinetochores: from epigenetics to mitotic checkpoint signaling. *Cell*, **112**, 407-421.
52 Kallio, M.J., Beardmore, V.A., Weinstein, J. and Gorbsky, G.J. (2002) Rapid microtubule-independent dynamics of Cdc20 at kinetochores and centrosomes in mammalian cells. *The Journal of cell biology*, **158**, 841-847.
53 Shah, J.V., Botvinick, E., Bonday, Z., Furnari, F., Berns, M. and Cleveland, D.W. (2004) Dynamics of centromere and kinetochore proteins; implications for checkpoint signaling and silencing. *Current biology : CB*, **14**, 942-952.
54 Holland, A.J. and Taylor, S.S. (2006) Cyclin-B1-mediated inhibition of excess separase is required for timely chromosome disjunction. *Journal of cell science*, **119**, 3325-3336.
55 Fukasawa, K. (2005) Centrosome amplification, chromosome instability and cancer development. *Cancer letters*, **230**, 6-19.
56 Schatten, H. (2008) The mammalian centrosome and its functional significance. *Histochemistry and cell biology*, **129**, 667-686.

57 Dammermann, A., Muller-Reichert, T., Pelletier, L., Habermann, B., Desai, A. and Oegema, K. (2004) Centriole assembly requires both centriolar and pericentriolar material proteins. *Developmental cell*, **7**, 815-829.
58 Korzeniewski, N., Hohenfellner, M. and Duensing, S. (2013) The centrosome as potential target for cancer therapy and prevention. *Expert opinion on therapeutic targets*, **17**, 43-52.
59 Kitagawa, D., Vakonakis, I., Olieric, N., Hilbert, M., Keller, D., Olieric, V., Bortfeld, M., Erat, M.C., Fluckiger, I., Gonczy, P. *et al.* (2011) Structural basis of the 9-fold symmetry of centrioles. *Cell*, **144**, 364-375.
60 Anderhub, S.J., Kramer, A. and Maier, B. (2012) Centrosome amplification in tumorigenesis. *Cancer letters*, **322**, 8-17.
61 Yang, J., Adamian, M. and Li, T. (2006) Rootletin interacts with C-Nap1 and may function as a physical linker between the pair of centrioles/basal bodies in cells. *Mol Biol Cell*, **17**, 1033-1040.
62 Mayor, T., Stierhof, Y.D., Tanaka, K., Fry, A.M. and Nigg, E.A. (2000) The centrosomal protein C-Nap1 is required for cell cycle-regulated centrosome cohesion. *The Journal of cell biology*, **151**, 837-846.
63 Bornens, M. (2012) The centrosome in cells and organisms. *Science*, **335**, 422-426.
64 Ou, Y., Zhang, M. and Rattner, J.B. (2004) The centrosome: The centriole-PCM coalition. *Cell motility and the cytoskeleton*, **57**, 1-7.
65 Nigg, E.A. (2007) Centrosome duplication: of rules and licenses. *Trends in cell biology*, **17**, 215-221.
66 Nigg, E.A. and Raff, J.W. (2009) Centrioles, centrosomes, and cilia in health and disease. *Cell*, **139**, 663-678.
67 Bettencourt-Dias, M. and Glover, D.M. (2007) Centrosome biogenesis and function: centrosomics brings new understanding. *Nature reviews. Molecular cell biology*, **8**, 451-463.
68 Tsou, M.F. and Stearns, T. (2006) Mechanism limiting centrosome duplication to once per cell cycle. *Nature*, **442**, 947-951.
69 Schockel, L., Mockel, M., Mayer, B., Boos, D. and Stemmann, O. (2011) Cleavage of cohesin rings coordinates the separation of centrioles and chromatids. *Nat Cell Biol*, **13**, 966-972.
70 Tsou, M.F., Wang, W.J., George, K.A., Uryu, K., Stearns, T. and Jallepalli, P.V. (2009) Polo kinase and separase regulate the mitotic licensing of centriole duplication in human cells. *Developmental cell*, **17**, 344-354.
71 Nigg, E.A. and Stearns, T. (2011) The centrosome cycle: Centriole biogenesis, duplication and inherent asymmetries. *Nat Cell Biol*, **13**, 1154-1160.
72 Hatch, E.M., Kulukian, A., Holland, A.J., Cleveland, D.W. and Stearns, T. (2010) Cep152 interacts with Plk4 and is required for centriole duplication. *The Journal of cell biology*, **191**, 721-729.
73 Inanc, B., Putz, M., Lalor, P., Dockery, P., Kuriyama, R., Gergely, F. and Morrison, C.G. (2013) Abnormal centrosomal structure and duplication in Cep135-deficient vertebrate cells. *Mol Biol Cell*, **24**, 2645-2654.
74 Kim, T.S., Park, J.E., Shukla, A., Choi, S., Murugan, R.N., Lee, J.H., Ahn, M., Rhee, K., Bang, J.K., Kim, B.Y. *et al.* (2013) Hierarchical recruitment of Plk4 and regulation of centriole biogenesis by two centrosomal scaffolds, Cep192 and Cep152. *Proceedings of the National Academy of Sciences of the United States of America*, **110**, E4849-4857.

75 Firat-Karalar, E.N. and Stearns, T. (2014) The centriole duplication cycle. *Philosophical transactions of the Royal Society of London. Series B, Biological sciences*, **369**.
76 Firat-Karalar, E.N., Rauniyar, N., Yates, J.R., 3rd and Stearns, T. (2014) Proximity interactions among centrosome components identify regulators of centriole duplication. *Current biology : CB*, **24**, 664-670.
77 Mattison, C.P. and Winey, M. (2006) The centrosome cycle. *Results and problems in cell differentiation*, **42**, 111-146.
78 Tsou, M.F. and Stearns, T. (2006) Controlling centrosome number: licenses and blocks. *Current opinion in cell biology*, **18**, 74-78.
79 Hinchcliffe, E.H., Li, C., Thompson, E.A., Maller, J.L. and Sluder, G. (1999) Requirement of Cdk2-cyclin E activity for repeated centrosome reproduction in Xenopus egg extracts. *Science*, **283**, 851-854.
80 Lacey, K.R., Jackson, P.K. and Stearns, T. (1999) Cyclin-dependent kinase control of centrosome duplication. *Proceedings of the National Academy of Sciences of the United States of America*, **96**, 2817-2822.
81 Matsumoto, Y., Hayashi, K. and Nishida, E. (1999) Cyclin-dependent kinase 2 (Cdk2) is required for centrosome duplication in mammalian cells. *Current biology : CB*, **9**, 429-432.
82 Meraldi, P., Lukas, J., Fry, A.M., Bartek, J. and Nigg, E.A. (1999) Centrosome duplication in mammalian somatic cells requires E2F and Cdk2-cyclin A. *Nat Cell Biol*, **1**, 88-93.
83 Avidor-Reiss, T. and Gopalakrishnan, J. (2013) Building a centriole. *Current opinion in cell biology*, **25**, 72-77.
84 Schmidt, T.I., Kleylein-Sohn, J., Westendorf, J., Le Clech, M., Lavoie, S.B., Stierhof, Y.D. and Nigg, E.A. (2009) Control of centriole length by CPAP and CP110. *Current biology : CB*, **19**, 1005-1011.
85 Franz, A., Roque, H., Saurya, S., Dobbelaere, J. and Raff, J.W. (2013) CP110 exhibits novel regulatory activities during centriole assembly in Drosophila. *The Journal of cell biology*, **203**, 785-799.
86 Graser, S., Stierhof, Y.D., Lavoie, S.B., Gassner, O.S., Lamla, S., Le Clech, M. and Nigg, E.A. (2007) Cep164, a novel centriole appendage protein required for primary cilium formation. *The Journal of cell biology*, **179**, 321-330.
87 JM Schrøder, M.R., L Jakobsen, K Vanselow, S Geimer, LB Pedersen and JS Andersen. (2012) Identification and characterization of two novel centriolar appendage component proteins. *cilia*, **1**.
88 Palazzo, R.E., Vogel, J.M., Schnackenberg, B.J., Hull, D.R. and Wu, X. (2000) Centrosome maturation. *Curr Top Dev Biol*, **49**, 449-470.
89 Panic, M., Hata, S., Neuner, A. and Schiebel, E. (2015) The centrosomal linker and microtubules provide dual levels of spatial coordination of centrosomes. *PLoS genetics*, **11**, e1005243.
90 Wang, G., Jiang, Q. and Zhang, C. (2014) The role of mitotic kinases in coupling the centrosome cycle with the assembly of the mitotic spindle. *Journal of cell science*, **127**, 4111-4122.
91 Mardin, B.R., Agircan, F.G., Lange, C. and Schiebel, E. (2011) Plk1 controls the Nek2A-PP1gamma antagonism in centrosome disjunction. *Current biology : CB*, **21**, 1145-1151.

92 Alieva, I.B. and Uzbekov, R.E. (2008) The centrosome is a polyfunctional multiprotein cell complex. *Biochemistry (Mosc)*, **73**, 626-643.
93 Tsang, W.Y., Spektor, A., Vijayakumar, S., Bista, B.R., Li, J., Sanchez, I., Duensing, S. and Dynlacht, B.D. (2009) Cep76, a centrosomal protein that specifically restrains centriole reduplication. *Developmental cell*, **16**, 649-660.
94 Sherr, C.J. and Roberts, J.M. (2004) Living with or without cyclins and cyclin-dependent kinases. *Genes & development*, **18**, 2699-2711.
95 R, B. (2012) Heide, S. (ed.), In *The centrosome: cell and molecular mechanisms of functions and dysfunctions in disease*. Humana Press, in press., pp. 187-197.
96 Chen, Z., Indjeian, V.B., McManus, M., Wang, L. and Dynlacht, B.D. (2002) CP110, a cell cycle-dependent CDK substrate, regulates centrosome duplication in human cells. *Developmental cell*, **3**, 339-350.
97 Nigg, E.A. (2002) Centrosome aberrations: cause or consequence of cancer progression? *Nature reviews. Cancer*, **2**, 815-825.
98 Duensing, A. and Duensing, S. (2010) Centrosomes, polyploidy and cancer. *Advances in experimental medicine and biology*, **676**, 93-103.
99 Pihan, G.A., Purohit, A., Wallace, J., Knecht, H., Woda, B., Quesenberry, P. and Doxsey, S.J. (1998) Centrosome defects and genetic instability in malignant tumors. *Cancer Res*, **58**, 3974-3985.
100 Vitre, B.D. and Cleveland, D.W. (2012) Centrosomes, chromosome instability (CIN) and aneuploidy. *Current opinion in cell biology*, **24**, 809-815.
101 Holland, A.J. and Cleveland, D.W. (2009) Boveri revisited: chromosomal instability, aneuploidy and tumorigenesis. *Nature reviews. Molecular cell biology*, **10**, 478-487.
102 Quintyne, N.J., Reing, J.E., Hoffelder, D.R., Gollin, S.M. and Saunders, W.S. (2005) Spindle multipolarity is prevented by centrosomal clustering. *Science*, **307**, 127-129.
103 Basto, R., Brunk, K., Vinadogrova, T., Peel, N., Franz, A., Khodjakov, A. and Raff, J.W. (2008) Centrosome amplification can initiate tumorigenesis in flies. *Cell*, **133**, 1032-1042.
104 Ganem, N.J., Godinho, S.A. and Pellman, D. (2009) A mechanism linking extra centrosomes to chromosomal instability. *Nature*, **460**, 278-282.
105 Godinho, S.A., Kwon, M. and Pellman, D. (2009) Centrosomes and cancer: how cancer cells divide with too many centrosomes. *Cancer metastasis reviews*, **28**, 85-98.
106 Pleasance, E.D., Cheetham, R.K., Stephens, P.J., McBride, D.J., Humphray, S.J., Greenman, C.D., Varela, I., Lin, M.L., Ordonez, G.R., Bignell, G.R. *et al.* (2010) A comprehensive catalogue of somatic mutations from a human cancer genome. *Nature*, **463**, 191-196.
107 Stratton, M.R., Campbell, P.J. and Futreal, P.A. (2009) The cancer genome. *Nature*, **458**, 719-724.
108 Futreal, P.A., Coin, L., Marshall, M., Down, T., Hubbard, T., Wooster, R., Rahman, N. and Stratton, M.R. (2004) A census of human cancer genes. *Nature reviews. Cancer*, **4**, 177-183.
109 Bettencourt-Dias, M., Hildebrandt, F., Pellman, D., Woods, G. and Godinho, S.A. (2011) Centrosomes and cilia in human disease. *Trends in genetics : TIG*, **27**, 307-315.
110 Badano, J.L., Teslovich, T.M. and Katsanis, N. (2005) The centrosome in human genetic disease. *Nature reviews. Genetics*, **6**, 194-205.

111 Oromendia, A.B. and Amon, A. (2014) Aneuploidy: implications for protein homeostasis and disease. *Disease models & mechanisms*, **7**, 15-20.
112 Barbelanne, M. and Tsang, W.Y. (2014) Molecular and cellular basis of autosomal recessive primary microcephaly. *BioMed research international*, **2014**, 547986.
113 Davenport JR, Y.B. (2005) An incredible decade for the primary cilium: a look at a onceforgotten
organelle. *American Journal of Physiology- Renal Physiology*, **289**, F1159 – F1169.
114 Davis, E.E., Brueckner, M. and Katsanis, N. (2006) The emerging complexity of the vertebrate cilium: new functional roles for an ancient organelle. *Developmental cell*, **11**, 9-19.
115 Wang, Q., Pan, J. and Snell, W.J. (2006) Intraflagellar transport particles participate directly in cilium-generated signaling in Chlamydomonas. *Cell*, **125**, 549-562.
116 Hassounah NB, B.T., McDermott KM. (2012) Molecular pathways: the role of primary cilia in cancer progression and therapeutics with a focus on Hedgehog signaling. *Clin Cancer Res*, **18**, 2429-2435.
117 Satir, P. and Christensen, S.T. (2007) Overview of structure and function of mammalian cilia. *Annual review of physiology*, **69**, 377-400.
118 Inglis, P.N., Boroevich, K.A. and Leroux, M.R. (2006) Piecing together a ciliome. *Trends in genetics : TIG*, **22**, 491-500.
119 Raychowdhury, M.K., McLaughlin, M., Ramos, A.J., Montalbetti, N., Bouley, R., Ausiello, D.A. and Cantiello, H.F. (2005) Characterization of single channel currents from primary cilia of renal epithelial cells. *The Journal of biological chemistry*, **280**, 34718-34722.
120 Quarmby, L.M. and Parker, J.D. (2005) Cilia and the cell cycle? *The Journal of cell biology*, **169**, 707-710.
121 Cole, D.G., Diener, D.R., Himelblau, A.L., Beech, P.L., Fuster, J.C. and Rosenbaum, J.L. (1998) Chlamydomonas kinesin-II-dependent intraflagellar transport (IFT): IFT particles contain proteins required for ciliary assembly in Caenorhabditis elegans sensory neurons. *The Journal of cell biology*, **141**, 993-1008.
122 Gerdes, J.M., Davis, E.E. and Katsanis, N. (2009) The vertebrate primary cilium in development, homeostasis, and disease. *Cell*, **137**, 32-45.
123 Goetz, S.C. and Anderson, K.V. (2010) The primary cilium: a signalling centre during vertebrate development. *Nature reviews. Genetics*, **11**, 331-344.
124 Silverman, M.A. and Leroux, M.R. (2009) Intraflagellar transport and the generation of dynamic, structurally and functionally diverse cilia. *Trends in cell biology*, **19**, 306-316.
125 Tsang, W.Y. and Dynlacht, B.D. (2013) CP110 and its network of partners coordinately regulate cilia assembly. *Cilia*, **2**, 9.
126 Reiter, J.F., Blacque, O.E. and Leroux, M.R. (2012) The base of the cilium: roles for transition fibres and the transition zone in ciliary formation, maintenance and compartmentalization. *EMBO reports*, **13**, 608-618.
127 Sorokin, S. (1962) Centrioles and the formation of rudimentary cilia by fibroblasts and smooth muscle cells. *The Journal of cell biology*, **15**, 363-377.
128 Sorokin, S.P. (1968) Reconstructions of centriole formation and ciliogenesis in mammalian lungs. *Journal of cell science*, **3**, 207-230.
129 Pedersen, L.B., Veland, I.R., Schroder, J.M. and Christensen, S.T. (2008) Assembly of primary cilia. *Developmental dynamics : an official publication of the American Association of Anatomists*, **237**, 1993-2006.

130 Hoyer-Fender, S. (2010) Centriole maturation and transformation to basal body. *Seminars in cell & developmental biology*, **21**, 142-147.
131 Dawe, H.R., Smith, U.M., Cullinane, A.R., Gerrelli, D., Cox, P., Badano, J.L., Blair-Reid, S., Sriram, N., Katsanis, N., Attie-Bitach, T. *et al.* (2007) The Meckel-Gruber Syndrome proteins MKS1 and meckelin interact and are required for primary cilium formation. *Hum Mol Genet*, **16**, 173-186.
132 Cardenas-Rodriguez, M. and Badano, J.L. (2009) Ciliary biology: understanding the cellular and genetic basis of human ciliopathies. *American journal of medical genetics. Part C, Seminars in medical genetics*, **151C**, 263-280.
133 Praveen K, D.E., Katsanis N. (2015) Unique among ciliopathies: primary ciliary dyskinesia, a motile cilia disorder. *F1000Prime Rep*, **36**.
134 Waters, A.M. and Beales, P.L. (2011) Ciliopathies: an expanding disease spectrum. *Pediatric nephrology*, **26**, 1039-1056.
135 Toftgard, R. (2009) Two sides to cilia in cancer. *Nature medicine*, **15**, 994-996.
136 Katsura Emoto, Y.M., Ken Yamazaki, Kathryn Effendi, Hanako Tsujikawa, Minoru Tanabe, Yuko Kitagawa, Michiie Sakamoto. (2014) Presence of primary cilia in cancer cells correlates with prognosis of pancreatic ductal adenocarcinoma. *human pathology*, **45**, 817-825.
137 Menzl, I., Lebeau, L., Pandey, R., Hassounah, N.B., Li, F.W., Nagle, R., Weihs, K. and McDermott, K.M. (2014) Loss of primary cilia occurs early in breast cancer development. *Cilia*, **3**, 7.
138 Otto, E.A., Loeys, B., Khanna, H., Hellemans, J., Sudbrak, R., Fan, S., Muerb, U., O'Toole, J.F., Helou, J., Attanasio, M. *et al.* (2005) Nephrocystin-5, a ciliary IQ domain protein, is mutated in Senior-Loken syndrome and interacts with RPGR and calmodulin. *Nature genetics*, **37**, 282-288.
139 Luo, X., He, Q., Huang, Y. and Sheikh, M.S. (2005) Cloning and characterization of a p53 and DNA damage down-regulated gene PIQ that codes for a novel calmodulin-binding IQ motif protein and is up-regulated in gastrointestinal cancers. *Cancer Res*, **65**, 10725-10733.
140 Otto, E.A., Helou, J., Allen, S.J., O'Toole, J.F., Wise, E.L., Ashraf, S., Attanasio, M., Zhou, W., Wolf, M.T. and Hildebrandt, F. (2008) Mutation analysis in nephronophthisis using a combined approach of homozygosity mapping, CEL I endonuclease cleavage, and direct sequencing. *Human mutation*, **29**, 418-426.
141 Estrada-Cuzcano, A., Koenekoop, R.K., Coppieters, F., Kohl, S., Lopez, I., Collin, R.W., De Baere, E.B., Roeleveld, D., Marek, J., Bernd, A. *et al.* (2011) IQCB1 mutations in patients with leber congenital amaurosis. *Invest Ophthalmol Vis Sci*, **52**, 834-839.
142 Stone, E.M., Cideciyan, A.V., Aleman, T.S., Scheetz, T.E., Sumaroka, A., Ehlinger, M.A., Schwartz, S.B., Fishman, G.A., Traboulsi, E.I., Lam, B.L. *et al.* (2011) Variations in NPHP5 in patients with nonsyndromic leber congenital amaurosis and Senior-Loken syndrome. *Arch Ophthalmol*, **129**, 81-87.
143 Chang, B., Khanna, H., Hawes, N., Jimeno, D., He, S., Lillo, C., Parapuram, S.K., Cheng, H., Scott, A., Hurd, R.E. *et al.* (2006) In-frame deletion in a novel centrosomal/ciliary protein CEP290/NPHP6 perturbs its interaction with RPGR and results in early-onset retinal degeneration in the rd16 mouse. *Hum Mol Genet*, **15**, 1847-1857.
144 Schafer, T., Putz, M., Lienkamp, S., Ganner, A., Bergbreiter, A., Ramachandran, H., Gieloff, V., Gerner, M., Mattonet, C., Czarnecki, P.G. *et al.* (2008) Genetic and physical interaction between the NPHP5 and NPHP6 gene products. *Hum Mol Genet*, **17**, 3655-3662.

145 Gerner, M., Haribaskar, R., Putz, M., Czerwitzki, J., Walz, G. and Schafer, T. (2010) The retinitis pigmentosa GTPase regulator interacting protein 1 (RPGRIP1) links RPGR to the nephronophthisis protein network. *Kidney international*, **77**, 891-896.
146 Sang, L., Miller, J.J., Corbit, K.C., Giles, R.H., Brauer, M.J., Otto, E.A., Baye, L.M., Wen, X., Scales, S.J., Kwong, M. *et al.* (2011) Mapping the NPHP-JBTS-MKS protein network reveals ciliopathy disease genes and pathways. *Cell*, **145**, 513-528.
147 Andersen, J.S., Wilkinson, C.J., Mayor, T., Mortensen, P., Nigg, E.A. and Mann, M. (2003) Proteomic characterization of the human centrosome by protein correlation profiling. *Nature*, **426**, 570-574.
148 Ohara, O., Nagase, T., Ishikawa, K., Nakajima, D., Ohira, M., Seki, N. and Nomura, N. (1997) Construction and characterization of human brain cDNA libraries suitable for analysis of cDNA clones encoding relatively large proteins. *DNA Res*, **4**, 53-59.
149 Sayer, J.A., Otto, E.A., O'Toole, J.F., Nurnberg, G., Kennedy, M.A., Becker, C., Hennies, H.C., Helou, J., Attanasio, M., Fausett, B.V. *et al.* (2006) The centrosomal protein nephrocystin-6 is mutated in Joubert syndrome and activates transcription factor ATF4. *Nature genetics*, **38**, 674-681.
150 Coppieters, F., Lefever, S., Leroy, B.P. and De Baere, E. (2010) CEP290, a gene with many faces: mutation overview and presentation of CEP290base. *Human mutation*, **31**, 1097-1108.
151 Valente, E.M., Brancati, F. and Dallapiccola, B. (2008) Genotypes and phenotypes of Joubert syndrome and related disorders. *Eur J Med Genet*, **51**, 1-23.
152 Kim, J., Krishnaswami, S.R. and Gleeson, J.G. (2008) CEP290 interacts with the centriolar satellite component PCM-1 and is required for Rab8 localization to the primary cilium. *Hum Mol Genet*, **17**, 3796-3805.
153 Stowe, T.R., Wilkinson, C.J., Iqbal, A. and Stearns, T. (2012) The centriolar satellite proteins Cep72 and Cep290 interact and are required for recruitment of BBS proteins to the cilium. *Mol Biol Cell*, **23**, 3322-3335.
154 Moradi, P., Davies, W.L., Mackay, D.S., Cheetham, M.E. and Moore, A.T. (2011) Focus on molecules: centrosomal protein 290 (CEP290). *Exp Eye Res*, **92**, 316-317.
155 Valente, E.M., Silhavy, J.L., Brancati, F., Barrano, G., Krishnaswami, S.R., Castori, M., Lancaster, M.A., Boltshauser, E., Boccone, L., Al-Gazali, L. *et al.* (2006) Mutations in CEP290, which encodes a centrosomal protein, cause pleiotropic forms of Joubert syndrome. *Nature genetics*, **38**, 623-625.
156 Anand, M. and Khanna, H. (2012) Ciliary transition zone (TZ) proteins RPGR and CEP290: role in photoreceptor cilia and degenerative diseases. *Expert opinion on therapeutic targets*, **16**, 541-551.
157 Cideciyan, A.V., Aleman, T.S., Jacobson, S.G., Khanna, H., Sumaroka, A., Aguirre, G.K., Schwartz, S.B., Windsor, E.A., He, S., Chang, B. *et al.* (2007) Centrosomal-ciliary gene CEP290/NPHP6 mutations result in blindness with unexpected sparing of photoreceptors and visual brain: implications for therapy of Leber congenital amaurosis. *Human mutation*, **28**, 1074-1083.
158 McEwen, D.P., Koenekoop, R.K., Khanna, H., Jenkins, P.M., Lopez, I., Swaroop, A. and Martens, J.R. (2007) Hypomorphic CEP290/NPHP6 mutations result in anosmia caused by the selective loss of G proteins in cilia of olfactory sensory neurons. *Proceedings of the National Academy of Sciences of the United States of America*, **104**, 15917-15922.

159 Garcia-Gonzalo, F.R., Corbit, K.C., Sirerol-Piquer, M.S., Ramaswami, G., Otto, E.A., Noriega, T.R., Seol, A.D., Robinson, J.F., Bennett, C.L., Josifova, D.J. *et al.* (2011) A transition zone complex regulates mammalian ciliogenesis and ciliary membrane composition. *Nature genetics*, **43**, 776-784.
160 Tsang, W.Y., Bossard, C., Khanna, H., Peranen, J., Swaroop, A., Malhotra, V. and Dynlacht, B.D. (2008) CP110 suppresses primary cilia formation through its interaction with CEP290, a protein deficient in human ciliary disease. *Developmental cell*, **15**, 187-197.
161 Spektor, A., Tsang, W.Y., Khoo, D. and Dynlacht, B.D. (2007) Cep97 and CP110 suppress a cilia assembly program. *Cell*, **130**, 678-690.
162 Murga-Zamalloa, C.A., Ghosh, A.K., Patil, S.B., Reed, N.A., Chan, L.S., Davuluri, S., Peranen, J., Hurd, T.W., Rachel, R.A. and Khanna, H. (2011) Accumulation of the Raf-1 kinase inhibitory protein (Rkip) is associated with Cep290-mediated photoreceptor degeneration in ciliopathies. *The Journal of biological chemistry*, **286**, 28276-28286.
163 Menotti-Raymond, M., David, V.A., Schaffer, A.A., Stephens, R., Wells, D., Kumar-Singh, R., O'Brien, S.J. and Narfstrom, K. (2007) Mutation in CEP290 discovered for cat model of human retinal degeneration. *J Hered*, **98**, 211-220.
164 Baye, L.M., Patrinostro, X., Swaminathan, S., Beck, J.S., Zhang, Y., Stone, E.M., Sheffield, V.C. and Slusarski, D.C. (2011) The N-terminal region of centrosomal protein 290 (CEP290) restores vision in a zebrafish model of human blindness. *Hum Mol Genet*, **20**, 1467-1477.
165 Craige, B., Tsao, C.C., Diener, D.R., Hou, Y., Lechtreck, K.F., Rosenbaum, J.L. and Witman, G.B. (2010) CEP290 tethers flagellar transition zone microtubules to the membrane and regulates flagellar protein content. *The Journal of cell biology*, **190**, 927-940.
166 Beales, P.L., Elcioglu, N., Woolf, A.S., Parker, D. and Flinter, F.A. (1999) New criteria for improved diagnosis of Bardet-Biedl syndrome: results of a population survey. *J Med Genet*, **36**, 437-446.
167 Bardet, G. (1995) On congenital obesity syndrome with polydactyly and retinitis pigmentosa (a contribution to the study of clinical forms of hypophyseal obesity). 1920. *Obes Res*, **3**, 387-399.
168 Green, J.S., Parfrey, P.S., Harnett, J.D., Farid, N.R., Cramer, B.C., Johnson, G., Heath, O., McManamon, P.J., O'Leary, E. and Pryse-Phillips, W. (1989) The cardinal manifestations of Bardet-Biedl syndrome, a form of Laurence-Moon-Biedl syndrome. *N Engl J Med*, **321**, 1002-1009.
169 Cramer, B., Green, J., Harnett, J., Johnson, G.J., McManamon, P., Farid, N., Pryse-Phillips, W. and Parfrey, P.S. (1988) Sonographic and urographic correlation in Bardet-Biedl syndrome (formerly Laurence-Moon-Biedl syndrome). *Urol Radiol*, **10**, 176-180.
170 Sheffield, V.C. (2010) The blind leading the obese: the molecular pathophysiology of a human obesity syndrome. *Trans Am Clin Climatol Assoc*, **121**, 172-181; discussion 181-172.
171 Sattar, S. and Gleeson, J.G. (2011) The ciliopathies in neuronal development: a clinical approach to investigation of Joubert syndrome and Joubert syndrome-related disorders. *Dev Med Child Neurol*, **53**, 793-798.
172 Scheidecker, S., Etard, C., Pierce, N.W., Geoffroy, V., Schaefer, E., Muller, J., Chennen, K., Flori, E., Pelletier, V., Poch, O. *et al.* (2014) Exome sequencing of Bardet-Biedl syndrome patient identifies a null mutation in the BBSome subunit BBIP1 (BBS18). *J Med Genet*, **51**, 132-136.

173 Xu, Q., Zhang, Y., Wei, Q., Huang, Y., Li, Y., Ling, K. and Hu, J. (2015) BBS4 and BBS5 show functional redundancy in the BBSome to regulate the degradative sorting of ciliary sensory receptors. *Sci Rep*, **5**, 11855.
174 Loktev, A.V., Zhang, Q., Beck, J.S., Searby, C.C., Scheetz, T.E., Bazan, J.F., Slusarski, D.C., Sheffield, V.C., Jackson, P.K. and Nachury, M.V. (2008) A BBSome subunit links ciliogenesis, microtubule stability, and acetylation. *Developmental cell*, **15**, 854-865.
175 Nachury, M.V., Loktev, A.V., Zhang, Q., Westlake, C.J., Peranen, J., Merdes, A., Slusarski, D.C., Scheller, R.H., Bazan, J.F., Sheffield, V.C. *et al.* (2007) A core complex of BBS proteins cooperates with the GTPase Rab8 to promote ciliary membrane biogenesis. *Cell*, **129**, 1201-1213.
176 Seo, S., Baye, L.M., Schulz, N.P., Beck, J.S., Zhang, Q., Slusarski, D.C. and Sheffield, V.C. (2010) BBS6, BBS10, and BBS12 form a complex with CCT/TRiC family chaperonins and mediate BBSome assembly. *Proceedings of the National Academy of Sciences of the United States of America*, **107**, 1488-1493.
177 Leroux, M.R. (2007) Taking vesicular transport to the cilium. *Cell*, **129**, 1041-1043.
178 Jin, H., White, S.R., Shida, T., Schulz, S., Aguiar, M., Gygi, S.P., Bazan, J.F. and Nachury, M.V. (2010) The conserved Bardet-Biedl syndrome proteins assemble a coat that traffics membrane proteins to cilia. *Cell*, **141**, 1208-1219.
179 Seo, S., Zhang, Q., Bugge, K., Breslow, D.K., Searby, C.C., Nachury, M.V. and Sheffield, V.C. (2011) A novel protein LZTFL1 regulates ciliary trafficking of the BBSome and Smoothened. *PLoS genetics*, **7**, e1002358.
180 Yen, H.J., Tayeh, M.K., Mullins, R.F., Stone, E.M., Sheffield, V.C. and Slusarski, D.C. (2006) Bardet-Biedl syndrome genes are important in retrograde intracellular trafficking and Kupffer's vesicle cilia function. *Hum Mol Genet*, **15**, 667-677.
181 Domire, J.S., Green, J.A., Lee, K.G., Johnson, A.D., Askwith, C.C. and Mykytyn, K. (2011) Dopamine receptor 1 localizes to neuronal cilia in a dynamic process that requires the Bardet-Biedl syndrome proteins. *Cell Mol Life Sci*, **68**, 2951-2960.
182 Zhang, Q., Nishimura, D., Vogel, T., Shao, J., Swiderski, R., Yin, T., Searby, C., Carter, C.S., Kim, G., Bugge, K. *et al.* (2013) BBS7 is required for BBSome formation and its absence in mice results in Bardet-Biedl syndrome phenotypes and selective abnormalities in membrane protein trafficking. *Journal of cell science*, **126**, 2372-2380.
183 Zhang, Q., Seo, S., Bugge, K., Stone, E.M. and Sheffield, V.C. (2012) BBS proteins interact genetically with the IFT pathway to influence SHH-related phenotypes. *Hum Mol Genet*, **21**, 1945-1953.
184 Eguether, T., San Agustin, J.T., Keady, B.T., Jonassen, J.A., Liang, Y., Francis, R., Tobita, K., Johnson, C.A., Abdelhamed, Z.A., Lo, C.W. *et al.* (2014) IFT27 links the BBSome to IFT for maintenance of the ciliary signaling compartment. *Developmental cell*, **31**, 279-290.
185 Wei, Q., Zhang, Y., Li, Y., Zhang, Q., Ling, K. and Hu, J. (2012) The BBSome controls IFT assembly and turnaround in cilia. *Nat Cell Biol*, **14**, 950-957.
186 Ou, G., Blacque, O.E., Snow, J.J., Leroux, M.R. and Scholey, J.M. (2005) Functional coordination of intraflagellar transport motors. *Nature*, **436**, 583-587.
187 Blacque, O.E., Reardon, M.J., Li, C., McCarthy, J., Mahjoub, M.R., Ansley, S.J., Badano, J.L., Mah, A.K., Beales, P.L., Davidson, W.S. *et al.* (2004) Loss of C. elegans BBS-7 and BBS-8 protein function results in cilia defects and compromised intraflagellar transport. *Genes & development*, **18**, 1630-1642.

188 Seo, S., Guo, D.F., Bugge, K., Morgan, D.A., Rahmouni, K. and Sheffield, V.C. (2009) Requirement of Bardet-Biedl syndrome proteins for leptin receptor signaling. *Hum Mol Genet*, **18**, 1323-1331.
189 Sung, C.H. and Leroux, M.R. (2013) The roles of evolutionarily conserved functional modules in cilia-related trafficking. *Nat Cell Biol*, **15**, 1387-1397.
190 Lechtreck, K.F., Brown, J.M., Sampaio, J.L., Craft, J.M., Shevchenko, A., Evans, J.E. and Witman, G.B. (2013) Cycling of the signaling protein phospholipase D through cilia requires the BBSome only for the export phase. *The Journal of cell biology*, **201**, 249-261.
191 Lechtreck, K.F., Johnson, E.C., Sakai, T., Cochran, D., Ballif, B.A., Rush, J., Pazour, G.J., Ikebe, M. and Witman, G.B. (2009) The Chlamydomonas reinhardtii BBSome is an IFT cargo required for export of specific signaling proteins from flagella. *The Journal of cell biology*, **187**, 1117-1132.
192 Zhang, D. and Aravind, L. (2012) Novel transglutaminase-like peptidase and C2 domains elucidate the structure, biogenesis and evolution of the ciliary compartment. *Cell cycle*, **11**, 3861-3875.
193 Sillibourne, J.E., Hurbain, I., Grand-Perret, T., Goud, B., Tran, P. and Bornens, M. (2013) Primary ciliogenesis requires the distal appendage component Cep123. *Biol Open*, **2**, 535-545.
194 Joo, K., Kim, C.G., Lee, M.S., Moon, H.Y., Lee, S.H., Kim, M.J., Kweon, H.S., Park, W.Y., Kim, C.H., Gleeson, J.G. *et al.* (2013) CCDC41 is required for ciliary vesicle docking to the mother centriole. *Proceedings of the National Academy of Sciences of the United States of America*, **110**, 5987-5992.
195 Alvarado-Kristensson, M., Rodriguez, M.J., Silio, V., Valpuesta, J.M. and Carrera, A.C. (2009) SADB phosphorylation of gamma-tubulin regulates centrosome duplication. *Nat Cell Biol*, **11**, 1081-1092.
196 Bahe, S., Stierhof, Y.D., Wilkinson, C.J., Leiss, F. and Nigg, E.A. (2005) Rootletin forms centriole-associated filaments and functions in centrosome cohesion. *The Journal of cell biology*, **171**, 27-33.
197 Veleri, S., Manjunath, S.H., Fariss, R.N., May-Simera, H., Brooks, M., Foskett, T.A., Gao, C., Longo, T.A., Liu, P., Nagashima, K. *et al.* (2014) Ciliopathy-associated gene Cc2d2a promotes assembly of subdistal appendages on the mother centriole during cilia biogenesis. *Nature communications*, **5**, 4207.
198 Tateishi, K., Yamazaki, Y., Nishida, T., Watanabe, S., Kunimoto, K., Ishikawa, H. and Tsukita, S. (2013) Two appendages homologous between basal bodies and centrioles are formed using distinct Odf2 domains. *The Journal of cell biology*, **203**, 417-425.
199 Thauvin-Robinet, C., Lee, J.S., Lopez, E., Herranz-Perez, V., Shida, T., Franco, B., Jego, L., Ye, F., Pasquier, L., Loget, P. *et al.* (2014) The oral-facial-digital syndrome gene C2CD3 encodes a positive regulator of centriole elongation. *Nature genetics*, **46**, 905-911.
200 Tanos, B.E., Yang, H.J., Soni, R., Wang, W.J., Macaluso, F.P., Asara, J.M. and Tsou, M.F. (2013) Centriole distal appendages promote membrane docking, leading to cilia initiation. *Genes & development*, **27**, 163-168.
201 Moser, J.J., Fritzler, M.J. and Rattner, J.B. (2009) Primary ciliogenesis defects are associated with human astrocytoma/glioblastoma cells. *BMC cancer*, **9**, 448.
202 Wang, W.J., Tay, H.G., Soni, R., Perumal, G.S., Goll, M.G., Macaluso, F.P., Asara, J.M., Amack, J.D. and Tsou, M.F. (2013) CEP162 is an axoneme-recognition protein promoting ciliary transition zone assembly at the cilia base. *Nat Cell Biol*, **15**, 591-601.

203 Drivas, T.G. and Bennett, J. (2014) CEP290 and the primary cilium. *Advances in experimental medicine and biology*, **801**, 519-525.
204 Klinger, M., Wang, W., Kuhns, S., Barenz, F., Drager-Meurer, S., Pereira, G. and Gruss, O.J. (2014) The novel centriolar satellite protein SSX2IP targets Cep290 to the ciliary transition zone. *Mol Biol Cell*, **25**, 495-507.
205 Marshall, C.B., Nishikawa, T., Osawa, M., Stathopulos, P.B. and Ikura, M. (2015) Calmodulin and STIM proteins: Two major calcium sensors in the cytoplasm and endoplasmic reticulum. *Biochemical and biophysical research communications*, **460**, 5-21.
206 Ben-Johny, M. and Yue, D.T. (2014) Calmodulin regulation (calmodulation) of voltage-gated calcium channels. *J Gen Physiol*, **143**, 679-692.
207 Villarroel, A., Taglialatela, M., Bernardo-Seisdedos, G., Alaimo, A., Agirre, J., Alberdi, A., Gomis-Perez, C., Soldovieri, M.V., Ambrosino, P., Malo, C. *et al.* (2014) The ever changing moods of calmodulin: how structural plasticity entails transductional adaptability. *J Mol Biol*, **426**, 2717-2735.
208 Vetri, V. and Fodera, V. (2015) The route to protein aggregate superstructures: Particulates and amyloid-like spherulites. *FEBS letters*, in press.
209 Karamanos, T.K., Kalverda, A.P., Thompson, G.S. and Radford, S.E. (2015) Mechanisms of amyloid formation revealed by solution NMR. *Prog Nucl Magn Reson Spectrosc*, **88-89**, 86-104.
210 Surguchev, A. and Surguchov, A. (2010) Conformational diseases: looking into the eyes. *Brain Res Bull*, **81**, 12-24.
211 Goldstein, L.S. (2001) Kinesin molecular motors: transport pathways, receptors, and human disease. *Proceedings of the National Academy of Sciences of the United States of America*, **98**, 6999-7003.
212 Kim, J., Lee, J.E., Heynen-Genel, S., Suyama, E., Ono, K., Lee, K., Ideker, T., Aza-Blanc, P. and Gleeson, J.G. (2010) Functional genomic screen for modulators of ciliogenesis and cilium length. *Nature*, **464**, 1048-1051.
213 Kuribara, S., Kato, M., Kato-Minoura, T. and Numata, O. (2006) Identification of a novel actin-related protein in Tetrahymena cilia. *Cell motility and the cytoskeleton*, **63**, 437-446.
214 Aoto, K. and Trainor, P.A. (2015) Co-ordinated brain and craniofacial development depend upon Patched1/XIAP regulation of cell survival. *Hum Mol Genet*, **24**, 698-713.
215 Antoniades, I., Stylianou, P. and Skourides, P.A. (2014) Making the connection: ciliary adhesion complexes anchor basal bodies to the actin cytoskeleton. *Developmental cell*, **28**, 70-80.
216 Gijs, H.L., Willemarck, N., Vanderhoydonc, F., Khan, N.A., Dehairs, J., Derua, R., Waelkens, E., Taketomi, Y., Murakami, M., Agostinis, P. *et al.* (2015) Primary cilium suppression by SREBP1c involves distortion of vesicular trafficking by PLA2G3. *Mol Biol Cell*, **26**, 2321-2332.
217 Zhang, Q., Yu, D., Seo, S., Stone, E.M. and Sheffield, V.C. (2012) Intrinsic protein-protein interaction-mediated and chaperonin-assisted sequential assembly of stable bardet-biedl syndrome protein complex, the BBSome. *The Journal of biological chemistry*, **287**, 20625-20635.
218 Berbari, N.F., Lewis, J.S., Bishop, G.A., Askwith, C.C. and Mykytyn, K. (2008) Bardet-Biedl syndrome proteins are required for the localization of G protein-coupled

receptors to primary cilia. *Proceedings of the National Academy of Sciences of the United States of America*, **105**, 4242-4246.
219 Nigg, E.A. (1991) The substrates of the cdc2 kinase. *Semin Cell Biol*, **2**, 261-270.
220 Nigg, E.A. (1993) Cellular substrates of p34(cdc2) and its companion cyclin-dependent kinases. *Trends in cell biology*, **3**, 296-301.
221 Loncarek, J., Hergert, P. and Khodjakov, A. (2010) Centriole reduplication during prolonged interphase requires procentriole maturation governed by Plk1. *Current biology : CB*, **20**, 1277-1282.
222 Yang, X.J. and Seto, E. (2008) Lysine acetylation: codified crosstalk with other posttranslational modifications. *Mol Cell*, **31**, 449-461.
223 Zhao, S., Xu, W., Jiang, W., Yu, W., Lin, Y., Zhang, T., Yao, J., Zhou, L., Zeng, Y., Li, H. *et al.* (2010) Regulation of cellular metabolism by protein lysine acetylation. *Science*, **327**, 1000-1004.

Annexe 1 : Molecular and Cellular Basis of Autosomal Recessive Primary Microcephaly (MCPH)

Marine Barbelanne[1,2] and William Y. Tsang[1,2,3,*]

[1]Institut de recherches cliniques de Montréal, 110 avenue des Pins Ouest, Montréal, Québec H2W 1R7, Canada

[2]Faculté de Médecine, Université de Montréal, Montréal, Québec H3C 3J7, Canada

[3]Division of Experimental Medicine, McGill University, Montréal, Québec H3A 1A3, Canada

Abstract

Autosomal recessive primary microcephaly (MCPH) is a rare hereditary neurodevelopmental disorder characterized by a marked reduction in brain size and intellectual disability. MCPH is genetically heterogeneous and can exhibit additional clinical features that overlap with related disorders including Seckel syndrome, Meier-Gorlin syndrome and microcephalic osteodysplastic dwarfism. In this review, we discuss the key proteins mutated in MCPH. To date, MCPH-causing mutations have been identified in twelve different genes, many of which encode proteins that are involved in cell cycle regulation or are present at the centrosome, an organelle crucial for mitotic spindle assembly and cell division. We highlight recent findings on MCPH proteins with regard to their role in cell cycle progression, centrosome function and early brain development.

Keywords: Centrosome; Microcephaly; MCPH; SCKL; Neurogenesis; Cell division, Cell cycle

Introduction

Autosomal recessive primary microcephaly (MCPH) is a rare condition associated with developmental anomaly of the brain. This neurodevelopmental disorder is characterized by a reduced occipito-frontal head circumference (OFC) at birth to at least 2-3 standard deviations below the mean for sex, age and ethnicity, a slower than average growth in OFC after birth, and prenatal onset as early as the second trimester of gestation [1-6]. MCPH patients possess a small brain with simplified gyri and exhibit varying degrees of intellectual disability; however, the architecture of the brain in general is not grossly affected. In some instances, MCPH is associated with additional clinical features, including short stature, mild seizures or skeletal abnormalities, and shows genetic and clinical overlap with related disorders such as Seckel syndrome (SCKL; OMIM 210600, 606744, 608664, 613676, 613823, 614728, 614851, 615807), Meier-Gorlin syndrome (OMIM 224690, 613800, 613804) and microcephalic osteodysplastic dwarfism (OMIM 210710, 210720, 210730) [7-12]. Although MCPH was traditionally distinguished from other disorders by height, short stature is not longer a distinguishing feature. Furthermore, it is now known that mutations in the same gene can cause MCPH and SCKL. In light of these observations, it is tempting to speculate that there must be a considerable overlap between the pathological mechanisms underlying MCPH and related disorders.

MCPH loci and brain development

To date, twelve genetic loci (MCPH-MCPH12) are implicated in MCPH (Table 1). The majority of mutations reported in these genes are frameshift or nonsense mutations leading to truncated proteins that are non-functional (please refer to references in Table 1). Perhaps not surprisingly, MCPH gene products are shown to be highly expressed in neuroepithelial or neuroprogenitor cells during early brain development [13-17]. Brain size at birth is primarily dependent on the ability of neuroprogenitor cells to proliferate and self-renew [9,10,18,19]. While symmetrical division of a neuroprogenitor cell results in the generation of two identical neuroprogenitor cells (thereby increasing the progenitor pool), asymmetrical division leads to the production of one progenitor cell (thereby maintaining the progenitor pool) and a committed precursor, which eventually undergoes migration and differentiates into neurons [20,21]. Conceivably, any perturbation that upsets the balance between symmetric and asymmetric division can drastically reduce the number of neuroprogenitor and neuronal cells, leading to reduced brain size [10]. Although such a mechanism is appealing, it is important to note that additional mechanisms, including cell proliferation defects, enhanced cell death/apoptosis, abnormal neuronal migration and/or differentiation can also impair brain development and contribute to the development of MCPH [10]. Interestingly, a significant number of MCPH proteins identified thus far are found to be associated with the centrosome [15,16,22-29], an organelle intimately connected with cell division, suggesting that proper cell cycle control could play an important role in neurogenesis.

Centrosome structure and function

The centrosome is the major microtubule-organizing center in mammalian cells and modulates diverse cellular processes such as cell cycle progression, cell shape, polarity, adhesion and motility, cilia assembly, DNA damage response, intracellular transport, positioning of cellular organelles, mitotic spindle formation, positioning and orientation, and genome stability [30-35]. This organelle is composed of a pair of centrioles, a mother and a daughter, surrounded by an amorphous pericentriolar matrix (PCM) (Figure 1). Centrioles, cylindrical structures consisting of nine triplets of stabilized microtubules, organize the PCM, which in turn nucleates and anchors cytoplasmic microtubules necessary for mitotic spindle assembly and chromosome segregation. Centrosome number, morphology and function are tightly regulated during the cell cycle [36-39]. A cell in the G1 phase has one centrosome. Centrosome duplication occurs once in the S phase and entails the synthesis of two new centrioles or procentrioles adjacent to the existing centrioles. At the G2/M transition, the duplicated centrosomes separate and migrate to opposite poles of the cell, and through a process known as centrosome maturation, additional proteins are recruited to the PCM to increase its microtubule-nucleating and -anchoring capacity essential for cell division. Defects in centrosome duplication and/or maturation are known to compromise cell cycle progression and cell division, resulting in aneuploidy, cell cycle arrest, cell death and/or uncontrolled cell growth. Indeed, centrosome dysfunction has been linked to a wide variety of human diseases including MCPH, but how exactly does it impede the cell cycle and affect brain development at the mechanistic level? In the next section, we will highlight the current status of our knowledge on the role of each MCPH gene product in cell cycle regulation, centrosome function and neurogenesis.

MICROCEPHALIN

MCPH1/MICROCEPHALIN is the first disease gene identified for MCPH and it encodes MICROCEPHALIN, a multi-functional protein that participates in various cellular processes [13,40,41]. MICROCEPHALIN possesses three BRCT (BRCA1 C terminus) domains commonly found in proteins involved in cell cycle control, DNA damage response and DNA repair [42]. Indeed, it functions to recruit the chromatin remodelling complex SWI-SNF (switch/sucrose nonfermentable) to DNA lesions and interacts with the E2F1 transcription factor to regulate genes involved in DNA repair and apoptosis [43-45]. MICROCEPHALIN also associates with CONDENSIN II, a protein involved in chromosome condensation, perhaps explaining why a loss of MICROCEPHALIN function triggers early cell cycle progression and premature chromosome condensation [46,47]. Besides its nuclear localization, MICROCEPHALIN also localizes to the centrosome throughout the cell cycle and interacts with PERICENTRIN, a PCM component critical for centrosome maturation, to control the localization of CHK1 (checkpoint kinase 1) to the centrosome [22,48,49]. In the absence of MICROCEPHALIN, CHK1 is mis-localized and cannot phosphorylate and inactivate CDC25B (cell division cycle 25B), thereby triggering premature CDK1 (Cyclin-dependent kinase 1) activation and early mitotic entry. Interestingly, PERICENTRIN is also mis-localized from the centrosome in the absence of MICROCEPHALIN, suggesting that the latter recruits the former to the centrosome. Although two mouse models of *Mcph1* show no obvious brain phenotype [50,51], a conditional knock-out causes untimely entry into mitosis, mitotic spindle mis-orientation and a premature switch of neuroprogenitors from symmetric to asymmetric division, resulting in primary microcephaly (Table 2) [49,52].

Interestingly, silencing *Cdc25b* is sufficient to rescue these phenotypes, suggesting that proper mitotic entry and progression are needed to maintain a balance between neuroprogenitor proliferation and neuronal differentiation.

WDR62 (WD repeat-containing protein 62)

WDR62 is the second most frequently mutated gene in MCPH, accounting for about 10% of cases [16,23,53,54]. Its encoded protein product possesses several WD40 (beta-transducin repeat) domains that mediate protein-protein interactions. WDR62 is predominantly a nuclear protein during interphase and accumulates at the spindle poles during mitosis [16,55,56]. The primary function of WDR62 is to preserve centrosome/spindle pole integrity after bipolar spindle formation, since a loss of this protein leads to the dispersal of PCM components PERICENTRIN, γ-TUBULIN and CDK5RAP2 (CDK5 regulatory subunit-associated protein 2) (these three PCM proteins are known to interact with each other) from metaphase centrosomes [55,56]. In addition, WDR62 is a substrate of c-Jun N-terminal kinase (JNK), active at the centrosome during mitosis, and phosphorylation of WDR62 by JNK is required for mitotic spindle organization [55,57]. Depletion of either Wdr62 (shRNA knock-down, Table 2) or Jnk induces spindle mis-orientation and triggers the asymmetric division of neuroprogenitors in the rat telencephalon, leading to their premature differentiation into neurons [58]. In another study, morpholino-mediated knock-down of wdr62 or two other microcephaly proteins, aspm (abnormal spindle-like microcephaly-associated protein) and sil (*STIL* in human*;* SCL/TAL1-interrupting locus), in zebrafish causes a significant reduction in head and eye size [59]. This phenotype is believed to be due to a failure in metaphase progression, leading to increased cell death [59].

Likewise, neuroprogenitor cells of mice deficient in Wdr62 exhibit spindle assembly checkpoint activation, delayed mitotic progression and cell death, resulting in reduced brain size (Table 2) [60]. Finally, lymphoblastoid cells derived from patients with compound heterozygous mutations in *WDR62* exhibit mitotic spindle defects as well as abnormal centrosomal protein localization [56]. Mechanistically, WDR62 physically and genetically interacts with AURORA A [60], a serine/threonine protein kinase that controls centrosome maturation, spindle formation and mitotic progression. AURORA A is a PCM protein, and its targeting to and subsequent activation at the mitotic spindle is dependent on another centrosomal protein CEP192 (centrosomal protein of 192 kDa) (discussed later) [61]. Thus, WDR62 appears to control the fate of neuroprogenitors cells partially through AURORA A.

CDK5RAP2 (CDK5 regulatory subunit-associated protein 2)

By virtue of its ability to interact with γ-TUBULIN, CDK5RAP2 is a PCM protein crucial for microtubule nucleation [62,63]. Depletion of CDK5RAP2 de-localizes γ-TUBULIN from centrosomes, thereby preventing centrosomal microtubule formation. Another PCM component, PERICENTRIN also physically interacts with CDK5RAP2, and recruitment of the latter to the centrosome depends on the former but not vice versa [64-66]. In addition to its role in PCM regulation, CDK5RAP2 is also required for centriole and centrosome cohesion, and ablation of this protein induces unscheduled centriole splitting, leading to amplified centrosomes and multipolar spindles [67,68]. Furthermore, CDK5RAP2 has the capacity to bind DNA and functions as a transcription activator to regulate the expression of two spindle checkpoint genes, *BUBR1* (budding uninhibited by benzimidazole-related 1) and *MAD2* (mitotic arrest deficient 2) [69].

Recently, the role of Cdk5rap2 in neurogenesis was examined in mice. Consistent with the functional relationship between Cdk5rap2 and Pericentrin, knock-down of either protein depletes the neural progenitor pool and triggers cell cycle exit, leading to premature neuronal differentiation without substantial apoptosis in the developing mouse neocortex of an in utero electroporation model (Table 2) [70]. In contrast, a different study showed that although the *Hertwig's anemia* mouse exhibits microcephaly, most neuroprogenitor cells undergo apoptosis instead of differentiating into neurons after exiting the cell cycle abruptly (Table 2) [71]. Thus, CDK5RAP2 could play a role in neuroprogenitor cell death and neuronal differentiation.

CASC5 (cancer susceptibility candidate 5)

CASC5 is among the most recently identified gene responsible for MCPH [72]. Unlike most MCPH proteins which localize to centrosomes, CASC5 is a kinetochore scaffold protein required for the proper attachment of chromatin to the mitotic apparatus [73]. It also associates with BUB1 (budding uninhibited by benzimidazoles 1) and BUBR1 to control the spindle assembly checkpoint. Depletion of this protein induces chromosome misalignment and accelerates entry into mitosis, a phenotype reminiscent of MICROCEPHALIN loss [74-77]. Future experiments, including the use of animal models, are needed to further delineate the molecular and cellular function of CASC5 and to define its role in neurogenesis.

ASPM (abnormal spindle-like microcephaly-associated protein)

Mutations in the *ASPM* gene constitute the most common cause of MCPH and accounts for about 25-50% of cases [6,10,14,78-90]. ASPM contains a microtubule-binding domain, two calponin homology domains commonly found in cytoskeletal proteins, and multiple IQ calmodulin-binding motifs. This protein may be required for the maintenance of centrosome/spindle integrity because, like WDR62, it is mostly concentrated in the nucleus and only relocates to the spindle pole during mitosis [24]. Furthermore, CALMODULIN, a calcium-binding protein known to interact with PERICENTRIN and ASPM, also exhibits strong staining at the spindle poles [91]. Localization of ASPM to the spindle pole is greatly diminished in fibroblasts derived from a patient carrying a homozygous *ASPM* mutation [92]. Depletion of ASPM in human cells affects spindle positioning and alters the division symmetry from symmetrical to asymmetrical, leading to cytokinesis failure [92]. Similarly, ablation of Aspm enhances asymmetric cell division and premature differentiation of mouse telencephalic neuroprogenitor cells without causing cell cycle arrest (Table 2) [93]. Likewise, *aspm* mutant flies display spindle-positioning defects, in addition to increased apoptosis [94,95]. In contrast, mutant mice ($Aspm^{1-25}$ and $Aspm^{1-7}$) expressing truncated proteins show no major alteration of cleavage plane orientation but are still microcephalic [96]. Taken together, ASPM may have additional function besides spindle positioning and division axis orientation critical for symmetric cell division. Of note, although *Aspm* mutant mice and flies exhibit microcephaly, these animals also have impaired fertility due to a massive loss of germ cells [96-99]. These observations, coupled with findings that ASPM and MICROCEPHALIN are highly up-regulated in different types of cancer [100-103], suggest that these two proteins could also positively regulate cell proliferation in multiple cell types.

CENPJ (centromere protein J)

A handful of core centrosomal components, including four microcephaly proteins CENPJ, STIL, CEP135 (centrosomal protein of 135 kDa) and CEP152 (centrosomal protein of 152 kDa) were recently identified as essential regulators of centriole duplication [104-106]. Centriole duplication is thought to occur in several sequential steps, wherein CEP152 and CEP192 first interact with each other to recruit polo-like kinase 4 (PLK4) to the site of centriole assembly [107-111]. This event is followed by the recruitment of SAS-6 (spindle assembly abnormal protein 6 homolog) and STIL, proteins that dictate the nine-fold radial symmetric arrangement of microtubules in centrioles, and finally CENPJ, to new centrioles [106,112-117]. CENPJ is known to interact with STIL, CEP135 and CEP152, and in addition, possesses the capacity to bind microtubules and to associate with CEP120 (centrosomal protein of 120 kDa) and SPICE1 (spindle and centriole associated protein 1), two proteins essential for centriole elongation [110,111,118-123]. Indeed, CENPJ is specifically involved in the elongation step of centriole duplication, and depletion of this protein leads to the formation of nascent centrioles that fail to reach full length, whereas over-expression promotes the formation of elongated centrioles [124-126]. Both moderate and excessive centriole elongation are detrimental to cells, causing loss of centrosome integrity and formation of multipolar spindles [126,127]. In addition to its role in centriole biogenesis, CENPJ also interacts with several PCM components to regulate the size of the PCM [128-130]. CENPJ was also found to play an important role in controlling the prefrontal cortex development in human [131]. Targeted inactivation of *Cenpj* in mice recapitulates many of the clinical features of MCPH and SCKL, including mitotic failure and massive cell death during embryonic development (Table 2) [132].

Notably, of the 12 MCPH proteins identified to date, only deficiencies in CENPJ and CEP152 are known to cause both MCPH and SCKL, the latter of which is a disorder traditionally characterized by short stature [132,133]. Since CENPJ regulates several aspects of centrosome function, a loss of this protein may lead to deficits in multiple cellular pathways which act together to cause dwarfism.

STIL (SCL/TAL1-interrupting locus)

STIL is a centrosomal protein localized to newly synthesized centrioles [118,134,135]. Immediately after PLK4 is recruited by CEP152 and CEP192, SAS-6 and STIL are brought to the site of centriole assembly. SAS-6 directly interacts and forms a complex with STIL, and these two proteins resemble each other in many ways in terms of functionality, sub-cellular localization pattern and expression levels during the cell cycle [118,134,135]. Ablation of one protein causes mis-localization of the other, suggesting that STIL and SAS-6 are mutually dependent for their localization to centrioles. Moreover, up-regulation of STIL induces the formation of multiple nascent centrioles around the parental centriole, mimicking the phenotype of SAS-6 or PLK4 over-expression [106,136,137]. STIL appears to be important for spindle positioning and mitotic progression [59,138,139]. Inactivation of sil in zebrafish or Stil in mice results in embryonic lethality (Table 2), indicating that this protein may play additional roles beyond brain development [139,140].

CEP135 (centrosomal protein of 135 kDa)

As an important regulator of centrosome biogenesis, CEP135 is a centriolar protein that associates with SAS-6 and CENPJ [123,141,142]. The precise relationship between CEP135 and SAS-6 is not completely clear at this point, although these proteins do not appear to depend on each other for localization to the centriole. On the other hand, CEP135 recruits CENPJ to centrioles, and not vice versa, indicating that CEP135 likely functions upstream of CENPJ [123]. Furthermore, in contrast to the loss of PLK4, SAS-6 or STIL, which completely suppresses centriole duplication, ablation of CEP135 results in a less severe phenotype with shorter centrioles and atypical centriolar structure [123,143]. By the same token, abnormal centrioles are also observed in *Drosophila*, *Chlamydomonas*, *Tetrahymena* and *Paramecium cep135* mutants (Table 2), and these results collectively suggest that the structural integrity of centrioles is compromised [144-150]. Since these structural anomalies are known to induce mitotic defects, including the formation of monopolar spindles, it would be interesting in the long run to investigate their consequences on prenatal neurogenesis [123,143].

CEP152 (centrosomal protein of 152 kDa)

Although CEP152 is deficient in both MCPH and SCKL, mutations in *CEP152* are by far the most common cause of SCKL, accounting for the majority of cases [27,151]. During the early step of centriole duplication, CEP152 and its associated partner, CEP192 form a discrete ring around parental centrioles, making the site of PLK4 recruitment and nascent centriole assembly [107,108,152]. The centrosomal localization of CEP152 is also dependent on CEP192, but not vice versa.

In addition, CEP152 is known to interact with CEP57 (centrosomal protein of 57 kDa) and CEP63 (centrosomal protein of 63 kDa), the latter of which is a SCKL protein [28,153,154]. While CEP152 and CEP63 are mutually dependent for one another for their centrosomal localization, only the former is absolutely required for centriole duplication, and a loss of this protein leads to severe mitotic defects and the formation of monopolar spindles [109-111]. In addition, CEP152 binds to CINP, a CDK2-interacting protein involved in DNA damage response and genome maintenance [151], thereby regulating cell cycle checkpoints. Indeed, centrosomes and nuclei show numerical and morphological abnormalities, indicative of aberrant cell division and cell cycle checkpoint, in CEP152-deficient patient fibroblasts/lymphocytes [151].

ZNF335 (zinc finger protein 335)

ZNF335 is a nuclear protein and a novel component of the H3K4 methyltransferase complex involved in chromatin-remodelling and transcriptional regulation [155,156]. One critical function of ZNF335 is its binding to the promoter region of REST/NRSF (RE1-silencing transcription factor/neuron-restrictive silencer factor), a master regulator of neuroprogenitor proliferation and neuronal differentiation. Elegant studies using *Znf335* deficient mice have demonstrated that this protein is required for many aspects of neurodevelopment, including neurogenesis and neuronal cell fate specification, morphogenesis and differentiation (Table 2) [156]. Perhaps because of the multi-faceted nature of ZNF335, its inactivation in humans leads to a more severe phenotype compared to most reported cases of microcephaly.

PHC1 (polyhomeotic-like protein 1)

PHC1 belongs to a member of the polycomb group which modulates chromatin remodelling [157]. This protein localizes to the nucleus and functions as an E3 ubiquitin ligase to promote the ubiquitination of histone H2A and to regulate the levels of GEMININ, a protein that partially localizes to the centrosome and is involved in cell cycle control [158,159]. Depletion of PHC1 induces aberrant DNA damage repair and polyploidy, again reinforcing the view that proteins involved in cell cycle regulation and/or checkpoints are critical for brain development [157].

CDK6 (cyclin-dependent kinase 6)

Hussain and co-workers have recently identified mutations in a new gene that can cause MCPH. Interestingly, this gene encodes CDK6, a well-known member of the cyclin/cyclin-dependent kinase family crucial for cell cycle progression in G1 and S phases [29,160]. Although several previous reports have shown that CDK6 exhibits both cytoplasmic and nuclear localization during interphase, this protein, like WDR62 and ASPM, becomes enriched at the spindle poles during mitosis [29,161-163]. Ablation of CDK6 impairs cell polarity and induces supernumerary centrosomes and aneuploidy, but it is not clear whether these phenotypes arise from cell cycle and/or spindle pole defects [29]. Interestingly, *Cdk6* knock-out mice are viable and develop normally (Table 2), suggesting that this protein is dispensable for proliferation in most cell types [164].

Paradoxically, a more recent study illustrates the importance of Cdk6 in embryonic neurogenesis and demonstrates that inactivation of *Pax6*, a transcription factor that directly represses the expression of *Cdk6,* leads to inappropriate activation of Cdk6 and over-proliferation of neuroprogenitor cells in mice [165]. Another study also highlighted a role for CDK6 in the regulation of G1 length during adult neurogenesis, although its potential contribution to embryonic neurogenesis was not addressed [166].

A multi-protein complex in brain development

In summary, almost all MCPH proteins are linked to the centrosome with varying levels of intimacy (Figure 2). CENPJ, STIL and CEP135 are core centriolar components; MICROCEPHALIN, CDK5RAP2 and CEP152 form an integral part of the PCM; WDR62, ASPM and CDK6 are transiently associated with the centrosome; and two other microcephaly proteins, CASC5 and PHC1 interact with known centrosomal constituents. In addition, a handful of microcephaly proteins are physically linked to each other, either directly or indirectly, suggesting the existence of a large network of protein-protein interactions essential for prenatal neurogenesis. We believe that the loss of a single protein or protein-protein interaction could cripple the interaction network, thereby increasing susceptibility to disease. Tellingly, mutations in PERICENTRIN, a protein in the network that interacts with MICROCEPHALIN and CDK5RAP2, cause SCKL and primordial dwarfism [167]. Furthermore, up-regulation of Plk4 is shown to impede brain development and cause microcephaly in mice, although there have been no reported cases in humans so far [168]. Moreover, CEP63 is a protein deficient in SCKL and known to interact with CEP152 [28].

As additional disease genes are being rapidly discovered, it is intriguing to speculate on their identity and whether they encode proteins in the interaction network.

Conclusion

During the past decade, substantial progress has been made in our understanding of brain development and the genetic basis of MCPH. It is now apparent that microcephaly proteins control a number of cellular processes, including centriole biogenesis, centrosome maturation, cell cycle and DNA damage checkpoint, spindle positioning and mitosis, all of which impinge on brain growth and size (Figure 3). While neuronal homeostasis is thought to be maintained by a complex interplay between the opposing actions of cell proliferation and cell death, symmetric and asymmetric division, and/or normal and aberrant differentiation, to what extent does each of these contribute to brain development? Despite our knowledge of microcephaly proteins, many important questions remain. For instance, why do some proteins appear to have a better-defined role in regulating the switch between symmetric and asymmetric division in the developing brain, and why others are more frequently involved in SCKL and/or have additional functions in more than one cell/tissue type? Is the centrosome a central hub for coordinating and integrating various molecular events crucial for prenatal neurogenesis? We firmly believe that the answers to these questions hinge on our ability to fully understand the functional importance of each microcephaly protein and build upon the existing protein interaction network. These studies would help to better define microcephaly disorders and to facilitate early diagnosis and prognosis.

Acknowledgements

We wish to thank an anonymous reviewer for critical reading of the manuscript. W.Y.T. was a Canadian Institutes of Health Research New Investigator and a Fonds de recherche Santé Junior 1 Research Scholar. This work was supported by the Canadian Institutes of Health Research (MOP-115033) to W.Y.T. and IRCM-Emmanuel Triassi scholarship to M.B.

Conflict of Interest

The authors have no conflicts of interest to declare.

References

1. Cox J, Jackson AP, Bond J, Woods CG (2006) What primary microcephaly can tell us about brain growth. Trends Mol Med 12: 358-366.
2. Mahmood S, Ahmad W, Hassan MJ (2011) Autosomal Recessive Primary Microcephaly (MCPH): clinical manifestations, genetic heterogeneity and mutation continuum. Orphanet J Rare Dis 6: 39.
3. Woods CG, Parker A (2013) Investigating microcephaly. Arch Dis Child 98: 707-713.
4. Woods CG, Bond J, Enard W (2005) Autosomal recessive primary microcephaly (MCPH): a review of clinical, molecular, and evolutionary findings. Am J Hum Genet 76: 717-728.
5. Passemard S, Kaindl AM, Verloes A (2013) Microcephaly. Handb Clin Neurol 111: 129-141.
6. Passemard S, Titomanlio L, Elmaleh M, Afenjar A, Alessandri JL, et al. (2009) Expanding the clinical and neuroradiologic phenotype of primary microcephaly due to ASPM mutations. Neurology 73: 962-969.
7. Mochida GH, Walsh CA (2001) Molecular genetics of human microcephaly. Curr Opin Neurol 14: 151-156.
8. Kerzendorfer C, Colnaghi R, Abramowicz I, Carpenter G, O'Driscoll M (2013) Meier-Gorlin syndrome and Wolf-Hirschhorn syndrome: two developmental disorders highlighting the importance of efficient DNA replication for normal development and neurogenesis. DNA Repair (Amst) 12: 637-644.
9. Thornton GK, Woods CG (2009) Primary microcephaly: do all roads lead to Rome? Trends Genet 25: 501-510.

10. Kaindl AM, Passemard S, Kumar P, Kraemer N, Issa L, et al. (2010) Many roads lead to primary autosomal recessive microcephaly. Prog Neurobiol 90: 363-383.
11. Klingseisen A, Jackson AP (2011) Mechanisms and pathways of growth failure in primordial dwarfism. Genes Dev 25: 2011-2024.
12. O'Driscoll M, Jackson AP, Jeggo PA (2006) Microcephalin: a causal link between impaired damage response signalling and microcephaly. Cell Cycle 5: 2339-2344.
13. Jackson AP, Eastwood H, Bell SM, Adu J, Toomes C, et al. (2002) Identification of microcephalin, a protein implicated in determining the size of the human brain. Am J Hum Genet 71: 136-142.
14. Bond J, Roberts E, Mochida GH, Hampshire DJ, Scott S, et al. (2002) ASPM is a major determinant of cerebral cortical size. Nat Genet 32: 316-320.
15. Bond J, Roberts E, Springell K, Lizarraga SB, Scott S, et al. (2005) A centrosomal mechanism involving CDK5RAP2 and CENPJ controls brain size. Nat Genet 37: 353-355.
16. Nicholas AK, Khurshid M, Desir J, Carvalho OP, Cox JJ, et al. (2010) WDR62 is associated with the spindle pole and is mutated in human microcephaly. Nat Genet 42: 1010-1014.
17. Issa L, Kraemer N, Rickert CH, Sifringer M, Ninnemann O, et al. (2013) CDK5RAP2 expression during murine and human brain development correlates with pathology in primary autosomal recessive microcephaly. Cereb Cortex 23: 2245-2260.
18. Huttner WB, Kosodo Y (2005) Symmetric versus asymmetric cell division during neurogenesis in the developing vertebrate central nervous system. Curr Opin Cell Biol 17: 648-657.
19. Peyre E, Morin X (2012) An oblique view on the role of spindle orientation in vertebrate neurogenesis. Dev Growth Differ 54: 287-305.
20. Taverna E, Gotz M, Huttner WB (2014) The Cell Biology of Neurogenesis: Toward an Understanding of the Development and Evolution of the Neocortex. Annu Rev Cell Dev Biol.
21. Fish JL, Dehay C, Kennedy H, Huttner WB (2008) Making bigger brains-the evolution of neural-progenitor-cell division. J Cell Sci 121: 2783-2793.
22. Zhong X, Pfeifer GP, Xu X (2006) Microcephalin encodes a centrosomal protein. Cell Cycle 5: 457-458.
23. Yu TW, Mochida GH, Tischfield DJ, Sgaier SK, Flores-Sarnat L, et al. (2010) Mutations in WDR62, encoding a centrosome-associated protein, cause microcephaly with simplified gyri and abnormal cortical architecture. Nat Genet 42: 1015-1020.
24. Zhong X, Liu L, Zhao A, Pfeifer GP, Xu X (2005) The abnormal spindle-like, microcephaly-associated (ASPM) gene encodes a centrosomal protein. Cell Cycle 4: 1227-1229.
25. Kumar A, Girimaji SC, Duvvari MR, Blanton SH (2009) Mutations in STIL, encoding a pericentriolar and centrosomal protein, cause primary microcephaly. Am J Hum Genet 84: 286-290.
26. Hussain MS, Baig SM, Neumann S, Nurnberg G, Farooq M, et al. (2012) A truncating mutation of CEP135 causes primary microcephaly and disturbed centrosomal function. Am J Hum Genet 90: 871-878.

27. Guernsey DL, Jiang H, Hussin J, Arnold M, Bouyakdan K, et al. (2010) Mutations in centrosomal protein CEP152 in primary microcephaly families linked to MCPH4. Am J Hum Genet 87: 40-51.
28. Sir JH, Barr AR, Nicholas AK, Carvalho OP, Khurshid M, et al. (2011) A primary microcephaly protein complex forms a ring around parental centrioles. Nat Genet 43: 1147-1153.
29. Hussain MS, Baig SM, Neumann S, Peche VS, Szczepanski S, et al. (2013) CDK6 associates with the centrosome during mitosis and is mutated in a large Pakistani family with primary microcephaly. Hum Mol Genet 22: 5199-5214.
30. Alieva IB, Uzbekov RE (2008) The centrosome is a polyfunctional multiprotein cell complex. Biochemistry (Mosc) 73: 626-643.
31. Bornens M (2012) The centrosome in cells and organisms. Science 335: 422-426.
32. Debec A, Sullivan W, Bettencourt-Dias M (2010) Centrioles: active players or passengers during mitosis? Cell Mol Life Sci 67: 2173-2194.
33. Nigg EA, Raff JW (2009) Centrioles, centrosomes, and cilia in health and disease. Cell 139: 663-678.
34. Tsang WY, Dynlacht BD (2013) CP110 and its network of partners coordinately regulate cilia assembly. Cilia 2: 9.
35. Hossain D, Tsang WY (2013) Centrosome dysfunction and senescence: coincidence or causality? Aging Sci 1: 113.
36. Hinchcliffe EH, Sluder G (2001) "It takes two to tango": understanding how centrosome duplication is regulated throughout the cell cycle. Genes Dev 15: 1167-1181.
37. Nigg EA, Stearns T (2011) The centrosome cycle: Centriole biogenesis, duplication and inherent asymmetries. Nat Cell Biol 13: 1154-1160.
38. Palazzo RE, Vogel JM, Schnackenberg BJ, Hull DR, Wu X (2000) Centrosome maturation. Curr Top Dev Biol 49: 449-470.
39. Brownlee CW, Rogers GC (2013) Show me your license, please: deregulation of centriole duplication mechanisms that promote amplification. Cell Mol Life Sci 70: 1021-1034.
40. Jackson AP, McHale DP, Campbell DA, Jafri H, Rashid Y, et al. (1998) Primary autosomal recessive microcephaly (MCPH1) maps to chromosome 8p22-pter. Am J Hum Genet 63: 541-546.
41. Venkatesh T, Suresh PS (2014) Emerging roles of MCPH1: expedition from primary microcephaly to cancer. Eur J Cell Biol 93: 98-105.
42. Jeffers LJ, Coull BJ, Stack SJ, Morrison CG (2008) Distinct BRCT domains in Mcph1/Brit1 mediate ionizing radiation-induced focus formation and centrosomal localization. Oncogene 27: 139-144.
43. Yang SZ, Lin FT, Lin WC (2008) MCPH1/BRIT1 cooperates with E2F1 in the activation of checkpoint, DNA repair and apoptosis. EMBO Rep 9: 907-915.
44. Peng G, Lin SY (2009) BRIT1/MCPH1 is a multifunctional DNA damage responsive protein mediating DNA repair-associated chromatin remodeling. Cell Cycle 8: 3071-3072.
45. Peng G, Yim EK, Dai H, Jackson AP, Burgt I, et al. (2009) BRIT1/MCPH1 links chromatin remodelling to DNA damage response. Nat Cell Biol 11: 865-872.
46. Wood JL, Liang Y, Li K, Chen J (2008) Microcephalin/MCPH1 associates with the Condensin II complex to function in homologous recombination repair. J Biol Chem 283: 29586-29592.

47. Trimborn M, Schindler D, Neitzel H, Hirano T (2006) Misregulated chromosome condensation in MCPH1 primary microcephaly is mediated by condensin II. Cell Cycle 5: 322-326.
48. Tibelius A, Marhold J, Zentgraf H, Heilig CE, Neitzel H, et al. (2009) Microcephalin and pericentrin regulate mitotic entry via centrosome-associated Chk1. J Cell Biol 185: 1149-1157.
49. Gruber R, Zhou Z, Sukchev M, Joerss T, Frappart PO, et al. (2011) MCPH1 regulates the neuroprogenitor division mode by coupling the centrosomal cycle with mitotic entry through the Chk1-Cdc25 pathway. Nat Cell Biol 13: 1325-1334.
50. Liang Y, Gao H, Lin SY, Peng G, Huang X, et al. (2010) BRIT1/MCPH1 is essential for mitotic and meiotic recombination DNA repair and maintaining genomic stability in mice. PLoS Genet 6: e1000826.
51. Trimborn M, Ghani M, Walther DJ, Dopatka M, Dutrannoy V, et al. (2010) Establishment of a mouse model with misregulated chromosome condensation due to defective Mcph1 function. PLoS One 5: e9242.
52. Zhou ZW, Tapias A, Bruhn C, Gruber R, Sukchev M, et al. (2013) DNA damage response in microcephaly development of MCPH1 mouse model. DNA Repair (Amst) 12: 645-655.
53. Bilguvar K, Ozturk AK, Louvi A, Kwan KY, Choi M, et al. (2010) Whole-exome sequencing identifies recessive WDR62 mutations in severe brain malformations. Nature 467: 207-210.
54. Bacino CA, Arriola LA, Wiszniewska J, Bonnen PE (2012) WDR62 missense mutation in a consanguineous family with primary microcephaly. Am J Med Genet A 158A: 622-625.
55. Bogoyevitch MA, Yeap YY, Qu Z, Ngoei KR, Yip YY, et al. (2012) WD40-repeat protein 62 is a JNK-phosphorylated spindle pole protein required for spindle maintenance and timely mitotic progression. J Cell Sci 125: 5096-5109.
56. Farag HG, Froehler S, Oexle K, Ravindran E, Schindler D, et al. (2013) Abnormal centrosome and spindle morphology in a patient with autosomal recessive primary microcephaly type 2 due to compound heterozygous WDR62 gene mutation. Orphanet J Rare Dis 8: 178.
57. MacCorkle-Chosnek RA, VanHooser A, Goodrich DW, Brinkley BR, Tan TH (2001) Cell cycle regulation of c-Jun N-terminal kinase activity at the centrosomes. Biochem Biophys Res Commun 289: 173-180.
58. Xu D, Zhang F, Wang Y, Sun Y, Xu Z (2014) Microcephaly-Associated Protein WDR62 Regulates Neurogenesis through JNK1 in the Developing Neocortex. Cell Rep 6: 104-116.
59. Novorol C, Burkhardt J, Wood KJ, Iqbal A, Roque C, et al. (2013) Microcephaly models in the developing zebrafish retinal neuroepithelium point to an underlying defect in metaphase progression. Open Biol 3: 130065.
60. Chen JF, Zhang Y, Wilde J, Hansen KC, Lai F, et al. (2014) Microcephaly disease gene Wdr62 regulates mitotic progression of embryonic neural stem cells and brain size. Nat Commun 5: 3885.
61. Joukov V, De Nicolo A, Rodriguez A, Walter JC, Livingston DM (2010) Centrosomal protein of 192 kDa (Cep192) promotes centrosome-driven spindle assembly by

engaging in organelle-specific Aurora A activation. Proc Natl Acad Sci U S A 107: 21022-21027.
62. Fong KW, Choi YK, Rattner JB, Qi RZ (2008) CDK5RAP2 is a pericentriolar protein that functions in centrosomal attachment of the gamma-tubulin ring complex. Mol Biol Cell 19: 115-125.
63. Choi YK, Liu P, Sze SK, Dai C, Qi RZ (2010) CDK5RAP2 stimulates microtubule nucleation by the gamma-tubulin ring complex. J Cell Biol 191: 1089-1095.
64. Lee K, Rhee K (2011) PLK1 phosphorylation of pericentrin initiates centrosome maturation at the onset of mitosis. J Cell Biol 195: 1093-1101.
65. Kim S, Rhee K (2014) Importance of the CEP215-Pericentrin Interaction for Centrosome Maturation during Mitosis. PLoS One 9: e87016.
66. Megraw TL, Sharkey JT, Nowakowski RS (2011) Cdk5rap2 exposes the centrosomal root of microcephaly syndromes. Trends Cell Biol 21: 470-480.
67. Barrera JA, Kao LR, Hammer RE, Seemann J, Fuchs JL, et al. (2010) CDK5RAP2 regulates centriole engagement and cohesion in mice. Dev Cell 18: 913-926.
68. Graser S, Stierhof YD, Nigg EA (2007) Cep68 and Cep215 (Cdk5rap2) are required for centrosome cohesion. J Cell Sci 120: 4321-4331.
69. Zhang X, Liu D, Lv S, Wang H, Zhong X, et al. (2009) CDK5RAP2 is required for spindle checkpoint function. Cell Cycle 8: 1206-1216.
70. Buchman JJ, Tseng HC, Zhou Y, Frank CL, Xie Z, et al. (2010) Cdk5rap2 interacts with pericentrin to maintain the neural progenitor pool in the developing neocortex. Neuron 66: 386-402.
71. Lizarraga SB, Margossian SP, Harris MH, Campagna DR, Han AP, et al. (2010) Cdk5rap2 regulates centrosome function and chromosome segregation in neuronal progenitors. Development 137: 1907-1917.
72. Genin A, Desir J, Lambert N, Biervliet M, Van Der Aa N, et al. (2012) Kinetochore KMN network gene CASC5 mutated in primary microcephaly. Hum Mol Genet 21: 5306-5317.
73. Cheeseman IM, Hori T, Fukagawa T, Desai A (2008) KNL1 and the CENP-H/I/K complex coordinately direct kinetochore assembly in vertebrates. Mol Biol Cell 19: 587-594.
74. Bolanos-Garcia VM, Lischetti T, Matak-Vinkovic D, Cota E, Simpson PJ, et al. (2011) Structure of a Blinkin-BUBR1 complex reveals an interaction crucial for kinetochore-mitotic checkpoint regulation via an unanticipated binding Site. Structure 19: 1691-1700.
75. Krenn V, Wehenkel A, Li X, Santaguida S, Musacchio A (2012) Structural analysis reveals features of the spindle checkpoint kinase Bub1-kinetochore subunit Knl1 interaction. J Cell Biol 196: 451-467.
76. Kiyomitsu T, Obuse C, Yanagida M (2007) Human Blinkin/AF15q14 is required for chromosome alignment and the mitotic checkpoint through direct interaction with Bub1 and BubR1. Dev Cell 13: 663-676.
77. Varma D, Salmon ED (2012) The KMN protein network--chief conductors of the kinetochore orchestra. J Cell Sci 125: 5927-5936.
78. Bond J, Scott S, Hampshire DJ, Springell K, Corry P, et al. (2003) Protein-truncating mutations in ASPM cause variable reduction in brain size. Am J Hum Genet 73: 1170-1177.

79. Kumar A, Blanton SH, Babu M, Markandaya M, Girimaji SC (2004) Genetic analysis of primary microcephaly in Indian families: novel ASPM mutations. Clin Genet 66: 341-348.
80. Pichon B, Vankerckhove S, Bourrouillou G, Duprez L, Abramowicz MJ (2004) A translocation breakpoint disrupts the ASPM gene in a patient with primary microcephaly. Eur J Hum Genet 12: 419-421.
81. Shen J, Eyaid W, Mochida GH, Al-Moayyad F, Bodell A, et al. (2005) ASPM mutations identified in patients with primary microcephaly and seizures. J Med Genet 42: 725-729.
82. Gul A, Hassan MJ, Mahmood S, Chen W, Rahmani S, et al. (2006) Genetic studies of autosomal recessive primary microcephaly in 33 Pakistani families: Novel sequence variants in ASPM gene. Neurogenetics 7: 105-110.
83. Gul A, Tariq M, Khan MN, Hassan MJ, Ali G, et al. (2007) Novel protein-truncating mutations in the ASPM gene in families with autosomal recessive primary microcephaly. J Neurogenet 21: 153-163.
84. Desir J, Cassart M, David P, Van Bogaert P, Abramowicz M (2008) Primary microcephaly with ASPM mutation shows simplified cortical gyration with antero-posterior gradient pre- and post-natally. Am J Med Genet A 146A: 1439-1443.
85. Muhammad F, Mahmood Baig S, Hansen L, Sajid Hussain M, Anjum Inayat I, et al. (2009) Compound heterozygous ASPM mutations in Pakistani MCPH families. Am J Med Genet A 149A: 926-930.
86. Nicholas AK, Swanson EA, Cox JJ, Karbani G, Malik S, et al. (2009) The molecular landscape of ASPM mutations in primary microcephaly. J Med Genet 46: 249-253.
87. Saadi A, Borck G, Boddaert N, Chekkour MC, Imessaoudene B, et al. (2009) Compound heterozygous ASPM mutations associated with microcephaly and simplified cortical gyration in a consanguineous Algerian family. Eur J Med Genet 52: 180-184.
88. Darvish H, Esmaeeli-Nieh S, Monajemi GB, Mohseni M, Ghasemi-Firouzabadi S, et al. (2010) A clinical and molecular genetic study of 112 Iranian families with primary microcephaly. J Med Genet 47: 823-828.
89. Kousar R, Nawaz H, Khurshid M, Ali G, Khan SU, et al. (2010) Mutation analysis of the ASPM gene in 18 Pakistani families with autosomal recessive primary microcephaly. J Child Neurol 25: 715-720.
90. Jamieson CR, Fryns JP, Jacobs J, Matthijs G, Abramowicz MJ (2000) Primary autosomal recessive microcephaly: MCPH5 maps to 1q25-q32. Am J Hum Genet 67: 1575-1577.
91. Tsang WY, Spektor A, Luciano DJ, Indjeian VB, Chen Z, et al. (2006) CP110 cooperates with two calcium-binding proteins to regulate cytokinesis and genome stability. Mol Biol Cell 17: 3423-3434.
92. Higgins J, Midgley C, Bergh AM, Bell SM, Askham JM, et al. (2010) Human ASPM participates in spindle organisation, spindle orientation and cytokinesis. BMC Cell Biol 11: 85.
93. Fish JL, Kosodo Y, Enard W, Paabo S, Huttner WB (2006) Aspm specifically maintains symmetric proliferative divisions of neuroepithelial cells. Proc Natl Acad Sci U S A 103: 10438-10443.
94. Gonzalez C, Saunders RD, Casal J, Molina I, Carmena M, et al. (1990) Mutations at the asp locus of Drosophila lead to multiple free centrosomes in syncytial embryos, but restrict centrosome duplication in larval neuroblasts. J Cell Sci 96 (Pt 4): 605-616.

95. Riparbelli MG, Callaini G, Glover DM, Avides Mdo C (2002) A requirement for the Abnormal Spindle protein to organise microtubules of the central spindle for cytokinesis in Drosophila. J Cell Sci 115: 913-922.
96. Pulvers JN, Bryk J, Fish JL, Wilsch-Brauninger M, Arai Y, et al. (2010) Mutations in mouse Aspm (abnormal spindle-like microcephaly associated) cause not only microcephaly but also major defects in the germline. Proc Natl Acad Sci U S A 107: 16595-16600.
97. Casal J, Gonzalez C, Wandosell F, Avila J, Ripoll P (1990) Abnormal meiotic spindles cause a cascade of defects during spermatogenesis in asp males of Drosophila. Development 108: 251-260.
98. Fujimori A, Itoh K, Goto S, Hirakawa H, Wang B, et al. (2013) Disruption of Aspm causes microcephaly with abnormal neuronal differentiation. Brain Dev.
99. Xu XL, Ma W, Zhu YB, Wang C, Wang BY, et al. (2012) The microtubule-associated protein ASPM regulates spindle assembly and meiotic progression in mouse oocytes. PLoS One 7: e49303.
100. Kouprina N, Pavlicek A, Collins NK, Nakano M, Noskov VN, et al. (2005) The microcephaly ASPM gene is expressed in proliferating tissues and encodes for a mitotic spindle protein. Hum Mol Genet 14: 2155-2165.
101. Hagemann C, Anacker J, Gerngras S, Kuhnel S, Said HM, et al. (2008) Expression analysis of the autosomal recessive primary microcephaly genes MCPH1 (microcephalin) and MCPH5 (ASPM, abnormal spindle-like, microcephaly associated) in human malignant gliomas. Oncol Rep 20: 301-308.
102. Lin SY, Pan HW, Liu SH, Jeng YM, Hu FC, et al. (2008) ASPM is a novel marker for vascular invasion, early recurrence, and poor prognosis of hepatocellular carcinoma. Clin Cancer Res 14: 4814-4820.
103. Alsiary R, Bruning-Richardson A, Bond J, Morrison EE, Wilkinson N, et al. (2014) Deregulation of microcephalin and ASPM expression are correlated with epithelial ovarian cancer progression. PLoS One 9: e97059.
104. Gonczy P (2012) Towards a molecular architecture of centriole assembly. Nat Rev Mol Cell Biol 13: 425-435.
105. Leidel S, Gonczy P (2005) Centrosome duplication and nematodes: recent insights from an old relationship. Dev Cell 9: 317-325.
106. Kleylein-Sohn J, Westendorf J, Le Clech M, Habedanck R, Stierhof YD, et al. (2007) Plk4-induced centriole biogenesis in human cells. Dev Cell 13: 190-202.
107. Sonnen KF, Gabryjonczyk AM, Anselm E, Stierhof YD, Nigg EA (2013) Human Cep192 and Cep152 cooperate in Plk4 recruitment and centriole duplication. J Cell Sci 126: 3223-3233.
108. Kim TS, Park JE, Shukla A, Choi S, Murugan RN, et al. (2013) Hierarchical recruitment of Plk4 and regulation of centriole biogenesis by two centrosomal scaffolds, Cep192 and Cep152. Proc Natl Acad Sci U S A 110: E4849-4857.
109. Hatch EM, Kulukian A, Holland AJ, Cleveland DW, Stearns T (2010) Cep152 interacts with Plk4 and is required for centriole duplication. J Cell Biol 191: 721-729.
110. Cizmecioglu O, Arnold M, Bahtz R, Settele F, Ehret L, et al. (2010) Cep152 acts as a scaffold for recruitment of Plk4 and CPAP to the centrosome. J Cell Biol 191: 731-739.

111. Dzhindzhev NS, Yu QD, Weiskopf K, Tzolovsky G, Cunha-Ferreira I, et al. (2010) Asterless is a scaffold for the onset of centriole assembly. Nature 467: 714-718.
112. van Breugel M, Hirono M, Andreeva A, Yanagisawa HA, Yamaguchi S, et al. (2011) Structures of SAS-6 suggest its organization in centrioles. Science 331: 1196-1199.
113. Kitagawa D, Vakonakis I, Olieric N, Hilbert M, Keller D, et al. (2011) Structural basis of the 9-fold symmetry of centrioles. Cell 144: 364-375.
114. Qiao R, Cabral G, Lettman MM, Dammermann A, Dong G (2012) SAS-6 coiled-coil structure and interaction with SAS-5 suggest a regulatory mechanism in C. elegans centriole assembly. EMBO J 31: 4334-4347.
115. Lettman MM, Wong YL, Viscardi V, Niessen S, Chen SH, et al. (2013) Direct binding of SAS-6 to ZYG-1 recruits SAS-6 to the mother centriole for cartwheel assembly. Dev Cell 25: 284-298.
116. Delattre M, Canard C, Gonczy P (2006) Sequential protein recruitment in C. elegans centriole formation. Curr Biol 16: 1844-1849.
117. Pelletier L, O'Toole E, Schwager A, Hyman AA, Muller-Reichert T (2006) Centriole assembly in Caenorhabditis elegans. Nature 444: 619-623.
118. Tang CJ, Lin SY, Hsu WB, Lin YN, Wu CT, et al. (2011) The human microcephaly protein STIL interacts with CPAP and is required for procentriole formation. EMBO J 30: 4790-4804.
119. Hung LY, Chen HL, Chang CW, Li BR, Tang TK (2004) Identification of a novel microtubule-destabilizing motif in CPAP that binds to tubulin heterodimers and inhibits microtubule assembly. Mol Biol Cell 15: 2697-2706.
120. Hsu WB, Hung LY, Tang CJ, Su CL, Chang Y, et al. (2008) Functional characterization of the microtubule-binding and -destabilizing domains of CPAP and d-SAS-4. Exp Cell Res 314: 2591-2602.
121. Comartin D, Gupta GD, Fussner E, Coyaud E, Hasegan M, et al. (2013) CEP120 and SPICE1 cooperate with CPAP in centriole elongation. Curr Biol 23: 1360-1366.
122. Lin YN, Wu CT, Lin YC, Hsu WB, Tang CJ, et al. (2013) CEP120 interacts with CPAP and positively regulates centriole elongation. J Cell Biol 202: 211-219.
123. Lin YC, Chang CW, Hsu WB, Tang CJ, Lin YN, et al. (2013) Human microcephaly protein CEP135 binds to hSAS-6 and CPAP, and is required for centriole assembly. EMBO J 32: 1141-1154.
124. Tang CJ, Fu RH, Wu KS, Hsu WB, Tang TK (2009) CPAP is a cell-cycle regulated protein that controls centriole length. Nat Cell Biol 11: 825-831.
125. Schmidt TI, Kleylein-Sohn J, Westendorf J, Le Clech M, Lavoie SB, et al. (2009) Control of centriole length by CPAP and CP110. Curr Biol 19: 1005-1011.
126. Kohlmaier G, Loncarek J, Meng X, McEwen BF, Mogensen MM, et al. (2009) Overly long centrioles and defective cell division upon excess of the SAS-4-related protein CPAP. Curr Biol 19: 1012-1018.
127. Cho JH, Chang CJ, Chen CY, Tang TK (2006) Depletion of CPAP by RNAi disrupts centrosome integrity and induces multipolar spindles. Biochem Biophys Res Commun 339: 742-747.
128. Gopalakrishnan J, Mennella V, Blachon S, Zhai B, Smith AH, et al. (2011) Sas-4 provides a scaffold for cytoplasmic complexes and tethers them in a centrosome. Nat Commun 2: 359.

129. Hung LY, Tang CJ, Tang TK (2000) Protein 4.1 R-135 interacts with a novel centrosomal protein (CPAP) which is associated with the gamma-tubulin complex. Mol Cell Biol 20: 7813-7825.
130. Gopalakrishnan J, Chim YC, Ha A, Basiri ML, Lerit DA, et al. (2012) Tubulin nucleotide status controls Sas-4-dependent pericentriolar material recruitment. Nat Cell Biol 14: 865-873.
131. Shi L, Lin Q, Su B (2014) Human-specific hypomethylation of CENPJ, a key brain size regulator. Mol Biol Evol 31: 594-604.
132. McIntyre RE, Lakshminarasimhan Chavali P, Ismail O, Carragher DM, Sanchez-Andrade G, et al. (2012) Disruption of mouse Cenpj, a regulator of centriole biogenesis, phenocopies Seckel syndrome. PLoS Genet 8: e1003022.
133. Ladha S (2011) Step to CEP152: uncovering a new mutation implicated in Seckel syndrome. Clin Genet 79: 428-430.
134. Vulprecht J, David A, Tibelius A, Castiel A, Konotop G, et al. (2012) STIL is required for centriole duplication in human cells. J Cell Sci 125: 1353-1362.
135. Arquint C, Sonnen KF, Stierhof YD, Nigg EA (2012) Cell-cycle-regulated expression of STIL controls centriole number in human cells. J Cell Sci 125: 1342-1352.
136. Habedanck R, Stierhof YD, Wilkinson CJ, Nigg EA (2005) The Polo kinase Plk4 functions in centriole duplication. Nat Cell Biol 7: 1140-1146.
137. Leidel S, Delattre M, Cerutti L, Baumer K, Gonczy P (2005) SAS-6 defines a protein family required for centrosome duplication in C. elegans and in human cells. Nat Cell Biol 7: 115-125.
138. Kitagawa D, Kohlmaier G, Keller D, Strnad P, Balestra FR, et al. (2011) Spindle positioning in human cells relies on proper centriole formation and on the microcephaly proteins CPAP and STIL. J Cell Sci 124: 3884-3893.
139. Pfaff KL, Straub CT, Chiang K, Bear DM, Zhou Y, et al. (2007) The zebra fish cassiopeia mutant reveals that SIL is required for mitotic spindle organization. Mol Cell Biol 27: 5887-5897.
140. Izraeli S, Lowe LA, Bertness VL, Good DJ, Dorward DW, et al. (1999) The SIL gene is required for mouse embryonic axial development and left-right specification. Nature 399: 691-694.
141. Kim K, Lee S, Chang J, Rhee K (2008) A novel function of CEP135 as a platform protein of C-NAP1 for its centriolar localization. Exp Cell Res 314: 3692-3700.
142. Kumar A, Rajendran V, Sethumadhavan R, Purohit R (2013) CEP proteins: the knights of centrosome dynasty. Protoplasma 250: 965-983.
143. Inanc B, Putz M, Lalor P, Dockery P, Kuriyama R, et al. (2013) Abnormal centrosomal structure and duplication in Cep135-deficient vertebrate cells. Mol Biol Cell 24: 2645-2654.
144. Carvalho-Santos Z, Machado P, Alvarez-Martins I, Gouveia SM, Jana SC, et al. (2012) BLD10/CEP135 is a microtubule-associated protein that controls the formation of the flagellum central microtubule pair. Dev Cell 23: 412-424.
145. Roque H, Wainman A, Richens J, Kozyrska K, Franz A, et al. (2012) Drosophila Cep135/Bld10 maintains proper centriole structure but is dispensable for cartwheel formation. J Cell Sci 125: 5881-5886.

146. Matsuura K, Lefebvre PA, Kamiya R, Hirono M (2004) Bld10p, a novel protein essential for basal body assembly in Chlamydomonas: localization to the cartwheel, the first ninefold symmetrical structure appearing during assembly. J Cell Biol 165: 663-671.
147. Hiraki M, Nakazawa Y, Kamiya R, Hirono M (2007) Bld10p constitutes the cartwheel-spoke tip and stabilizes the 9-fold symmetry of the centriole. Curr Biol 17: 1778-1783.
148. Jerka-Dziadosz M, Gogendeau D, Klotz C, Cohen J, Beisson J, et al. (2010) Basal body duplication in Paramecium: the key role of Bld10 in assembly and stability of the cartwheel. Cytoskeleton (Hoboken) 67: 161-171.
149. Bayless BA, Giddings TH, Jr., Winey M, Pearson CG (2012) Bld10/Cep135 stabilizes basal bodies to resist cilia-generated forces. Mol Biol Cell 23: 4820-4832.
150. Mottier-Pavie V, Megraw TL (2009) Drosophila bld10 is a centriolar protein that regulates centriole, basal body, and motile cilium assembly. Mol Biol Cell 20: 2605-2614.
151. Kalay E, Yigit G, Aslan Y, Brown KE, Pohl E, et al. (2011) CEP152 is a genome maintenance protein disrupted in Seckel syndrome. Nat Genet 43: 23-26.
152. Avidor-Reiss T, Gopalakrishnan J (2013) Building a centriole. Curr Opin Cell Biol 25: 72-77.
153. Brown NJ, Marjanovic M, Luders J, Stracker TH, Costanzo V (2013) Cep63 and cep152 cooperate to ensure centriole duplication. PLoS One 8: e69986.
154. Lukinavicius G, Lavogina D, Orpinell M, Umezawa K, Reymond L, et al. (2013) Selective chemical crosslinking reveals a Cep57-Cep63-Cep152 centrosomal complex. Curr Biol 23: 265-270.
155. Garapaty S, Xu CF, Trojer P, Mahajan MA, Neubert TA, et al. (2009) Identification and characterization of a novel nuclear protein complex involved in nuclear hormone receptor-mediated gene regulation. J Biol Chem 284: 7542-7552.
156. Yang YJ, Baltus AE, Mathew RS, Murphy EA, Evrony GD, et al. (2012) Microcephaly gene links trithorax and REST/NRSF to control neural stem cell proliferation and differentiation. Cell 151: 1097-1112.
157. Awad S, Al-Dosari MS, Al-Yacoub N, Colak D, Salih MA, et al. (2013) Mutation in PHC1 implicates chromatin remodeling in primary microcephaly pathogenesis. Hum Mol Genet 22: 2200-2213.
158. Tachibana KE, Gonzalez MA, Guarguaglini G, Nigg EA, Laskey RA (2005) Depletion of licensing inhibitor geminin causes centrosome overduplication and mitotic defects. EMBO Rep 6: 1052-1057.
159. Lu F, Lan R, Zhang H, Jiang Q, Zhang C (2009) Geminin is partially localized to the centrosome and plays a role in proper centrosome duplication. Biol Cell 101: 273-285.
160. Bertoli C, Skotheim JM, de Bruin RA (2013) Control of cell cycle transcription during G1 and S phases. Nat Rev Mol Cell Biol 14: 518-528.
161. Mahony D, Parry DA, Lees E (1998) Active cdk6 complexes are predominantly nuclear and represent only a minority of the cdk6 in T cells. Oncogene 16: 603-611.
162. Kohrt DM, Crary JI, Gocheva V, Hinds PW, Grossel MJ (2009) Distinct subcellular distribution of cyclin dependent kinase 6. Cell Cycle 8: 2837-2843.
163. Kwon TK, Buchholz MA, Gabrielson EW, Nordin AA (1995) A novel cytoplasmic substrate for cdk4 and cdk6 in normal and malignant epithelial derived cells. Oncogene 11: 2077-2083.

164. Malumbres M, Sotillo R, Santamaria D, Galan J, Cerezo A, et al. (2004) Mammalian cells cycle without the D-type cyclin-dependent kinases Cdk4 and Cdk6. Cell 118: 493-504.
165. Mi D, Carr CB, Georgala PA, Huang YT, Manuel MN, et al. (2013) Pax6 exerts regional control of cortical progenitor proliferation via direct repression of Cdk6 and hypophosphorylation of pRb. Neuron 78: 269-284.
166. Beukelaers P, Vandenbosch R, Caron N, Nguyen L, Belachew S, et al. (2011) Cdk6-dependent regulation of G(1) length controls adult neurogenesis. Stem Cells 29: 713-724.
167. Rauch A, Thiel CT, Schindler D, Wick U, Crow YJ, et al. (2008) Mutations in the pericentrin (PCNT) gene cause primordial dwarfism. Science 319: 816-819.
168. Marthiens V, Rujano MA, Pennetier C, Tessier S, Paul-Gilloteaux P, et al. (2013) Centrosome amplification causes microcephaly. Nat Cell Biol 15: 731-740.
169. Roberts E, Jackson AP, Carradice AC, Deeble VJ, Mannan J, et al. (1999) The second locus for autosomal recessive primary microcephaly (MCPH2) maps to chromosome 19q13.1-13.2. Eur J Hum Genet 7: 815-820.
170. Moynihan L, Jackson AP, Roberts E, Karbani G, Lewis I, et al. (2000) A third novel locus for primary autosomal recessive microcephaly maps to chromosome 9q34. Am J Hum Genet 66: 724-727.
171. Jamieson CR, Govaerts C, Abramowicz MJ (1999) Primary autosomal recessive microcephaly: homozygosity mapping of MCPH4 to chromosome 15. Am J Hum Genet 65: 1465-1469.
172. Pattison L, Crow YJ, Deeble VJ, Jackson AP, Jafri H, et al. (2000) A fifth locus for primary autosomal recessive microcephaly maps to chromosome 1q31. Am J Hum Genet 67: 1578-1580.

Tables

Table 1. Gene table: autosomal recessive primary microcephaly (MCPH)

Gene	Locus	Gene Product	References (gene and/or locus)	OMIM
MCPH1 MICROCEPHALIN	MCPH1	MICROCEPHALIN	[40]	607117
WDR62 (WD repeat-containing protein 62)	MCPH2	WDR62	[169]	613583
CDK5RAP2 (CDK5 regulatory subunit-associated protein 2)	MCPH3	CDK5RAP2	[170]	608201
CASC5 (cancer susceptibility candidate 5)	MCPH4	CASC5	[171]	609173
ASPM (abnormal spindle-like microcephaly-associated protein)	MCPH5	ASPM	[172]	605481
CENPJ (centromere protein J)	MCPH6	CENPJ	[15]	609279
STIL (SCL/TAL1-interrupting locus)	MCPH7	STIL	[25]	181590
CEP135 (centrosomal protein of 135 kDa)	MCPH8	CEP135	[26]	611423
CEP152 (centrosomal protein of 152 kDa)	MCPH9	CEP152	[27]	613529
ZNF335 (zinc finger protein 335)	MCPH10	ZNF335	[156]	610827
PHC1 (polyhomeotic-like protein 1)	MCPH11	PHC1	[157]	602978
CDK6 (cyclin-dependent		CDK6	[29]	603368

kinase 6)				

Table 2. Animal models of MCPH

Gene	**Model**	**Method**	**Phenotype**
MCPH1 *MICROCEPHALIN*	mouse	knock-out (deletion of exon 2)	genomic instability, growth retardation, male infertility and increased radiation sensitivity
	mouse	knock-out (gene trap)	shorter life span, improper chromosome condensation
	mouse	conditional knock-out (recombination)	specific reduction of the cerebral cortex at birth
	fly	knock-out (p-element excision)	abnormal spindles during embryonic cell cycle
WDR62	rat	shRNA knock-down	premature differentiation of neuroprogenitors into neurons
	zebrafish	morpholino-mediated knock-down	reduction in head and eye size
	mouse	knock-out (deletion of the WDR62 locus)	reduced brain size
CDK5RAP2	fly	knock-out (chemical mutagenesis)	disconnection between centrosome and PCM
	mouse	shRNA knock-down	premature neuronal differentiation
	Hertwig's anemia mouse	inversion of exon 4	reduced brain size
ASPM	zebrafish	morpholino-mediated knock-down	reduction in head and eye size
	mouse	siRNA knock-down	premature differentiation of telencephalic neuroprogenitor cells
	mouse	knock-out (removal of exon 2 and 3)	reduced brain size
	mouse	knock-out (gene trap)	mild microcephaly, massive loss of

			germ cells
	fly	mutagenesis (x-irradiation)	spindle positioning defects, increased apoptosis
CENPJ	mouse	conditional knock-out (truncated mRNA)	intrauterine growth retardation
	fly	knock-out (transposon insertion)	loss of centrioles, abnormal spindle
	worm	siRNA knock-down	loss of centrioles, abnormal centrosome size/organization
STIL	mouse	knock-out (removal of exon 3 to 5)	embryonic lethality
	zebrafish	morpholino-mediated knock-down	embryonic lethality
CEP135	fly	knock-out (transposon insertion)	abnormal centrioles, immotile cilium
	alga	insertion mutagenesis	abnormal centrioles, abnormal cell division and slow growth
	protozoa	siRNA knock-down	abnormal centrioles
CEP152	fly	chemical mutagenesis	defective centrosomes, no zygotic division
	zebrafish	morpholino-mediated knock-down	ciliary defects
ZNF335	mouse	shRNA knock-down	impaired progenitor cell proliferation
	mouse	knock-out (removal of promoter and exons 1&2)	severely reduced cortical size
	mouse	knock-out (gene trap insertion)	embryonically lethal
CDK6	mouse	knock-out (removal of 1st coding exon)	viable, develop normally, hematopoiesis slightly impaired

Figure legends

Figure 1. Centrosome structure

Centrosomes are small organelles composed of two perpendicular centrioles (orange cylinders), a mother and a daughter, linked together by interconnecting fibres (dark green). The centrioles are surrounded by an amorphous pericentriolar matrix (dotted orange background) involved in the nucleation and anchoring of cytoplasmic microtubules. Contrary to the daughter centriole, the mother centriole possesses distal (purple) and sub-distal (blue) appendages necessary for cilia assembly and microtubule anchoring, respectively.

Figure 2. Microcephaly protein interaction network

The majority of microcephaly proteins (red) are associated with centrosomes. CENPJ, STIL and CEP135 are components of centrioles (green box), while MICROCEPHALIN, CDK5RAP2 and CEP152 are part of the PCM (orange background). WDR62, ASPM and CDK6 temporarily localize to the PCM. In addition, CASC5 and PHC1 are known to interact with proteins at the centrosome. For ZNF335, its precise connection to the centrosome is not understood. Microcephaly proteins are physically linked to one another either directly or indirectly (solid black lines) to form a protein network.

Figure 3. Cellular processes involved in microcephaly

A model depicting how malfunction of microcephaly proteins perturbs neurogenesis. A loss of microcephaly proteins can disturb various cellular processes, including chromatin remodelling, kinetochore integrity, centrosome biogenesis or centrosome maturation, which impair cell cycle checkpoints and mitosis. These perturbations disrupt the equilibrium between cell proliferation and cell death, symmetric and asymmetric division, and/or normal and abnormal differentiation, reducing the total number of neuroprogenitor cells and differentiated neurons in the developing brain, leading to microcephaly.

Figures

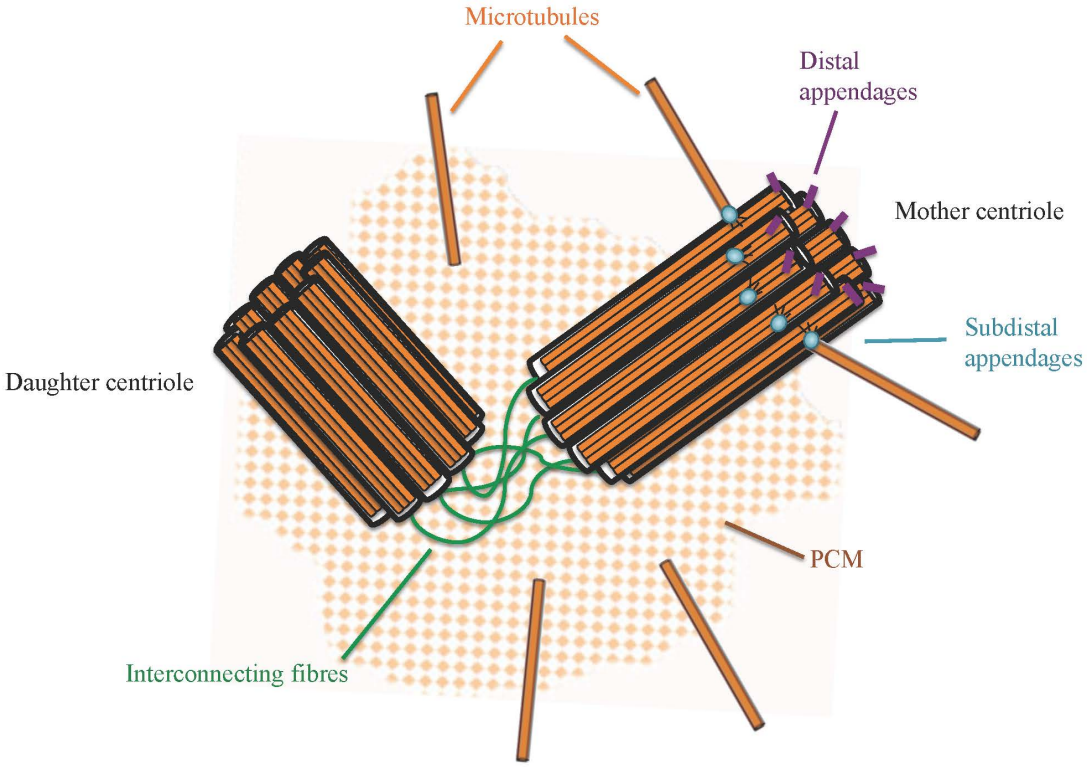

Figure 1. Centrosome structure

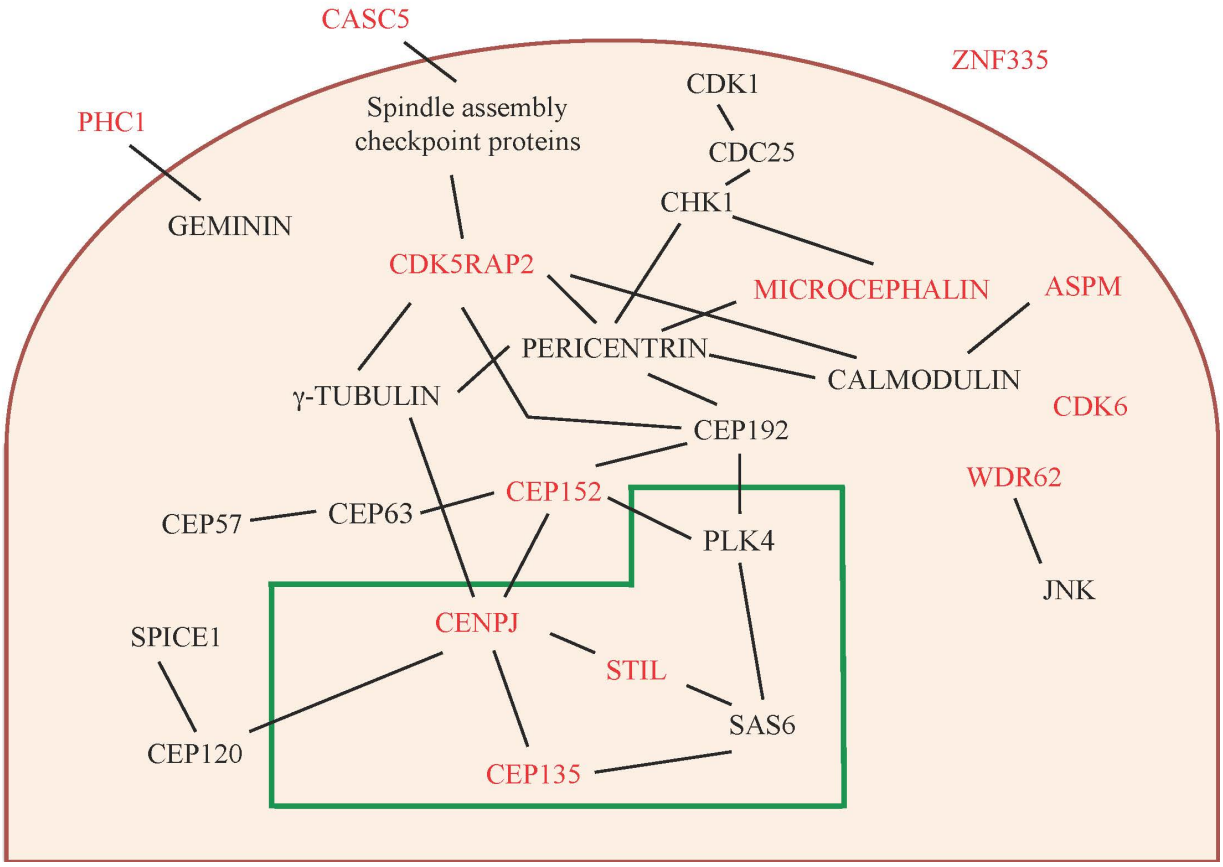

Figure 2. Microcephaly protein interaction network

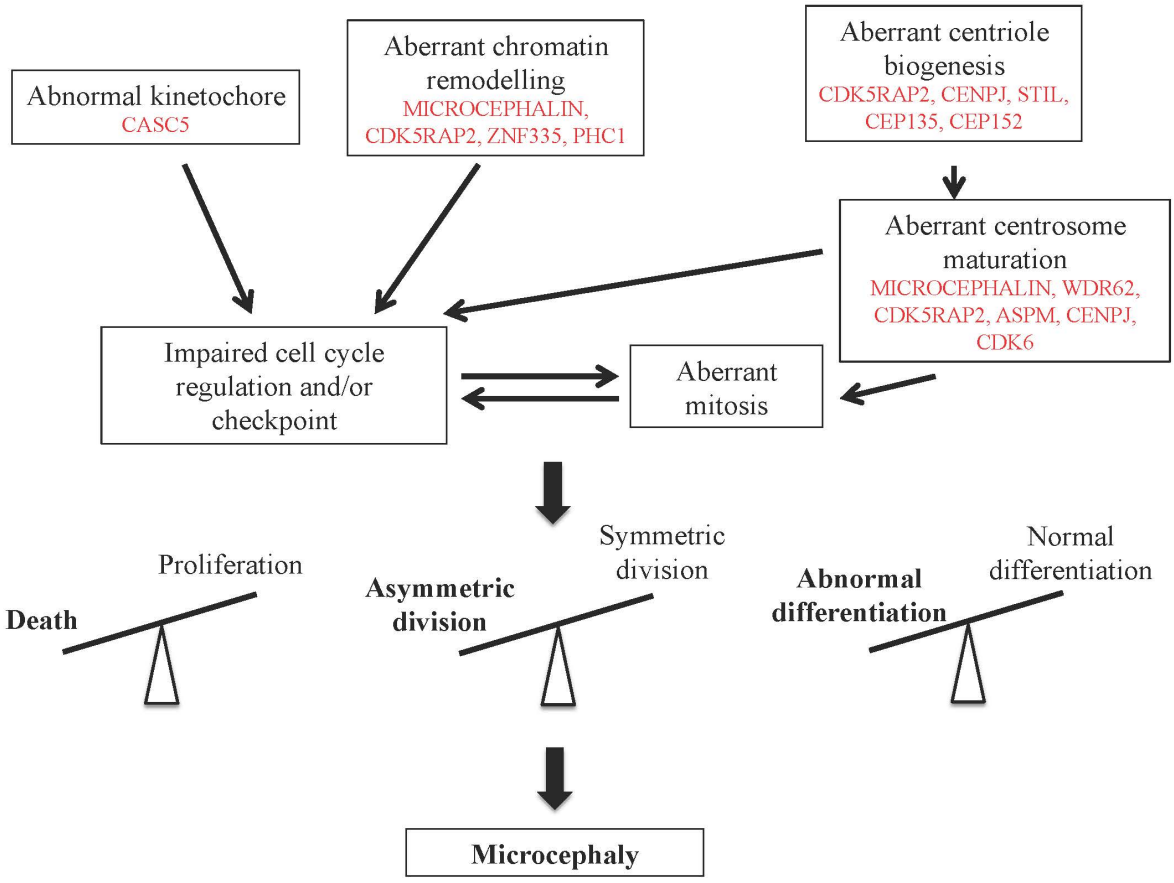

Figure 3. Cellular processes involved in microcephaly